Respiration, Acid/Base, Ammonia and Ionoregulatory Strategies in the Pacific hagfish
(*Eptatretus stoutii*)

by

Alexander Michael Clifford

A thesis submitted in partial fulfillment of the requirements for the degree of

Doctor of Philosophy
in
Physiology, Cell and Developmental Biology

Department of Biological Sciences
University of Alberta

Abstract

Hagfish feed on putrefied carrion, which poses several environmental challenges to the scavenger including hypoxia (Low P_{O_2}), hypercapnia (high P_{CO_2}) and high environmental ammonia (HEA). To any other organism, these conditions would be physiologically challenging; however, hagfish seem to have adapted to survive and thrive in this type of environment. While feeding, hagfish immerse their head and gills in the decaying flesh leaving their trunk exterior to the carcass, allowing for potential cutaneous exchange of acid/base (A/B) equivalents, ammonia and O_2. Hagfish are osmoconformers and do not regulate plasma [Na^+] or [Cl^-] but do regulate the divalent ions SO_4^{2-}, Mg^{2+} and Ca^{2+}; however, the hormone(s) controlling this regulation have remained elusive.

In this thesis, I describe some of the physiological strategies that Pacific hagfish (*Eptatretus stoutii*) employ to withstand and recover from stresses in A/B status, and exposure to ammonia and hypercapnia. Furthermore I identify the relative branchial and cutaneous contributions to overall maintenance of A/B status, ammonia excretion, and O_2 acquisition through the use of custom designed separated-flux chambers. Finally I characterize the glucocorticoid and mineralocorticoid responses of the hagfish and identify the role of the corticosteroids previously shown to act on hagfish corticosteroid receptor.

An environment with a high P_{CO_2} will initially cause acidification of the blood followed by compensatory metabolic plasma [HCO_3^-] elevations. I simulated these perturbations in hagfish through injections of either HCl or $NaHCO_3$ (total H^+/HCO_3^- load: 6000 μmol kg^{-1}). Hagfish excreted the acid load *via* excretion of acid equivalents in

the gill region while the resultant base load was excreted in the skin-only posterior region, indicating that the gills may not be involved in recovery from acute metabolic hypercarbia. However, following chronic hypercapnia exposure (72 h; 0.6% CO_2) to induce hypercarbia, hagfish utilized both gill and skin mechanisms to similar degrees for HCO_3^- excretion, indicating that the gills are capable of excreting base equivalents.

Hagfish exposed to chronic hypercapnia (48 h; 4% CO_2) compensated for blood acidosis by mounting an ~70 mmol L^{-1} plasma $[HCO_3^-]$ response. Upon reintroduction into normocapnic seawater, plasma $[HCO_3^-]$ was rapidly corrected within 8 h. This correction occurred with impressive rates of plasma HCO_3^- loss (at peak: ~10 mmol kg^{-1} h^{-1}) occurring primarily *via* carbonic anhydrase mediated CO_2 offloading with only minor contributions from direct HCO_3^-/Cl^- flux and insignificant contributions from increased glomerular filtration.

During 48 h HEA (20 mmol L^{-1} $[T_{Amm}]$; [total ammonia]) exposure, plasma $[T_{Amm}]$ increased 100-fold to over 5000 μmol L^{-1} while ammonia excretion (J_{Amm}) was transiently inhibited. Plasma $[T_{Amm}]$ stabilized after 24–48 h exposure, possibly through lowering NH_3 influx by reducing body NH_3 permeability. Ammonia balance was subsequently maintained through the reestablishment of J_{Amm} against inwardly directed ΔP_{NH_3} and NH_4^+ electrochemical gradients. Restoration of J_{Amm} by the hagfish during ammonia exposure likely involves secondary active transport of NH_4^+, possibly mediated by Na^+/NH_4^+ (H^+) exchange. Recovery from HEA in ammonia-free water was characterized by considerable ammonia washout, and restoration of plasma $[T_{Amm}]$ within 24 h. During recovery, J_{Amm} occurred *via* branchial (70-80%) and cutaneous (20-30%) mechanisms. Excised hagfish skin fluxes revealed concentration-dependent (0.05 – 5

mmol L^{-1}) J$_{Amm}$ with 8-fold greater J$_{Amm}$ across skin excised from HEA-exposed hagfish. Using immunohistochemical staining with a hagfish-specific Rhcg (ammonia/ammonium transporter) antibody, I demonstrated that Rhcg is present in cutaneous epidermal layers consistent with physiological data.

Cutaneous O$_2$ uptake by the hagfish has been previously suggested as the major site of systemic O$_2$ acquisition. However, I show that hagfish rely primarily (85%) on branchial O$_2$ uptake. When the branchial region was locally immersed in hypoxic conditions (4.6 kPa O$_2$), hagfish did not utilize cutaneous mechanisms to acquire available O$_2$ in the normoxic anterior chamber, suggesting that even when presented with restricted O$_2$ availability, hagfish do not use cutaneous mechanisms to supplement metabolic O$_2$ requirements.

Using handling stress and mineral challenges (SO$_4^{2-}$ injections), I show that hagfish are capable of eliciting glucocorticoid and mineralocorticoid responses. Furthermore I show that these responses are not mediated by alterations in plasma cortisol, corticosterone, 11-deoxycorticosterone or 11-deoxycortisol.

Overall in this thesis, I show that hagfish have developed novel cutaneous A/B and ammonia handling mechanisms along with extraordinary tolerances and effective recovery strategies to cope with exposure to extreme perturbations (*e.g.* hypercapnia, hypoxia, HEA). It is these strategies and mechanisms that allow this unique organism to survive and thrive in their demersal environment.

Preface

This thesis is an original work by Alexander Michael Clifford. The research project, of which this thesis is a part, received research ethics approval from the University of Alberta Animal Care and Use Committee and Bamfield Marine Sciences Animal Care Committee. The following protocols governed the research described herein: University of Alberta: Project Name "Acid/base and ionoregulation in fishes" AUP0001126 (2010-2016). BMSC: Project Name "Acid/base and ionoregulation in ancient fishes" RS 10-42, RS-11-26, RS-12-10, RS-13-24, RS-14-13, RS-15-31. (2010-2016).

Some of the research conducted for this thesis forms part of an international research collaboration, led by Professor G.G. Goss at the University of Alberta. I (Alexander M. Clifford) performed the majority of the work presented in this original Ph.D. thesis. However, parts of this thesis were the result of collaborative efforts. Parts of **Chapter 1** were published in the book titled *"Hagfish Biology"* (2015) Edwards, S.L., Goss, G.G. Eds., CRC Press – Taylor & Francis Group. **Chapters 2 and 5** have been published in Comparative Biochemistry and Physiology - Part A, which is a peer-reviewed journal. **Chaper 6** is currently under consideration for publication in American Journal of Physiology - Regulatory, Integrative and Comparative Physiology. **Chapter 7** is currently under consideration for publication in General and Comparative Endocrinology and Journal of Experimental Biology, respectively. **Chapter 8** has been published in the Journal of Experimental Biology. **Chapter 3** will be submitted for possible publication in Journal of Experimental Biology. **Chapter 4** will be submitted pending collection of further data in July 2016. The separating chambers described in

Chapter 2 were designed by me with the assistance Dr. G. Goss and J. Johnston (University of Alberta). The biographical details for the introduction and data chapters are listed below and indicated at the beginning of each chapter. The role and contributions of all authors for each chapter are briefly described below.

Chapter 1:

Clifford, A.M., Goss, G.G., Roa, J.N., Tresguerres, M., 2015. Acid/base and ionic regulation in hagfish, in: Edwards, S.L., Goss, G.G. (Eds.), Hagfish Biology. CRC Press, Boca Raton, Fl, pp. 277–298. doi:10.1201/b18935-12

This review was conceived by AMC, GGG and MT. AMC drafted the manuscript. AMC, MT and GGG revised the manuscript. All authors approved the manuscript. This review is the result of my individual efforts with the following exceptions: Figure 1 was adapted with permission from Tresguerres et al. (2006) Comparative Biochemistry and Physiology Part A. 145:312-321; Figure 3 was contributed by JNR.

Chapter 2:

Clifford, A.M., Guffey, S.C., Goss, G.G., 2014. Extrabranchial mechanisms of systemic pH recovery in hagfish (*Eptatretus stoutii*). Comp. Biochem. Physiol. A 168, 82–89. doi: 10.1016/j.cbpa.2013.11.009.

The study was conceived and designed by AMC and GGG. AMC performed the experiments and SCG aided. AMC conducted sample analysis and analyzed the data. GGG contributed analysis tools, materials and reagents. AMC drafted the manuscript. All authors revised and approved the manuscript. All experiments performed in Chapter 2 are

the result of my individual efforts with the following exception: SCG aided in data collection.

Chapter 3:

Clifford, A.M., Weinrauch, A.M., Goss, G.G. Recovery from hypercapnia-induced hypercarbia in Pacific hagfish (*Eptatretus stoutii*) occurs primarily *via* passive loss of CO_2 mediated by carbonic anhydrase conversion of HCO_3^-

The study was conceived and designed by AMC and GGG. AMC performed the experiments and AMW aided. AMC conducted sample analysis and analyzed the data. GGG contributed analysis tools, materials and reagents. AMC drafted the manuscript. AMC and GGG revised the manuscript. All authors approved of the manuscript. All experiments performed in Chapter 3 are the result of my individual efforts with the following exception: AMW aided in data collection

Chapter 4:

Clifford, A.M., Weinrauch, A.M., Goss, G.G. Extrabranchial recovery strategies from hypercapnia-induced hypercarbia in Pacific hagfish

The study was conceived and designed by AMC and GGG. AMC performed the experiments and AMW aided AMC performed sample analysis. AMC analyzed the data. GGG contributed analysis tools, materials and reagents. AMC drafted the manuscript. AMC and GGG revised the manuscript. All authors approved of the manuscript. All experiments performed in Chapter 4 are the result of my individual efforts with the following exception: AMW aided in data collection.

Chapter 5:

Clifford, A.M., Goss, G.G., Wilkie, M.P., 2015b. Adaptations of a deep sea scavenger: High ammonia tolerance and active NH_4^+ excretion by the Pacific hagfish (Eptatretus stoutii). Comp. Biochem. Physiol. A 182C, 64–74. doi:10.1016/j.cbpa.2014.12.010

The study was conceived and designed by AMC, GGG and MPW. AMC, and MPW performed the experiments, sample analysis and analyzed the data. GGG and MPW contributed analysis tools, materials and reagents. AMC and MPW drafted the manuscript. All authors revised and approved of the manuscript.

Chapter 6:

Clifford, A.M., Weinrauch, A.M., Edwards, S.L. Wilkie, M.P., Goss, G.G., Flexible ammonia handling strategies using the skin and gill contribute to the high ammonia tolerance of the Pacific hagfish. American Journal of Physiology - Regulatory, Integrative and Comparative Physiology. Submitted 31 pages on August 15, 2016. Manuscript ID: R-00351-2016

The study was conceived and designed by AMC and GGG. AMC performed the experiments. AMC, AMW and SLE analyzed the samples. AMC analyzed the data. MPW aided in data interpretation. GGG and SLE contributed analysis tools, materials and reagents. AMC drafted the manuscript. All authors revised and approved of the manuscript. All experiments performed in Chapter 6 are the result of my individual efforts with the following exceptions: AMW contributed H&E staining and SLE contributed immunohistochemistry.

Chapter 7:

Clifford, A.M., Bury, N.R., Schultz, A.G., Ede, J.D., Goss, B.L. Goss, G.G., Regulation of plasma glucose and sulfate excretion rates in Pacific hagfish, Eptatretus stoutii is not mediated by 11-deoxycortisol. General and Comparative Endocrinology. Submitted 37 pages on April 27, 2016. Manuscript ID: GCE-S-16-00236

The study was conceived and designed by NRB and GGG. AMC, BLG, JDE, NRB and GGG performed experiments. AMC, AGS, JDE, NRB and GGG analyzed samples. AMC, GGG and NRB analyzed the data. GGG contributed analysis tools, materials and reagents. AMC and GGG drafted the manuscript. AMC, AGS, GGG and NRB revised the manuscript. All authors approved of the manuscript.

Chapter 8

Clifford, A.C., Zimmer, A.M., Wood, C.M., Goss, G.G. 2016. It's all in the gills: Evaluation of O2 uptake in Pacific hagfish refutes a major respiratory role for the skin. Journal of Experimental Biology. In Press, doi: 10.1242/jeb.141598

The study was conceived and conducted by AMC and AMZ. AMC and AMZ analyzed the samples. AMC analyzed the data. GGG and CMW contributed analysis tools, materials and reagents. AMC drafted the manuscript; all authors revised and approved the final manuscript. All experiments performed in Chapter 8 are the result of my individual efforts with the following exceptions: AMC and AMZ conducted the experiments collaboratively.

*This thesis is dedicated to **Monica Niereisel** – With me every step of the way.*

Acknowledgements

I'll start by thanking my supervisor Dr. Greg Goss. I can't thank you enough for all the opportunities that you've afforded me. Through you, I've learned not just about the science but also how to be a better kind of researcher (Work hard - Play Hard). Even though I've heard you quote Charles Barkley "I am not a role model" countless times I truly believe the opposite is true. Thank you for all the Bamfield seasons, conference trips and most importantly all the good times. Not only are you a fantastic supervisor, you're a stellar friend, buddy and pal. Beyond the science, valuable lessons such as "Keep your tip up" and "Don't horse it" will be sure to keep the "Fish On" for me in the years to come. I look forward to future fishing trips and ski weekends whenever we can find the time. 'til the next Caucasian.. Cheers.

I've had the opportunity to work alongside some really wonderful people both inside the lab and out. Special mention goes out to fellow hagfishologist Alyssa Weinrauch and my fishing buddy Samuel Guffey. Alyssa, you're a truly wonderful woman and it has been a privilege to watch you grow from that bright ZOOL344 student in my classroom to the established young researcher you are today. You've been the ultimate friend and amazing companion and I am so fortunate to have worked, lived, Bamfield'ed and travelled side by side with you. I'm sad that we are parting ways, but I know that our paths will cross again. Sam, the expert baker and most astute man I know. I'll never forget that day in the boat where we pulled up (then ate) big Bob. Thank you for the late night discussions and crazy Bamfield hours. Resurrecting Heisler's method of $J_{H^+}^{Net}$ measurement wouldn't have been possible without you. Here's to always hoping that "If this works, it'll be awesome!"

Components of this thesis and of the collaborations I've been able to contribute to over the years involve molecular techniques, which I never would have acquired, were it not for Aga Dymowska. Thank you Aga for not only the guidance in the molecular biology and for the help throughout my program, but also for the kindness that you showed me, especially in those early years when I came to Edmonton not knowing anyone. Thanks also to Van Ortega for his tutelage in Western techniques.

Science just wouldn't be the same without being able to work with some amazing people. Thank you to Dylan Cole, Sal Blair, Tamzin Blewitt, Lindsey Felix, James Ede, Perinne Delompré, Erik Folkerts, Kim Ong, Aaron Schultz, David Boyle, Brain Zhang, Henry Ye, Joy, li and Danauta Chamot. You guys are a fantastic crew.

Nearly half of my program was spent at Bamfield Marine Sciences Centre. Given the remoteness that BMSC, the people you meet there end up feeling like family. Thank you to all my "Bamily" member including Suz Anthony, Kat Anderson, Nicole Webster, Travis Tai, Amanda Khan, Courtney Deck, Kylee Pawluk, Bridget Clarkston, Allen Roberts, Carley Wall, Kim Thornton, Nic Weber, Jessica Leonard, Javier Luque and Kiesha Kerr de Luque. A special thanks to Sam Starko for the good times in Cabin 4-Down and the nightly spirited science tangents we explored.

I was fortunate enough to land a T.A. ship for Directed Studies and through this I was able to teach and learn from a great set of students (Fall Programmers 2014). Your drive to pursue research was wholly refreshing. Thanks Guys!

Table of Contents

List of Tables

Table of Figures

List of symbols, nomenclature and abbreviations

11-DOC	11-Deoxycortisol
A.D.U.	Average Densitometry Units
A/B	Acid/Base
AE	Anion exchanger
α_{O_2}	Solubility coefficient of oxygen
ANOVA	Analysis of variance
Ant	Anterior
AQP	Aquaporin
AR	Androgen receptor
β	Buffering capacity
BGI	Beijing Genomics institute
BMSC	Bamfield Marine Sciences Centre
Branch	Branchial
CA	Carbonic anhydrase
CBE	Chloride bicarbonate exchanger
cDNA	Complementary DNA
CDS	Coding sequence
Cl^-	Chloride ion
CO_2	Carbon dioxide
COG	Clusters of Orthologous Groups
Con	Control
Cp	Capillary

CPM	Counts per minute
CR	Corticoid receptor
cRNA	Capped RNA
Cutan	Cutaneous
D	dermis
DNA	Deoxyribonucleic acid
DOC	11-deoxycorticosterone
E	Epidermis
ECF	Extracellular fluid
$E_{NH_4^+}$	Nernst equilibrium potential for NH_4^+
EPOC	Excess post-exercise Oxygen consumption
ER	Estrogen
ERR	estrogen "like" receptor
Exp	Experimental
G	Gauge
g	gravitational force
GFR	Glomerular filtration rate
GR	Glucocorticoid receptor
h	hour
H^+	Hydrogen ion or Proton
HC	Hypercapnia
HCl	Hydrochloric acid
HCO_3^-	Bicarbonate ion

HEA	High environmental ammonia
HPA	Hypothalamic-pituitary axis
J_{Amm}	Ammonia excretion rate
$J_{H^+}^{Net}$	Net Proton excretion
KEGG	Kyoto Encyclopedia of Gene and Genome
Kg	kilogram
kPa	kilopascals
L	Litre
m	mass of animal
MC	Mucus Cell
mCi	millicurie
min	minute
mmol	millimol
mmol L^{-1}	millimolar
M_{O_2}	Rate of oxygen consumption or Metabolic rate
mPa	millipascals
MR	Mineralocorticoid receptors
MRC	Mitochondrion rich cell
Na^+	Sodium ion
Na^+K^+-ATPase	Sodium Potassium ATPase enzyme
Na_2SO_4	Sodium sulfate
$NaHCO_3$	Sodium bicarbonate
NaOH	Sodium hydroxide

NBC	Sodium bicarbonate co-transporter
NC	Normocapnia
NH_3	Ammonia or Ammonia gas
NH_4^+	Ammonium
NHE	Sodium Hydrogen Exchanger
O_2	Oxygen or Oxygen gas
OH^-	hydroxide ion
ORF	Open reading frame
P	Partial Pressure
PBS	Phosphate buffered saline
PCA	Perchloric acid
PCR	Polymerase Chain Reaction
pH_i	intracellular pH
Post	Posterior
ppt	Parts per thousand
PR	Progesterone receptors
Rhxg	Rhesus glycoprotein type x
RIA	Radioimmunoassay
RNA	ribonucleic acid
s.e.m.	Standard error of the mean
SA	Specific Activity
sAC	soluble adenylyl cyclase
SLC	Solulte carrier

SO_4^{2-}	Sulfate ion
SR	steroid receptor
t	time
T_1	initial time
T_2	final time
T_{Amm}	Total ammonia
TCO_2	Total carbon dioxide content
TMS	Tricaine methanesulfonate
$U\ mL^{-1}$	Units per milliliter
UTR	Untranslated region
V	Volume
VHA	Vacuolar H^+-ATPase
WGD	Whole genome duplication
μCi	Microcurie
$\mu equiv$	microequivalents
μmol	micromol
$\mu mol\ L^{-1}$	micromolar

Chapter 1: General introduction to hagfish respiration, acid/base, ammonia and ionoregulation

Introduction

Hagfish are extant representatives of the most basal craniate and share an ionic profile similar to that seen in marine invertebrates, representing the evolutionary transition between invertebrate and vertebrate organisms. It is these unique physiological traits and evolutionary positions that make hagfish an excellent model to study the evolution of respiration, acid/base (A/B) homeostasis and ionic regulation. Hagfishes diverged from the main vertebrate lineage more than 500 million years ago (Bardack, 1991) with fossil evidence supporting the inference that their morphology has remained unchanged for ~450 million years (Holland and Chen, 2001). Hagfishes are exclusively marine animals with most living at considerable depths world-wide (Fernholm, 1998; Martini, 1998; Wisner and McMillan, 1995), and are the only living vertebrates to passively maintain their plasma Na^+ and Cl^- concentrations at levels almost iso-osmotic to that of seawater (Robertson, 1976). Coupling the unique osmoregulatory characteristics of hagfish along with the fact that fossil evidence comes solely from marine-based sediments, it is inferred that the ancestors of hagfish never entered a fresh water environment. Fossil evidence further suggests that the morphology of extant hagfishes has remained relatively unchanged compared to their ancestral relatives. Thus, is can be inferred that their current physiology may reflect the physiology of vertebrate ancestors prior to invasion of estuaries, fresh waters and land (Hardisty, 1979; Holland and Chen, 2001; Janvier, 2007).

Hagfish are stenohaline osmoconformers who maintain their blood osmolarity slightly hypertonic in comparison to seawater. Capable of withstanding only small deviations in salinity (violent struggling observed in hagfish held in seawater that is < 31

ppt and rapid death at 20-27 ppt; Adam, 1960; Gustafson, 1935; Strahan, 1962) they have no ability to regulate Na^+ and Cl^- concentrations to control levels (Sardella et al., 2009) similar to proto-vertebrate lineages (*e.g. Ciona, Amphioxus*), but distinct from lamprey and all other vertebrates (Robertson, 1954). While hagfish do not regulate Na^+ and Cl^-, they do actively regulate plasma concentrations of the divalent ions, Ca^{2+}, Mg^{2+} and SO_4^{2-} to 30-50% of seawater concentrations (Bellamy and Chester Jones, 1961). Despite the inability to regulate Na^+ and Cl^-, a number of studies have identified genes associated with ion transport and A/B regulation (Choe et al., 1999; Choe et al., 2002; Edwards et al., 2001; Karnaky, 1998; Tresguerres et al., 2006a) . Regulation of A/B is linked to monovalent ion movement through the Na^+/H^+ exchanger (NHE), Na^+/HCO_3^- Exchange and Cl^-/HCO_3^- exchange (CBE) transporter families. Thus hagfish are an excellent model for studying acid/base physiology as the confounding effect of Na^+ and Cl^- regulation can be negated.

A well-known feeding strategy of the hagfish involves burrowing into rotting carcasses of animals that fall to the ocean floor (Martini, 1998), presenting a feeding environment which would have high [ammonia], have a low P_{O_2} (Partial pressure of O_2; hypoxic), and high P_{CO_2} (hypercapnic) due to micro-organisms also feeding on the carcass. Furthermore, hagfish partially burrow into the decaying flesh while feeding, ventilation of the hagfish would be restricted and the branchial (gill) region, typically the dominant site of respiration, acid/base ammonia and ion exchange (Evans et al., 2005), would be fully immersed in this physiologically challenging environment. These perturbations would generally be toxic or deleterious to any other aquatic organism; however, hagfish have somehow adapted to withstand these physiological stresses. Thus

3

is derived the central theme of my thesis, *viz*, to identify and describe the mechanisms by which hagfish survive and thrive in what can only be considered otherwise pernicious conditions to other organisms.

In this general introduction, I will give an overview on key lines of research regarding hagfish physiology leading up to my hypotheses which are set in four overarching topics; namely: 1) Acid/base regulation 2) Nitrogen handling 3) Ionoregulation and 4) Respiration. These topics ultimately compose the major sections of my dissertation, and within each I provide unique and valuable insights into the physiology of the hagfish based on hypothesis-driven research.

Acid/base regulation

A/B regulation is one of the most tightly regulated physiological processes (Heisler, 1986b) and all organisms must maintain this homeostasis as the concentration of H^+ (~pH) affects the kinetics of chemical reactions and the structure and function of proteins (Srivastava et al., 2007; Whitten et al., 2005). Fish, similar to terrestrial vertebrates, use a strategy of buffering and excretion to defend against both intracellular and extracellular pH alterations. The processes of intracellular metabolism generates free H^+ and HCO_3^- from CO_2 which exist in equilibrium as:

$$CO_2 + H_2O \Leftrightarrow H_2CO_3 \Leftrightarrow H^+ + HCO_3^-$$
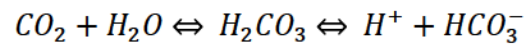
and speciate according to the Henderson-Hasselbach equation (Reviewed by Claiborne et al., 2002). While the intracellular buffering capacity in hagfishes is not well characterized, in higher fishes both inorganic and organic phosphates, proteins and amino acid residues have been shown to limit free H^+. However, to maintain intracellular pH, critical for proper cellular function, cells must additionally actively import and export H^+ and HCO_3^- *via* transport proteins located in the cell membrane (Roos and Boron, 1981). The ability of fishes to compensate for metabolic and environmental disturbances is limited by the aquatic environment in which they reside, therefore most fishes regulate blood pH by secreting and absorbing excess H^+ and HCO_3^- across specialized epithelia including gills and skin (reviewed by Perry, 1997). Other factors that help maintain or affect extracellular fluid (ECF) and blood A/B homeostasis are buffer systems, including CO_2/HCO_3^-, NH_3/NH_4^+, phosphates and proteins (Boron, 2004; Heisler, 1986a).

Hagfish are demersal and either burrow into the sediment (Genus *Myxini*) or reside on top of the ocean bed (Genus *Eptatretus*) (Martini, 1998). These environments are usually quite hypoxic or even anoxic (McInerney and Evans, 1970; Smith and Hessler, 1974), and likely determine the low metabolic rates observed in hagfish (Drazen et al., 2011; Forster, 1990; Munz and Morris, 1965). Hagfish also have a high capacity for anaerobic respiration (Sidell et al., 1984) which can lead to metabolic acidosis.

Hagfish have traditionally been considered to be scavengers; however, recently at least one species has been observed to also actively hunt live prey, dragging their victims back to their burrows (Zintzen et al., 2011). Hagfish consume a wide variety of prey types including polychaetes, squid, shrimp, crab, and teleosts (Shelton, 1978), sometimes robbing food captured by other fauna (Auster and Barber, 2006). Active hunting behaviour is likely associated with burst swimming activity potentially causing acute blood acidosis (Ruben and Bennett, 1980). However, hagfish are able to readily recover from energetic bouts with little disturbance to their blood A/B status (Davison et al., 1990).

Hagfish are best known for their opportunistic scavenging behaviour, as they have been regularly reported to feed on dead and decaying carrion that falls to the ocean floor (Auster and Barber, 2006; Collins et al., 1999; Martini, 1998; Smith, 1985). Sources of carrion may include by-catch from commercial fishing (Collins et al., 1999) or large expired mammals (Smith and Baco, 2003), but the most likely source is leftovers from other predator-prey interactions. Hagfish burrow into the decomposing carcass (Jensen, 1966; Martini, 1998), which presents both opportunities and challenges. As the carcass is

6

being consumed, decomposition of the tissues by bacteria is believed to generate an environment that is rich in nutrients including amino acids and phosphate, which hagfish may absorb across gills and skin (Glover et al., 2011; Schultz et al., 2014). However, the metabolism of bacteria, other animals and hagfish themselves feeding inside the carcass likely also results in depletion of P_{O_2} and elevations in P_{CO_2}, [ammonia], [H$^+$] and weak acids including as butyric acid, putrescine and formic acid, which are known to cause acute acidification of tissues.

Acid/base regulatory organs

The gill is the main blood A/B regulatory organ in adult fish (Evans et al., 2005), and certain areas of the skin fulfill this role in larval fish before gills develop (Wells and Pinder, 1996). Similarly, gills were considered as the main A/B organ in hagfish (Edwards et al., 2001; Evans, 1984); however, my early research has demonstrated that the skin, especially in the posterior body, also plays an important role in blood A/B homeostasis (Clifford et al., 2014). While the renal system in more derived aquatic species (*e.g.* chondrichthyes, osteichthyes) plays a distinctive role in A/B regulation (Claiborne et al., 2002), the hagfish renal output is quite low (0.1-1.0 mL 100 g^{-1} day^{-1}; Hardisty, 1979; Morris, 1965). Furthermore, all fish lack the ability to resorb fluid and are unable to concentrate solutes in their urine (Alt et al., 1981) leading to the assumption that the hagfish renal system is likely unable to significantly contribute to acute A/B regulation. Nonetheless, hagfish kidneys have been shown to resorb Na$^+$ (McInerney, 1974), which may play a significant role in nutrient uptake from the filtrate (discussed below).

Gills

The gill pouches of the hagfish are morphologically different compared to gills from lampreys, chondrichthyan and osteichthyan fishes (Figure 1). Gill pouches are found along the length of the anterior half of the body, and range from 6 to 13 pairs in number displaying both intra- and inter-species variability (Rauther, 1937; Weinrauch et al., 2015) . All gill pouches are morphologically similar, and consist of a muscular wall lined up with an epithelium known as the 'primary filament', from which multiple 'lamella' radiate towards the pouch lumen (Mallatt and Paulsen, 1986). Whether or not all gill pouches are also functionally identical has not yet been discerned.

Ultrastructural studies on hagfish gills have revealed the presence of pavement, basal and intermediate cells and ionocytes (Bartels, 1984; Bartels, 1985; Elger and Hentschel, 1983; Mallatt and Paulsen, 1986; Weinrauch et al., 2015). Ionocytes, which are cells characterized by possessing large number of mitochondria, typically support transepithelial ATPase-driven ion transporting processes. The ionocytes in hagfish gills have been shown to express ion transporter mRNAs and proteins associated with the excretion and absorption of H^+ and HCO_3^- for A/B regulation (Choe et al., 1999; Edwards et al., 2001; Evans, 1984; Mallatt et al., 1987; Parks et al., 2007b; Tresguerres et al., 2007a), and they have also been demonstrated to take up inorganic phosphate (Schultz et al., 2014) and amino acids (Glover et al., 2011).

Cellular mechanisms for gill acid/base regulation

In all organisms, transepithelial A/B regulation is achieved by the combined action of various ion-transporting proteins differentially expressed in the basolateral or

apical membranes, or in the cytoplasm; the overall result is excretion of excess H^+ and absorption of HCO_3^- to correct blood acidosis, and excretion of excess HCO_3^- and absorption of H^+ to correct blood alkalosis. In marine organisms, the most typical ion-transporters/proteins involved in A/B regulation are Na^+-K^+-ATPase (NKA, located in the basolateral membrane), carbonic anhydrase (CA, cytoplasmic and membrane-bound), Na^+/H^+ exchangers (NHE; HUGO gene family SLC9), Na^+/HCO_3^- co-transporters (NBC; HUGO gene family SLC4) and Cl^-/HCO_3^- exchangers (CBE; HUGO gene family SLC26) (with the latter three located in either apical or basolateral membrane, depending on the specific isoform and cell type). Another A/B relevant protein is the V-type H^+-ATPase (VHA), which is intracellularly localized and its specific role varies depending on the species, cell type and A/B condition (for review, see Evans et al. 2005).

In a generalized model, CO_2 enters the ionocytes from blood plasma (through a mechanism that may depend on plasma membrane-bound CA; Esbaugh et al., 2009) and is also produced in mitochondria. Once in the ionocyte, the hydration of CO_2 is catalyzed by cytoplasmic CA into H^+ and HCO_3^-, which are subsequently differentially excreted to seawater or absorbed into the blood, depending on the A/B regulatory needs. To compensate for blood acidosis, H^+ are excreted to the surrounding seawater in exchange for Na^+ through apical NHEs; this transport is secondarily energized by basolateral NKA (Evans et al., 2005). The proteins responsible for HCO_3^- absorption are not as well characterized, although suitable candidates are basolateral CBEs and Na^+/HCO_3^- co-transporters (NBCs) (Parks et al., 2007a). To compensate for blood alkalosis, HCO_3^- is excreted in exchange for Cl^- through apical CBEs. However, the rest of the mechanism is much less understood and may vary considerably from species to species. The driving

force may be provided by NKA, for example by creating a cell membrane potential that favours a low intracellular [Cl^-], or by linkage of apical Cl^-/HCO_3^- exchange with Na^+ uptake (*e.g.* Na^+-dependent CBE) (Parks et al., 2009). In this case, H^+ transport from the ionocyte into the blood most likely takes place by basolateral NHEs, as described in the intestine of marine fish (Grosell and Genz, 2006) and crab gills (Tresguerres et al., 2008).

Another option for acid/base compensation involves basolateral VHA as described in shark gill ionocytes; in this mechanism VHA 'pumps' H^+ into the blood, driving apical Cl^-/HCO_3^- exchange by removing H^+ from the cytosol (which prevents CA inhibition and reversal by law of mass action), and by promoting Cl^- absorption into the blood across channels in the basolateral membrane (due to the membrane potential generated by H^+ transport; Tresguerres et al., 2006b). Regardless of the specific mechanisms, lampreys, elasmobranchs and bony fish have developed gill ionocyte subtypes specialized for acid or base secretion (reviewed in Evans et al. 2005). Hagfish follow the general model of Na^+/H^+ and Cl^-/HCO_3^- exchange across the gill epithelium (Evans 1984: Figure 2a). However, histochemical and immunohistochemical evidence suggests that hagfish gills have a single type of ionocyte that alternatively performs H^+ or HCO_3^- secretion depending on the blood A/B condition (Tresguerres et al., 2006a). The vast majority of experiments on hagfish A/B regulation have been conducted on either Atlantic hagfish (*Myxini glutinosa*), or Pacific hagfish (*Eptatretus stoutii*) with little information on the other species (*e.g. E. burgeri*). Based on the published results, this chapter assumes that the cellular mechanisms for A/B regulation are similar for all hagfish species; for details about the experimental species used in each study the reader is directed to the cited literature.

Hagfish decrease net H^+ or HCO_3^- secretion when placed in Na^+- or Cl^--free seawater, respectively (Evans, 1984). Given that hagfishes represent the only chordate group assumed to have never entered freshwaters (Hardisty, 1979; Janvier, 2007), the presence of these transport mechanisms led to the hypothesis that these mechanisms evolved for pH balance prior to their use in ionoregulation, and that these mechanisms were co-opted for Na^+ and Cl^- absorption for ionoregulation by the chordates that originally invaded estuarine and freshwater environments (Evans, 1984).

The first suggestion that hagfish gill ionocytes are involved in blood A/B regulation was biochemical evidence of NKA and CA activities in hagfish gill pouches histological sections (Mallatt et al. 1987). Two subsequent studies used immunohistochemistry to localize NKA and NHEs in hagfish gill epithelium (Choe et al., 1999; Choe et al., 2002), and a third study suggested co-localization of NKA, V-H^+-ATPase, and an NHE2-like in a single gill cell type (Tresguerres et al., 2006a). The anti-NKA and anti-VHA antibodies used in those studies were raised against amino acid regions that are highly conserved in all animals and therefore it is likely they are able to specifically recognize hagfish NKA and VHA proteins. However, the anti-NHEs antibodies used were against mammalian NHE isoforms that are not as well conserved in other animals, so these results should be interpreted with caution. Another potential limitation of Tresguerres et al. (2006a) was that co-localization of NKA, VHA and NHE2 was inferred from consecutive histological gill sections, which do not always contain the same cells (in fact, co-localization was not evident in all sections examined). However, more recent dual immunolocalization of NKA and VHA on the same gill section confirm that these two proteins are indeed present in the same cells (Figure 1.3).

Responses to metabolic acidosis

Hagfish have an outstanding capacity for recovering from metabolic acidosis; this has been determined from experiments that induced blood acidosis by injections of H_2SO_4 (3 mequiv H^+ kg^{-1}; Edwards et al., 2001; McDonald et al., 1991) or HCl (6 mequiv H^+ kg^{-1}; Parks et al. 2007b) into the posterior caudal blood sinus. Blood pH suffered initial sharp reductions between ~0.6 (McDonald et al., 1991) and up to ~1.6 pH units (Parks et al., 2007b). However, blood pH was fully (McDonald et al., 1991) or near fully (Parks et al., 2007b) rectified within 6 h demonstrating a significant capacity for rapid A/B regulation. In the latter study, subsequent injections caused significantly smaller reductions in blood pH compared to the initial injection, indicating increased capacity for acid secretion upon sustained acidosis. Metabolic acidosis resulted in up-regulation in gill NHE2-like mRNA (Edwards et al., 2001) and protein abundance (Parks et al., 2007b) and involved protein insertion in the apical membrane of gill ionocytes (Parks et al. 2007b) (Figure 2a). In addition, the protein abundance of NKA and VHA remained unchanged (Parks et al. 2007b). These results indicate that apical NHEs are involved in acid secretion, and suggest that the basal levels of NKA are sufficient to sustain upregulated acid secretion. However, other NKA-activating mechanisms (NKA isoforms, phosphorylation) cannot be ruled out.

Responses to metabolic alkalosis

Little research has been conducted evaluating hagfish responses to metabolic alkalosis. It is also less clear which conditions would result in blood alkalosis in the wild. One possibility is following feeding in a hypercapnic environment (*e.g.* after feeding on a

decaying carcass), when there may be excess HCO_3^- that had accumulated to compensate acidosis as described in other fishes (Brauner and Baker, 2009). Hagfish have recently been demonstrated to rapidly (24 – 48 h) accumulate large plasma [HCO_3^-] (up to ~70 mmol HCO_3^- L^{-1}) during exposure to compensation from the respiratory acidosis experienced from elevated P_{CO_2} tensions (Baker et al., 2015) (discussed below). Another potential source of blood alkalosis is a post-prandial alkaline tide as observed in elasmobranchs (Tresguerres et al., 2007b; Wood et al., 2005a), and both freshwater (Bucking and Wood, 2008) and seawater-acclimated trout (*Oncorhynchus mykiss*) (Bucking et al., 2009). However, post-prandial digestive strategies of hagfishes remain to be identified.

Nonetheless, it is clear that hagfish possess efficient mechanisms to rectify blood metabolic alkalosis (Tresguerres et al., 2007a). Injection of base ($NaHCO_3$; 6 mequiv HCO_3^- kg^{-1}) caused sharp increases in blood pH and HCO_3^-, and both were rectified within 6 h. Similar to the acid injections described above, the impact of subsequent base injections on blood pH was diminished, indicating capacity for up-regulation of base secretory mechanisms. After four $NaHCO_3$ injections at 6 h intervals (24 h), there was an increase in VHA protein abundance both in gill homogenates and in enriched gill cell membrane fractions, estimated from Western blots. Since accumulation of VHA in the apical membrane was not evident in immunostained gill sections, these results suggest a translocation of VHA to the basolateral membrane to counteract blood alkalosis as described in dogfish sharks (Tresguerres et al., 2005). However, the tubulovesicular system in hagfish gill ionocytes complicates differentiating between cytoplasm and basolateral membrane localization using immunohistochemistry techniques, unlike shark

ionocytes that lack a tubulovesicular system (*e.g.* see Tresguerres et al. 2005). While there were no significant changes in NKA abundance in gill homogenates, a reduction of NKA abundance was detected in enriched gill cell membrane fractions, also by Western blot analysis. Since hagfish gills posses only one ionocyte subtype that is rich in both NKA and VHA, it was postulated that the differential activation of acid and base secretion occurs *via* differential insertion of NKA and VHA into the basolateral membrane, and of NHE and of a yet unidentified CBE into the apical membrane (Parks et al., 2007b; Tresguerres et al., 2006a; Tresguerres et al., 2007a). In addition, my initial research has suggested that, at least at shorter time points (4 h), extrabranchial, rather than branchial mechanisms are primarily relied upon for recovering from blood alkalosis (Clifford et al., 2014; see *Extrabranchial* section below).

In all other chordates studied, there exist two or more ionocyte subtypes (Doyle and Gorecki, 1961; Lin et al., 2006) with distinct utility for regulating acid/base status (Goss et al., 2011; Reid et al., 2003). In the case of lampreys and elasmobranchs, acid and base secretion is likely split between two subtypes; NKA-containing and V-H$^+$-ATPase-containing (Choe et al., 2004; Piermarini and Evans, 2001; Piermarini et al., 2002; Tresguerres et al., 2005; Tresguerres et al., 2006a). The same is true for teleost fish, where at least 2 or more different subtypes have been identified with at least one subtype capable of acid secretion and another for base secretion (for review see Hwang and Lee, 2007; Hwang et al., 2011). The presence of a single ionocyte type in hagfish suggests it is an ancestral character trait and that more derived groups evolved multiple ionocyte subtypes in relation to novel environmental and metabolic challenges (Tresguerres et al., 2006a).

Responses to hypercapnia

Given the feeding lifestyle of the hagfish, one physiological challenge that may be frequently encountered during feeding bouts involving decaying carcasses is hypercapnia. Considerable amounts of CO_2 are generated during land-based decomposition, due in part by microorganisms consuming decaying flesh (Carter et al., 2007; Putman, 1978). Similar CO_2 generation and build-up (hypercapnia or high P_{CO_2} tension) can be inferred during aquatic decomposition. Hypercapnia presents organisms with an interesting set of physiological A/B challenges. CO_2 diffuses across epithelia (gills/skin) and rapidly causes a respiratory acidosis (as opposed to a metabolic acidosis – see above) resulting in reduction in intracellular and extracellular pH (pH_i and pH_e, respectively). Generally animals, including hagfish (Baker et al., 2015), will compensate for these reductions in pH elevating plasma $[HCO_3^-]$ in an equimolar exchange with plasma $[Cl^-]$. Thus, hypercapnia results in an initial acidosis, which the animal attempts to correct for, followed by an alkaline load at the conclusion of exposure, which also must be excreted. Full compensation (full correction of pH) appears to be limited by the capacity for the organism to elevate HCO_3^- beyond $27 - 33$ mmol L^{-1} during acute hypercapnia exposure – previously thought to be the "apparent $[HCO_3^-]$ threshold" (Heisler, 1986b) for HCO_3^- compensation. Recently however, Baker et al. (2015) reported on the extraordinary tolerance of the hagfish to hypercapnia. In their study, hagfish exposed to up to 5% CO_2 were able to withstand exposure to periods of at least 96 h. More interesting however, was the reported HCO_3^- compensation exhibited by the hagfish, reaching plasma $[HCO_3^-]$ concentrations of up to ~70 mmol L^{-1}, exchanged equimolarly with plasma $[Cl^-]$. Baker et al. (2015) further hypothesize that this degree of compensation is possible in hagfish due

in part by their osmoconforming strategy, thereby providing a greater amount of Cl^- ions to exchange for HCO_3^- (Baker et al., 2015). Whether or not hagfish are capable of recovering from these impressive plasma $[HCO_3^-]$ loads, and how recovery is mediated warrants further investigation.

Nitrogen balance and handling

Build-up of total ammonia (T_{Amm}; $NH_4^+ + NH_3$) within organisms is toxic, causing a variety of impairments including disruption of biochemical pathways, interference of ionic movement across transmembrane surfaces *via* ion substitution of other monovalent ions including Na^+ and K^+, and also disruption of extracellular and intracellular pH *via* the strongly basic NH_3 (Walsh, 1997). The high protein diet of hagfishes (Auster and Barber, 2006; Collins et al., 1999; Martini, 1998; Smith, 1985) results in uptake of a large amount of amino acids. Catabolism of these ingested amino acids not only supplies the carbon backbone, necessary for conversion into fatty acids, and carbohydrates (Nelson et al., 2008), but also contributes to the net nitrogen load of the fish, which must be excreted (for excellent reviews see Evans et al., 2005; Wood, 2001). Other sources of nitrogen include the deamination of proteins during fasting periods or, perhaps more relevant to the scavenging behaviour of the hagfishes, from a decaying food source. No data exists on the physicochemical characteristics inside or surrounding decaying carrion in aquatic environments; however, in Chapter 5, I suggest that this environment would be similar to decomposition in terrestrial environments where putrefactive gases (hydrogen sulfide and ammonia) generated by anaerobic microflora lead to high deposits (~30 mmol L^{-1}) of nitrogenous compounds in the surrounding soil (Carter et al., 2007). These deposits in an aquatic environment would present high inwardly directed ammonia gradients to an encapsulated animal during a prandial event (Chapter 5; Clifford et al., 2015a).

Nitrogen handling organs

Gills

The gills are a primary site of NH_3 excretion for many aquatic vertebrates (Wood and Evans, 1993; Wright, 1995) and most aquatic invertebrates (Henry et al., 2012). Additionally, various strategies exist to combat high ammonia including ureotelosis as in the lake Magadi tilapia (*Oreochromis alcalicus grahami*; Randall and Wright, 1989) and Gulf toadfish (*Opsanus beta*; Walsh et al., 1990), glutamine production in the swamp eel (*Monopterus albus*; Ip et al., 2010), and active NH_4^+ excretion used by the mudskipper (*Periophthalmodon schlosseri*) while burrowed (Randall et al., 1999; Wilson et al., 2000). Recently, hagfish have been shown to have low basal rates of NH_3/NH_4^+ and urea excretion, with both the gills and the skin being hypothesized as sites of passive excretion (Braun and Perry, 2010).

Cellular mechanisms for nitrogen excretion

Despite reported low basal rates of nitrogenous waste excretion, hagfish have the remarkable ability to excrete excess nitrogen. Excess nitrogen uptake can be induced by either exposure to high environmental ammonia (HEA; Clifford et al. 2015a) or *via* direct infusion of NH_4Cl (Edwards et al., 2015; McDonald et al., 1991) or urea (Braun and Perry, 2010). Transcellular transport of ammonia and urea may be respectively facilitated by Rh glycoproteins (Hugo gene family SLC42) (Marini and Urrestarazu, 1997) and urea transporters (UT; Hugo gene family SLC14) proteins (Levine et al., 1973a; Levine et al., 1973b; You et al., 1993). The Rh glycoproteins are homologues of the Amt superfamily and have multiple isoforms (Huang and Peng, 2005); however, the isoforms of interest to

fish physiology and ammonia excretion are Rhag, Rhbg and Rhcg (Hung et al., 2007; Nakada et al., 2007; Nawata et al., 2007; Tsui et al., 2009). In gills from the marine teleost *Takifugu rubripes*, Rhag localizes to the apical and basolateral membranes of the pillar cells and mediates ammonia transport from red blood cells through pillar cells (Nakada et al., 2007). Rhbg localizes to the basolateral membrane of pavement cells while Rhcg2 localizes to the apical membrane. Finally Rhcg-b localizes on ionocytes on apical, gill/water interface. However, teleost fishes are highly derived compared to the hagfishes so the roles and localizations of any hagfish specific Rh glycoproteins may differ.

To date two Rh glycoprotein isoforms from hagfish have been cloned; Rhbg and Rhcg and are expressed in hagfish gill and skin (Edwards et al., 2015) with the presence of Rhag so far remaining elusive. Hagfish specific Rhcg protein and mRNA expression has been demonstrated in both gill and skin tissues. In gill, Rhcg is localized to the basal aspect of the filament epithelium along the region of the filament closest to the blood margin and in the skin *h*Rhcg (hagfish specific Rhcg) immunoreactive cells were localized to regions surrounding mucous glands (Edwards et al., 2015). In addition, by using heterologous antibodies and immunohistochemistry, Braun and Perry (2010) found Rhbg localized to the lining of larger blood vessels (i.e. non-capillary vessels), while Rhcg1 co-localized apically to NKA enriched gill cells. Localization of Rhbg to the blood vessels points to a different role for this isoform in hagfish, likely mediating transcellular transport of ammonia from tissues to the blood (Braun and Perry, 2010).

Responses to nitrogen challenges

Basal ammonia excretion rates for hagfish are about 40-60 µmol kg^{-1} hr^{-1} (Braun and Perry, 2010; Clifford et al., 2014; Clifford et al., 2015a), half that of most ammonotelic fishes (100-350 µmol kg^{-1} hr^{-1}; Evans et al., 2005; Wood, 2001) and on par with larval and parasitic sea lamprey (*Peteromyzon marinus*; 20-50 µmol kg^{-1} hr^{-1}; Wilkie et al., 2004; Wilkie et al., 1999) and the ureotelic elasmobranchs (~50 µmol kg^{-1} hr^{-1}; reviewed by Wood 2001). A few studies have described the ability of the hagfish to survive high inwardly directed ammonia gradients with survival reported following 9 h exposure to 100 mmol L^{-1} NH_4Cl in seawater (Braun and Perry, 2010) and 48 – 72 h exposure to 20 mmol L^{-1} NH_4Cl (Clifford et al., 2015a). These studies have also highlighted the capacity of hagfish to tolerate extremely high plasma ammonia loads with the highest reported plasma ammonia load peaking at 5450 µmol L^{-1} following 24 h exposure to 20 mmol L^{-1} HEA (Clifford et al., 2015a). Remarkably, during continued exposure to HEA, hagfish are able to excrete ammonia/ammonium against massively inwardly directed gradients thus stabilizing rates of uptake (Clifford et al., 2015a). During recovery from HEA exposure hagfish are capable of excreting ammonia/ammonium at high rates (~3000 µmol kg^{-1} hr^{-1}; Clifford et al. 2015a). The high rate of ammonia excretion is composed of both branchial and extrabranchial transport with the branchial contribution comprising approximately 70-80% and excretion through the skin comprising the remainder (Clifford et al. 2014; 2015a; see *Extrabranchial* section).

A recent study where hagfish were injected with 3 mmol kg^{-1} NH_4Cl demonstrated that elevated plasma ammonia concentrations paralleled elevated ammonia

excretion rates and coincided with initial significant up-regulation of Rhcg mRNA expression in the gill & the skin. These results suggest that the transcriptional regulation of Rh glycoproteins may respond to elevated plasma ammonia. The study also used hagfish-specific antibodies to demonstrate the subsequent significant up-regulation of hagfish Rhcg protein, suggesting that Rh glycoproteins are involved in the regulation of ammonia excretion in hagfish (Edwards et al., 2015).

Basal excretion of urea in hagfish has been reported to be $\sim$30 μmol kg^{-1} hr^{-1} (Braun and Perry, 2010), again on par with excretion rates observed in parasitic lamprey (Wilkie et al., 2004). In *E. stoutii*, urea excretion did not change during exposure to high environmental ammonia (10 – 100 mmol L^{-1}) nor during recovery in nominally-ammonia free seawater (Braun and Perry, 2010; Clifford et al., 2015a). However, following infusion of NH_4Cl that raised plasma ammonia to 10 mmol L^{-1}, three-fold increases in urea excretion were observed following a 6 h period. Direct infusion of urea (to raise plasma urea to $\sim$100 mmol L^{-1}) caused an immediate (0-3 h) 1000-fold surge in urea excretion which tapered to $\sim$250-fold compared to control animals (Braun and Perry, 2010).

Ionoregulation

Similar to A/B balance, the maintenance of stable plasma ionic composition is crucial for normal physiological function. Ionic regulation is traditionally associated with Na^+ and Cl^- transport because these are the two major constituents of internal fluids and therefore are the major contributors to total osmolarity. However, plasma ions including K^+, Ca^{2+}, Mg^{2+} and SO_4^{2-} are also maintained at significantly lower concentrations compared to the environment; these are especially relevant for hagfish plasma since they are the only ions whose concentrations are significantly lower than seawater (Bellamy and Chester Jones, 1961; Currie and Edwards, 2010). Ions that contribute to A/B balance (*e.g.* H^+, HCO_3^-, NH_4^+) are discussed in previous sections.

Ionic gradients between internal fluids and the marine environment originated in the first unicellular organisms; these gradients were essential for processes such as energy generation, uptake of molecules from the environment, and counteraction of negatively-charged proteins (Yancey, 2005). Ionic gradients are associated with water flux which can disrupt cells by swelling and shrinking; thus, cells also accumulate other solutes including proteins, amino acids and other osmolytes to account for the osmotic gap with the environment.

The osmolarity of hagfish plasma is essentially the same as in seawater (Smith, 1932) and therefore hagfish do not experience major water fluxes with the environment; except perhaps when entering a carcass. Later works demonstrated hagfish plasma is also similar to seawater in ionic composition (Bellamy and Chester Jones, 1961; Robertson, 1976), with the exception of Ca^{2+}, Mg^{2+} and SO_4^{2-} (Bellamy and Chester Jones, 1961). Due to the similarity of osmotic strategies, hagfish have been considered to have more in

common with invertebrates than the vertebrates (Currie and Edwards, 2010). Indeed, Na^+ and Cl^- are the major osmolytes in hagfish plasma, and they lack the capacity to regulate plasma osmolality and $[Na^+]$ and $[Cl^-]$ (Sardella et al., 2009), similar to most marine invertebrates. The strict osmoconforming strategy likely reflects an exclusive evolutionary history of hagfish in seawater, and it can also explain why there are no fossil records of hagfish in sediments other than of marine origin, and why there are not extant estuarine or freshwater hagfishes (Janvier, 2007).

While plasma $[Na^+]$ and $[Cl^-]$ are similar to seawater, plasma $[Ca^{2+}]$, $[Mg^{2+}]$ and $[SO_4^{2-}]$ are regulated to levels 1/2 to 1/3 that of seawater (Bellamy and Chester Jones, 1961; Robertson, 1976; Robertson, 1954). For example, unlike $[Na^+]$ and $[Cl^-]$ (Sardella et al. 2009), hagfish can actively regulate SO_4^{2-} levels in the absence of any changes in glomerular filtration rate (Chapter 8; Clifford et al. submitted). Similarly, information about mechanisms for active regulation of plasma $[Ca^{2+}]$ and $[Mg^{2+}]$ is still lacking. Given the phylogenetic position of the hagfish and its ability to regulate these divalent ions but not Na^+ and Cl^-, it seems that ionoregulation of divalent ions evolved prior to regulation of monovalent ions. However, validation of this hypothesis requires further study examining the ionoregulatory capacities of organisms from major clades that diverged prior to and following the divergence of the agnathans.

Respiration

Given the demersal habitat of hagfishes, with some species known to burrow into mud (Genus *Myxine*) (Martini, 1998), and the scavenging nature of their feeding regimes (Lesser et al., 1996; Martini, 1998), hagfishes are likely to frequently encounter hypoxic or even anoxic conditions. Depending on location, water exchange at depth is low, leading to limited available oxygen. While feeding the ability for the hagfish to draw water through their nostril into the pharynx may be impaired thus impairing ventilation (Burggren et al., 1985; Steffensen et al., 1984; Welsch and Potter, 1998). Furthermore, organisms other than hagfish also consume the carrion, further depleting the already scarce oxygen. As a result, this shared feeding environment is likely severely hypoxic or even anoxic. Despite these environmental challenges, hagfish readily survive and thrive in these conditions that would be deleterious to most other aquatic organisms. Survival by the hagfish in these extreme oxygen-limited conditions results from employing several physiological strategies and/or adaptations. In particular, as a strict osmoconformer (Smith, 1932), hagfish do not need to expend energy to actively regulate plasma ions and this can help to maintain low metabolic rates (Forster, 1990; Munz and Morris, 1965). Indeed, hagfish have been shown to have the lowest measured metabolic rate among fishes (Brauner and Berenbrink, 2007). Further adaptations relating to hypoxia/anoxia tolerance include the ability of rapid metabolic rate (M_{O_2}) suppression (Cox et al., 2011; Drazen et al., 2011), altered kinetics of key glycolytic enzymes (Baldwin and Davison, 1989; Sidell and Beland, 1980) and monomeric hemoglobin with a high affinity for O_2 at low P_{O_2} tensions (Manwell, 1963). Finally, despite the low reported contribution to whole-animal oxygen uptake by the gills (see below), Malte and Lomholt (1998) reported

that oxygen extraction efficiency of the gills of hagfish may be as high as 75 – 80%.

Thus, the hagfish is well adapted to handle very low oxygen challenges.

Extrabranchial contributions to respiration, acid/base, ammonia and ionoregulation

The structure and functioning of the gill epithelia (gill pouches) of hagfish is considerably different when compared to that of teleosts and chondrichthyan fishes. In more derived teleost and chondrichthyan fishes, the gills represent the dominant site for ion, A/B, and ammonia regulation and respiration. Several reports however, suggest that cutaneous mechanisms are prominent in hagfish physiology with regard to respiration and ionoregulation. Furthermore, my preliminary studies also suggest that the skin of hagfish is important in excretion of HCO_3^- and ammonia.

Two previous reports examining oxygen exchange in hagfish provide evidence suggesting that cutaneous oxygen uptake acts as the predominant route of oxygen acquisition. Studies comparing ventilation and oxygen uptake in burrowed and unburrowed hagfish have suggested that ventilation in hagfish can only account for ~20% of whole animal O_2 extraction (Steffensen et al., 1984). Furthermore, given the prominent capillary networks in the subepidermis (Hans and Tabencka, 1938; Lametschwandtner et al., 1989), Steffensen et al. (1984) further suggested that hagfish are well suited for cutaneous respiration. Lending support to this hypothesis was the finding that when gill apertures of hagfish were sutured shut, hagfish retained 89% of M_{O_2} (Lesser et al., 1996). Cutaneous O_2 uptake would be beneficial as while feeding, the anterior end of the hagfish remains burrowed, thus impairing ventilation *via* water current through the nostrils into the pharynx, while the trunk of the animal remains exposed to oxygenated water (Burggren et al., 1985; Steffensen et al., 1984; Welsch and Potter, 1998). On the contrary, Malte & Lomholt (1998) have argued against the capability of cutaneous O_2 uptake in the hagfish, citing the impracticality for O_2 exchange across the 70-100 µm epidermal layer

(Welsch and Potter, 1998), the perfusion of capillaries with arterial blood with a high P_{O_2}, and the impact of a boundary layer surrounding the skin on diffusion (Malte and Lomholt, 1998). An important consideration with regard to the studies of Steffensen et al. (1984) and Lesser et al. (1996) is that measurements of cutaneous oxygen exchange were made, or inferred, indirectly. Thus, an in-depth study into the true cutaneous oxygen uptake abilities of the hagfish is warranted.

Recent developments in hagfish physiology have begun to highlight the extrabranchial aspects of A/B and ionoregulatory status, specifically, the novel findings of the skin performing nutrient acquisition. Glover et al. (2011) proposed that the feeding environment (i.e. putrefied carrion) of the hagfish would be high in amino acid content and that hagfish may have adapted to take up nutrients across multiple epithelia. It was hypothesized that while burrowing into a carcass to feed, hagfish could optimize nutritional uptake *via* amino acid transport through use of both the skin and gill in addition to the intestine. The findings from this study did indeed show *in vitro* uptake of L-alanine and L-glycine through the intestine, as expected. However, more importantly for this thesis, uptake was also present in the gills and the skin (Glover and Bucking, 2015; Glover et al., 2011; Glover et al., 2013) thus highlighting the novel adaptations that hagfish have acquired to maximize nutrient uptake while burrowing into decaying food sources. Further work by members of my laboratory has demonstrated that in addition to intestine, the skin and gills of hagfish also facilitate uptake of inorganic phosphate, a limiting nutrient at the demersal habitat of the hagfish (Schultz et al., 2014).

In addition to being nutrient rich, the environment in and around the putrefying carrion is also likely high in P_{CO_2}, [ammonia] and likely has an acidic pH (see above:

Hagfish habitat and behaviour). I hypothesized that hagfish may have also developed similar extrabranchial adaptations in ionoregulatory capacity to cope with these environmental stressors when hagfish burrow into carrion (Evans, 1984; Jensen, 1966; Martini, 1998). Observationally, it is known that while feeding, the posterior portion of the animal often remains outside the carrion (Strahan, 1963). Thus, it is likely that the caudal region is immersed in seawater that has far lower concentrations of putrefactive gases and would present more favourable gradients to offload toxicants including excess NH_4^+, NH_3, H^+, HCO_3^-, CO_2). In this thesis, I investigate the potential role of extrabranchial tissues (specifically skin, intestine and kidney) in ionoregulation, A/B regulation nitrogen handling and respiration as unique adaptations to the hagfish feeding behaviour/strategy.

Perspectives and objectives

Hagfish have been a model organism for physiologists and morphologists since Homer Smith's seminal 1932 review on the evolution of water regulation (Smith, 1932). Since this time, many interesting physiological traits have been described for this phylogenetically ancient organism including hypoxia and anoxia tolerance (Cox et al., 2011; Forster et al., 1992; Perry and Gilmour, 2006; Perry et al., 2009), tolerance to extreme environmental hypercapnia (Baker et al., 2015) and ammonia (Braun and Perry, 2010) and an extraordinary ability to regulate blood acid/base status (McDonald et al., 1991; Parks et al., 2007b; Tresguerres et al., 2007a). Indeed, for some scientists, the hagfish is considered the basal state of vertebrate physiology; based primarily on the fact that at least the morphology of the organism is similar to the fossil record, gone unchanged since it's suspected divergence (Holland and Chen, 2001). Alternatively, the numerous distinct physiological traits of hagfish may be entirely derived given the unique environment it inhabits and the long evolutionary time frame (~500 million years) since divergence from the rest of the vertebrate lineage (Bardack, 1991). A discussion on the debates and arguments surrounding the basal phylogenetic relationships of the hagfish to the early vertebrate evolution is beyond the scope of my thesis. However, my thesis is based upon the presumption that valuable insights can come from an in-depth understanding of the unique physiology of the hagfish. These insights, which I aim to provide through this dissertation, can certainly be used from a comparative/evolutionary physiological standpoint and provide useful information towards an understanding of early vertebrate evolution. My overall goal is to highlight the mechanisms and

adaptations in hagfish that allow this animal to survive and thrive in a physiologically challenging environment.

My PhD research was initiated as an investigation into the strategies for acid/base regulation and the unusual tolerance of the hagfish to withstand extreme acid/base regulatory challenges. From these initial studies, and with the aid of numerous collaborators, my thesis grew into the story presented herein. Specifically the main goals of my thesis were to:

1) Investigate the branchial and extrabranchial mechanisms hagfish employ to recover from systemic acid and base disturbances.

2) Define the mechanisms by which hagfish are able to recover from hypercapnia-induced hypercarbia.

3) Investigate the physiological basis by which hagfish are able to tolerate and recover from high ammonia environments.

4) Identify whether Pacific hagfish (*Eptatretus stoutii*) possess and employ glucocorticoid and mineralocorticoid responses.

5) Investigate the metabolic physiology of the hagfish following exhaustive exercise and examine the role of the skin in oxygen transport.
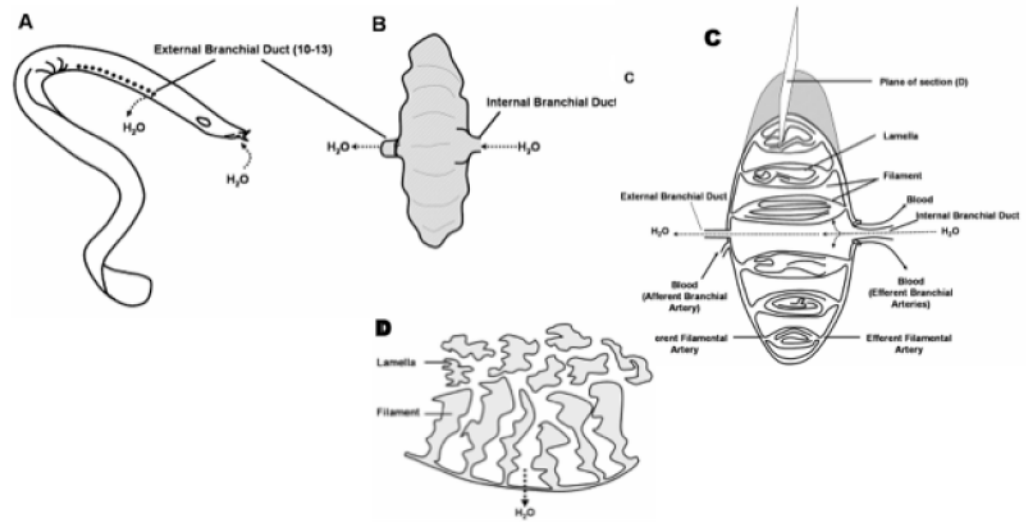
Figure 1.1 Schematic of the hagfish gill pouch gross anatomy and fine structure.

(A) Water enters the hagfish through the nasopharyngeal duct, and it leaves across the 10 to 13 pairs of gill pouches located at each side of the body. (B) External morphology of a gill pouch. (C) Cross section of a gill pouch (modified from Mallat and Paulsen, 1986). Water and blood flow in counter-current fashion. The surface area of filaments and lamella is enlarged by radial infoldings, as opposed to the typical structures found in lampreys, elasmobranchs and teleosts. The plane of section used in the immunohistochemistry study is illustrated on top of the pouch, which is also shown in more detail in D. (D) Section across the gill pouch in the orientation indicated in C. The gill filaments and lamella are shown in the same view as the immunohistochemistry sections of Figure 1.3. Notice how the radial infolding of the lamella results in an apparent separation from the filaments in this plane of section. (Adapted from Tresguerres et al. (2006a) *Comp Biochem Physiol A* 145:312-321)
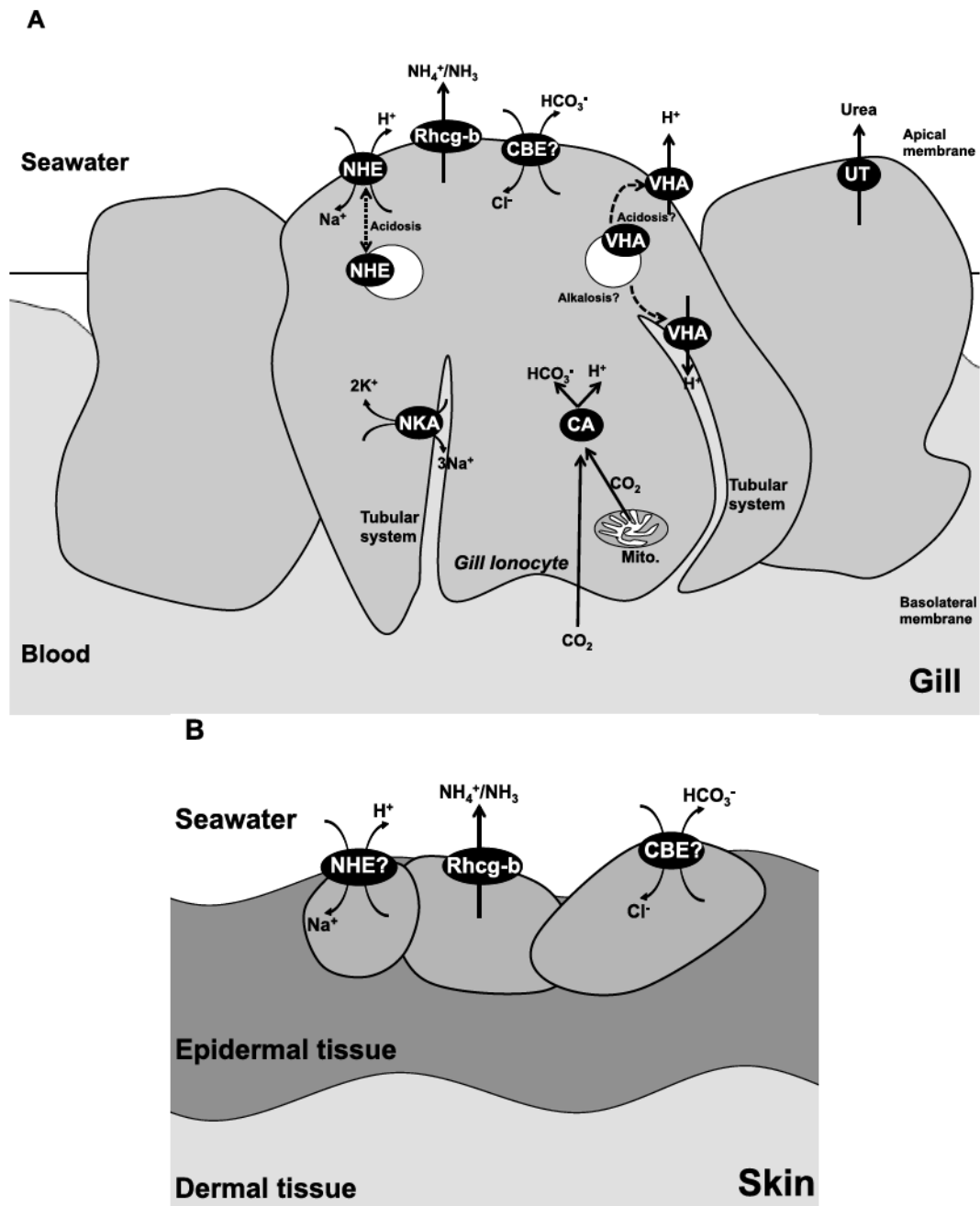
Figure 1.2 Molecular components of hagfish acid/base and ionoregulation.

Molecular components of hagfish acid/base and ionoregulation in (A) gill and (B) skin. NKA=Na^+/K^+- ATPase, VHA = V-H^+-ATPase, NHE = Na^+/H^+ exchanger, Rhcg-b = Rh glycoprotein c1, UT = Urea Transporter, CBE = Chloride Bicarbonate Exchanger, CA = Carbonic Anhydrase.

VHA **NKA**
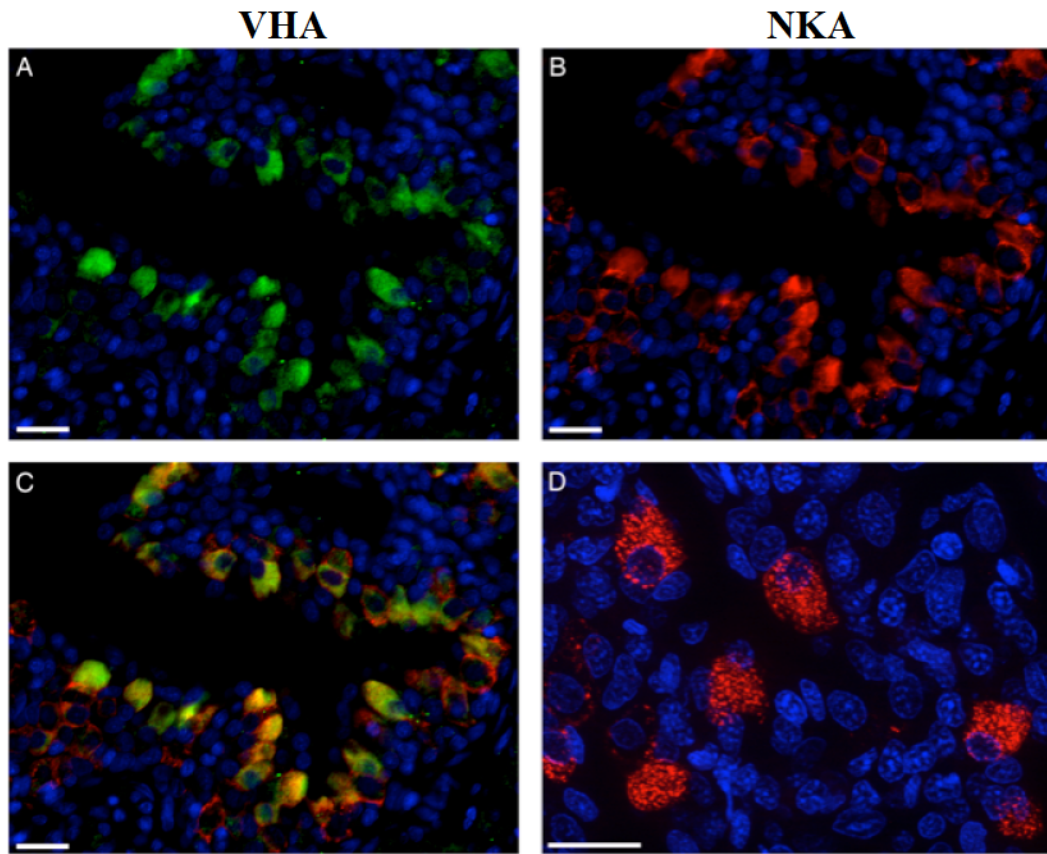
Figure 1.3 VHA- and NKA-rich cells in hagfish gills.

Dual immunolocalization of VHA (A, green) and NKA (B, red), with VHA and NKA immunoreactivity found in the same gill cells (C). At higher magnification with optical sectioning NKA immunoreactivity was visible as punctate staining throughout the edge of cell, indicative of NKA localization along the basolateral membrane (D). Nuclei in blue. Scale bar = 20 μm.

SECTION I:

ACID/BASE REGULATION

Chapter 2: Extrabranchial mechanisms of systemic pH recovery in hagfish (Eptatretus stoutii)

Introduction

The hagfish are the oldest extant representatives of an organism that split from the rest of the vertebrate lineage approximately 500-600 million years ago (Bardack, 1991). Possessing a plasma composition that is isosmotic to seawater, the hagfish does not ionoregulate plasma sodium and chloride levels (Robertson, 1976). This lack of regulation is interesting given the abundant presence of gill mitochondrion rich cells (MRCs) in hagfish (Bartels, 1985; Elger and Hentschel, 1983), cells that are, in marine teleosts, associated with both acid/base balance and salt regulation (Foskett and Scheffey, 1982; Goss and Wood, 1990a; Goss and Wood, 1990b; Karnaky, 1986; Philpott, 1980). The hagfish does not use these MRCs for sodium and chloride regulation; therefore, it has been hypothesized that these cells are present primarily for pH regulation (Evans, 1984; Mallatt et al., 1987). In jawed vertebrates, there exist two or more MRC types with one cell type thought to be responsible for acid excretion and another for base excretion (for review see Dymowska et al., 2012) . In contrast, hagfish are only believed to possess one cell type based on common immunocytochemical localization of transport proteins in hagfish gills (Tresguerres et al., 2006a).

The ability of the hagfish to recover from disturbances to blood pH is well documented, being able to return blood pH to normal levels within 6 h following injection of 1500 μmol kg^{-1} H$_2$SO$_4$ (McDonald et al., 1991) and being able to withstand and recover from repeated injections (6000 μmol kg^{-1}) of either HCl or NaHCO$_3$ (Parks et al., 2007b; Tresguerres et al., 2007a). Recovery by the hagfish from these acid/base disturbances *via* the single MRC they possess was postulated to occur by MRC

remodeling depending on the disturbance; however, the true mechanisms of this dual recovery has yet to be elucidated (Tresguerres et al., 2006a).

Past research efforts have primarily focused on branchial mechanisms of ion transport in hagfish (Choe et al., 1999; Edwards et al., 2001; Evans, 1984; McDonald et al., 1991; Parks et al., 2007b; Tresguerres et al., 2007a); however, extrabranchial ion exchange has largely been overlooked. Hagfish are scavengers that feed on decaying animal carcasses that have fallen to the ocean floor (Martini, 1998). While burrowing into a decaying carcass to feed, the anterior portion of the hagfish would constantly be interfacing with a nutrient rich environment. With this in mind, Glover et al. (2011) investigated amino acid transport through the skin and gill of hagfish with the hypothesis that, given this nutrient rich environment, hagfish would optimize nutritional uptake *via* transport through both the skin and gill. The findings from this study demonstrated uptake of amino acids by an excised gill or skin preparation. Glover et al. (2011) further demonstrated that uptake of amino acids was sodium dependent and suggested a role of SLC (solute carrier) transport proteins being involved in this uptake (as opposed to mass diffusion). This study has provided interesting results by demonstrating extrabranchial nutrient and ion uptake in hagfish in isolated tissue preparations. However, to date there have been no studies conducted *in vivo* demonstrating the capacity of the skin to contribute to ionic or nutrient homeostasis.

In addition to the feeding environment (inside the carcass) being nutrient rich, other significant physiological impairments would also be present, namely low pH, high P_{CO_2} and high [ammonia], all produced by microorganisms feeding off the same carcass. The raspers and feeding appendages are in close proximity to the branchial region of the

hagfish. While the hagfish feeds on the decaying carcass, there is an opportunity for undesirable branchial uptake of CO_2 and ammonia. Observations of feeding behavior in hagfish show that while burrowing into the carcass, the posterior part of the hagfish often remains outside. Thus, there is an opportunity for partitioned ion and acid/base regulation using extrabranchial mechanisms. Therefore, I hypothesized that the skin can serve as an extrabranchial mechanism for both regulating acid/base status and excreting ammonia. Using hagfish compartmentalizing flux chambers, I was able to separate flux of ammonia and acid/base equivalents into anterior (skin and gill contributions combined) and posterior regions (posterior to gill pores, skin and intestinal contributions combined). In addition, by sealing the cloacal opening and eliminating the intestinal contribution, I document the extrabranchial strategies employed by the hagfish to recovery from either acid or base injections.

Materials and methods

Experimental animals and holding

Pacific hagfish (*Eptatretus stoutii*; N=42; 86.64 ± 2.02 g; mean $\pm$ s.e.m.) were lured with bait (rotting hake) and captured *via* a bottom-dwelling trap from the Trevor channel, Vancouver Island, BC, Canada. The fish were immediately brought to the Bamfield Marine Sciences Centre and housed in aerated, darkened 20 m^3 tanks receiving seawater in a flow-through design. Fish were fed bi-weekly with rotting fish during captivity. Fish were fasted at least for one week prior to experimentation. All animals were used under the licenses of Department of Fisheries and Oceans Canada collection permit XR 146 2012 and Bamfield Marine Science Centre Animal Care protocol number BMSC RS-12-10

Chemicals

Unless noted, all chemical compounds, reagents and enzymes were supplied by Sigma-Aldrich Chemical Company (St. Louis, MO).

Experimental protocol

pH disturbances

Hagfish were anaesthetized in seawater with 1 g L^{-1} tricaine methanesulfonate (TMS; Syndel Laboratories Ltd., Vancouver, British Columbia, Canada) buffered with 2 g L^{-1} sodium bicarbonate. This dose of TMS was sufficient to keep the animal sedated for ~5 minutes while pre-experimental protocols were conducted. Weight was recorded and

42

fish were then held vertically causing pooling of blood in the caudal subcutaneous sinus within 20 seconds. A 200μl non-injected control blood sample was then removed from the sinus with a heparinized 21G needle and 1 mL disposable syringe. The animals were then injected with one of the following solutions: acid saline (250 mmol L^{-1} HCl [pH=0.60], 250 mmol L^{-1} NaCl), alkaline saline (250 mmol L^{-1} NaHCO$_3$, 250 mmol L^{-1} NaCl, [pH≈8.43]) or control saline (500 mmol L^{-1} NaCl) at a standard volume of 2.4 μl g^{-1} body mass to induce an acid/alkaline/saline load of 6000 μmol kg^{-1} body mass. Similar injection protocols have been employed in previous studies involving hagfish (McDonald et al., 1991; Parks et al., 2007b; Tresguerres et al., 2007a) with no adverse effects noted.

The injection site was then sealed by adhering a 0.5mm X 0.5mm square of nitrile rubber with instant cyanoacrylate glue (Krazy Glue: Elmer's Products Inc., Columbus, Ohio, USA) to ensure no acid/base seepage from the injection site. Animals were then gently inverted five times to facilitate mixing of the blood and injected solution. At this point, half of the animals also underwent the cloacal seal protocol (below) prior to being fitted for insertion into the compartmentalizing flux chamber.

Fitting of cloacal seal

The kidney and gut of the hagfish empty directly into the cloaca. In order to determine cutaneous flux without the potential additional flux coming from the cloacal compartment, half of all injected fish were fitted with a cloacal seal. First the cloacal region of the animal was blotted dry with a Kimwipe and then instant cyanoacrylate glue was applied to seal the cloaca shut (drying times ~15 seconds). A nitrile rubber bandage (2.0cm X 1.0 cm) was then applied to the cloacal region by gluing the perimeter around

the cloacal region. Animals were then fitted for insertion into the compartmentalizing flux chamber.

Fitting of latex collar

The anterior and posterior portions of the chambers are separated by collar assemblies (two square Plexiglas plates with 2.5 cm diameter central holes; see supplementary material) that are fitted onto the hagfish first prior to insertion into the flux chambers. These assemblies sandwich a finger from non-powdered latex gloves (8 cm long x 2 cm unstretched diameter) and are tightened together with plastic wing nuts and screws. Hagfish (either cloacally sealed or non-sealed) were patted dry in the region 2 cm to 4 cm posterior to the most posterior branchiopores. The latex sheath was slid onto the animal from the anterior end until the sheath was in the area to be glued. Cyanoacrylate glue was applied to this region around the circumference of the animal and the latex glued to the skin to form a watertight seal.

Fitting of hagfish into compartmentalizing flux chambers

Hagfish were then placed into a specially constructed hagfish compartmentalizing flux chamber (designed by AC, manufactured by Jeffery Johnston – UofA fabrication workshop; see supplementary material) in order to partition ammonia and acid/base fluxes into anterior and posterior regions. With no cloacal seal, the posterior compartment receives both cutaneous and cloacal flux while with a cloacal seal, only cutaneous flux is measured. The hagfish were then rinsed in fresh seawater and placed into the chamber where the collar assembly was fitted into slots. A thin layer of Silly Putty (Crayola LLC, Easton, Pennsylvania, USA) lined the perimeter of the Plexiglas plates to ensure a

watertight seal between chambers. Measured amounts of seawater were added to the anterior portion of the chamber only and a check for leaks was conducted. Only those preparations that demonstrated no leakage against the head pressure of the anterior region were used in this study. Following the leak test, seawater was subsequently added to the posterior chamber. Initial water samples were removed and the lid secured in place with plastic wing nuts. The entire chamber was then placed onto a water table with flowing seawater for temperature control (~12 ˚C) for the 4 h flux period.

Blood sample analysis and terminal sampling

Blood samples (200 µl) were obtained as described above prior to injection and following conclusion of the 4 h flux period. Following sampling, blood was added into a 1.5 mL Eppendorf tube and placed into a water bath held at 10 ˚C. Blood pH was measured immediately using a thermojacketed Orion ROSS Micro pH electrode (Fisher Scientific, Ottawa, ON). Blood samples were then centrifuged (12,000 g for 2 min) to obtain plasma, which was immediately analyzed for total CO_2 content (TCO_2) using a Corning 965 carbon dioxide analyzer (Ciba Corning Diagnostic, Halstead, Essex, UK).

Measured values of blood pH and total CO_2 were used to calculate plasma [HCO_3^-] and blood P_{CO_2} at 10°C by the Henderson-Hasselbalch equation, using the general formulas derived by Heisler and cited in Boutilier et al. (1984) using the solubility of CO_2 (Weiss, 1974) and the dissociation constant of carbonic acid as a function of pH, temperature, and ionic strength for seawater as a surrogate for hagfish plasma (Mehrbach, 1973).

Proton fluxes

Net H$^+$ fluxes from hagfish anterior and posterior regions were determined using techniques modified from Heisler and Weitz (1976) and Evans (1982). Under the assumptions proposed by Heisler and Weitz (1976), if the P_{CO_2} and temperature of a water sample is maintained constant while recording pH, then according to the Henderson-Hasselbalch equation, after a correction for seawater buffering capacity, any net change in recorded pH can only be the result of a net acid or base addition from the animal.

Using a disposable 25 mL pipette, water samples (25 mL) were removed from both the anterior and posterior chambers at *t=0 h* and *t=4 h* and added to 50 mL conical tubes. The tubes were then placed in a water bath held at 10 ˚C and the samples were bubbled with 6% CO_2. During bubbling, water pH was measured using a thermojacketed Orion ROSS Micro pH electrode until a stable reading was obtained (drift < 0.002 pH units 10 sec^{-1} for 1 min). pH readings were converted into μequiv H$^+$ and differentials between *t=0 h* and *t=4 h* were calculated. The presence of the hagfish may change the buffering capacity of the experimental water. In order to correct calculated H$^+$ differentials, buffering capacity of seawater from both the anterior and posterior compartments was determined at *t=4 h* over the pH range observed during the course of the flux period. To determine buffering capacity, changes in pH were measured following the addition of known amounts of 0.1066 N HCl or 0.10 N NaOH to a separate 25 mL water sample. Buffering capacity was calculated as the slope from the linear regression of μequivalent H$^+$ change per μequiv acid/base added. All corrected H$^+$ differentials were

compared to differentials calculated in control chambers containing no fish and with buffering capacity determined at $t=0$ h.

Thus, H$^+$ flux produced by the animal could be calculated according to the following equation:

$$J_{H^+}^{Net} = \left[\left[\frac{\left(_{exp}H_{final}^+ - _{exp}H_{initial}^+ \right)}{_{exp}\beta} \cdot {_{exp}V} \right] - \left[\frac{\left(_{con}H_{final}^+ - _{con}H_{initial}^+ \right)}{_{con}\beta} \cdot {_{con}V} \right] \right] \cdot \frac{1}{m} \cdot \frac{1}{t} \qquad (1)$$

where $J_{H^+}^{Net}$ is the net proton flux, $_{exper}H_{final}^+$ and $_{exper}H_{initial}^+$ are the total proton concentration in the experimental samples, $_{control}H_{final}^+$ and $_{control}H_{initial}^+$ are the total proton concentrations in the control samples, $_{exper}\beta$ and $_{control}\beta$ are the determined buffering capacities of the experimental water and the control water, $_{exp}V$ and $_{con}V$ are the water volumes of the experimental and the control chambers, m is the mass of the hagfish and t is the total flux time.

Ammonia fluxes

Water samples (1 mL) for ammonia analysis were removed at $t=0$ h and $t=4$ h and added to 1.5 mL tubes and acidified with 1 µl of 1.999 N HCl to trap ammonia. Water total ammonia (T$_{Amm}$) concentration was determined using methods modified from Verdouw et al., (1978) using a salicylate-hypochlorite colourimetric assay and measured using a microplate spectrophotometer (Spectramax 190, Molecular Devices, Sunnyvale, CA). Ammonia flux (J$_{Amm}$) was calculated for both the anterior and posterior chambers as based on the T$_{Amm}$ accumulation using the following equation:

$$J_{Amm} = \left([T_{Amm}]_{initial} - [T_{Amm}]_{final} \cdot _{exp}V\right) \cdot \frac{1}{m} \cdot \frac{1}{\Delta t} \qquad (2)$$

where $[T_{Amm}]$ is the initial or final concentration of ammonia in the water (μmol L^{-1}); V is the volume of water (mL); m is the animal mass (g) and Δt the duration of the flux period.

Statistical analysis

All data presented are reported as mean ± s.e.m. (*n*). Differences between groups were tested using one-way analysis of variance followed by Fisher's Least Significant Difference multiple comparison *post-hoc* tests (Fisher, 1949) with pre-planned comparisons. Statistical significance was defined as $p < 0.05$. Comparisons were not made between (Saline/No Seal) vs. (Acid/Seal) or (Base/Seal) groups, (Saline/Seal) vs. (Acid/No Seal) or (Base/No Seal) groups, (Acid/Seal) vs. (Base/No Seal), and (Acid/No Seal) vs. (Base/Seal). All statistical analyses were completed using GraphPad Prism 6.0 (GraphPad Software, San Diego, USA).

Determination of epaxial muscle pH$_i$

Samples of epaxial muscle excised terminally were immediately freeze clamped (clamps pre-chilled in liquid nitrogen) and stored in liquid nitrogen. Intracellular tissue pH was determined within 30 days of sampling using techniques modified from Pörtner et al., (1990). Briefly, samples were removed from liquid nitrogen and a portion (100-200 mg) was broken off from the frozen fillet. The subsample was pulverized under liquid nitrogen into a fine powder and added to an Eppendorf tube containing 400 μl of metabolic inhibitor (150 mmol L^{-1} potassium fluoride + 6 mmol L^{-1} nitrilotriacetic acid). The resulting slurry was mixed with an 18G needle and an additional 400 μl of inhibitor

solution was added. Tubes were then capped, vortexed and stored on ice. After 10 minutes, the pH of the slurry was measured using a thermojacketed Orion ROSS Micro pH electrode until a stable reading was obtained.

Results

Blood and plasma variables 4 h after HCl injection

Blood pH in non-injected control animals was 7.97 ± 0.02, $n = 41$. No differences were observed in blood pH between non-injected controls and saline-injected animals without the cloacal seal (7.83 ± 0.05, $n = 7$). Saline-injected, sealed animals exhibited a small but reliable depression in blood pH (7.64 ± 0.10, $n = 4$) 4 h after injection. Acid-injected animals (6000 μmol kg^{-1} HCl) exhibited significant blood acidosis after 4 h with blood pH reduced to 6.94 ± 0.17, $n = 8$, in unsealed animals. However, hagfish with a cloacal seal displayed a greater acidosis with a measured blood pH of 5.98 ± 0.24, $n = 7$ (Figure 2.1A).

Plasma TCO$_2$ values displayed nearly the same pattern (Figure 2.1B). No significant differences after 4 h were observed between non-injected controls (7.61 ± 0.27 mmol CO$_2$ L^{-1}, $n = 41$) and saline-injected animals (8.52 ± 1.00 mmol CO$_2$ L^{-1}, $n = 7$ and 6.62 ± 1.43 mmol CO$_2$ L^{-1}, $n = 4$ in unsealed and sealed hagfish, respectively). While acid-injected hagfish without a cloacal seal did not exhibit a significant reduction in TCO$_2$ 4 h post-injection (5.78 ± 1.01 mmol CO$_2$ L^{-1}, $n = 8$) compared to non-injected controls, a significant reduction in TCO$_2$ was observed in acid-injected animals with a cloacal seal (2.00 ± 0.54 mmol CO$_2$ L^{-1}, $n = 7$).

Calculation of plasma [HCO$_3^-$] and P_{CO_2} in all non-injected fish revealed a plasma [HCO$_3^-$] of 7.52 ± 0.27 mmol HCO$_3^-$ L^{-1}, $n = 41$ (Figure 2.1C). Saline injection resulted in no change in either plasma [HCO$_3^-$] or P_{CO_2} after 4 h ($p > 0.99$). However, injection of HCl resulted in both a reduced plasma [HCO$_3^-$] combined with a significant increase in

P_{CO_2} in animals either with (2.17 ± 0.24 kPa, $n = 7$) or without (1.97± 0.42 kPa, $n = 8$) a cloacal seal compared to control P_{CO_2} values (0.22± 0.012 kPa, $n = 41$).

Blood and plasma variables 4 h after NaHCO₃ injection

No disturbances in blood pH were evident in either sealed (7.81 ± 0.07, $n = 8$) or unsealed base-injected animals (7.98 ± 0.06, $n = 8$) after 4 h (Figure 2.1A).

In base-injected animals, plasma TCO_2 disturbances remained 4 h after injection (Figure 2.1B). Unsealed, base-injected hagfish still had significant elevations of TCO_2 4 h post-injection (17.52 ± 1.82 mmol CO_2 L^{-1}, $n = 8$) both compared to non-injected controls and to unsealed, saline injected animals. The elevation in plasma TCO_2 after 4 h was less pronounced in base-injected hagfish fitted with a cloacal seal (11.93 ± 0.63 mmol CO_2 L^{-1}, $n = 8$).

Calculation of plasma [HCO_3^-] and P_{CO_2} indicated that HCO_3^- remained elevated 4 h post injection in both sealed and unsealed animals (11.70 ± 0.63 mmol HCO_3^- L^{-1}, $n = 8$ and 17.33 ± 1.83 mmol HCO_3^- L^{-1}, $n = 8$, respectively; Figure 2.1C) and that this was also associated with a slight but not significant rise in plasma P_{CO_2} in each group (0.51 ± 0.04 kPa, $n = 8$, or 0.58± 0.12 kPa, $n = 8$, in both sealed and unsealed animals, respectively) compared to control animals.

Partitioning of H^+ flux following acid injection

Unsealed hagfish injected with saline exhibited minimal net H^+ flux from the anterior region during the 4 h post-injection period (Figure 2.2A; 69.80 ± 282.70 µequiv H^+ kg^{-1} h^{-1}, $n = 7$). The same animals exhibited considerable net base efflux in the

51

posterior region (Figure 2.2B; -917.14 ± 177.24 µequiv H^+ $kg^{-1} h^{-1}$, $n = 7$; where negative outward H^+ flux is equivalent to positive outward base flux). Mean anterior H^+ flux from saline-injected animals with a cloacal seal (559.08 ± 550.33 µequiv H^+ $kg^{-1} h^{-1}$, $n = 4$) was not statistically different from that of unsealed animals due to considerable variability in the responses. Base efflux in the posterior region was significantly reduced in sealed animals (-33.68 ± 77.97 µequiv H^+ $kg^{-1} h^{-1}$, $n = 4$). During the 4 h post-injection period, unsealed, acid-injected hagfish excreted 13.5 times more H^+ in the anterior region (948.70 ± 187.74 µequiv H^+ $kg^{-1} h^{-1}$, $n = 8$) than unsealed saline-injected controls. However, acid-injected hagfish with a cloacal seal exhibited only a small net base efflux in the anterior region (-62.92 ± 178.37 µequiv H^+ $kg^{-1} h^{-1}$, $n = 7$) that was not statistically different from sealed, saline-injected animals. In the posterior region, unsealed, acid-injected animals tended to excrete less base (-421.99 ± 138.10 µequiv H^+ $kg^{-1} h^{-1}$, $n = 8$) than the saline injected animals (-917.14 ± 177.24 µequiv H^+ $kg^{-1} h^{-1}$, $n = 7$), but this was not statistically significant. The cloacal seal did not significantly affect net base excretion by the posterior region of acid-injected fish.

Partitioning of H^+ flux following base injection

No changes in anterior net H^+ flux were observed in base-injected animals with or without a cloacal seal compared to saline-injected controls (Figure 2.2A; 139.13 ± 278.15 µequiv H^+ $kg^{-1} h^{-1}$, $n = 8$, for unsealed and 178.00 ± 428.02 µequiv H^+ $kg^{-1} h^{-1}$, $n = 8$, for animals with a cloacal seal). In the posterior region, base injection did not lead to differences in H^+ flux in unsealed animals (-1239.53 ± 321.73 µequiv H^+ $kg^{-1} h^{-1}$, $n = 8$) compared to unsealed, saline injected controls (-917.14 ± 164.10 µequiv H^+ $kg^{-1} h^{-1}$, $n = 7$) (Figure 2.2B). However, application of the cloacal seal after base injection

significantly increased base efflux by the skin (-2521.15 ± 309.94 µequiv H^+ kg^{-1} h^{-1}, $n =$ 8).

Partitioning of ammonia flux following both acid and base injection

Saline-injected hagfish excreted ammonia in the anterior region at a rate of 50.63 $\pm$ 10.26 µmol amm kg^{-1} h^{-1}, $n = 7$ (Figure 2.3A) and in the posterior region at 9.28 $\pm$ 3.74 µmol amm kg^{-1} h^{-1}, $n = 7$ (Figure 2.3B). Application of the cloacal seal did not result in any statistically significant differences, with an ammonia flux of 23.30 $\pm$ 18.45 µmol amm kg^{-1} h^{-1}, $n = 4$ in the anterior region and 9.21 $\pm$ 0.93 µmol amm kg^{-1} h^{-1}, $n = 4$ in the posterior region. There were no significant effects of acid injection on ammonia excretion rate during the 4 h post-injection period in either the anterior or posterior region in either sealed or unsealed animals. Similarly, in the base-injected animals, no statistically significant differences were observed in ammonia flux from the anterior region with or without a cloacal seal compared to saline injected controls.

Measurement of epaxial muscle pH$_i$ 4 h post-injection

The tissue pH$_i$ in excised epaxial muscle was 7.06 $\pm$ 0.05, $n = 8$, in control non-injected animals. No statistically significant differences were observed between any of the groups after 4 h (Figure 2.4; $p > 0.5$, $n = 6 - 8$).

Discussion

Partitioning of net acid or base secretion in hagfish

The present experiment demonstrates that after acidosis, hagfish excrete protons primarily into the anterior compartment. Furthermore, since the skin and skin+cloacal inputs in the posterior did not play a role in acid secretion, I suggest that acid excretion primarily occurs at the gills. In contrast, after alkalosis, hagfish excrete base through non-branchial (*i.e.* posterior) mechanisms with little contribution from the anterior/branchial region. Whether the skin of the anterior and posterior regions exhibit similar rates of transport is unknown and warrants further study.

Values of net H^+ flux in this study come from measurement of the change in pH of the water. The major chemical species contributing to this flux, which cannot be distinguished from one another, are likely H^+, OH^-, HCO_3^-. The total balance of acid/base equivalents transferred between the animal and the seawater would then be the sum of net H^+ flux and net ammonia (NH_3/NH_4^+) flux.

The values of net H^+ flux show that saline-injected hagfish normally excrete minimal H^+ in the anterior region and exhibit a considerable net base efflux in the posterior region. A control base efflux rate of ~-250 μequiv H^+ kg^{-1} h^{-1} for whole animals was observed by McDonald et al. (1991) in non-injected Atlantic hagfish (*Myxine glutinosa*) using similar flux protocols and the present study extends those results to demonstrate anterior/posterior partitioning of net acid and net base flux, respectively. After sealing the cloaca, base efflux by the posterior region was eliminated, suggesting cloacal constituents of base flux were significant under control conditions. Hagfish have

low urinary output, less than 5.4 mL kg^{-1} day^{-1} (Morris, 1965) which, in the case of the average hagfish (86.64 g) in the current study would equate to ~78µl of urine output in 4 h. Even in unsealed animals, this rate of urine production would likely account for less than 1% of observed net flux. This suggests that the gut or cloacal tissues are routes of base excretion in the resting hagfish. This raises an interesting point as it has recently been demonstrated that seawater teleosts utilize increased HCO_3^- secretion by the intestine and calcium and magnesium mediated carbonate precipitation for hyposmotic regulation (Grosell, 2006; Taylor and Grosell, 2006). Preliminary studies found no indication of hyperosmotic mediated increased in HCO_3^- secretion by the hagfish gut (Taylor, 2009). However, it should be noted that disturbances in acid/base balance were not investigated. If the intestine can indeed respond to base challenges by upregulating intestinal HCO_3^- secretion, it would suggest that the mechanisms for elevated HCO_3^- secretion by the intestine under hyperosmotic conditions were co-opted from acid/base regulatory mechanisms. This interesting but important evolutionary hypothesis will form the subject of future studies.

My results show that this protocol induced significant acidosis in hagfish (Figure 2.1A) with disturbances in blood pH to as low as 6.94 ± 0.17 in non-sealed animals and 5.89 ± 0.24 in sealed acid-injected animals 4 h post-injection. Based on results obtained by Parks et al. (2007b), who measured blood pH equal to 6.21 at 3 h post-injection of the same acid load, it seems likely that some recovery occurred before the 4 h sampling point in the present study. Parks et al. (2007b) also demonstrated that 3 h post acid injection, plasma TCO_2 was as low as 0.08 mmol CO_2 L^{-1}; however, the present study observed a recovery of TCO_2 after 4 h to levels similar to controls. While the observed blood

acidifications are substantial, hagfish have been shown to demonstrate similar blood acidification (0.7 pH units) during recovery from exercise (Ruben and Bennett, 1980). The NaHCO$_3$ injections in the present study were intended to induce a substantial HCO$_3^-$ load with an associated elevation in blood pH. Although significant rises in blood pH were not observed 4 h post base injection, based on the alkalizations recorded by Tresguerres et al. (2007) 3 h post-injection (pH=8.05 to 8.13) using the same injection protocol, it is likely that the hagfish had already significantly recovered blood pH by the 4 h post-injection sampling time. The TCO$_2$ measurements in the base-injected animals indicate that a significant part of the bicarbonate load remained after 4 h. As indicated in the pH/HCO$_3^-$ plot in Figure 2.1C, blood pH at 4 h after base injection was similar to control values due to a rise in plasma P_{CO_2} that balanced the increased plasma HCO$_3^-$ load.

In the present study, my results show that following acidosis, the main route of blood pH recovery is through branchial acid excretion, which increased by 13.5-fold in the 4 h post-injection period compared to saline-injected controls. There was also a trend toward moderately decreased base excretion by the posterior region. Proton flux results are in line with previous measurements by McDonald et al. (1991) who injected hagfish with sulphuric acid (3000 μequiv H$^+$ kg^{-1}) and observed a maximal H$^+$ excretion rate of 608 μequiv H$^+$ kg^{-1} h^{-1} in the first 1.5 h of recovery.

It is interesting to note that there was a greatly decreased branchial acid flux in acid injected animals fitted with a cloacal seal. This result is also supported by the fact that in these same animals, there was a greater reduction of blood pH in cloacally sealed animals. This interesting finding suggests that there is a mechanism of crosstalk between

the cloacal net H^+ flux and gill net H^+ flux. The mechanism by which this might occur is currently unknown and warrants further investigation.

Surprisingly, there were no observed differences in anterior H^+ flux in the 4 h period post base injection, suggesting that the branchial region is not responsible for base excretion. This result runs contrary to a previous suggestion (Tresguerres et al., 2006a) that MRCs in the gill are responsible for the majority of both acid and base excretions. In all other fishes studied, there are at least two or more types of MRCs with at least one population capable of acid secretion and another capable of base secretion (Dymowska et al., 2012). Based on immunohistochemical labeling of several ion transport proteins, hagfish are thought to only possess a single gill MRC type (Tresguerres et al., 2006a). Since hagfish do not regulate plasma $[Na^+]$ and $[Cl^-]$, these cells have been proposed to be primarily responsible for systemic pH regulation. Given the presence of a single MRC type and the remarkable ability for the hagfish to recover from a wide array of acid/base perturbations (McDonald et al., 1991; Parks et al., 2007b; Tresguerres et al., 2007a) it was postulated by Tresguerres et al. (2006) that the hagfish gill MRC is responsible for both acid excretion and base excretion. In light of the results of the current study, I suggest that hagfish MRCs are acid-secreting only and that the majority of base excretion occurs through extrabranchial mechanisms. This result also forces a reconsideration of the evolution of MRCs and how multiple MRC types arose throughout the vertebrate lineage.

For base-injected hagfish without a cloacal seal, the posterior region excreted base at approximately the same rate as control NaCl-injected hagfish suggesting that there was an inability to upregulate this cloacal flux. However, when the cloaca was sealed, net

base excretion was reduced in NaCl-injected animals but was substantially increased in base-injected cloacal sealed animals. This suggests that hagfish are able to upregulate base secretion *via* the skin. These results are supported by Tresguerres et al. (2007), who showed that hagfish demonstrated full recovery from base injection after 6 h and an enhanced ability to deal with subsequent base loads. The observed effects of the cloacal seal noted above, *viz.*, that a cloacal seal either prevented up-regulation of acid flux in the anterior of the animal or enhanced base flux in the posterior region through the skin, reveals that there is some as yet unidentified communication amongst these epithelia. To ensure that differences were not the result of transfer of acidic or basic equivalents into the intracellular compartment, pH_i in epaxial muscle was terminally measured tissue however, no differences between any of the groups 4 h post-injection were noted. These findings raise an interesting point (as noted previously) where the cloacal seal reveals that mechanisms for communication between the skin, gill and intestine/cloaca occur within the hagfish. While this is an important finding, a logical and experimentally supported explanation is unable to be provided at this time. Future studies should focus on the possibility that there are mechanisms for cross-talk between tissues to allow for adjustments in acid/base regulatory processes.

Partitioning of ammonia flux

This study clearly demonstrates that the skin of hagfish, at least in the posterior region, is capable of excreting a substantial amount of ammonia. However, ammonia efflux is not a factor in acid/base regulation in the hagfish because flux was similar and unchanging across all treatments.

The most notable observation of ammonia flux is that ammonia efflux in the posterior chamber continued even in the presence of a cloacal seal, indicating that hagfish are capable of excreting ammonia across the skin. In the anterior region, ammonia flux contains both gill and skin components. In this study, partitioning of skin from the whole animals was ~40% in the anterior and 60% in the posterior chamber. Ammonia flux from the skin of the posterior region alone was in the range of 10-30% of total ammonia flux. While ammonia transport through the isolated skin has previously been reported by Braun and Perry, (2010) using Ussing chamber protocols, here I provide the first physiological *in vivo* evidence demonstrating ammonia excretion through the hagfish skin. It should also be noted that when total anterior and posterior flux of ammonia are combined, the total ammonia flux rates observed was nearly an order of magnitude lower compared to McDonald et al. (1991). This difference was noted in both restrained (current study) and unrestrained animals (Chapter 6). This discrepancy could be due to species differences or perhaps differences in capture and feeding regimes.

The ability to excrete ammonia extrabranchially is not surprising considering the scavenging behavior of the hagfish. Within a decaying carcass, decomposition would create a source of ammonia, reversing the ammonia and pH gradients between the environment and the feeding hagfish. In order to prevent the deleterious effects of elevated ammonia levels (for reviews see Cooper and Plum, 1987; Mommsen and Walsh, 1992; Wilkie, 2002) an exchange system featuring ammonia efflux from the posterior skin would be beneficial.

Conclusions

In summary, my results have provided insight into how hagfish regulate systemic acid/base status after exogenous loads. Acid excretion occurs through the branchial region, while the ability to increase base excretion occurs by a non-branchial mechanism located in the posterior region, likely through the skin. Future studies will focus on identifying the mechanism(s) of recovery from alkalosis and determining the normal role of the cloacal region in acid/base balance, characterizing the regulatory capacity of ammonia transport in the skin, and investigating the ammonia transport capacity along the length of the organism. Finally, with the use of new hagfish separating chambers, many new avenues of research surrounding the unique aspects of hagfish physiology are available.

Figures

a)
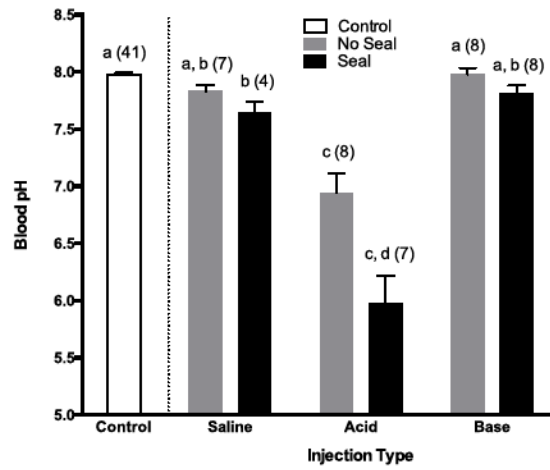
b)
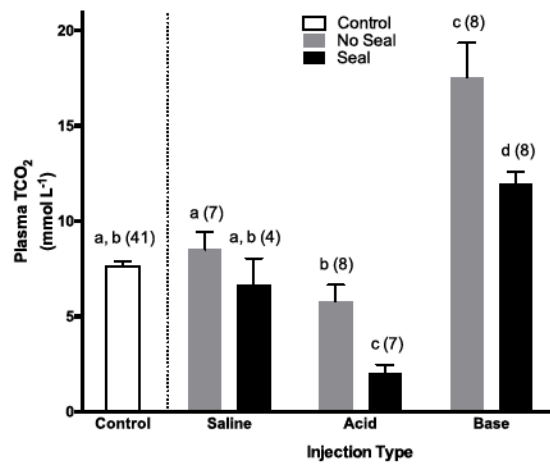
c)
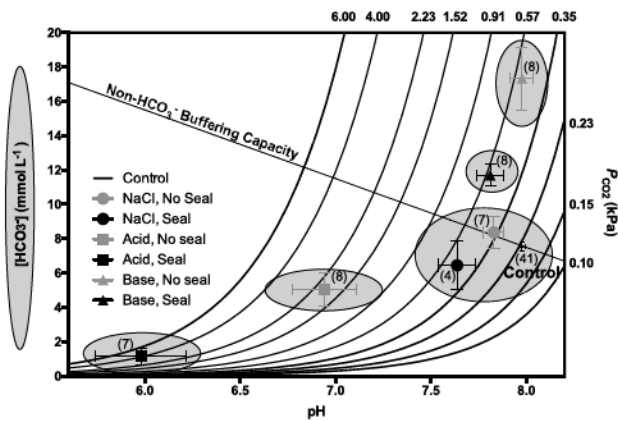
Figure 2.1 Recovery of hagfish blood and plasma acid/base parameters of following acid or base infusion.

Hagfish were injected with 2.4 µl g^{-1} body mass of one of the following: 250 mmol L^{-1} HCl/250 mmol L^{-1} NaCl (Acid; 6000 µmol H$^+$ kg^{-1} body mass), 250 mmol L^{-1} NaHCO$_3$/250 mmol L^{-1} NaCl (Base; 6000 µmol HCO$_3^-$ kg^{-1} body mass) or an equivalent volume of 500 mmol L^{-1} NaCl (Saline) then placed into darkened separated chamber apparatus for 4 h. (A) Blood pH (B) plasma total CO$_2$ of non-injected hagfish (Control; White bar), hagfish with an non-sealed cloaca (No Seal; grey bars) or a sealed cloaca (Seal; back bars). Data are presented as mean ± 1 s.e.m. (*n*). Bars sharing the same letter are not significantly different. (c) Blood pH/[HCO$_3^-$] diagram depicting the acid/base status of the blood of hagfish. The solid straight line is the non-bicarbonate buffer line determined by (Wells et al., 1986). Non-statistically different HCO$_3^-$ values are grouped within grey ovals. For difference in blood pH values refer to (A)
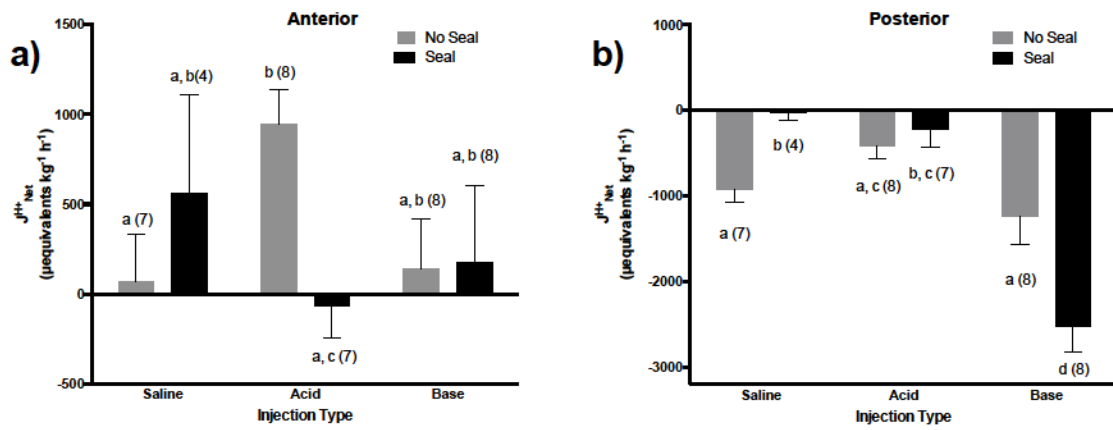
Figure 2.2 Measured net H^+/HCO_3^- during 4 h recovery from acid or base infusion.

(A) Net outward anterior and (B) posterior H^+ fluxes during 4 h period in separated chamber apparatus. Hagfish were treated as described in Figure 2.1. Hagfish either had a non-sealed cloaca (No Seal; grey bars) or a sealed cloaca (Seal; back bars). Data presented as mean $\pm$ 1 s.e.m. (n). Bars sharing the same letter are not significantly different.
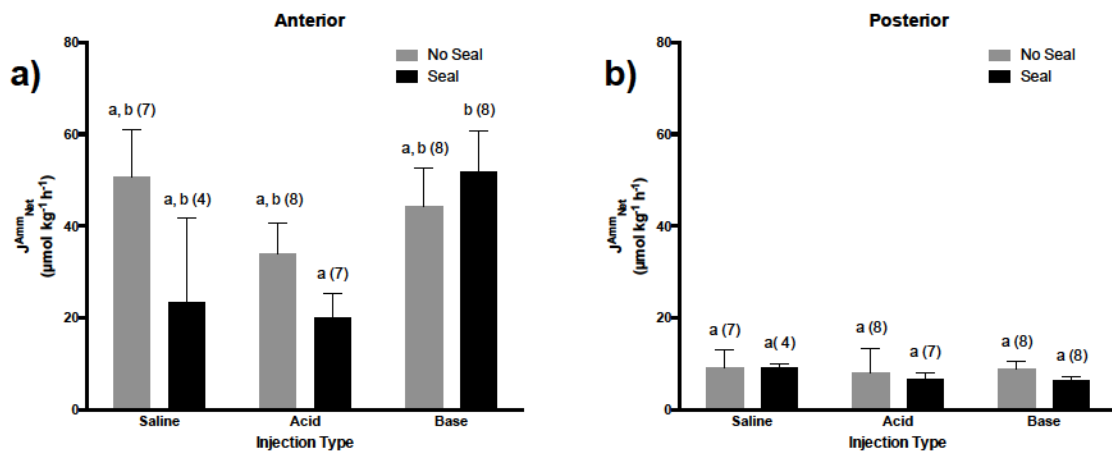
Figure 2.3 Measured net NH$_3$/NH$_4^+$ during 4 h recovery from acid or base infusion.

(A) Net outward anterior and (B) posterior ammonia fluxes during 4 h post injection period in separated chamber apparatus. Hagfish were treated as described in Figure 2.1. Data presented as mean ± 1 s.e.m. (n). Hagfish either had a non-sealed cloaca (No Seal; grey bars) or a sealed cloaca (Seal; black bars)
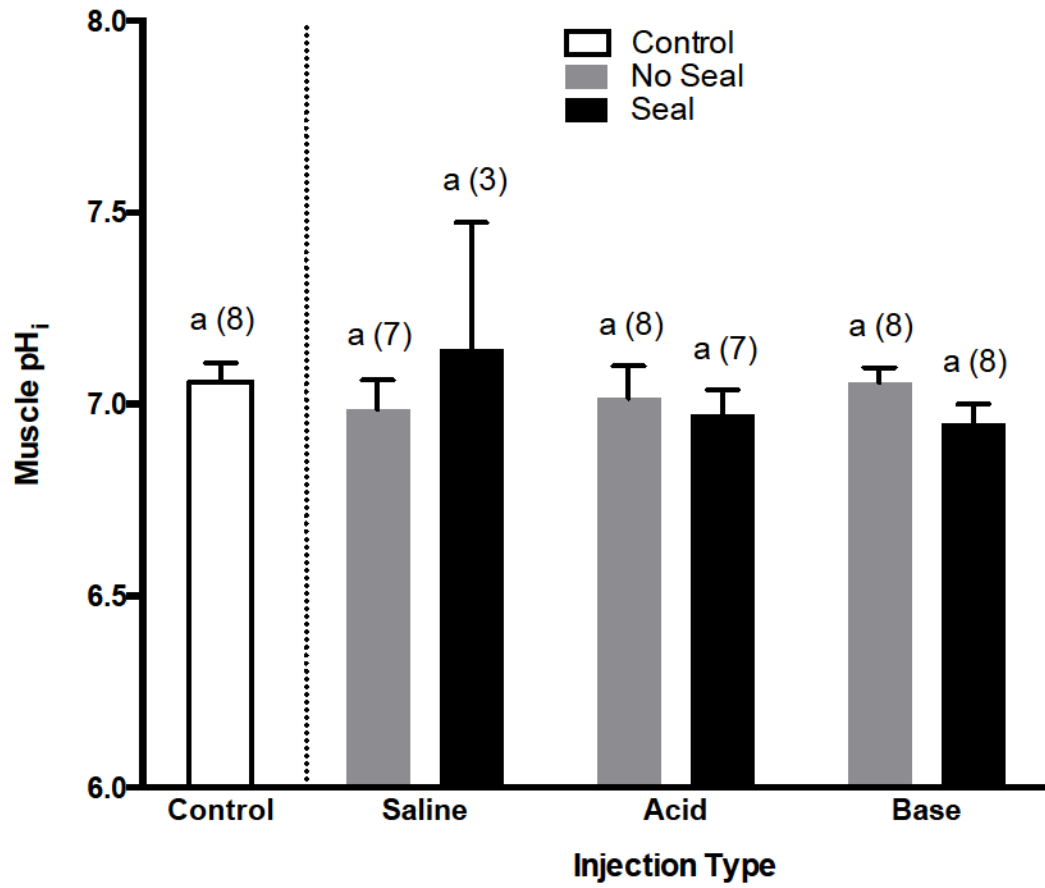
Figure 2.4 Measured muscle pH$_i$ during 4 h recovery from acid or base infusion.

Measurement of intracellular pH (pH_i) before (control) and following a 4 h post injection period in separated chamber apparatus. Hagfish were treated as described in Figure 2.1. Hagfish either had a non-sealed cloaca (No Seal; grey bars) or a sealed cloaca (Seal; black bars). Data presented as mean ± 1 s.e.m. (*n*). Bars sharing the same letter are not significantly different.

Supplemental figures
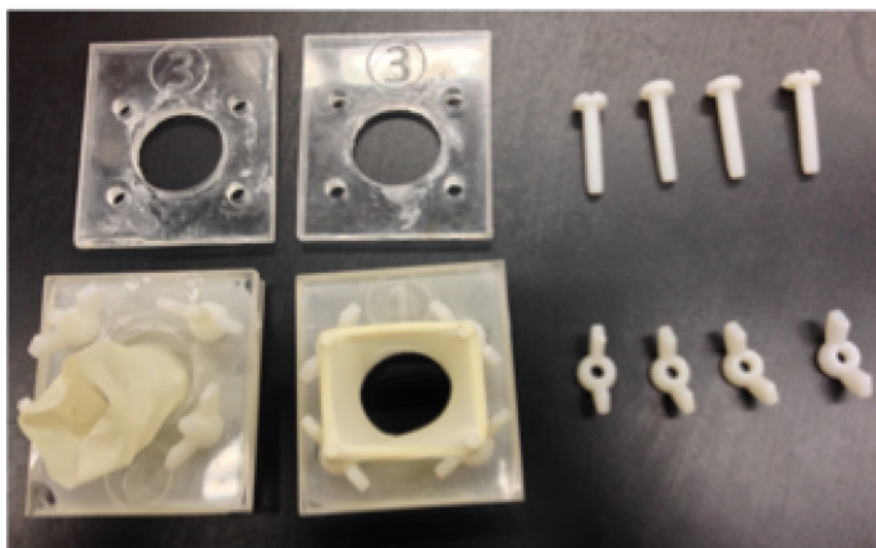
Supplemental Figure 2.1 Photograph of collar assembly.

Picture showing deconstructed Plexiglas collar assembly and fully assembled collar including latex sheath (non-powdered latex glove finger). The collar was fitted on hagfish posterior to branchiopores and the sheath was glued into place with cyanoacrylate glue.
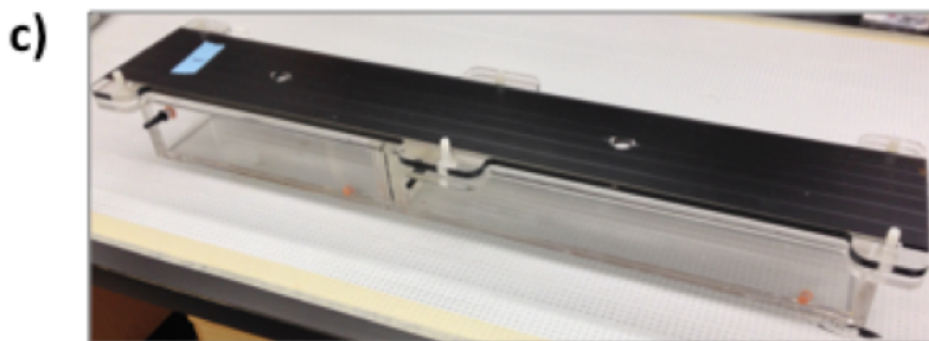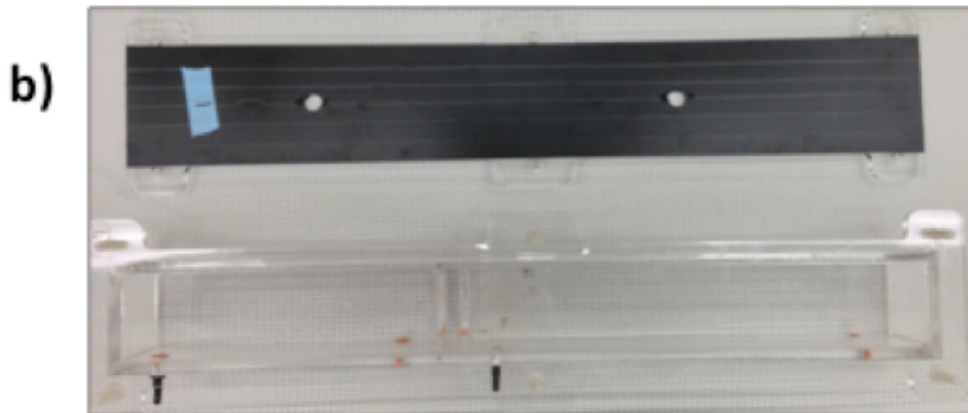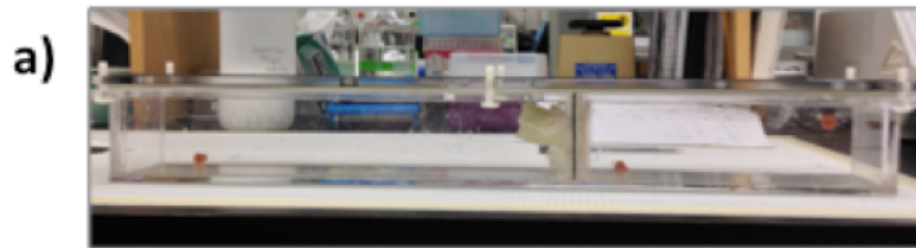
Supplemental Figure 2.2 Separating chamber apparatus.

(A) Side view of hagfish separating chamber with collar assembly inserted. (B) Top view of chamber with darkened lid. (C) Aerial side view of chamber with darkened lid.
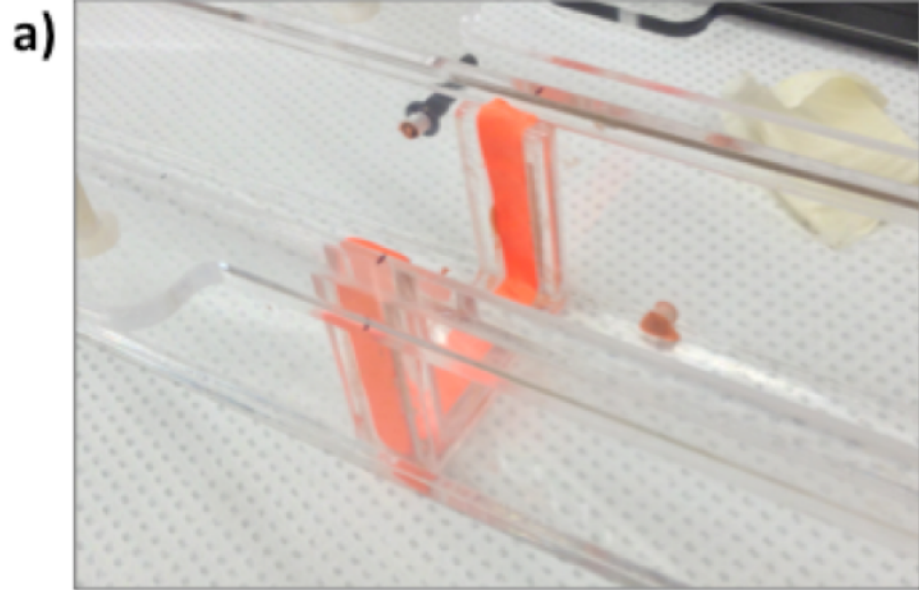
Supplemental Figure 2.3 Seperating chamber slot for collar.

(A) Picture illustrating how collar slots were lined with silly putty in order to achieve leak-proof seal between the anterior and posterior chambers. (B) Aerial view of hagfish properly fitted into apparatus.

Chapter 3: Recovery from extreme hypercapnia in the Pacific hagfish (*Eptatretus stoutii*)

Introduction

Hagfish are touted as physiological champions due to their tolerance to noxious environmental stresses such as high ammonia (Clifford et al., 2015a), hypoxia (Axelsson et al., 1990; Forster et al., 1992), anoxia (Cox et al., 2011) and hypercapnia (Baker et al., 2015). While the tolerance and physiological impacts to these stressors have been well characterized, little data exists on the mechanisms and strategies for recovery from these stressors. Physiologically speaking, acid/base homeostasis is a tightly regulated process amongst vertebrates (Heisler, 1986b) and hagfish are no exception. Several studies have highlighted the extraordinary capabilities for hagfish to regulate their blood pH in the face of severe perturbations. When injected with H_2SO_4 (McDonald et al., 1991) or HCl (Parks et al., 2007b) (1500 $\mu mol\ kg^{-1}$ and 6000 $\mu mol\ kg^{-1}$ respectively) the acidosis that hagfish experienced (H_2SO_4: > 0.6 pH unit acidosis; HCl: ~2 pH unit acidosis) was recovered within 6 h of injection. When injected with base (6000 $\mu mol\ kg^{-1}$ $NaHCO_3$); blood pH only rose ~0.3 pH units after 1 h and was fully recovered within 6 h, demonstrating that hagfish have a pronounced capacity to withstand acid/base challenges (Tresguerres et al., 2007a). Perhaps more profound is how hagfish are capable of tolerating very high partial pressures of CO_2 (P_{CO_2}; termed: hypercapnia), withstanding P_{CO_2} tensions of up to 50 torr (~6.6% CO_2) for 96 h. Hagfish compensate such P_{CO_2} tensions by building up plasma [HCO_3^-] (termed: hypercarbia) to the highest levels ever observed in any organism (~70 $mmol\ L^{-1}$; Baker et al., 2015). Plasma [HCO_3^-] compensation for hypercapnia-induced acidosis takes place over 24 – 48 h in an equimolar trade-off with plasma [Cl^-] (Baker et al., 2015).

Hypercapnia tolerance in hagfish is well characterized and it seems apparent that hagfish are capable of rapidly recovering from minor hypercarbia loads induced by base injection (~20 mmol HCO_3^-; Tresguerres et al., 2007a) easily clearing repeated alkaline infusions. However, it remains to be seen whether hagfish are capable of recovering from high hypercarbia loads as reported by Baker et al. (2015). Furthermore, if recovery is possible, the kinetics and mechanisms merit investigation. Indeed, during extended bouts of hypercapnia, hagfish appear to be 'sluggish', presenting themselves in a distended or uncoiled manner (personal observation) rather than the traditional coiling observed in normal healthy hagfish (Martini, 1998).

The goal of this study was to characterize the recovery strategies of the hagfish in response to hypercapnia-induced hypercarbia. Hagfish were exposed to hypercapnia (4% CO_2) for 48 h to induce hypercarbia at high levels. Over the next 24 h, hagfish were allowed to recover in normocapnic seawater while measurements of blood acid/base status, [Cl^-] and net H^+/HCO_3^- flux were made in an effort to describe the recovery strategies of the hagfish. While it is hypothesized that the majority of TCO_2 (total CO_2 content: comprised of the sum of both P_{CO_2} and [HCO_3^-] in a biological system) recovery will occur *via* direct HCO_3^- excretion in an equimolar trade-off with Cl^- mediated *via* chloride-bicarbonate exchanger (CBE), other means of TCO_2 off-loading exist (see Figure 3.1). These include increases in glomerular filtration rate (GFR) and carbonic anhydrase (CA) -mediated recovery/reduction of plasma HCO_3^-, which would involve the catalyzed hydration of HCO_3^- to CO_2 at the gills and rapid clearance of gaseous CO_2 across the gill epithelium.

The renal system in hagfish is known to be rudimentary with a low urinary flow rate (Morris, 1965) and also lacking concentrative abilities (Alt et al., 1981). Thus it is hypothesized that GFR will not play a substantial role in recovery. The relative role(s) of CA-mediated and CA-independent recovery can be investigated by inhibition of CA using the CA inhibitor acetazolamide; however, based on the previously reported hypercapnia compensation with equimolar exchanges of plasma $[HCO_3^-]$ and $[Cl^-]$ during exposure, CA-mediated recovery is not hypothesized to play a major role in recovery.

Materials and methods

Animals and holding

Pacific hagfish (*Eptatretus stoutii*; $N = 24$; average mass $= 77.27 \pm 5.89$ g) were captured from Trevor channel, Vancouver Island, BC, Canada *via* a bottom-dwelling trap baited with rotting hake. Hagfish were transferred to Bamfield Marine Sciences Centre and housed in aerated, darkened 20 m^3 tanks receiving flow-through seawater. Hagfish were fed bi-weekly with rotting fish during captivity and fasted at least for one week prior to experimentation. All animals were used under the licenses of Department of Fisheries and Oceans Canada collection permit XR-310 2015 and University of Alberta Animal Care protocol number AUP0001126.

Chemicals

Unless noted, all other chemical compounds, reagents and enzymes were supplied by Sigma-Aldrich Chemical Company (St. Louis, MO).

Experimental protocol

Hypercapnia exposure and recovery in normocapnic seawater

One day prior to experiments, Pacific hagfish were transferred to 1.0 L containers with tight fitting lids, receiving continuously flowing normocapnic seawater to acclimate. Containers were placed in a sea-table receiving flow-through seawater for temperature regulation ($\sim$12 °C). The next morning, hagfish were exposed to hypercapnia (nominal $P_{CO_2} = 4\%\ CO_2$) in continuously flowing seawater within the 1.0 L containers, maintained

by aeration with ~10% CO_2 (administered *via* utilization of a dual-supply precision gas blender (FM4333/FM4336 Matheson, Basking Ridge, New Jersey) receiving 100% CO_2 (Praxair) and house air) which was controlled by a P_{CO_2}/pH feedback controller (DAQ-M, Loligo systems Inc, Viborg, Denmark) connected to a pH meter/ pH electrode (Portable meter ProfiLine pH 3310 / Sentix HWD electrode, Wissenschaftlich-Technische Werkstätten GmbH, Weilheim, Germany). This system was calibrated and controlled using CapCTRL software (Loligo Systems Inc).

Following 48 h hypercapnia exposure, CO_2 administering airlines were removed, water refreshed and hagfish were allowed to recover in their individual, aerated 1.0 L containers receiving normocapnic seawater for up to 24 h. Modifications to this protocol for blood sampling, or for flux/GFR protocols are listed below.

Series 1: Blood and plasma responses during recovery from hypercapnia-induced hypercarbia

Immediately following acclimation to exposure chambers, flow-through seawater was temporarily shut off, and ~half the water in the 1.0 L container was removed. Hagfish were anaesthetized *via* addition of 0.5 g L^{-1} tricaine methanesulfonate (TMS; Syndel Laboratories Ltd., Vancouver, British Columbia, Canada) neutralized with 0.15 g NaOH pre-dissolved in ~10 mL of seawater. This dose caused rapid sedation, lasting for ~5 minutes and also allowed for rapid recovery (typically < 5 min) from blood sampling/sedation. Fish were weighed, and then held vertically causing pooling of blood in the caudal subcutaneous sinus within 20 seconds. A 200 µl control (pre-exposure) blood sample was then drawn from the sinus with a 21G needle and 1mL disposable

syringe that was rinsed with heparinized hagfish saline (50 U mL^{-1} heparin in 0.5 mol L^{-1} NaCl). Hagfish were immediately returned to containers with refreshed seawater and flow-through re-established, with the administration of CO_2 as described above. Blood samples were immediately analyzed (see below) for pH and TCO_2. Hagfish were sampled for blood in a similar manner following the conclusion of 48 h hypercapnia exposure, at 2 h intervals from 0 – 12 h recovery and then at 4 h intervals from 12 – 24 h recovery. Throughout recovery, flow-through seawater was dispensed to the container.

Blood sample analysis

Blood pH was measured immediately using a thermojacketed (10 ˚C) Orion ROSS Micro pH electrode (Fisher Scientific, Ottawa, ON). Blood samples were then centrifuged (12,000 g for 2 min) to obtain plasma, which was then analyzed for total CO_2 (TCO_2) using a Corning 965 carbon dioxide analyzer (Ciba Corning Diagnostic, Halstead, Essex, UK). Plasma [Cl$^-$] was measured with a Buchler Digital Chloridometer. Measured values of blood pH and TCO_2 were used to calculate [HCO$_3^-$] and P_{CO_2} at 10°C by the Henderson-Hasselbalch equation, using the general formulas derived by Heisler and cited in Boutilier et al. (1984) using the solubility of CO_2 (Weiss, 1974) and the dissociation constant of carbonic acid as a function of pH, temperature, and ionic strength for seawater as a surrogate for hagfish plasma (Mehrbach, 1973).

Series 2: Hagfish acid/base and ammonia excretion patterns during recovery from hypercapnia-induced hypercarbia

Net H$^+$ flux and J$_{Amm}$ (ammonia excretion rate) were measured in the 2 h period prior to hypercapnia exposure, in the final 2 h of hypercapnia exposure and at 2 h

intervals throughout recovery from 0 – 10 h recovery. Net H^+ flux was measured using techniques modified from Heisler and Weitz, (1976) and described by Clifford et al. (2014). Briefly, flow-through water to the individual 1.0 L containers was terminated and water was removed such that ~750 mL of water remained. Two water samples (1 mL and 25 mL) were removed at the beginning and end of the flux period. At the conclusion of each flux period, the container containing the hagfish and experimental water was weighed and water samples taken (see below). Following the conclusion of each flux period, water in the containers was refreshed. At the conclusion of the recovery period, hagfish were anaesthetized and then weighed.

The 25 mL water samples were placed in a water bath held at 10 ˚C and bubbled with 100% CO_2. Water pH was measured using a thermojacketed Orion ROSS Micro pH electrode until a stable reading was obtained (drift < 0.002 pH units 10 sec^{-1} for 1 min). pH readings were converted into μequiv H^+ and differences between initial and final time-points calculated. As the hagfish itself may change the buffering capacity of the seawater, H^+ differentials (between initial and final) were corrected by determining the buffering capacity of the experimental water over the observed pH range. Buffering capacity was determined in the final 25 mL water sample by measuring changes in pH following the addition of known amounts of 0.1011 N HCl or 0.1 N NaOH (Standardized via volumetric titration) while being aerated with 100% CO_2. Buffering capacity was calculated as the slope from the linear regression of μequivalent acid change per μequivalent acid/base added. Differences between corrected H^+ differentials were compared to differentials calculated in control chambers (containing no fish; in tandem with experimental chambers and with buffering capacity determined at initial time-

points). Thus, H$^+$ flux produced by the animal could be calculated (See calculations below).

The 1 mL water samples were acidified with1 µL of 2 M HCl to trap ammonia. Water [ammonia] was determined using methods modified from Verdouw et al. (1978) using a salicylate-hypochlorite colourimetric assay measured at 650 nm on a plate spectrophotometer (Spectramax 190, Molecular Devices, Sunnyvale, CA).

Series 3: Determining the role of glomerular filtration during recovery from hypercapnia

In a third experimental series, hagfish were allowed to acclimate to the containers overnight and were then anaesthetized (as above), weighed, and injected with ^{14}C-inulin (Perkin Elmer as ^{14}C-inulin:(250 µCi in 1 mL; 2.1 mCi g^{-1}) as a plasma space marker in order to calculate glomerular filtration rate (GFR) (Munger et al., 1991). Hagfish were injected with 0.12 µCi g^{-1} of ^{14}C-inulin animal weight administered as 0.06 µCi ^{14}C µL^{-1} hagfish saline (500 mmol L^{-1} NaCl). Hagfish were then placed into individual flux containers so that ^{14}C-inulin activity was allowed to equilibrate in the plasma for 6 h. Preliminary experiments (Chapter 7) determined that plasma concentrations were fully mixed and stable in the 6 – 12 h post-injection period. Following the 6 h mixing period, hagfish were anaesthetized (as above) and a 100 µL blood sample drawn (as above) at 6 h post-radiolabeled inulin injection. GFR was measured in 2 h time-spans before exposure, before recovery and in 2 h blocks throughout 10 h recovery. Blood was also sampled at the conclusion of the hypercapnia exposure and at the conclusion of the recovery period. To begin each measurement period, 2 water samples (4 mL – weighed precisely on a fine balance) were collected from the flux container (T$_1$) and each flux was terminated after 2

h by withdrawing final water samples (T_2). Flux containers were weighed at the end of the flux period to determine the flux volume (minus the weight of the fish).

Plasma was separated *via* centrifugation (as above) and plasma was separated into two 30 µL aliquots (measured on a fine balance) in 20 mL scintillation vials. ACS scintillation fluid (Fisher chemical) was added to plasma samples (4 mL scintillation fluid) and water samples (10 mL scintillation fluid) both of which were mixed and later analyzed for ^{14}C radioactivity using a Beckman LS-6000.

Series 4: Determining the role of carbonic anhydrase during recovery

To examine the involvement of carbonic anhydrase in recovery from hypercapnia-induced hypercarbia, hagfish were sampled and exposed to hypercapnia as in Series 1 (above). However, following the conclusion of hypercapnia exposure, but prior to pre-recovery blood sampling, hagfish were injected with acetazolamide (40 mg kg^{-1}; administered as 0.016 mg µL^{-1} in hagfish saline). Blood sampling and analysis for pH and TCO_2 occurred (as above) every 2 h.

Calculations

H$^+$ flux ($J_{Net}^{H^+}$) was calculated as:

$$J_{Net}^{H^+} = \left[\left(\frac{\left(_{exp}H_{final}^+ - _{exp}H_{initial}^+ \right)}{_{exp}\beta} \cdot _{exp}V \right) - \left(\frac{\left(_{con}H_{final}^+ - _{con}H_{initial}^+ \right)}{_{con}\beta} \cdot _{con}V \right) \right] \cdot \frac{1}{m} \cdot \frac{1}{\Delta t} \quad (1)$$

where $J_{Net}^{H^+}$ is the net proton flux, $_{exp}H_{final}^+$ and $_{exp}H_{initial}^+$ are the net H$^+$ content in the experimental samples (µmol), $_{con}H_{final}^+$ and $_{con}H_{initial}^+$ are the net H$^+$ content in the

control samples (μmol), $_{exp}\beta$ and $_{con}\beta$ are the determined buffering capacities of the experimental water and the control water, $_{exp}V$ and $_{con}V$ is the volume of experimental and control water (L), m is the animal mass (kg), and Δt is the duration of the flux period.

Ammonia flux (J_{Amm}) was calculated as:

$$J_{Amm} = \left([T_{Amm}]_{initial} - [T_{Amm}]_{final} \cdot V\right) \cdot \frac{1}{m} \cdot \frac{1}{\Delta t} \qquad (2)$$

where $[T_{Amm}]$ is the initial or final concentration of ammonia in the water (μmol L^{-1}), V is the flux volume (L) and other notations correspond as above.

Glomerular filtration rate was calculated based on ^{14}C excretion rate using the following equation:

$$GFR = \left[\left(CPM_{water}^{T_2} - CPM_{water}^{T_1}\right) \cdot \frac{1}{m} \cdot \frac{1}{\Delta t}\right] \cdot V \cdot SA \qquad (3)$$

where $CPM_{water}^{T_2}$ and $CPM_{water}^{T_1}$ correspond to average final and initial CPM in water samples based on duplicate samples, and SA refers to specific activity and all other notations are as listed above. Note for the pre-exposure period, SA was determined by the radioactivity in only the pre-exposure blood sample, while the SA in the pre-recovery period was determined by the pre-recovery period blood sample. For all other measurement periods throughout recovery, SA was determined as:

$$SA = \frac{\left(\dfrac{volume}{CPM_{plasma}^{T_2}} + \dfrac{volume}{CPM_{plasma}^{T_1}}\right)}{2} \qquad (4)$$

Plasma [HCO$_3^-$] and [Cl$^-$] values throughout exposure and recovery were converted to changes in whole-animal solutes (either HCO$_3^-$ and Cl$^-$) assuming equilibration of each across the whole animal using the following equation

$$\Delta \text{ Whole-animal ion} = \left([\text{ion}]_{T_2} - [\text{ion}]_{T_1}\right) \cdot m \tag{5}$$

where $[\text{ion}]_{T_2}$ and $[\text{ion}]_{T_1}$ refer to measured final and initial [HCO$_3^-$] and [Cl$^-$].

Rate of [HCO$_3^-$] loss $\left(\dfrac{dHCO_3^- \cdot \frac{1}{m}}{dt}\right)$ was calculated as:

$$\frac{dHCO_3^- \cdot \frac{1}{m}}{dt} = \left[\left([HCO_3^-]_{T_2} - [HCO_3^-]_{T_1}\right) \cdot m\right] \cdot \frac{1}{m} \cdot \frac{1}{\Delta t} \tag{6}$$

Statistics

All data are presented are given as mean $\pm$ s.e.m. Differences from pre-exposure (control) values were tested using repeated-measured one-way ANOVA followed by Holm-Sidak *post-hoc* test. For acetazolamide experiments, differences were measured using repeated-measured two-way ANOVA followed by Holm-Sidak *post-hoc* test for comparison to control values or Fisher's LSD test for comparison between groups. For $\dfrac{dHCO_3^- \cdot \frac{1}{m}}{dt}$ with and without acetazolamide, differences across time periods were measured using repeated-measured two-way ANOVA followed by Tukey's multiple comparisons test. Statistical significance was inferred when $p < 0.05$. All statistical analyses were completed using GraphPad Prism 6.0 (GraphPad Software, San Diego, USA).

Results

Recovery of blood and plasma acid/base homeostasis following hypercapnia-induced hypercarbia

Following 48 h of hypercapnia (4% CO_2) exposure, hagfish blood pH (7.84 ± 0.04 pH units) was not significantly different from pre-exposure levels (7.95 ± 0.04 pH units; Figure 3.2A) indicating near complete blood pH compensation. In the post-hypercapnic recovery period, blood pH was significantly elevated throughout the first 10 h, peaking at 4 h recovery (8.66 ± 0.03 pH units) and returning to levels not significantly different to pre-exposure levels by 12 h recovery (blood pH < 8.133 ± 0.06 pH units from 12 – 24 h).

Compensation from hypercapnia exposure was accomplished by a substantial increase in plasma TCO_2 reaching 66.96 ± 5.08 mmol TCO_2 L^{-1} compared to pre-exposure control levels (4.91 ± 0.32 mmol L^{-1}; Figure 3.2B). Post-hypercapnic alkalosis was accompanied with steady reductions in TCO_2 over the first 10 h of recovery, reaching concentrations not significantly different compared to pre-hypercarbic levels within 8 h (13.56 ± 3.19 mmol CO_2 L^{-1}) and remaining unchanged for the remainder of the 24 h recovery period (range = 5.01 – 8.35 mmol CO_2 L^{-1}).

Calculation of plasma [HCO_3^-] and P_{CO_2} in pre-exposed hagfish yielded a plasma [HCO_3^-] of 4.84 ± 0.31 mmol HCO_3^- L^{-1} and P_{CO_2} of 1.24 ± 0.02 Torr (Figure 3.1C). Following 48 h exposure to 4% CO_2, these same animals displayed significant elevations in both [HCO_3^-] (65.83 ± 2.11 mmol HCO_3^- L^{-1}) and P_{CO_2} (22.00 ± 2.08 Torr) as a result of hypercapnia exposure. In the post-hypercapnic recovery period, plasma P_{CO_2} was rapidly restored to control tensions (< 2 h) after initiation of post-hypercapnia recovery

(2.61 ± 0.41 Torr) and remained stable throughout the duration of the recovery period while plasma [HCO_3^-] declined to control concentrations over the next 8 h of recovery and stabilized thereafter (Figure 3.2C).

Effect of hypercapnia-induced hypercarbia on plasma solutes

Plasma [Cl^-] was significantly diminished in hagfish (392.2 ± 2.3 mmol L^{-1}) following 48 h hypercapnia exposure compared to pre-exposure levels (448.5 ± 3.1 mmol L^{-1}; Figure 3.3B). Over the course of the post-hypercapnia recovery, plasma [Cl^-] steadily recovered to levels not significantly different to pre-exposure levels within 8 h of recovery (438.5 ± 4.2 mmol L^{-1}). Comparing change in plasma HCO_3^- content to change in plasma Cl^- content (Figure 3.3B) demonstrates a clear trend that as plasma HCO_3^- returns to control levels, so too does plasma Cl^- in approximately equimolar amounts. No statistical differences between the two metrics were observed at any time-point.

Hagfish H^+/HCO_3^- and ammonia excretion during recovery from hypercapnia-induced hypercarbia

During pre-exposure conditions, basal H^+ excretion rate was 50.8 ± 175.8 µequiv H^+ kg^{-1} h^{-1} (Figure 3.4A), while at 48 h of 4% CO_2 hypercapnia (46 – 48 h exposure), H^+ excretion was slightly, but not significantly increased to 369.4 ± 177.8 µequiv H^+ kg^{-1} h^{-1}, perhaps indicating that compensation was not quite complete. Within the first two hours of recovery from hypercapnia exposure, hagfish net H^+/HCO_3^- equivalent excretion was minor and not different from pre-exposure levels (7.7 ± 160.2 µequiv HCO_3^- kg^{-1} h^{-1}). However, in the 2 – 4 h time period, the rate of net H+/HCO_3^- excretion increased ~200 fold compare to control rates (2327 ± 880, 2092 ± 426 and 2320 ± 401 µequiv HCO_3^- kg^{-1}

h^{-1} at $t = 2 - 4$, $4 - 6$ and $6 - 8$ h) before declining steadily to levels not significantly different to pre-hypercapnia exposure levels by 10 h.

Pre-exposed hagfish excreted ammonia at a rate of 30.6 ± 9.9 µmol kg^{-1} h^{-1} (Figure 3.4B). Ammonia excretion did not significantly differ from pre-exposure levels throughout the duration of the experiment; however, rates were ~2-fold higher in the final 2 h of exposure (55.7 ± 12.5 µmol kg^{-1} h^{-1}) and ~2.5-fold higher in the first 2 h of recovery (75.6 ± 9.92 µmol kg^{-1} h^{-1}).

Glomerular filtration patterns during recovery from hypercapnia-induced hypercarbia

In pre-exposed animals, GFR averaged 1.08 ± 0.36 mL kg^{-1} h^{-1} (Figure 3.5). Despite the variability in the measure throughout the duration of the experiment, GFR was significantly elevated (4.19 ± 0.56 mL kg^{-1} h^{-1}) in the 2 - 4 h recovery period and appeared equally elevated, albeit non-significantly ($p > 0.15$) at the 0 - 2 and 4 - 6 h recovery periods (3.88 ± 0.76 and 4.21 ± 1.14 mL kg^{-1} h^{-1}, respectively).

Effect of carbonic anhydrase inhibition on hypercarbia recovery

Acetazolamide (40 mg kg^{-1}) was injected into the caudal sinus of hypercapnia exposed hagfish immediately following the 0 h recovery blood sample and immediately prior to allowing hagfish to recover in normocapnic seawater. While hagfish that were to be acetazolamide-injected did have a slight blood acidosis (7.66 ± 0.05 pH units; Figure 3.6A) following hypercapnia exposure ($t = 0$ h) compared to pre-exposure levels (7.99 ± 0.01 pH units), no significant differences were observed between the control and acetazolamide-injected animals either prior to (7.95 ± 0.04 vs. 7.99 ± 0.01 pH units) or following 48 h exposure (7.84 ± 0.04 vs. 7.66 ± 0.04 pH units). Compared to control

animals, blood pH in acetazolamide-injected animals remained significantly more acidotic at the 2 h (8.48 ± 0.05 vs. 8.03 ± 0.08 pH units), 4 h (8.66 ± 0.03 vs. 8.17 ± 0.08 pH units) and 6 h (8.59 ± 0.06 vs. 8.28 ± 0.06 pH units) recovery time-points. However, only at the 4 and 6 h recovery times was blood pH significantly alkalotic compared to pre-exposure control values. For the remainder of recovery (8, 10 h), blood pH remained elevated in both control and acetazolamide-injected animals compared to pre-exposure values; however, did not differ between control and injected animals.

Prior to hypercapnia exposure, blood P_{CO_2} averaged 1.24 ± 0.22 and 0.63 ± 0.04 Torr while plasma [HCO_3^-] averaged 4.84 ± 0.31 and 2.84 ± 0.17 mmol HCO_3^- L^{-1} in pre-exposed control hagfish and hagfish to be injected with acetazolamide, respectively (Figure 3.6B,C). Blood P_{CO_2} and plasma [HCO_3^-] were significantly elevated in both control hagfish (22.00 ± 2.08 Torr and 65.83 ± 2.11 mmol HCO_3^- L^{-1}) and hagfish to be injected with acetazolamide (30.11 ± 2.19 Torr and 57.58 ± 5.10 mmol HCO_3^- L^{-1}) following hypercapnia exposure compared to pre-exposure values (Figure 3.6B,C). Injection of acetazolamide impaired recovery of plasma P_{CO_2} during the first 4 h of recovery wherein plasma P_{CO_2} remained significantly elevated (9.60 ± 1.06 and 5.71 ± 1.14 Torr and at $t = 2$ and 4 h respectively) in acetazolamide-injected hagfish compared to both pairwise controls (2.61 ± 0.41 and 1.05 ± 0.18 Torr and at 2 and 4 h recovery respectively) and pre-exposure control values. At 6, 8 and 10 h recovery, plasma [HCO_3^-] was significantly elevated in acetazolamide-injected animals (32.60 ± 3.29, 22.76 ± 2.70 and 17.48 ± 2.11 mmol HCO_3^- L^{-1}) compared to pair-wise control animals (23.54 ± 2.91, 13.54 ± 3.18 and 8.31 ± 1.62 mmol HCO_3^- L^{-1}) and at 10 h recovery, plasma [HCO_3^-]

only remained elevated in acetazolamide-injected hagfish compared to pre-exposure levels.

Following exposure to hypercapnia, hagfish plasma $[HCO_3^-]$ decreased at a rate of 4470 µmol ± 675 µmol kg^{-1} h^{-1} over the first 2 h of recovery (Figure 3.7). Interestingly, hagfish demonstrated a delay in increasing capacity for HCO_3^- loss, significantly increasing rate of HCO_3^- loss during the 4 – 6 h recovery period to 9761 ± 1528 µmol kg^{-1} h^{-1}, suggesting time is required to upregulate HCO_3^- excretion mechanisms following hypercapnia. In the remainder of the recovery period, rates of HCO_3^- loss decreased (5057 ± 451 and 2574 ± 934 µmol kg^{-1} h^{-1} at the 6 – 8 and 8 – 10 h recovery periods respectively) as plasma $[HCO_3^-]$ returned to control values (Figure 3.2C).

By comparison, rate of HCO_3^- loss in acetazolamide-injected animals remained unchanging throughout the entirety of the recovery period ranging between 2372 – 5130 µmol kg^{-1} h^{-1} (Figure 3.7).

Discussion

This study is the first to characterize the mechanistic aspects of hypercapnia recovery strategies in any fish species. Previously, Baker et al. (2015) reported that when exposed to hypercapnia (30 torr or 4% CO_2), hagfish rapidly accumulate HCO_3^- to offset the acidosis, attaining the highest measured plasma $[HCO_3^-]$ in any vertebrate to date (~55 mmol L^{-1} and ~80 mmol L^{-1} by 24 and 48 h, respectively). This rise in plasma $[HCO_3^-]$ was also associated with equimolar decreases in plasma $[Cl^-]$, which is supported by results from the current study. This equimolar exchange may suggest that Cl^-/HCO_3^- exchange is the dominant mechanism used to directly elevate plasma HCO_3^- to compensate for the hypercapnia-induced acidosis. However, an alternative mechanism to increase plasma HCO_3^- is to utilize the high P_{CO_2} gradients to convert CO_2 to HCO_3^- (either CA- dependent or CA-independent) with the resultant H^+ and Cl^- being excreted into the environment. Indeed, at the conclusion of hypercapnia (current study), and when hagfish are branchially exposed to hypercapnia (Chapter 4, unpublished results), net H^+ equivalent excretion is observed from the whole animal.

Few other examples exist of this degree of compensation, the closest likely being the channel catfish (*Ictalurus punctatus;* ~50 mmol HCO_3^- L^{-1} after exposure to progressive hypercapnia; 60 torr) and the blue crab (*Callinectes sapidu;* ~40 mmol HCO_3^- L^{-1} following progressive hypercapnia; 50 torr) (Cameron and Iwama, 1987). However, for each of these organisms, no differences in plasma $[Cl^-]$ were detected, likely due to their inability to measure differences against high plasma $[Cl^-]$ levels (Cameron and Iwama, 1987). When exposed to ~24 Torr CO_2 (~3.16% CO_2) for 96 h, white sturgeon (*Acipenser transmontanus*) experienced elevations in plasma $[HCO_3^-]$ to 21.2 mmol

HCO_3^- L^{-1} (Crocker and Cech, 1998). However, in the three species listed above, HCO_3^- accumulation did not effectively compensate the blood acidosis experienced by the organisms (Cameron and Iwama, 1987; Crocker and Cech, 1998).

My results suggest that as impressive as it is for the hagfish to mount the incredible hypercarbia load within 48 h, still more impressive is the fact that the hagfish can recover to basal levels within 8 h and the associated alkalosis is also corrected for within ~10 h. Substantial rates in whole-animal HCO_3^- loss ($\frac{dHCO_3^- \cdot \frac{1}{m}}{dt}$) were noted throughout recovery, peaking at ~10,000 μmol kg^{-1} h^{-1} within the $4 - 6$ h recovery time-frame (Figure 3.7). By comparison, white sturgeon experienced plasma HCO_3^- loss at a rate of ~570 μmol kg^{-1} h^{-1} from hypercapnia-induced hypercarbia over a period of 24 h, based on utilizing equation 6 and their reported values (Crocker and Cech, 1998). Crocker and Cech, measured only a single recovery time-point at 24 h and considerably less time may have been taken to recover plasma [HCO_3^-] to control values. Even if full recovery was realized rapidly within the unlikely window of 2 h of recovery, $\frac{dHCO_3^- \cdot \frac{1}{m}}{dt}$ would still only be ~6800 μmol kg^{-1} h^{-1}; again highlighting that hagfish are still champions of acid/base regulation (Crocker and Cech, 1998).

Possible routes for reducing HCO_3^- in the plasma include tissue/red blood cell accumulation, direct excretion, diffusion into the surrounding seawater, metabolic consumption, glomerular filtration and production of alkaline urine, and CA-mediated conversion of HCO_3^- to CO_2 at the gill membrane. Given the lack of HCO_3^- permeability in hagfish red blood cells (Peters et al., 2000), and the lack of changes in epaxial muscle intracellular pH during recovery from base injection (6000 μequiv kg^{-1} as $NaHCO_3$;

Clifford et al., 2014), muscle tissue or red blood cell accumulation can likely be ruled out. Diffusion into seawater can also likely be ruled out given that repeated $NaHCO_3$ injections (6000 μequiv kg^{-1} as $NaHCO_3$) had diminished blood pH and plasma TCO_2 effects, suggesting that HCO_3^- excretion was actively regulated (Tresguerres et al., 2007a). Metabolic consumption of HCO_3^- can be accomplished by the OUC (ornithine urea cycle) -mediated conversion of NH_3. However, given that only minor increases in J_{Amm} were observed in the current study, and considering hagfish lack a complete complement of OUC enzymes (Braun and Perry, 2010; Read, 1975), metabolic consumption can also be ruled out.

I also investigated the potential for renal HCO_3^- loss as a mechanism using GFR as a surrogate, assuming no concentrative ability of the hagfish kidney as has been previously demonstrated for Atlantic hagfish (Alt et al., 1981). I did measure statistically significant increases in GFR within the $2 - 4$ h recovery period, alongside arguably biologically significant increases at the $0 - 2$ and $4 - 6$ h recovery periods. However, the fact that all fish lack the ability to resorb fluid and cannot concentrate HCO_3^- in their urine (Alt et al., 1981), means that these increases can only account for less than 5% of the realized restorations in plasma HCO_3^- (Table 3.1). This, combined with the low urinary flow rates previously described in Atlantic hagfish (Morris, 1965) suggests that the contribution of the kidneys to overall HCO_3^- excretion is nominal.

I hypothesized that following hypercapnia exposure, TCO_2 recovery would be characterized by rapid passive CO_2 loss from the hagfish due to the considerable internal vs. external P_{CO_2} gradients. Secondarily, I hypothesized that the largest component of the remaining TCO_2 load would be secondarily excreted *via* Cl^-/HCO_3^- mediated exchange,

since the rapid diminishment of the P_{CO_2} gradients reduces loss by passive CO_2 diffusion. In the present study, during recovery TCO_2 declined rapidly recovering within $6 - 8$ h while sustaining an impressive ~0.7 pH unit alkalosis. Blood P_{CO_2} re-equilibrated rapidly within 2 h while plasma HCO_3^- declined more-or-less steadily throughout the first 8 h of recovery. HCO_3^- flux remained negligible within the first two hours but was significantly elevated between 2 and 8 h of recovery.

At first glance, these data support my hypothesis for the possible route of TCO_2 recovery. Plasma P_{CO_2} rapidly equilibrates over the first 2 h; however, the remaining TCO_2 load (pre-dominantly speciated as HCO_3^-) is excreted *via* an epithelial HCO_3^- excretion mechanism that must be up-regulated or activated. However, the continual alkalization of blood pH (Figure 3.2A) is not explained by this mechanism and suggests that TCO_2 recovery continues to be mediated *via* a gaseous CO_2 loss from the animal. More importantly, following the 2 h recovery period there was a significant and sustained increase in $J_{Net}^{HCO_3^-}$ to ~2330 µequiv HCO_3^- kg^{-1} h^{-1}, lasting until 8 h recovery (Figure 3.4A). This metric is a measure of direct HCO_3^- flux, likely mediated *via* a CBE. However, total $\frac{dHCO_3^- \cdot \frac{1}{m}}{dt}$ based on plasma HCO_3^- exceeded $J_{Net}^{HCO_3^-}$ by ~3 – 4-fold over the same recovery periods peaking at >10,000 µmol kg^{-1} h^{-1} (see Figure 3.7), strongly suggesting another mechanism for TCO_2 recovery was at play.

Based on the alkalization of the blood during recovery and these incongruences between $J_{Net}^{HCO_3^-}$ and $\frac{dHCO_3^- \cdot \frac{1}{m}}{dt}$, I hypothesized that the secondary mechanism for TCO_2 loss may be CA-mediated conversion of HCO_3^- to CO_2 (as CA-independent conversion occurs at low rates – see Figure 3.1). Therefore the next series of experiments were designed to

investigate this possibility by using the CA inhibitor acetazolamide to partition relative contributions of CA and CBE related mechanisms to HCO_3^- loss.

If this hypothesis were correct, as blood circulates and enters the gills, gaseous CO_2 diffuses across the gill epithelia, maintaining a driving gradient to convert residual plasma HCO_3^- to gaseous CO_2 which also diffuses across the gill epithelia. This rapid conversion between HCO_3^- and CO_2 at the gills is mediated by CA activity. Acetazolamide inhibits CA activity, impairing the normally rapid turnover. Following injection of acetazolamide, blood P_{CO_2} did not recover to pre-exposure levels until 6 h recovery. While gaseous CO_2 is still able to permeate across the gill epithelia, the conversion of HCO_3^- to CO_2 happens at a much lower rate and diffusion of CO_2 is perfusion-limited. This elevation in blood P_{CO_2} suppressed the normal post-recovery alkalosis (Figure 3.6A), and late in recovery (6 – 10 h) reduced the rate of CA-mediated $\frac{dHCO_3^- \cdot \frac{1}{m}}{dt}$ (Figure 3.7), explaining the delayed release of HCO_3^- until later time periods. This response clearly suggests that CA-mediated HCO_3^- to CO_2 conversion followed by passive CO_2 flux is the dominant mechanism for reduction in plasma $[HCO_3^-]$ in a hypercapnia compensated hagfish. Based on plasma $\frac{dHCO_3^- \cdot \frac{1}{m}}{dt}$ data, this CA-mediated mechanism must be either up-regulated or activated, as peak rates were observed at the 4 – 6 h recovery period.

Despite the stated importance of the CA-mediated TCO_2 loss, direct Cl^-/HCO_3^- flux still contributes to net loss. When comparing plasma $[HCO_3^-]$ and $[Cl^-]$ data, this suggests an equimolar exchange with the two solutes. This secondary recovery mechanism could possibly be mediated by an anion exchanger (SLC4 family of

transporters) or a CBE (SLC26 family of transporters). What is apparent is that the mechanism is up-regulated/activated, taking at least ~2 h of recovery to occur as hypothesized by Tresguerres et al. (2007). In their study, repeated HCO_3^- injections caused increases in V-H^+-ATPase (VHA) abundance in whole gill and gill membrane fractions suggesting insertion into the (likely basolateral) membrane during hypercarbia to allow resorption of H^+ into the blood was necessary to aid in HCO_3^- excretion. Unfortunately antibodies for these transporters and CA are not available at this time. However, qPCR analysis could be done following identification of potential transporters and CA isoforms in available hagfish transcriptomes and this is the subject of future investigations.

Whether these same mechanisms are responsible for recovery from infusion induced hypercarbia during $NaHCO_3$ infusion (*e.g.* Tresguerres et al., 2007) or other experiment manipulations is unknown and warrants further investigation. Furthermore, the cellular localization of the CA responsible could either be intracellular or exofacial on the membrane of mitochondrion-rich cells. Acetazolamide is a permeable inhibitor, able to inhibit both CA types. A potential future direction would be to use an impermeant extracellular CA inhibitor (*e.g.* benzolamide; Perry et al., 1999) to identify the localization of the CA responsible for mediating recovery.

For the hagfish to have the ability to rapidly adjust plasma HCO_3^- levels, there should be an ecological relevance to such an adaptation. It is unlikely for hagfish to ever experience P_{CO_2} tension levels used in the current, or previous studies (Baker et al., 2015) in nature. However, a possible scenario where hagfish experience mild hypercapnia tensions is during feeding (Evans, 1984). As active scavengers, hagfish consume

decaying flesh from carrion that falls to the ocean floor (Martini, 1998) whereby they may enter into large mammalian carrion (*e.g.* whale and other large carcasses; Smith and Baco, 2003) that while alive have CO_2 tensions of ~5% CO_2. Moreover, hagfish potentially reside inside these carcasses for considerable periods of time and this carrion would also be consumed by micro-organisms, which in turn would be producing considerable amounts of CO_2, thus presenting hypercapnic conditions to the hagfish. Given the recent advances describing cutaneous uptake of amino acids (Glover et al., 2011) and phosphate (Schultz et al., 2014), and my previous study demonstrating that base excretion is mediated by cutaneous means (Clifford et al., 2014), future research efforts should focus on identifying if cutaneous base excretion also occurs during hypercapnia-induced hypercarbia.

Conclusions

My results show that following extended hypercapnia (4% CO_2) exposure, the resultant compensatory plasma [HCO_3^-] load, which takes $24 - 48$ h to mount (Baker et al., 2015), is rapidly offloaded within $6 - 8$ hrs. While considerable increases in both $J_{HCO_3^-}$ and GFR are observed throughout recovery (>2 h), neither of these increases can account for the observed rates of whole-animal HCO_3^- loss from the hagfish (Figure 3.4,7 and Table 3.1). Instead, restoration of plasma TCO_2 and [HCO_3^-] from hypercapnia-induced hypercarbia is likely facilitated in a multi-staged manner, initially relying on passive CO_2 diffusion, and later relying primarily on CA-mediated conversion of HCO_3^- to CO_2 which is passively diffused across epithelia and, after $2 - 4$ h of recovery, up-regulation of CBE mediated HCO_3^- loss.

Tables

Table 3.1 Calculation of relative contribution of GFR to net HCO_3^- flux.
The volume of plasma filtered was based on measured GFR from Figure 3.5. Rate of HCO_3^- filtration was calculated as the plasma volume filtered in 2 h multiplied by the net HCO_3^- loss observed during the same time period and then converted into a rate. GFR-specific contribution to HCO_3^- flux was calculated as the percent of net HCO_3^- filtration (μmol kg^{-1} h^{-1}) compared to $J_{Net}^{HCO_3^-}$ (μmol kg^{-1} h^{-1}) at the same time period.

		Time period (h)				
		0 – 2	2 – 4	4 – 6	6 – 8	8 – 10
GFR	mL kg^{-1} h^{-1}	3.88	4.20	4.21	2.89	2.68
Plasma filtered in 2 h	mL kg^{-1}	7.77	8.40	8.41	5.78	5.37
Δ [HCO_3^-] in 2 h	mmol L^{-1}	11.5	10.8	20.0	10.0	5.2
Net HCO_3^- filtered in 2 h	μmol kg^{-1}	89.2	90.7	168.2	57.8	28.0
Rate of HCO_3^- filtration	μmol kg^{-1} h^{-1}	44.6	45.4	84.1	28.9	14.0
Rate of J_{HCO3^-}	μmol kg^{-1} h^{-1}	7.7	2327.3	2092.0	2319.6	1131.4
GFR-specific contribution to HCO_3^- Flux	%	100	1.95	4.02	1.25	1.24
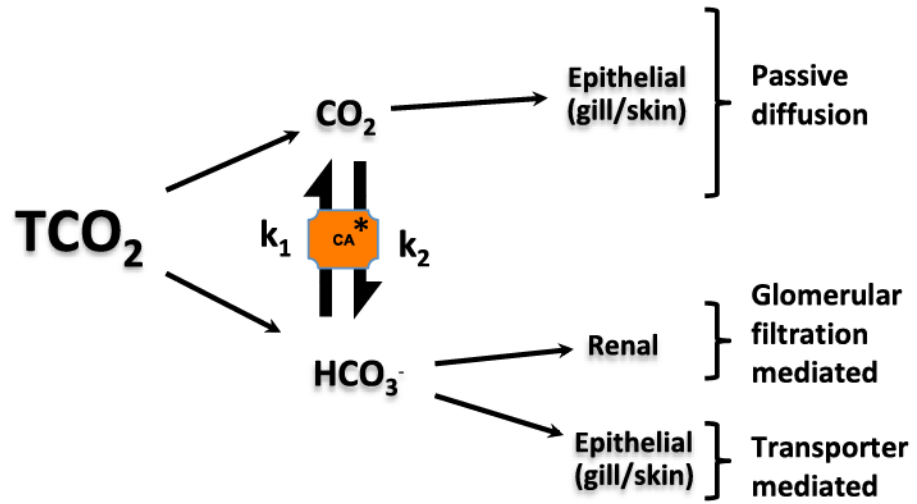
Figure 3.1 Prospective routes for TCO$_2$ (Total CO$_2$ content) loss in hagfish.

TCO_2 is comprised of the partial pressure of CO_2 (P_{CO_2}) and HCO_3^- in a biological system. Uncatalyzed hydration of CO_2 occurs rapidly ($K_1 = 3.5 \times 10^{-2}$ s^{-1}) while dehydration is rate limiting; occurring more slowly by ~3 orders of magnitude ($K_2 = 20$ s^{-1}; Edsall, 1968). In the presence of catalytic carbonic anhydrase (CA), conversion between CO_2 and HCO_3^- occurs at a near instantaneous rate (Henry and Heming, 1998). Gaseous CO_2 can be lost across epithelia passively or converted to HCO_3^-, while HCO_3^- loss can either be mediated *via* glomerular filtration or transported across epithelia *via* transporters. HCO_3^- can also be converted to gaseous CO_2 *via* CA mediated conversion.
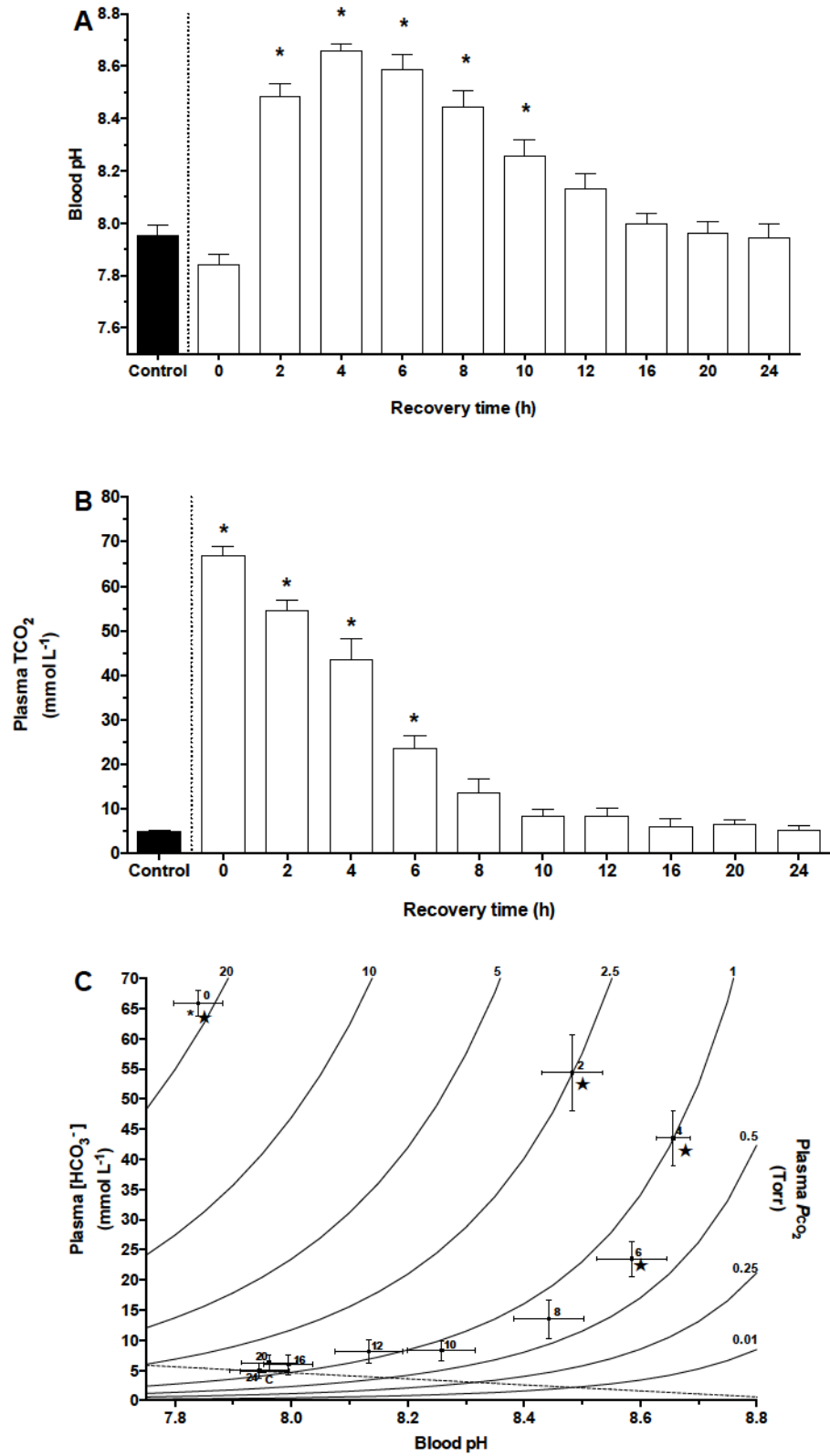
Figure 3.2 Blood and plasma acid/base parameters.

Blood and plasma acid/base parameters of hagfish prior to (Control; closed bar) and during 48 h recovery (open bars) from exposure to 4% CO_2 in normocapnic seawater. Blood pH (A) and plasma TCO_2 (B) were measured prior to exposure and throughout the 48 h recovery in normocapnic seawater. (C) Calculated blood pH/plasma HCO_3^- diagram depicting the acid/base status of hagfish blood following 48 h exposure to 4% CO_2 and during recovery in normocapnic seawater. The dotted line represents the non-bicarbonate buffering capacity as determined by Wells et al. (1986). Data are presented as mean + s.e.m. $n = 6$. Bars with an asterisk (*) are significantly different compared to control values; $p < 0.05$, one-way repeated measures ANOVA with Holm-Sidak $post$-hoc analysis. In (C), asterisk (*) depicts blood P_{CO_2} while star (★) depicts differences in plasma [HCO_3^-], compared to control values. For blood pH differences see Figure 2A.
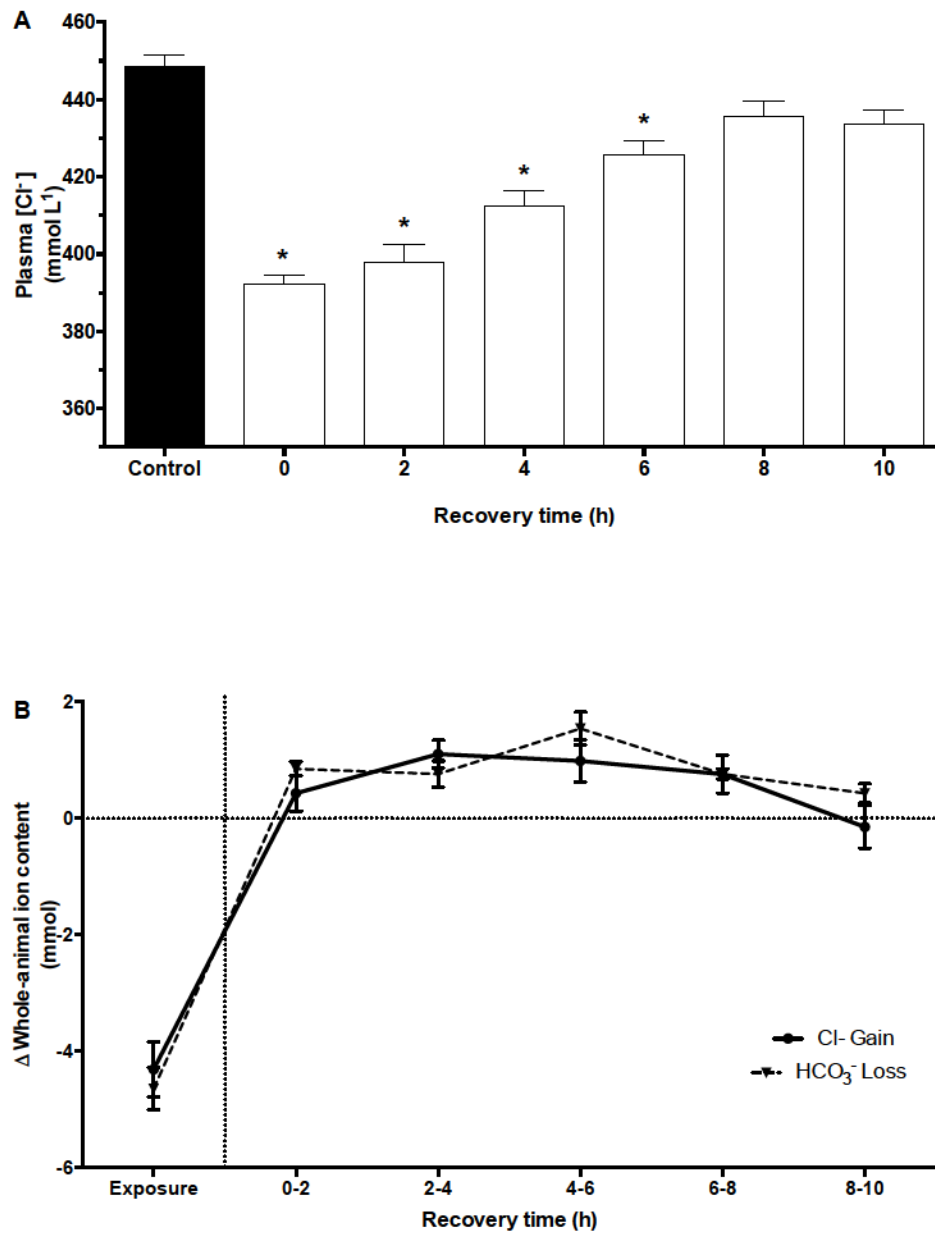
Figure 3.3 Plasma ion concentrations during recovery.

Plasma ion concentrations of hagfish exposed to 4% CO_2 for 48 h and during 10 h recovery. (A) Plamsa $[Cl^-]$ was measured prior to (Control; closed bar) and immediately following exposure (0) and throughout the 24 h recovery in normocapnic seawater. (B) Changes in total plasma HCO_3^- loss in relation to changes in total plasma Cl^- gain. Data are presented as mean + s.e.m. $n = 6$. In (A) bars with an asterisk (*) are significantly different to control values; $p < 0.05$, one-way repeated measures ANOVA with Holm-Sidak *post-hoc* analysis. No differences were observed in (B).
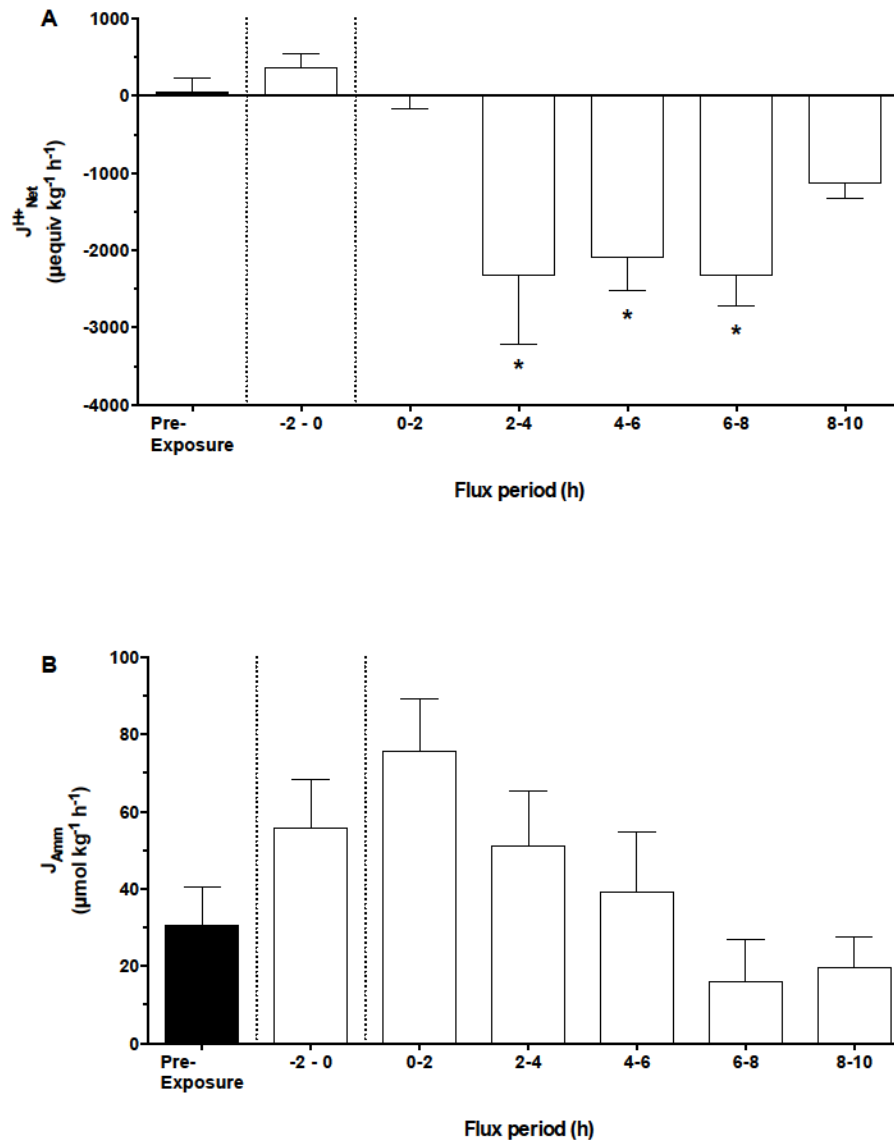
Figure 3.4 H$^+$/HCO$_3^-$ and ammonia flux during recovery.

(A) Net outward H^+ (positive values) or HCO_3^- (negative values) equivalent flux and (B) J_{Amm} from hagfish prior to 4% hypercapnia exposure (Control; closed bar), prior to recovery (-2 – 0 h) and during recovery (open bars) in normocapnic seawater. Data are presented as mean + s.e.m. n = 6. Data with an asterisk (*) are significantly different compared to control values; $p < 0.05$, one-way repeated measures ANOVA with Holm-Sidak correction.
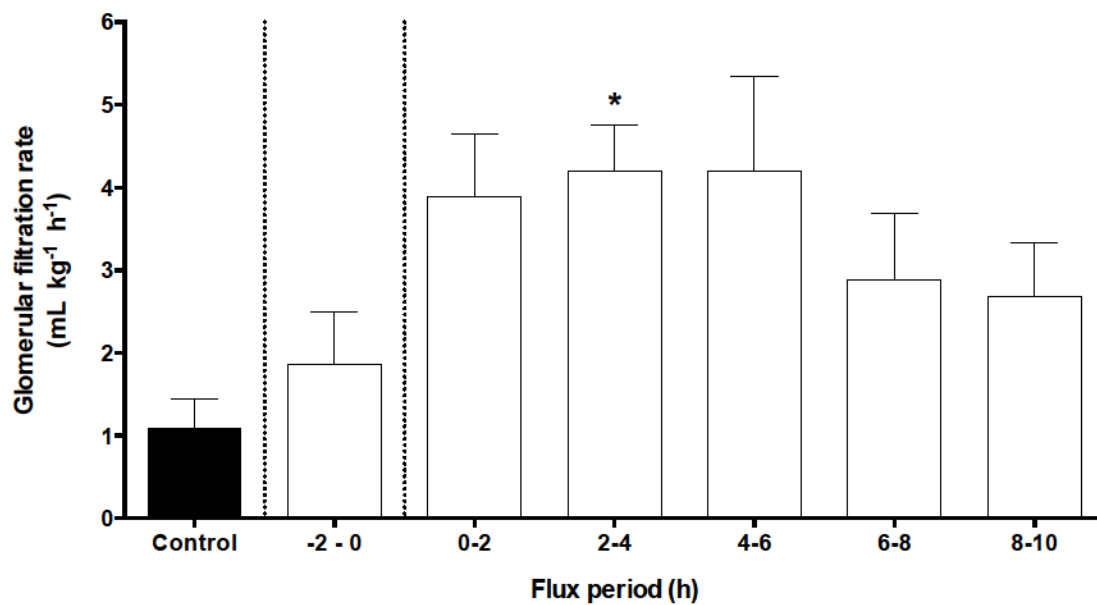
Figure 3.5 Glomerular filtration rate during recovery.

Glomerular filtration rate in hagfish measured prior to exposure (48 h) to 4% CO_2 (Control; closed bar), prior to recovery (-2 – 0 h) and during recovery (open bars) in normocapnic seawater. Data are presented as mean + s.e.m. $n = 6$. Data with an asterisk (*) are significantly different compared to control values; $p < 0.05$, one-way repeated measures ANOVA with Holm-Sidak correction.
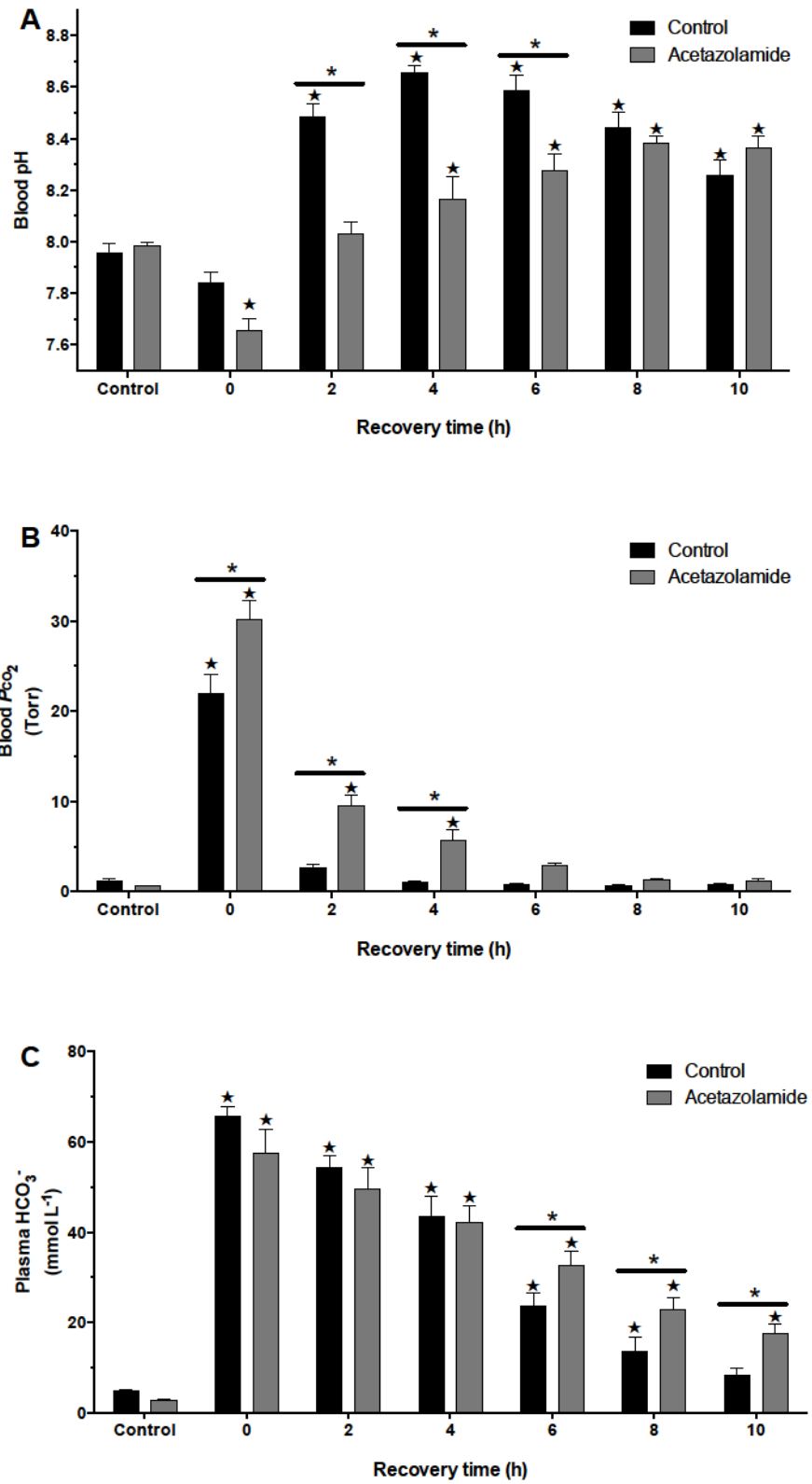
Figure 3.6 Effect of acetazolamide on blood and plasma acid/base parameters.

Blood and plasma acid/base parameters in hagfish exposed to 4% CO_2 for 48 h prior to being injected with carbonic anhydrase inhibitor (40 mg kg^{-1}) acetazolamide (closed bars) or receiving no injection (Control; previously reported in figure 3.2), and then allowed to recover in normocapnic water. Measured blood pH (A) and plasma TCO_2 (not shown) were measured prior to exposure and throughout the 48 h recovery in normocapnic seawater and converted into blood P_{CO_2} (B) and plasma $[HCO_3^-]$ (C). Data are presented as mean + s.e.m. $n = 6$. Bars with a star ($\star$) are significantly different compared to pre-exposure control values; $p < 0.05$, two-way repeated measures ANOVA with Holm-Sidak *post-hoc* test. Significant differences between control and acetazolamide values are signified with a horizontal bar and asterisk (_*_); $p < 0.05$, two-way repeated measures ANOVA with Fisher's LSD *post-hoc* test.
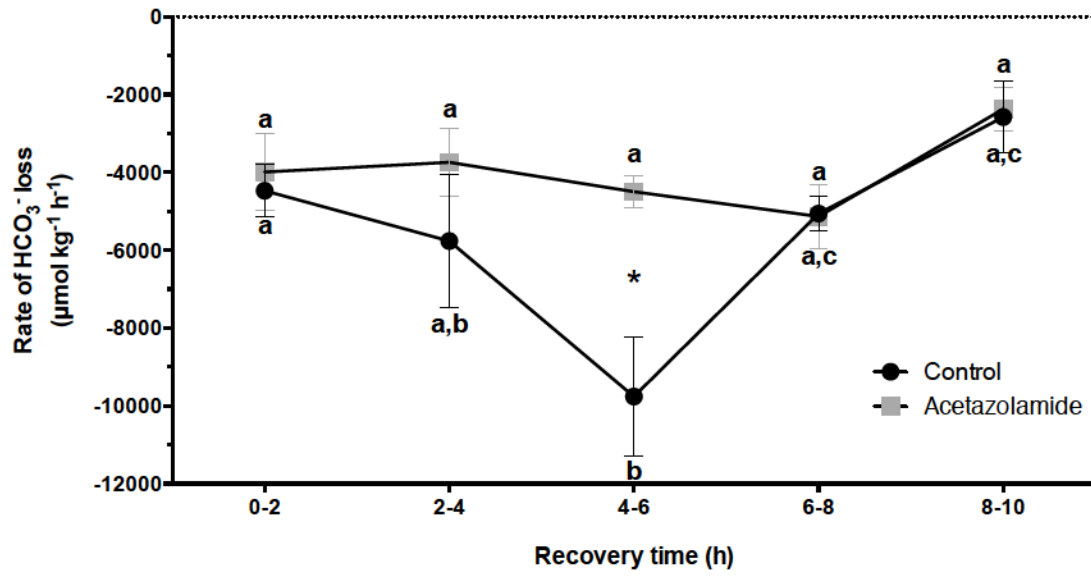
Figure 3.7 Calculated $\frac{dHCO_3^- \cdot \frac{1}{m}}{dt}$ **or rate of HCO$_3^-$ loss.**

Calculated $\dfrac{dHCO_3^- \cdot \frac{1}{m}}{dt}$ or rate of HCO$_3^-$ loss in hagfish exposed to 4% CO$_2$ for 48 h prior to injection with carbonic anhydrase inhibitor (40 mg kg^{-1}) acetazolamide (grey squares) or receiving no injection (control; black circles), then allowed to recover in normocapnic water. Values sharing the same letter within a group are not significantly different; $p < 0.05$, two-way repeated measures ANOVA with Tukey's *post-hoc* test. Values between groups with an asterisks (*) are significantly different; $p < 0.05$, two-way repeated measures ANOVA with Fisher's LSD *post-hoc* test.

Chapter 4: Extrabranchial recovery strategies from hypercapnia-induced hypercarbia in Pacific hagfish

Introduction

The scavenging hagfish feeds by burrowing into decaying carrion and consuming soft tissue (Strahan, 1963). This feeding lifestyle likely presents several physiological challenges to the scavenger. During land-based mammalian decomposition, micro-organisms feeding on carcasses yield considerable amounts of ammonia (Carter et al., 2007), and CO_2 (Carter et al., 2007; Putman, 1978) presenting severe acid/base challenges to the scavenger (Clifford et al., 2014; Clifford et al., 2015a; Clifford et al., 2015b).

While numerous studies exist on hagfish acid/base regulation following acid/base stress, all previous studies have used supra-physiological stresses [*e.g.* 4% P_{CO_2} (partial pressure of CO_2) exposure (Baker et al., 2015; Chapter 2), injection of 3000 μequiv kg^{-1} H_2SO_4 (McDonald et al., 1991), injection of 6000 μmol kg^{-1} HCl or $NaHCO_3$ (Clifford et al., 2014; Parks et al., 2007b; Tresguerres et al., 2007a)], to characterize the physiological responses to such challenges. Furthermore, past research efforts on hagfish acid/base and ammonia physiology have primarily focused on gill (branchial) mechanisms of regulation (Clifford et al., 2015a; Edwards et al., 2001; Edwards et al., 2015; McDonald et al., 1991; Parks et al., 2007b; Tresguerres et al., 2007a) while extrabranchial mechanisms are generally overlooked. Partial burrowing into carrion by the hagfish (Strahan, 1963) leaves the branchial region of the animal directly exposed to the putrefied environment while the tail-region remains distal to the carcass thereby providing an excretory route for anteriorly-acquired acid/base constituents. Indeed, the capillary vasculature in the subepidermal skin of the hagfish is extensive (Hans and Tabencka, 1938; Lametschwandtner et al., 1989) and the simplistic body plan of the hagfish provides a

high epidermal surface area to volume ratio. Thus the skin represents a considerable epithelial tissue that may contribute to overall homeostasis. Furthermore, recent studies have begun to highlight the involvement of hagfish skin in the acquisition of trace metals (Glover et al., 2015), nutrients such as amino acids and phosphate (Glover et al., 2011; Schultz et al., 2014) and in acid/base balance (Clifford et al., 2014).

Recently, Baker et al. (2015) demonstrated then when exposed to extreme levels of hypercapnia (6.6% CO_2), hagfish were able to tolerate long exposures by mounting a compensatory HCO_3^- loading response to offset the acidosis. However, the mechanism(s) by which this response is mediated are unknown.

An elevation in environmental P_{CO_2} will result in CO_2 entering down partial pressure gradients, leading to an acidosis within the organism. HCO_3^- compensation occurs then by one of two mechanisms (or perhaps both). One possibility is for hagfish to directly exchange available plasma Cl^- for environmental HCO_3^-. Under this scenario, exchange of Cl^- and HCO_3^- would be directed *via* a chloride bicarbonate exchanger (CBE). A secondary route for mounting the noted elevation in plasma HCO_3^- in response to the induced acidosis is for the animal to rapidly hydrate the CO_2 into H^+ and HCO_3^-, with secondary excretion of H^+ into the environment across epithelia either by VHA (Vacuolar H^+-ATPase) or NHE (Na^+/H^+ Exchanger) -mediated mechanisms, thereby correcting plasma pH. Thermodynamically, secondary excretion of H^+ must be associated with an equimolar loss of Cl^- through a Cl^- channel. In either scenario, gain of HCO_3^- is either directly or indirectly exchanged for Cl^- (Baker et al., 2015; Cameron and Iwama, 1987; Goss and Wood, 1990a,b; 1991).

The primary goal of this study was to characterize if lower, environmentally realistic P_{CO_2} tensions induce similar extrabranchial pH recovery strategies in hagfish as higher tensions do. Furthermore, I aimed to directly compare these results to my previous study (Chapter 2) where hagfish were directly injected with $NaHCO_3$ (Clifford et al., 2014) and the posterior skin was proposed to play a significant (perhaps dominant) role in overall base excretion. A final goal was to describe how hagfish respond to localized hypercapnia exposure with respect to how the HCO_3^- compensation response is mounted.

In this study, Pacific hagfish (*Eptatretus stoutii*) were exposed to mild hypercapnia (0.6% CO_2) for 72 h to simulate a low-level hypercapnic environment similar to that which the organism may experience naturally. Using custom designed separating chambers, I then allowed hagfish to recover in normocapnic water for 4 h thereby allowing me to determine anterior (branchial + cutaneous) and posterior (cutaneous only) contributions to net acid/base equivalent flux. Based on results from Clifford et al. (2014), I hypothesized that hagfish will excrete resultant hypercarbia loads *via* posteriorly (i.e. extrabranchially) -mediated mechanisms. In a second series of experiments, utilizing the separating chambers, hagfish were exposed to either anteriorly- or posteriorly-localized hypercapnia to determine the effects of localized hypercapnia (as might be experienced during partial burrowing) on the animal's response. I predicted that when exposed to either anteriorly- or posteriorly-localized hypercapnia, hagfish will mount hypercarbia responses similarly in each condition and that net acid excretion (or base absorption) would be observed over the course of the exposure period.

Materials and methods

Experimental animals and holding

Pacific hagfish (*Eptatretus stoutii*) were captured from Trevor channel, Vancouver Island, BC, Canada *via* a bottom-dwelling trap baited with rotting hake. Hagfish were transferred to Bamfield Marine Sciences Centre and housed in aerated, darkened 20 m^3 tanks receiving flow-through seawater. Hagfish were fed bi-weekly with rotting fish during captivity and fasted at least for one week prior to experimentation. All animals were used under the licenses of Department of Fisheries and Oceans Canada collection permit XR 192 2014 and University of Alberta Animal Care protocol number AUP0001126

Chemicals

Unless noted, all other chemical compounds, reagents and enzymes were supplied by Sigma-Aldrich Chemical Company (St. Louis, MO).

Experimental protocol

Series 1: Partitioning of hypercarbic recovery following chronic 0.6% hypercapnia

Hagfish (N=28; 103.92 ± 4.81 g; mean ± s.e.m.) were anaesthetized in seawater with 0.5 g L^{-1} tricaine methanesulfonate (TMS; Syndel Laboratories Ltd., Vancouver, British Columbia, Canada) neutralized with 0.15 g NaOH. This dose of TMS was sufficient to keep the animal sedated for ~5 minutes and allowed for rapid recovery from blood sampling and insertion into separating chambers (see below). Fish were then held

vertically causing pooling of blood in the caudal subcutaneous sinus within 20 seconds. A 200 μl control (pre-exposure) blood sample was then drawn from the sinus with a 21G needle and 1 mL disposable syringe that was rinsed with heparinized hagfish saline (50 U mL^{-1} heparin in 0.5 mol L^{-1} NaCl). Blood samples were immediately analyzed (see below) and hagfish were transferred into individual 5 L containers with tight-fitting lids receiving seawater aerated with either air (Normoxia) or 0.6% CO_2 in air (Hypercapnia) equilibrated water from a 40 L header tank. Normoxia and hypercapnia levels were further maintained within individual containers *via* direct aeration with either air or hypercapnic 0.6% CO_2 in air. Hypercapnic P_{CO_2} levels were achieved *via* utilization of a dual-supply precision gas blender (FM4333/FM4336 Matheson, Basking Ridge, New Jersey) receiving 20% CO_2 in air (Praxair) and normoxic air.

Hagfish were exposed to either normoxic or hypercapnic conditions for 72 h after which time animals were anaesthetized and blood sampled (as above) then quickly blotted dry and weighed. To determine cutaneous acid/base flux without the potential for additional acid or base equivalents coming from the cloacal compartment, the cloaca was sealed by first blotting the cloacal region of the animal dry with Kim wipe and then applying instant cyanoacrylate glue to seal the cloaca shut, allowing the glue to air dry for ~15 seconds. A nitrile rubber bandage (2.0cm X 1.0 cm) was then affixed to the cloacal region using cyanoacrylate. This technique has been previously validated (Clifford et al; 2014).

Hagfish were placed into divided chambers that isolated the posterior body region from the anterior region (see Clifford et al., 2014 for apparatus and protocol details). Seawater was then added to the anterior compartment only, and partitioning-seal efficacy

checked by monitoring for water appearance in the posterior compartment. Seawater was then added to the posterior compartment and a lid secured. The chamber was placed in a wet table receiving flowing seawater for temperature control (10 ˚C). Two 25 mL water samples were collected for H^+ determination following placement of hagfish into the chamber and following the 4 h recovery period. After final sample collection, the patency of the seal was visually inspected, the hagfish removed from the apparatus, and anaesthetized and sampled (as above). Only those preparations that demonstrated no leakage were used for calculations of flux.

Series 2: Physiological responses to localized hypercapnia

The effects of localized hypercapnia (0.6% CO_2) exposure in anterior vs. posterior body regions were determined by aerating each region individually to hypercapnia with the opposite region receiving aeration with normocapnic air. For control animals both anterior and posterior chambers were aerated with normocapnic air. To supply sufficient aeration, the perimeter of the chambers was lined with perforated airline tubing. First, hagfish were sampled for blood and placed in the divided chambers, sampled, then sealed (as above). After 4 h of exposure to the listed treatments, final water samples were taken and the animals removed and immediately blood sampled.

Blood sample analysis

Blood pH was measured immediately using a thermojacketed Orion ROSS Micro pH electrode (Fisher Scientific, Ottawa, ON). Blood samples were then centrifuged (12,000 *g* for 2 min) to obtain plasma which was then analyzed for total CO_2 (TCO_2)

using a Corning 965 carbon dioxide analyzer (Ciba Corning Diagnostic, Halstead, Essex, UK).

Measured values of blood pH and TCO_2 were used to calculate $[HCO_3^-]$ and P_{CO_2} at 10°C by the Henderson-Hasselbalch equation, using the general formulas derived by Heisler and cited in Boutilier et al. (1984) using the solubility of CO_2 (Weiss, 1974) and the dissociation constant of carbonic acid as a function of pH, temperature, and ionic strength for seawater as a surrogate for hagfish plasma (Mehrbach, 1973).

Proton fluxes

Net H^+ fluxes ($J_{H^+}^{Net}$) from anterior and posterior regions of hagfish were measured using techniques modified from (Heisler and Weitz, 1976) and described by Clifford et al. (2014). Briefly, water samples (25 mL) were removed from both the anterior and posterior chambers at *t=0* and *t=4 h* recovery and placed in a water bath held at 10 ˚C and the samples were bubbled with 20% CO_2. Water pH was measured using a thermojacketed Orion ROSS Micro pH electrode until a stable reading was obtained (drift < 0.002 pH units/10 sec for 1 min). pH readings were converted into μequivalents H^+ and differences between *t=0 h* and *t=4 h* were calculated. As the presence of the hagfish may change the buffering capacity of the experimental water, calculated H^+ differentials were corrected by measuring the buffering capacity of the seawater. The buffering capacity of seawater from both the anterior and posterior compartments was determined at *t=4 h* over the pH range observed during the course of the flux period. To determine buffering capacity, changes in pH were measured following the addition of known amounts of 0.1066 N HCl or 0.1 N NaOH to a separate 25 mL water sample. Buffering capacity was

calculated as the slope from the linear regression of μequivalent acid change per μequivalent acid/base added.

All corrected H$^+$ differentials were compared to differentials calculated in control chambers containing no fish and with buffering capacity determined at $t=0$ h. Thus, H$^+$ flux produced by the animal could be calculated. H$^+$ flux was calculated as (corrected experimental H$^+$ differential – corrected control H$^+$ differential)/weight of organism/time.

Thus, net H$^+$ flux produced by the animal could be calculated according to the following equation:

$$J_{H^+}^{Net} = \left[\left[\frac{\left(_{exp}H_{final}^+ - _{exp}H_{initial}^+ \right)}{_{exp}\beta} \cdot {_{exp}V} \right] - \left[\frac{\left(_{con}H_{final}^+ - _{con}H_{initial}^+ \right)}{_{con}\beta} \cdot {_{con}V} \right] \right] \cdot \frac{1}{m} \cdot \frac{1}{t} \qquad (1)$$

where $J_{H^+}^{Net}$ is the net proton flux, $_{exp}H_{final}^+$ and $_{exp}H_{initial}^+$ are the total proton concentration in the experimental samples, $_{con}H_{final}^+$ and $_{con}H_{initial}^+$ are the total proton concentrations in the control samples, $_{exp}\beta$ and $_{con}\beta$ are the determined buffering capacities of the experimental water and the control water, m is the mass of the hagfish and t is the total flux time.

Statistical analysis

All data are presented are given as mean ± s.e.m. Differences between groups were tested using one-way analysis of variance followed by Holm-Sidak *post-hoc* tests with pre-planned comparisons. Statistical significance was inferred when $p < 0.05$. All

statistical analyses were completed using GraphPad Prism 6.0 (GraphPad Software, San

Diego, USA).

Results

Blood and plasma responses during recovery from 72 h hypercapnia

Prior to exposure to hypercapnia (0.6% CO_2), hagfish blood pH averaged 7.98 ± 0.03 pH units (Figure 4.1A). Blood pH in paired unexposed hagfish prior to being fitted into the separating chamber apparatus did not significantly differ from pre-exposure values (7.97 ± 0.05 pH units), while in animals exposed to 0.6% CO_2 for 72 h, there was a marked blood alkalosis (8.31 ± 0.03 pH units). During the ensuing 4 h post-exposure recovery period, blood pH in both control fish and hypercapnia-exposed fish was significantly reduced (7.81± 0.02 and 8.04 ± 0.04 pH units respectively) compared to their respective 0 h (paired) blood pH.

Plasma TCO_2 values in control animals did not significantly differ from pre-exposure levels (8.56 ± 0.79 mmol CO_2 L^{-1}) either prior to (5.38 ± 0.87 mmol CO_2 L^{-1}) or after (7.13 ± 1.18 mmol CO_2 L^{-1}) the 4 h recovery period (Figure 4.2B). In contrast, animals pre-exposed to 0.6% CO_2 for 72 h demonstrated significantly increased plasma TCO_2 levels (40.23 ± 1.52 mmol CO_2 L^{-1}), which recovered by ~50% (23.1 ± 2.1 mmol CO_2 L^{-1}) after only 4 h of post-exposure recovery, towards pre-exposure values (Figure 4.2B)

Calculation of plasma [HCO_3^-] and P_{CO_2} in pre-exposed animals revealed a plasma [HCO_3^-] of 8.46 ± 0.79 mmol HCO_3^- L^{-1} and P_{CO_2} of 0.24 ± 0.02 kPa (Figure 4.1C), which did not significantly differ from control animals (5.32 ± 0.87 mmol HCO_3^- L^{-1} and 0.15 ± 0.02 kPa, respectively) prior to insertion into separating chambers. An elevation in P_{CO_2} was noted in control animals following the 4 h recovery period 0.34 ± 0.07 kPa that

differed only from initial but not pre-exposure P_{CO_2} values. Following exposure to 0.6% CO_2 for 72 h, hagfish displayed a substantial elevation in both plasma P_{CO_2} (0.45 ± 0.03 kPa) and [HCO_3^-] (40.06 ± 1.53 mmol HCO_3^- L^{-1}). Plasma [HCO_3^-] recovered by nearly 50% towards control values (22.87 ± 2.14 mmol HCO_3^- L^{-1}) following 4 h of post-exposure recovery (Figure 4.1C)

No significant differences in plasma [Cl^-] were detected between exposure and recovery (Figure 4.2A), likely due to high variability in response. However, a linear regression analysis of ΔPlasma [Cl^-] vs. ΔPlasma [HCO_3^-] displayed a clear linear trend between the two metrics with a slope of -0.5568. The calculated slope for the line of best fit did not significantly differ from a slope of -1.0 (Linear regression analysis; $F_{(1,24)}$ = 2.392, p = 0.1350; Figure 4.2B).

Partitioning of H^+ flux during recovery

Hagfish held under control (normocapnic exposure) conditions excreted minimal net H^+ flux from both the anterior (Figure 3A; 72.8 ± 96.1 μequiv H^+ kg^{-1} h^{-1}) and posterior (Figure 3B; 128.8 ± 167.2 μequiv H^+ kg^{-1} h^{-1}) regions during the 4 h recovery period. However, after 72 h of hypercapnia, post-hypercapnic exposed hypercarbic fish excreted significant amounts of base equivalents from both anterior (-258.1 ± 36.0 μequiv H^+ kg^{-1} h^{-1}; negative outward H^+ flux is equivalent to positive outward base flux) and posterior (-177.4 ± 42.2 μequiv H^+ kg^{-1} h^{-1}) segments.

Acid/base effects of localized hypercapnia.

Prior to exposure, hagfish blood pH averaged 7.82 ± 0.02 pH units (Figure 4.4a). Separation of these animals into the three treatment groups showed that all groups likely displayed a mild acidosis (control: 7.65 ± 0.04 pH units) due to the dividing chamber. Nevertheless, while anteriorly-exposed (7.69 ± 0.03 pH units) had the same blood pH as non-hypercapnic control hagfish, posteriorly-exposed (7.33 ± 0.05 pH units) displayed a significant acidosis. Interestingly, plasma TCO_2 and $[HCO_3^-]$ in pre-exposed animals (4.88 ± 0.23 mmol CO_2 L^{-1} and 4.80 ± 0.23 mmol HCO_3^- L^{-1} respectively) differed only from anteriorly-exposed animals (8.51 ± 0.35 mmol CO_2 L^{-1} and 8.31 ± 1.97 mmol HCO_3^- L^{-1} respectively; Figure 4.4B,C). Furthermore, hagfish that were anteriorly-exposed to hypercapnia displayed an ~2-fold increase in plasma $[HCO_3^-]$ (8.31 ± 1.97 mmol HCO_3^- L^{-1}) compared to post-exposure control animals (4.26 ± 1.53 mmol HCO_3^- L^{-1}); the acidosis displayed by posteriorly-exposed animals appeared uncompensated (4.71 ± 0.57 mmol HCO_3^- L^{-1}). Hagfish exposed to hypercapnia both anteriorly and posteriorly had significantly elevated plasma P_{CO_2} levels (0.52 ± 0.10 and 0.72 ± 0.09 kPa respectively) compared to control levels (0.30 ± 0.03 kPa) that approximated the expected 0.6% hypercapnia target (Figure 4.4C).

Partitioning of H^+ flux during localized hypercapnia

Non-exposed hagfish receiving aeration with normocapnic air in both anterior and posterior compartments excreted small amounts of base equivalents (-64.3 ± 8.3 µequiv H^+ kg^{-1} h^{-1} anteriorly and -81.5 ± 29.6 µequiv H^+ kg^{-1} h^{-1} posteriorly; Figure 4.5). During anteriorly-applied 0.6% hypercapnia, hagfish excreted substantial quantities of acid

equivalents (565.5 ± 252.9 μequiv $H^+ kg^{-1} h^{-1}$) anteriorly while posterior excretion remained unchanged (-69.2 ± 39.8 μequiv $H^+ kg^{-1} h^{-1}$). During posteriorly-applied hypercapnia, both anterior (16.4 ± 73.2 μequiv $H^+ kg^{-1} h^{-1}$) and posterior (-202.7 ± 59.1 μequiv $H^+ kg^{-1} h^{-1}$) excretion rates were not significantly different compared to control rates.

Discussion

Hagfish are extraordinary adept at overcoming acid/base challenges administered in a variety of different methods including acid and base infusion (McDonald et al., 1991; Parks et al., 2007b; Tresguerres et al., 2007a) and exposure to hypercapnia (Baker et al., 2015). Tolerance to acid/base stress is likely associated with the feeding lifestyle of the hagfish whereby they partially burrow into the flesh and soft tissues of decaying organisms (Evans, 1984; Martini, 1998; Strahan, 1963). The data in this chapter supports conclusions from Chapter 3 demonstrating that in addition to the hagfish being adept at compensating acid/base status during hypercapnia exposure (Baker et al., 2015), they can also readily offload large quantities of plasma TCO_2 /HCO_3^- rapidly following egress from hypercapnic sources.

In the current study, following 72 h of mild hypercapnia (0.6% CO_2), hagfish experienced substantial hypercarbia loads up to ~40 mmol HCO_3^- L^{-1} which were reduced by roughly 20 mmol HCO_3^- L^{-1} or ~50% recovered to control values within 4 h recovery in separating chambers (Figure 4.1). Comparing rates of HCO_3^- loss or $\frac{dHCO_3^- \cdot \frac{1}{m}}{dt}$ (see Chapter 3 for calculation) based on plasma data in the current study, hagfish were able to reduce plasma HCO_3^- at a rate of ~4300 μmol kg^{-1} h^{-1} over the 0-4 hour recovery period, in direct agreement with the rates reported in the similar recovery time period in Chapter 3.

During recovery, anterior + posterior measurements of H^+/HCO_3^- equivalent flux can be summed and total to ~435 μequiv HCO_3^- kg^{-1} h^{-1}. By comparison, in the first 4 hours of recovery following 48 h exposure to 4% CO_2, (Chapter 3), hagfish had a delay in

direct base excretion in the first $0 - 2$ h post-hypercapnia recovery period where negligible H^+/HCO_3^- equivalent flux was noted. However, in that study, in the $2 - 4$ h post-hypercapnic period, hagfish mounted a base excretory response of ~2200 μequiv HCO_3^- kg^{-1} h^{-1} (Chapter 3).

I proposed that this increase in base excretion was mediated by both an up-regulation/activation of Cl^-/HCO_3^- transporters and a co-incident up-regulation of CA-mediated TCO_2 loss as suggested by previous CA inhibitor studies (Chapter 3). While increases in GFR were noted in the past study, I did rule out that the flux of HCO_3^- was not mediated by an alteration in kidney function since hagfish produce urine at low rates (Morris, 1965) and their rudimentary kidney is not capable of fluid reabsorption, thereby lacking the ability to concentrate HCO_3^- in their urine (Alt et al., 1981). Future experimentation will be required to identify the molecular components responsible for the noted increase in flux rate (Chapter 3).

Comparing ΔPlasma $[Cl^-]$ vs. ΔPlasma $[HCO_3^-]$ values demonstrated a clear linear trend with respect to the two measured metrics. Similar 1:1 ratiometric patterns in Cl^-/HCO_3^- exchange have been noted in other studies involving acid base challenges (Baker et al., 2015; Cameron, 1978; Goss and Wood, 1990a,b;1991). This suggests that a Cl^-/HCO_3^- transport mechanism is responsible for recovery of blood pH from either acidosis or alkalosis during exposure when plasma HCO_3^- stores are built-up and during recovery when plasma $[HCO_3^-]$ is subsequently offloaded and supports conclusions made in Chapter 3. Thus the transporter(s) involved during exposure and recovery is/are most likely from the SLC26 family (Cl^-/HCO_3^- exchanger; CBE) or the SLC4 related family members (AE family of transporters) which are Cl^- linked HCO_3^- transport proteins

(Alper, 2006; Alper and Sharma, 2013). In the Goss lab hagfish Illumina transcriptomes, I have identified several SLC26 and SLC4 homologues, and future research will focus on obtaining full-length transcripts for these hagfish CBE and AE transporters followed by full phylogenetic analysis to successfully identify true molecular identity. qPCR analysis will also be used to ascertain potential involvement of various SLC26 and SLC4 isoforms during exposure to and recovery from hypercapnia.

Interestingly, in my previous study looking at branchial and extrabranchial recovery from infused blood alkalosis (Chapter 2; Clifford et al., 2014), hagfish utilized only posterior (skin) mechanisms to offload the resultant hypercarbia load in the 4 h recovery period immediately following injection. When infused with acid, acid excretion was observed in the anterior compartment. Based on this, I proposed that hagfish mitochondrion rich cells (MRCs), of which hagfish are proposed to possess only one type (Tresguerres et al., 2006a), are exclusively acid secreting with base excretion occurring *via* extrabranchial means. In the current study where hypercarbia was achieved *via* hypercapnia exposure, hagfish utilized both anterior (gills + skin) and posterior (skin only) mechanisms for base excretion. Thus, the results of the current study thus require a reconsideration of the capabilities of hagfish MRCs as it appears that branchial base excreting mechanisms must be up-regulated or activated to allow function. The single type of hagfish MRCs was originally identified by co-localization of NHE (Na^+/H^+ Exchanger), NKA (Na^+-K^+-ATPase) and VHA. Future co-localization studies should include CBE and NBC localization following different types of hypercarbic stress in order to determine the physiology of hagfish MRCs.

Possible explanations for differences in up-regulation/activation of HCO_3^- equivalent excretion include method of acid/base challenge administration (hypercapnia vs. infusion), degree of hypercarbia or length of acid/base disturbance. Considering metabolic alkalization *via* infusion yielded hypercarbia without the signal of high environmental P_{CO_2} as in the current chapter, perhaps a CO_2 signal is necessary in order to stimulate the gills for base excretion. Results in Chapter 3 suggest that that Cl^-/HCO_3^- transporting mechanisms (*e.g.* SLC26-like) must be up-regulated or activated, and that this only occurs at least 2 h after egress from hypercapnia. In the present study, it appears as though base excretion mechanisms in both the anterior and posterior segments of the hagfish are 'ready to go' within 4 h of recovery. One hypothesis for these different responses is perhaps the environmental CO_2 may be to act as a signal, up-regulating acid/base related transporters. Tresguerres et al. (2007) did note an increase in some transporter abundance (*e.g.* gill VHA) but only following repeated (4 times over 18 h) infusion with 6000 μmol kg^{-1} $NaHCO_3$. Studies involving measuring Cl^-/HCO_3^- transporter expression and abundance are needed to resolve this discrepancy in response. Localized hypercapnia experiments in the current study further support this theory suggesting that CO_2 sensing may be responsible for mounting compensatory responses during hypercapnia (see below).

The infusion protocol used previously (Chapter 2; Clifford et al., 2014) should yield a TCO_2 load of ~22 mmol L^{-1} based on Tresguerres et al. (2007) while in the current study TCO_2 loads were nearly double that. Perhaps the lower hypercarbia induced by infusion (Chapter 2; Clifford et al., 2014), was so readily handled by posterior mechanisms that involvement of the gill region was not necessary while the higher TCO_2

loads in the current study necessitated involvement of branchial mechanisms to facilitate recovery.

Finally, the noted differences between the results of this study and the previous short-term study may also be due to the length/persistence of the acid/base challenge. This study used a chronic hypercapnia to induce an acid/base disturbance while the infusion protocol induced an acute hypercarbia followed by immediate recovery. To determine which of the explanations are responsible for these differences, Western blot or qPCR analysis will need to be conducted on gill tissue following acute and chronic hypercapnia exposure/ alkaline infusion.

The goal of series 2 experiments was to evaluate how hagfish respond to localized hypercapnia; a situation that may be observed during feeding bouts while burrowing into carcasses (Heisler and Weitz, 1976; Strahan, 1963). Furthermore, I wished to elucidate the mechanism by which hagfish mount metabolic compensation during hypercapnia exposure. When either anteriorly- or posteriorly-exposed to 0.6% hypercapnia, hagfish do experience a respiratory acidosis (Figure 4.4). Hagfish anteriorly-exposed to hypercapnia responded as hypothesized, excreting considerable net amount of acid equivalents in the anterior chamber while also mounting a compensatory HCO_3^- response in their plasma. It is important to remember that net acid equivalent excretion also can be accomplished by base equivalent absorption and these cannot be separated experimentally. For example, there is no difference to the animal if they absorb HCO_3^- by a CBE-mediated mechanism or directly excrete H^+ *via* an NHE or VHA.

One of the more interesting and novel findings in this study is that only animals which were anteriorly-exposed appear to compensate for this acidosis by raising plasma

[HCO$_3^-$] levels and further excrete H$^+$ equivalents anteriorly. Despite experiencing a prominent respiratory acidosis (Figure 4.4C), posteriorly-exposed hagfish displayed no metabolic HCO$_3^-$ compensation or acid excretion patterns. These results may suggest an anteriorly-mediated CO$_2$ sensor, rather than a proximal blood pH-mediated sensor, is responsible for activating bicarbonate compensation. This intriguing finding requires further careful experimentation to rule out mixing effects (*e.g.* accounting for low circulatory rate in hagfishes; Forster et al. 2011) and this will form the subject of my future research. The identity of a CO$_2$ sensor will be investigated by using known HCO$_3$-sensor (soluble adenylyl cyclase; sAC) inhibitors (i.e. KH7 or 4CE) to elucidate the potential pH/CO$_2$ sensing mechanism(s) in hagfish.

The observation that hagfish that were posteriorly-exposed to hypercapnia also experienced an acidosis is also interesting. In Chapter 8, I demonstrate that hagfish are incapable of utilizing their skin as a means for oxygen uptake; however, here I show that CO$_2$ can diffuse in to the animal across the skin. Given the physical constraint proposed against cutaneous O$_2$ diffusion (i.e. epidermal layer is too thick to allow for O$_2$ diffusion (Malte and Lomholt, 1998; See Chapeter 8), how can CO$_2$ diffuse across this same tissue? CO$_2$ transport has been demonstrated to be facilitated by Rh glycoproteins (SLC42 transporter family). Using ammonia-CO$_2$ competition experiments with Rh-knockdown zebrafish, Rh proteins have been demonstrated to facilitate transport of not only ammonia (Hung et al., 2007; Nakada et al., 2007; Nawata et al., 2007; Tsui et al., 2009), but also CO$_2$ (Perry et al., 2010). In Chapter 6, I demonstrate that hagfish demonstrate Rhcg-like (the purported ammonia transporter) immunoreactivity in their epidermal tissue. Another candidate for facilitated CO$_2$ diffusion is AQP1 (Endeward et

al., 2006; Musa-Aziz et al., 2009). Further investigation will be needed in order to inform about the mechanism of cutaneous CO_2 exchange.

Conclusions

In summary, in this chapter, I have provided evidence demonstrating that hagfish utilize both gill and skin mechanisms to recover from hypercapnia-induced hypercarbia loads. Furthermore it appears as though the proposed single MRC type in hagfish is capable of both acid and base excretion, provided the appropriate stimulus is provided. Finally, I provide preliminary evidence that hagfish utilize an anteriorly-mediated sensor to respond to hypercapnia-induced acid/base disturbances.

Figures
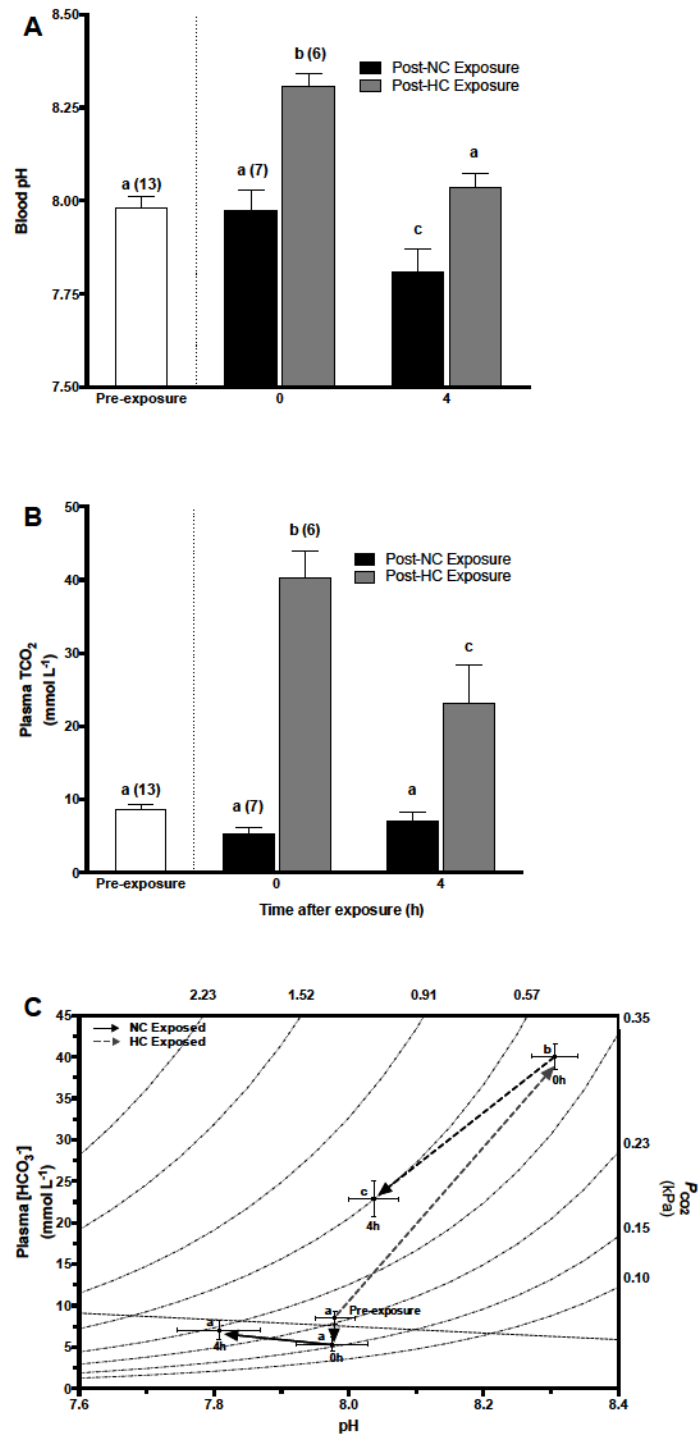
Figure 4.1 Blood and plasma acid/base parameters following exposure to and recovery from 0.6% hypercapnia.

Blood and plasma acid/base parameters of hagfish exposed to hypercapnia (0.6% CO_2; Post-HC Exposure; Grey bars) or normocapnia (Post-NC Exposure; Black bars) for 72 h with recovery allowed for 4 h in separating chambers. Blood pH (A) and plasma [TCO_2] (B) were measured prior to exposure (Pre-exposure; Open bars) and before (0 h) and after (4 h) recovery in normocapnic seawater. (C) Calculated blood pH/plasma HCO_3^- diagram depicting the blood acid/base status of hagfish exposed for 72 h to either hypercapnia (0.6% CO_2; HC Exposed; Dotted line) or normocapnia (NC Exposed; solid line). The dotted line represents the non-bicarbonate buffering capacity as determined by Wells et al. (1986). Data are presented as mean + s.e.m. (*n*). Differences between points sharing the same letter are not statistically significant. In (C) plasma [HCO_3^-] data sharing the same letter are not statistically different. For blood pH differences see Figure 4.1A.
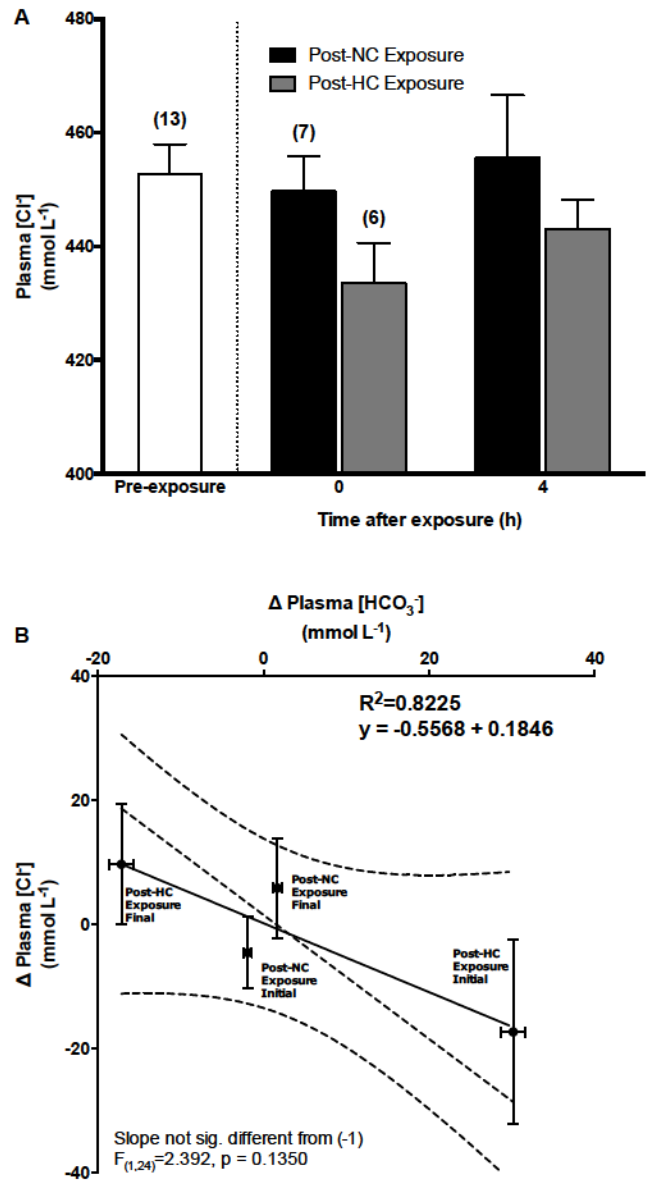
Figure 4.2 Plasma [Cl⁻] following exposure to and recovery from 0.6% hypercapnia.

Plasma [Cl⁻] of hagfish exposed to hypercapnia (0.6% CO_2; Post-HC Exposure; Grey bars) or normocapnia (Post-NC Exposure; Black bars) for 72 h with recovery allowed for 4 h in separating chambers. (A) Plamsa [Cl⁻] were measured prior to exposure (pre-exposure; Open bars) and immediately following exposure (0 h) and after (4 h) recovery in normocapnic seawater. (B) Linear regression analysis of Δplasma [HCO_3^-] vs. Δplasma [Cl⁻]. Initial values were calculated as the difference between pre-exposure and $t = 0$ values, while final points were calculated as the difference between $t = 0$ and $t = 4$ h recovery values.). Data are presented as mean + s.e.m. (n). Bars sharing the same letter are not statistically significant. Dotted lines represent 95% confidence intervals for the line of best fit (solid). Dotted line shows a line of slope = -1.0.
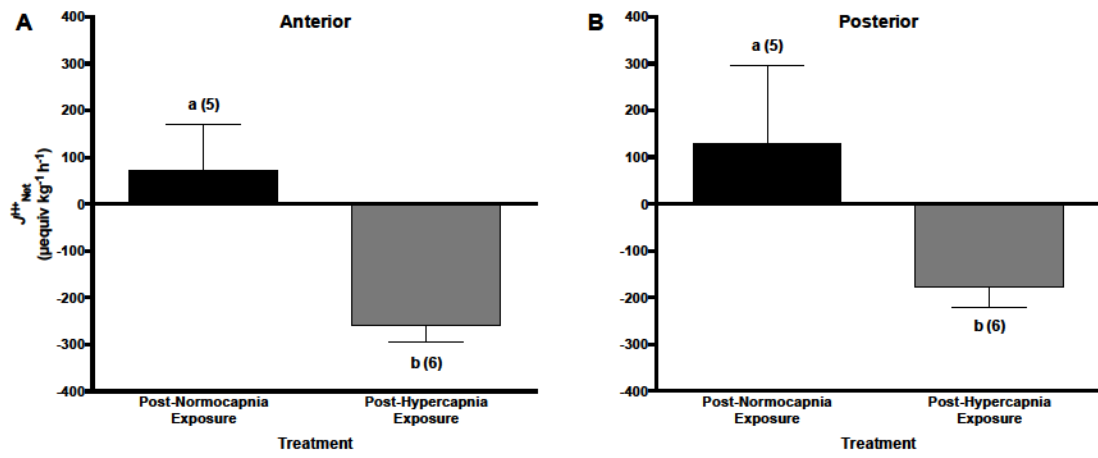
Figure 4.3 Net H$^+$/HCO$_3^-$ during recovery from 0.6% hypercapnia.

Net outward H^+ (positive values) or HCO_3^- (negative values) flux from the anterior (A) and posterior (B) portions of hagfish fitted into separating chambers. Hagfish were treated as described in Figure 4.1. Following removal from exposure, acid/base equivalent efflux was determined in anterior and posterior compartments of separating chamber. Data are presented as mean + s.e.m. (n). Bars sharing the same letter are not statistically significant.
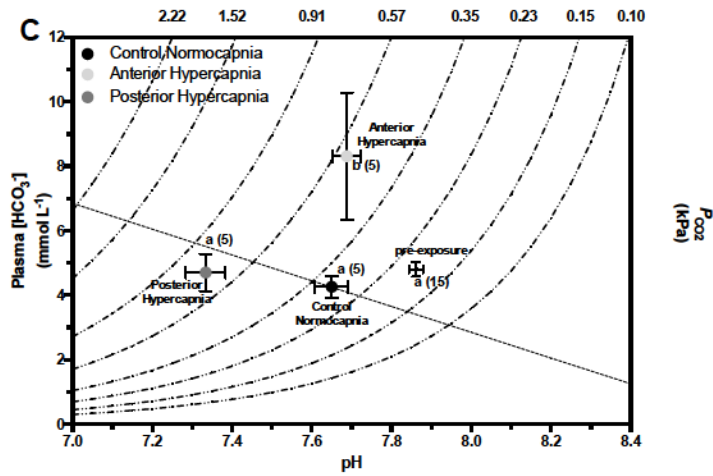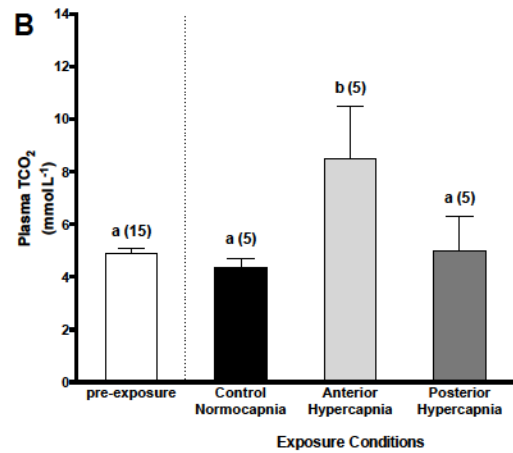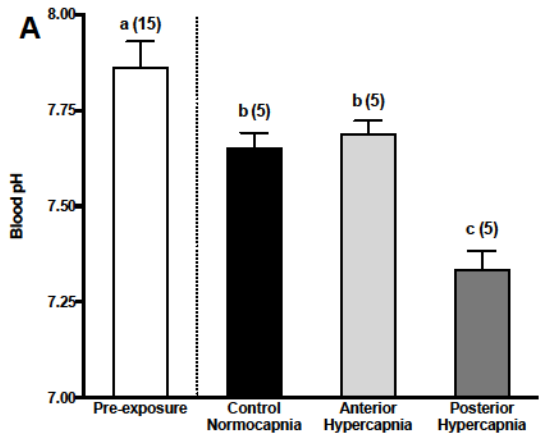
Figure 4.4 Blood and plasma acid/base parameters during localized hypercapnia exposure.

Blood pH (A) and plasma TCO_2 (B) were measured prior to exposure (Pre-exposure; Open bars) and after localized anterior (light grey bars) or posterior (Dark grey bars) exposure to 0.6% P_{CO_2} or symmetrical (non-localized) aeration with normocapnic air (Control; black bars) in separating chambers. (C) Calculated blood pH / plasma HCO_3^- diagram demonstrating the acid/base status of hagfish blood in control, anterior- and posterior-exposed hagfish. The dotted line represents the non-bicarbonate buffering capacity as determined by Wells et al. (1986). Data are presented as mean + s.e.m. (n). Plasma $[HCO_3^-]$ data sharing the same letter are not significantly different. For differences in pH see Figure 4.4A.
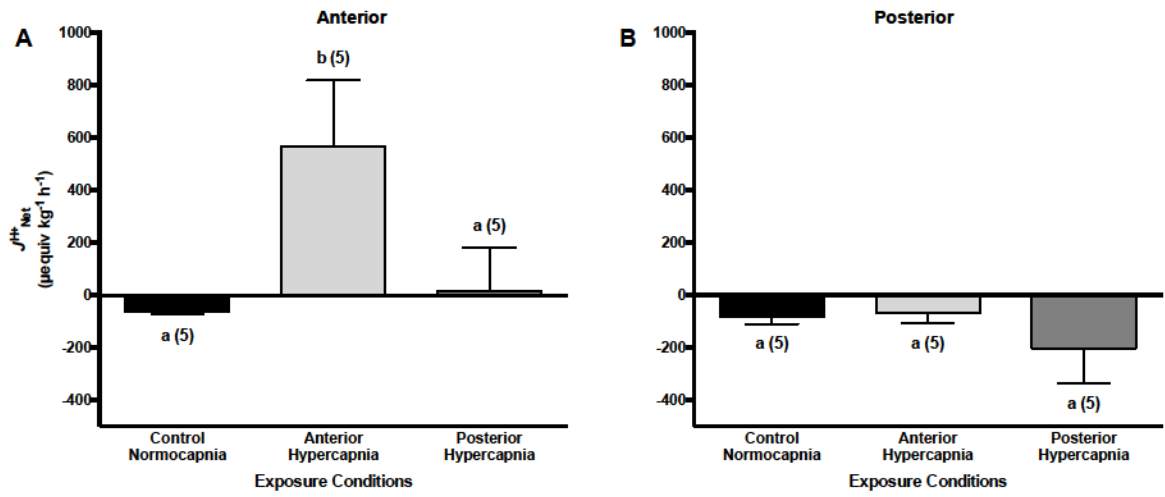
Figure 4.5 Net H$^+$/HCO$_3^-$ flux during localized hypercapnia exposure.

Net outward anterior (A) and posterior (B) H^+ (positive values) or HCO_3^- (negative values) flux in hagfish during exposure to 0.6% hypercapnia localized to the anterior (light grey bars) or posterior (dark grey bars) region or symmetrical aeration with normocapnic air (Control; black bars) in separating chambers. Data are presented as mean ± s.e.m (n). Bars sharing the same letter are not statistically different.

SECTION II:

NITROGEN EXCRETION

Chapter 5: High ammonia tolerance and active NH_4^+ excretion by the Pacific hagfish (*Eptatretus stoutii*)

A version of this chapter has been published.

Introduction

It has been long known that internal accumulations of ammonia in vertebrates leads to ammonia toxicity which is characterized by over-excitation of the nervous system due to N-methyl-D-aspartate overactivation, the generation of reactive oxygen species, apoptosis or necrosis of neurons and glial cells in the brain, ATP depletion, and potentially fatal encephalopathy caused by ionic disturbances and increases in brain water content (see Ip et al., 2001b; Felipo and Butterworth, 2002; Ip et al., 2001a; Walsh et al., 2007 for reviews). In mammals, ammonia toxicity can arise from liver damage which results in a failure to convert ammonia to less toxic urea *via* the ornithine urea cycle (Felipo and Butterworth, 2002). However, for fish living in aquatic environments, there is no need to convert ammonia to urea because the high water solubility and diffusability of ammonia allows it to be readily excreted across the gills in most aquatic environments (see Wright, 1995; Wilkie, 1997 for comprehensive reviews). For this reason, the major nitrogenous waste product in most teleost fishes is ammonia while urea predominates in marine elasmobranchs and coelacanths, which retain urea as an osmolyte in seawater (Ballantyne, 2001; Griffith, 1991). However, some teleosts either live in or are transiently exposed to environments that do not favour ammonia excretion such as the Lake Magadi tilapia (*Oreocrhomis alcalicus* graham) which lives in highly alkaline (~pH 10) water (Randall and Wright, 1989), and certain air breathing fishes including the lungfishes (Janssens and Cohen, 1968; Smith, 1930; Wood et al., 2005b). Strategies for detoxification include increases in glutamine production to detoxify ammonia as employed by the swamp eel *Monopterus albus* (Ip et al., 2010), ammonia volatilization as used by mangrove killifish (*Kryptolebias marmoratus)* during air exposure (Frick and

Wright, 2002), and even active NH_4^+ transport , as proposed for the mudskipper (*Periophthalmodon schlosseri*) and the climbing perch (*Anabas testudineus*) during exposure to air or exposure to high environmental ammonia (Randall et al., 1999; Wilson et al., 2000). The swamp eel and weatherloach (*Misgurnus anguillacaudatus*) are also able to withstand millimolar increases in plasma ammonia (Chew et al., 2001; Tsui et al., 2002; Ip et al., 2004). While a wealth of knowledge on ammonia excretion by teleosts and elasmobranchs has been generated in the last 20 years (see Weihrauch et al. 2009 for review), relatively little is known about how nitrogenous wastes are excreted by the agnathan fishes, as represented by the lampreys (Petromyzontidae) and the hagfishes (Myxinidae), which are the earliest extant representatives of the vertebrate lineage (Bardack, 1991). A better understanding of how these jawless fishes handle and excrete nitrogenous wastes should provide valuable insight into the patterns of nitrogenous waste production and excretion and how they evolved in the vertebrates (Weihrauch et al., 2009).

As opportunistic scavengers, hagfishes are amongst the first marine organisms to begin devouring "food drops", defined as carrion that sink to the ocean floor from the upper depths or water surface (Collins et al., 1999). Carrion may simply be fish, including by-catch from commercial fishing (Collins et al., 1999), or extremely large marine mammals (Smith and Baco, 2003). As the hagfish devour the carrion they may burrow into the decomposing carcass *via* orifices in the body, or beneath the operculum in the case of fishes (Collins et al., 1999).

In terrestrial environments, the early stages of decomposition mainly involves the breakdown of cells and tissues by anaerobic bacteria, leading to the generation of

"putrefactive gases" such as hydrogen sulfide and ammonia, which can lead to the deposition of very high concentrations of nitrogen compounds in the surrounding environment including $(NH_4^+)_2SO_4$, which can exceed 525 µg g^{-1} (~29 mmol L^{-1}; Carter et al., 2007). There is little data on the biochemical process of putrefaction in aquatic environments, but since many of the anaerobic bacteria involved in the putrefactive process arise from the gut (Carter et al., 2007), it seems reasonable to assume that decomposing fish or marine mammal carcasses would generate large amounts of ammonia. Thus, high ammonia tolerance is likely a pre-requisite for the scavenging life-style of hagfishes, which are also likely to encounter hypoxic and acidic conditions due to the generation of lactic acid and propionic acid in the early stages of decomposition, and perhaps high concentrations of CO_2 in later stages (Carter et al., 2007). Indeed, the ability of the hagfish to withstand and recover from acidic, hypoxic and hypercapnic conditions has been reported in recent years (Clifford et al., 2014; Cox et al., 2011; Tresguerres et al., 2007a, Parks et al., 2007b). However, less is known about hagfish nitrogenous waste metabolism and excretion. The main nitrogenous waste product for hagfishes is ammonia, with little reliance on urea excretion under routine conditions (Walsh et al., 2001). Hagfish can also withstand short-term exposure to high environmental ammonia (HEA; Braun and Perry, 2010), but the underlying mechanisms of their ammonia tolerance have not yet been identified. Immunohistochemical evidence suggests that the Pacific hagfish (*Eptatretus stoutii*) relies on Rhesus glycoprotein mediated-ammonia excretion under such conditions (Braun and Perry, 2010), but it is not known if the hagfish can withstand longer periods of HEA, or how acid/base balance, and ammonia balance are maintained under such extreme conditions.

In the present study, Pacific hagfish were exposed to nominal total ammonia concentrations (T_{Amm} equals the sum of $NH_3 + NH_4^+$) of 20 mmol L^{-1} for 48 h to determine how HEA affected blood T_{Amm} and other nitrogenous waste product concentrations (urea, glutamine). In addition, measurements were made to quantify how HEA influenced acid/base balance, to describe how ammonia and urea excretion (J_{Amm}, J_{Urea}) patterns across the body surface were affected by HEA, and to determine how these processes take place. I hypothesized that the Pacific hagfish would be able to tolerate long-term HEA exposure by converting it to less toxic urea and/or glutamine, and that the animals would be able to prevent ammonia from reaching toxic concentrations by excreting ammonia against large inwardly directed NH_3 and/or NH_4^+ electrochemical gradients, as previously suggested by Braun and Perry (2010).

Materials and methods

Experimental animals and holding

Pacific hagfish (*Eptatretus stoutii*; N=24; average mass = 118 ± 10 g, range 65 – 270 g) were captured using bottom-dwelling traps, baited with strips of Pacific hake (*Merluccius productus*), from Trevor Channel, off the southwest coast of Vancouver Island, BC, Canada. Traps were checked daily and captured hagfish were transported to the Bamfield Marine Sciences Centre where they were housed in aerated, darkened 20 m^3 tanks continuously receiving seawater. The hagfish were used for experiments within 3 weeks, and were fed bi-weekly with strips of hake, but fasted for at least one week prior to experimentation. All animals were collected with Department of Fisheries and Oceans Canada authorization (scientific collection permit no. XR-214-2011), and experiments were approved by the Bamfield Marine Science Centre Animal Care Committee (protocol number BMSC RS-11-26) and followed Canadian Council of Animal Care guidelines.

Experimental protocol

Exposure to high environmental ammonia

One day prior to experiments, Pacific hagfish (N=18) were transferred to 10 L buckets receiving continuously flowing seawater. The next morning, they were exposed to a nominal NH_4Cl concentration of 20 mmol L^{-1} in 5 L of aerated seawater, and held under static conditions for 24 – 48 h. Representative water samples (15 mL) were

collected daily to verify that the water total ammonia concentrations (T_{Amm} = [NH_3] + [NH_4^+]) matched target values.

Quantification of ammonia and urea excretion rates

Rates of ammonia excretion (J_{Amm}) and urea excretion (J_{Urea}) were measured in a sub-set of animals (*n*=6) under control (seawater only) conditions (mean [T_{Amm}] = 2.2 ± 1.0 μmol L^{-1} (SD); *n* = 6 measurements), during exposure to HEA (mean [T_{Amm}] = 21.6 ± 2.0 mmol L^{-1}; *n* = 72), and during a post-ammonia exposure recovery period in nominally ammonia-free sea water (mean [T_{Amm}] = 6.3 ± 2.2 μmol L^{-1}; n= 12). Under control conditions, water flow to the buckets was cut-off and the water volume lowered to exactly 1.0 L. The very low basal J_{Amm} and J_{Urea} rates of Pacific hagfish, determined in preliminary experiments (see Discussion), necessitated the low water volume used to measure control excretion rates. Water samples (15 mL) were then collected at the beginning of the measurement period (0 h) and after 4 h, and then frozen at -20ºC, until analyzed for water T_{Amm} and urea concentration. During the 48 h HEA exposure, water volume was adjusted to 3.0 L, and water samples (15 mL) were collected every 4 h, over three 8 h flux intervals (0 – 8 h, 8 – 16 h, 16 – 24 h) and one 12 h flux interval (36 – 48 h). Following each flux interval, 2/3 of the water in the 3.0 L bucket was replaced with fresh, aerated seawater containing a nominal concentration of 20 mmol L^{-1} NH_4Cl. All water samples were frozen at -20ºC until analyzed.

Following the 48 h HEA exposure, the animals were allowed to recover in nominally ammonia-free seawater for 24 h. Due to the rapid accumulation of water T_{Amm} that was anticipated, the flux measurement periods were of shorter duration than during

HEA (1 – 4 h rather than 8 h), and the volume of water in the buckets was adjusted to 5.0 L instead of 3.0 L to prevent increases in T_{Amm} that could subsequently impair J_{Amm}. Accordingly, post-HEA J_{Amm} and J_{Urea} were measured from 0 – 1 h, 1 – 2 h, and 2 – 4 h, at which point the water in the buckets was replaced with nominally ammonia-free seawater and another flux initiated from 4 to 8 h. Water flow was then re-established to the containers for 12 h, followed by a final J_{Amm} and J_{Urea} measurement period from 20 – 24 h. Immediately following this final flux measurement period, the animals were anaesthetized, and blood and gill samples collected, as described below.

Blood sample analysis and terminal sampling

Blood samples (~200 μL) were collected from the fish allowed to recover from HEA (n = 6; see above) and from separate sub-sets of hagfish (n =10-12) under control conditions (no ammonia), and after 4 h, 12 h, 24 h and/or 48 h of HEA exposure. At each blood sample period, the hagfish were anaesthetized with 1 g L^{-1} tricaine methanesulfonate (TMS; Syndel Laboratories Ltd., Nanaimo, British Columbia, Canada), buffered with 2 g L^{-1} sodium bicarbonate. After approximately 5 minutes, the anaesthetized fish was suspended by the head causing pooling of blood in the caudal subcutaneous sinus from which the blood sample was collected using a heparinized 21G needle and 1 mL disposable syringe. A similar blood sampling protocol was found to have minimal effect on the blood acid/base status of Pacific hagfish (Parks et al., 2007; Tresguerres et al., 2007). During sampling, animals were handled for less than 1 minute to minimize any potential repeated handling stress and all animals typically recovered from sampling and anesthesia within 5 – 10 minutes.

Following sampling, a sub-sample of blood (25 – 50 µL) was transferred to glass (borosilicate) hematocrit tubes, and centrifuged at $5000 \times g$ followed by measurement of hematocrit. The remaining blood was transferred into a 1.5 mL micro-centrifuge tube and placed in a water bath at 10 ˚C. Blood pH was then measured immediately using a thermojacketed Orion ROSS Micro pH electrode (Fisher Scientific, Ottawa, ON), which was directly immersed in the sample. Following pH determination, the blood sample was centrifuged in a microcentrifuge ($12,000 \times g$ for 2 min; Eppendorf, Model 5140C, Hamburg, Germany), and an aliquot of plasma drawn-off and analyzed for total CO_2 (T_{CO2}) using a Corning 965 carbon dioxide analyzer (Ciba Corning Diagnostic, Halstead, Essex, UK). Another aliquot (25 µL) of the plasma was then acidified with 8% perchloric acid (PCA; 2 parts plasma to 1 parts PCA) for later analysis of [lactate]. The remaining (unacidified) plasma was then flash-frozen in liquid N_2 for later determination of plasma ammonia, urea, and glutamine concentration.

Gill tissue was also collected and snap-frozen in liquid N_2 from control animals not exposed to HEA ($n = 6$), and from those exposed to HEA for 24 h (N=6) and 48 h (N=6), and from the animals that had recovered for 24 h in ammonia-free water ($n = 6$).

Analytical techniques

Unless noted, all chemical compounds, reagents and enzymes were supplied by Sigma-Aldrich Chemical Company (St. Louis, MO). Concentrations of water ammonia and urea, and plasma ammonia, glutamine and urea were determined spectrophotometrically using well-established techniques and a 96 well micro-well plate spectrophotometer (Spectramax 190, Molecular Devices, Sunnyvale, CA). Briefly, water

154

ammonia concentration was determined colorimetrically using the salicylate-hypochlorite assay at 650 nm (Verdouw et al., 1978). Control water samples were undiluted, but samples collected during HEA were diluted 200-fold in deionized (ammonia-free) water to ensure that water ammonia concentrations were within the linear dynamic range of the assay (10-200 μmol L^{-1}). Plasma T_{Amm} concentration was quantified enzymatically using a commercial kit (Sigma-Aldrich Procedure A001; glutamate dehydrogenase) at 340 nm, after diluting samples 2 – 4 fold in deionized water. Water and plasma urea concentrations were quantified colorimetrically using diacetylmonoxime at 540 nm (Crocker, 1967). Plasma glutamine was quantified using glutamine synthetase and ferric chloride at 540 nm (Mecke, 1985). Plasma lactate concentrations was determined enzymatically (lactate dehydrogenase), with samples read at 340 nm (Bergmeyer, 1983).

Electrophoresis and Western blot analysis

Frozen gill samples were pulverized and large chunks (~100 mg) were transferred to a centrifuge tube containing 1:10 w/v of ice-cold homogenization buffer (250 mmol L^{-1} sucrose, 1 mmol L^{-1} EDTA, 30 mmol L^{-1} Tris, 100 mg/mL containing protease inhibitor [cOmplete, Mini; Roche, Basal, Switzerland; 1 tablet:10 mL buffer). Samples were then homogenized on ice using a hand-held motorized mortar and pestle (Gerresheimer Kimble Kontes LLC, Dusseldorf, Germany) for 45 seconds. Homogenates were then centrifuged at 3000 × *g* for ten minutes at 4 ˚C and the supernatant drawn off. A subsample of the supernatant was assayed for protein determination *via* the BCA technique (Pierce, Rockford, IL, USA). Processed gill samples were diluted with 3X Laemmli buffer (Laemmli, 1970) and 15 μg of total protein was separated in a 10% SDS-

PAGE mini-gel. Protein was transferred for 1 h at 110V in a wet transfer cell (Bio-Rad Laboratories Inc., Hercules, CA, USA) to a nitrocellulose membrane.

Protein transfer was confirmed by soaking membranes in Ponsceau S staining solution (0.1% (w/v) Ponceau S in 1% (v/v) acetic acid). Following transfer confirmation, membranes were washed (2 min in distilled water followed by 3 x 1 min in 0.5 M Tris-Buffered Saline [TBS; pH=8.0] containing 0.1% Triton X-100 [TBST]) and then blocked (5% skim milk powder in TBST) on a shaking carousel overnight at 4 ˚C. Membranes were then washed (3x15 min in TBS and then 3x15 min in TBST) before incubation in blocking buffer containing 1˚ antibody (1:2500 rabbit anti-hagfish Rchg - Generously donated by S. Edwards or 1:5000 rabbit anti-Beta-actin - Sigma Aldrich) for 1 h at room temperature. Membranes were then washed again (3x15 min in TBS and then 3x15 min in TBST) then incubated with 2˚ antibody (1:20,000 goat anti-rabbit HRP; Santa Cruz Biotechnologies Inc., Dallas, TX, USA).

Labeled protein bands were detected *via* enhanced chemiluminescent (ECL; Pierce; SuperSignal West Pico Chemiluminescent Substrate; Rockford, Il, USA) and bands were compared to protein size marker (Fermentas Life Sciences, Pittsburgh, PA, USA).

Films were digitized on a computer scanner and densitometry was conducted using ImageJ (http://imagej.nih.gov/ij/). Films of blots were normalized using an identical sample loaded on each gel and samples were normalized against the endogenous loading control beta-actin.

Calculations and statistics

Measured values of blood pH and plasma total CO_2 were used to calculate the plasma $[HCO_3^-]$ and P_{CO_2} at 10°C by re-arrangement of the Henderson-Hasselbalch equation, with values for the solubility co-efficient of CO_2 (αCO_2) and the apparent dissociation constant of carbonic acid (pk'_{app}) calculated as functions of pH, salinity and temperature as described in Boutilier et al. (1984).

The cumulative metabolic acid-load (ΔH^+_m) added to the blood of hagfish was calculated as described by McDonald et al. (1991):

$$\Delta H^+_m = ([HCO_3^-]_i - [HCO_3^-]_f) - \beta(pH_i - pH_f) \tag{1}$$

where ΔH^+_m is expressed in mmol L^{-1}, i and f refer to the concentrations of HCO_3^- and pH measured in the plasma and blood of the hagfish at the beginning and end of a measurement period. The buffer capacity of hagfish blood [β = - 4.77 mmol L^{-1} pH unit^{-1} (Slykes)] was derived from average measurements of hematocrit (Hct) in control animals using the relationship described by (Wells et al., 1986) for New Zealand hagfish (*Eptatretus cirrhatus*) with the following formula:

$$\beta = -0.0675 \cdot Hct^2 + 0.94 \cdot Hct + 2.70 \tag{2}$$

The speciation of ammonia was also based on re-arrangement of the Henderson-Hasselbalch equation (Wright and Wood, 1985) as outlined below:

$$[NH_4^+] = T_{Amm}/(1 + antilog\ (pH - pk_a)) \tag{3}$$

$$[NH_3] = T_{Amm} - [NH_4^+] \tag{4}$$

where pH is the respective measured water pH or blood pH, and pK_a is the appropriate apparent dissociation constant for T_{Amm} calculated from nomograms as a function of salinity, the measured temperature and pH in plasma and water, respectively (Cameron and Heisler, 1983).

The partial pressure of NH_3 (P_{NH_3}) of plasma and water was then determined from the calculated NH_3 concentration, using the solubility of co-efficient for NH_3 (αNH_3) in seawater at 10°C provided by Boutilier et al. (1984) using the following equation:

$$P_{NH_3} = [NH_3]/\ \alpha NH_3 \tag{5}$$

where P_{NH_3} is expressed is expressed in mPa (For conversion to μTorr, multiply by 7.501 μTorr/mPa). The plasma and water P_{NH_3} were then used to calculate the plasma-water NH_3 diffusion gradient (ΔP_{NH_3}):

$$\Delta P_{NH_3} = Plasma\ P_{NH_3} - Water\ P_{NH_3} \tag{6}$$

where a positive ΔP_{NH_3} indicates an outwardly directed NH_3 partial pressure diffusion gradient.

The Nernst equilibrium potential for NH_4^+ ($E_{NH_4^+}$) between the plasma and the water was then calculated using the appropriate gas constant (R), Faraday's constant, and valence of NH_4^+ at the appropriate temperature (10°C = 283°K) using the following formula:

$$E_{NH_4^+} = 56.1 \log ([NH_4^+]_{SW} / [NH_4^+]_{Pl}) \qquad (7)$$

where $[NH_4^+]_{SW}$ and $[NH_4^+]_{Pl}$ are the respective concentrations of NH_4^+ in seawater and plasma.

The ammonia excretion (J_{Amm}) and urea excretion (J_{Urea}) rates were expressed in $\mu mol\ kg^{-1}\ h^{-1}$ based on differences in the respective concentrations of T_{Amm} and urea measured over 1 – 12 h (as appropriate) intervals when water flow was cut-off to the containers holding each individual hagfish, after correcting for the water volume of the container, time and the mass of the animal (*e.g.* Wilkie and Wood, 1991; Wright and Wood, 1985).

All data were expressed as the mean + 1 standard error of the mean (s.e.m.) unless otherwise noted, and analyzed using one-way ANOVA. Where data were not normally distributed and/or had unequal standard deviations, a Kruskal-Wallis non-parametric ANOVA was used. Where significant variation was observed, a Holm-Sidak pair-wise *post-hoc* test was used to identify significant differences amongst the different treatment groups. The limit of statistical significance was at the $p < 0.05$ level. All statistical analyses were performed using GraphPad Prism version 6.0 for MacOSX, GraphPad Software, San Diego California USA, www.graphpad.com.

Results

Ammonia tolerance of Pacific hagfish

The measured concentration of T_{Amm} to which Pacific hagfish were exposed averaged 21.7 ± 0.25 mmol L^{-1}, which was approximately 8.5% greater than the target concentration of 20 mmol L^{-1}. Nevertheless, the hagfish readily survived exposure to HEA, with no mortality observed. Exposure to HEA did however, lead to a reversal of J_{Amm} and a net-uptake of ammonia in the first $12 - 16$ h of exposure, along with related acid/base disturbances.

Effects of high external ammonia exposure on J_{Amm} and J_{Urea}

Under control conditions, routine rates of J_{Amm} averaged -50 μmol $kg^{-1} h^{-1}$ (negative values denote net excretion of ammonia) but during the first 8 h of exposure to HEA, J_{Amm} was directed inward at a rate of 8,170 μmol $kg^{-1} h^{-1}$. The rate of ammonia uptake by the hagfish dropped by approximately 50% over the next 8 h, averaging approximately 3,880 μmol $kg^{-1} h^{-1}$ (Figure 5.1A). By $16 - 24$ h, however, the fish had reversed the process with a net ammonia excretion of approximately -6,260 μmol $kg^{-1} h^{-1}$ noted. The last $12 - 13$ h of HEA exposure were characterized by 90% lower J_{Amm}, that remained outwardly directed averaging approximately -600 μmol $kg^{-1} h^{-1}$ (Figure 5.1A). The post-exposure period was characterized by a marked stimulation of J_{Amm} compared to the pre-exposure control measurements, fluctuating around -2,000 to -3,000 μmol $kg^{-1} h^{-1}$ during the first 6 h of recovery (Figure 5.1A). By 24 h of recovery, however, J_{Amm} was not significantly different from control rates (Figure 5.1A).

Despite the inhibition of J_{Amm} over the first 16 h of HEA exposure, J_{urea} did not significantly change from control rates of -1.4 μmol N kg^{-1}h^{-1} over the 48 h exposure period (Figure 5.1B). However, J_{Urea} increase by 2 – 3 fold during the first 4 h of the post-ammonia exposure recovery period. Thereafter, J_{Urea} was not significantly different from the pre-exposure control measurements (Figure 5.1B).

Accumulation of nitrogenous wastes in the plasma

The plasma T_{Amm} in hagfish prior to HEA-exposure averaged 39.2 μmol L^{-1}, but increased more than 50-fold to 2,163 μmol L^{-1} after 4 h of exposure to HEA (Figure 5.2A). Plasma T_{Amm} peaked near 5,450 μmol L^{-1} after 24 h, before stabilizing at approximately 5,000 μmol L^{-1} after 48 h of HEA exposure (Figure 5.2A). Upon reintroduction into control seawater, plasma ammonia concentrations dropped precipitously as the fish unloaded the accumulated ammonia, stabilizing near 80 μmol L^{-1} after 24 h, which was not significantly different from pre-exposure control values (Figure 5.2A). Neither plasma urea or glutamine concentrations significantly increased during the 48 h HEA exposure period. Nor were there any changes in the plasma urea or glutamine concentrations during the post-exposure recovery period (Figure 5.2B, C).

Changes in the ΔP_{NH_3} gradient and the Nernst Potential for NH_4^+ across the hagfish body surface during HEA

Under control conditions, ΔP_{NH_3} was approximately 1.33 mPa ($\sim$10 μtorr; positive), and outwardly directed from the plasma to salt water. Following exposure to HEA, however, the gradient was reversed (negative) and more than two orders of magnitude higher, at approximately 600 mPa ($\sim$4,500 μTorr) after 4 h (Figure 5.3A).

There was no significant change in the ΔP_{NH_3} gradient for the remainder of the exposure period, despite the measured increases in plasma T_{Amm} that were observed over the first 24 h of HEA exposure. Immediately following the return of the animals to ammonia-free water, a large outward ΔP_{NH_3} gradient was re-established, at approximately 173 mPa (~1,300 µTor; Figure 5.3A). However, the continual unloading of ammonia by the hagfish over the ensuing 24 h of recovery resulted in a substantial decrease in the ΔP_{NH_3} gradient to values near controls, but still outwardly directed (Figure 5.3A).

Under control conditions $E_{NH_4^+}$ was approximately –18 mV, but it was reversed, as indicated by a switch in the polarization and magnitude, to approximately +60 mV after the fish were exposed to HEA (Figure 5.3B). The $E_{NH_4^+}$ gradually declined over the first day of HEA exposure before stabilizing at approximately +38 mV after 24 h, at which time $E_{NH_4^+}$ was still inwardly directed (Figure 5.3B). The return of the hagfish to ammonia-free seawater was characterized by an immediate switch in the size and polarization of $E_{NH_4^+}$ to approximately -160 mV. By 24 h of recovery, $E_{NH_4^+}$ had returned to values that were comparable to control (pre-ammonia exposure) measurements (Figure 5.3B).

Effect of HEA on acid/base balance

Blood pH in control animals prior to HEA exposure was approximately pH 7.91, but following 4 h of HEA exposure, rose significantly to a value of pH 8.11 (Figure 5.4A). By 12 h of HEA exposure, however, blood pH was no longer significantly different from control values, and continued to be regulated downwards until 48 h at which time blood pH was approximately 7.80 (Figure 5.4A). Recovery in nominally

ammonia-free seawater for 24 h resulted in significant reduction in blood pH to approximately pH 7.56, which was significantly lower than the pre-HEA exposure control values (Figure 5.4A).

The alkalosis experienced by the hagfish was mainly due to the gain of metabolic base (metabolic base load), as revealed by a ΔH^+_m of -7.5 mmol L^{-1} after only 4 h at HEA (Figure 5.4B). Thereafter, the metabolic base load was gradually eliminated as ΔH^+_m shifted towards zero. Following 24 h of recovery in nominally ammonia-free seawater, the hagfish experienced a significant metabolic acid load of +5.0 mmol L^{-1}, suggesting that the initial metabolic base-load was offset by the simultaneous production of metabolic acid (Figure 5.4B). The absence of any changes in blood lactate (Figure 5.4C) indicated that the source of the counterbalancing metabolic acid was not likely lactic acid production.

Further analysis of blood acid/base status using a pH-bicarbonate (Davenport) diagram revealed more about the nature of the acid/base disturbances experienced by the hagfish during HEA (Figure 5.5). Under control conditions, hagfish had a plasma [HCO_3^-] of approximately 8.0 mmol L^{-1}, and a corresponding plasma P_{CO_2} of 0.24 kPa (~1.8 Torr). The increase in blood pH that was observed after the initial period of HEA exposure was due solely to a rapid pure metabolic alkalosis characterized by a two-fold rise in plasma [HCO_3^-] to 13 mmol L^{-1}, but plasma P_{CO_2} remained unchanged. By 12 h, plasma HCO_3^- had returned to and remained near pre-exposure values despite the continued presence of HEA (Figure 5.5). After 24 h recovery in nominally ammonia-free seawater, a pure metabolic acidosis was observed characterized by a 75% lower plasma

HCO$_3^-$ concentration relative to control measurements yet again, no changes in P_{CO_2} were noted (Figure 5.5).

Rhcg abundance in gill following HEA exposure and after ammonia-free recovery

Both α-hagfish Rhcg antibody and α-beta actin recognized a single band at the predicted size of ~50 kDa and ~37 kDa respectively. Following densitometry analysis (Figure 5.6), no differences in Rhcg abundance in any of the exposure or recovery groups were noted.

Discussion

Pacific hagfish exhibit high tolerance to ammonia

The present study unequivocally supports earlier suggestions that the Pacific hagfish is ammonia-tolerant (Braun and Perry, 2010; Bucking et al., 2011). This tolerance is likely due to an ability to decrease the permeability of the gills to NH_3, and likely involves the use of an as of yet undefined secondary active transport mechanism to excrete NH_4^+ against its electrochemical gradient. High neural tolerance to ammonia may also be important, but measurements of brain ammonia and glutamine concentration, water content and other biochemical indices will be needed to test this hypothesis.

Hagfish plasma ammonia concentrations peaked at 5,450 μmol L^{-1} after 24 h exposure to a measured T_{Amm} concentration of 21.7 mmol L^{-1}, and remained near 5,000 μmol L^{-1} for the remainder of the 48 h HEA period (Figure 5.1). Moreover, all fish survived the ammonia challenge, and were able to restore homeostasis following their re-introduction into nominally ammonia-free seawater, with only a metabolic acidosis persisting through the 24 h recovery period (see below). To my knowledge, these are amongst the highest plasma T_{Amm} concentrations ever reported in any organism following exposure to HEA. Previously, Braun and Perry (2010) reported that the plasma T_{Amm} concentration approached 3500 μmol L^{-1} in Pacific hagfish following exposure to 100 mmol L^{-1} T_{Amm}, but did not extend their exposure period beyond 9 h. Burrow-dwelling, larval sea lampreys (*Petromyzon marinus*), which belong to the only other group of extant agnathans readily survived up to 5 d when exposed to 2 mmol L^{-1} T_{Amm}, resulting in plasma T_{Amm} concentrations near 2,100 μmol L^{-1} (Wilkie et al., 1999).

In contrast to the Pacific hagfish, the plasma T_{Amm} concentrations in the goldfish (*Carassius auratus*) reached approximately 1,300 $\mu mol\ L^{-1}$ following 5 d exposure to 5 mmol L^{-1} ammonia in fresh water (Wilkie et al., 2011). Less ammonia tolerant teleosts such as the common carp (*Cyprinus carpio*) and the rainbow trout (*Oncorhynchus mykiss*) experienced respective plasma T_{Amm} levels of 1,400 $\mu mol\ L^{-1}$ and 2,200 $\mu mol\ L^{-1}$ during exposure to 1 mmol L^{-1} T_{Amm} in fresh water (Sinha et al., 2013). Amongst the fishes with the highest reported tolerances to ammonia are the air-breathing amphibious fishes, found predominately in tropical regions. For instance, the oriental weatherloach is able to withstand plasma T_{Amm} concentrations near 5,000 $\mu mol\ L^{-1}$ during air exposure (Chew et al., 2001), and 4,400 $\mu mol\ L^{-1}$ following 48 h exposure to 30 mmol L^{-1} T_{Amm} (Tsui et al., 2002). Plasma T_{Amm} concentrations peak near 2,300 $\mu mol\ L^{-1}$ in the air-breathing walking Indian catfish (*Heteropneustes fossillis*) during exposure to 25 mmol L^{-1} T_{Amm} over 7 days, but it should be noted that these fish possess a full complement of ornithine-urea enzymes, which enables them to convert the ammonia to less toxic urea, which can either be excreted or stored by the animals until conditions are more favourable or the animals are re-introduced into water (Saha and Ratha, 2007). The amphibious swamp eel (*Monopterus albus*) can withstand T_{Amm} concentrations of 75 mmol L^{-1} for 6 d, with plasma T_{Amm} concentrations approaching 3,500 $\mu mol\ L^{-1}$ (Ip et al., 2010). While the swamp eel could encounter ammonia concentrations approaching 90 mmol L^{-1} in the waters of fertilized rice fields (Ip et al., 2004), few other fish species would ever naturally encounter T_{Amm} concentrations greater than several mmol L^{-1} in aquatic environments. The hagfish, however, could be one exception given its propensity to scavenge on and within dead and dying marine organisms (Collins et al., 1999; Smith

and Baco, 2003), which would likely generate large amounts of putrefactive gases such as NH_3 due to decomposition by anaerobic bacteria (Carter et al., 2007).

Based on evidence in the current study, it was apparent that hagfish do not convert ammonia loads to less toxic end-products of nitrogen metabolism such as urea, which did not significantly increase in the plasma during HEA exposure. Nor did J_{Urea} significantly change in response to HEA, but there was a slight stimulation during recovery from HEA. Some ammonia tolerant fishes including the Lake Magadi tilapia, the gulf toadfish (*Opsanus beta*) and climbing catfish use the ornithine-urea cycle to detoxify ammonia (Mommsen and Walsh, 1989; Randall and Wright, 1989; Saha and Ratha, 2007). At least in the Magadi tilapia and the gulf toadfish, the excretion of urea is promoted by facilitated urea transport proteins found mainly in the gills (Walsh and Smith, 2001; Walsh et al., 2003) but there is emerging evidence that other fishes including the Pacific hagfish also use urea transport proteins (Braun and Perry, 2010). Although the Pacific hagfish did not produce physiologically relevant amounts of urea in the present study, immunohistochemical analysis suggests that they use facilitated urea excretion (Braun and Perry, 2010). Rather than *de novo* urea synthesis, it is more likely that such urea arises from ingested urea and/or the hydrolysis of dietary arginine. Indeed, parasitic sea lampreys excrete large quantities of urea due to the ingestion of urea from elasmobranchs, as well as through the hydrolysis of arginine ingested from teleost fishes (Wilkie et al., 2004; Wilkie et al., 2006).

Ammonia loaded hagfish furthermore did not demonstrate generalized conversion of ammonia to glutamine, at least in the blood/plasma circulation. Glutamine arises from a glutamine synthetase (GS) mediated reaction between ammonia and glutamate in many

tissues (*e.g.* liver, brain, muscle, intestine). As a neutral amino acid, glutamine is less toxic than ammonia, but the reaction is ATP dependent, which may explain why this strategy appears to be restricted to a few species of ammonia tolerant, air breathing fishes such as the four-eyed sleeper (*Bostrichythis sinensis*), marble goby (*Oxyeleotris marmoratus*) and the aforementioned weatherloach, swamp eel and walking Indian catfishes, which use glutamine synthetase (GS) in the liver, muscle, brain and other organs to convert ammonia to glutamine (Chew et al., 2001; Ip et al., 2001b; Jow et al., 1999; Saha and Ratha, 2007). Presumably, any conversion of ammonia to glutamine in organs such as the liver or muscle would have been reflected by an increase in the plasma glutamine concentrations of hagfish (*e.g.* Ip et al., 2001b; Levi et al., 1974; Tay et al., 2003). This does not rule out a potential role for ammonia detoxification *via* glutamine formation in the brain, in which glutamine increases markedly in response to HEA exposure (*e.g.* Ip et al., 2001b; Sanderson et al., 2010; Sinha et al., 2013; Tay et al., 2003; Veauvy et al., 2005; Wilkie et al., 2011) and following feeding (Wicks and Randall, 2002).

Ammonia enters hagfish via passive NH₃ diffusion

The reversal of the P_{NH_3} gradient and corresponding metabolic alkalosis that was observed strongly suggests that ammonia mainly entered the hagfish *via* NH₃ diffusion, most likely facilitated *via* the Rhcg-b glycoprotein recently localized to the apical regions of the Pacific hagfish pavement cells (Braun and Perry, 2010). In fact, the molar equivalents of metabolic base that accumulated in the blood (7.5 mmol L^{-1}; Figure 5.4B) exceeded the observed total plasma ammonia load (2.1 mmol L^{-1}; Figure 5.2A) by approximately 5 mmol L^{-1}.

Because Rh glycoproteins act as facilitated NH_3 transporters (Hung et al., 2007; Nakada et al., 2007; Nawata et al., 2007; Tsui et al., 2009), movements of NH_3 through the Rhcg channel would be dependent upon the direction of the ΔP_{NH_3} gradient (Wright and Wood, 2009), providing a route for the apical, inward diffusion of NH_3. Efforts by Braun and Perry (2010) to localize Rhbg, which normally has a basolateral location in the lamellar pavement cells of teleosts (Wright and Wood, 2009), suggested localization in blood vessels of the lamellar and filamental epithelium of the hagfish. Thus, it remains unclear how the NH_3 entered the blood of the hagfish from the cytoplasm of the gill or skin epithelial cells, but NH_3 diffusion *via* an Rh-like protein, which has not yet been identified, remains likely.

The likelihood of ionic NH_4^+ entering down its electrochemical gradient seems unlikely given the low cationic permeability of the hagfish body surface (Evans, 1984). This conclusion was based on several observations including a relatively low, slightly negative transepithelial potential (TEP) across the hagfish body surface and the absence of any appreciable change in TEP (3 mV) when the fish were transferred to Na^+-free seawater (Evans, 1984). In marine teleosts, the gills are somewhat leaky to Na^+ to facilitate its outward diffusion *via* the paracellular pathways between accessory cells and ionocytes (mitochondrion rich cells; Evans et al., 2005). Clearly, the maintenance of very high internal Na^+ concentrations and a lack of drinking compared to marine teleosts precludes a need to excrete Na^+ in such a manner. This would also eliminate a potential paracellular route favoring NH_4^+ uptake, despite the high likelihood of a massive inwardly directed electrochemical gradients that would favor such movement.

Ammonia uptake is limited by decreased NH₃ diffusing capacity

A notable observation was that despite massive inwardly directed P_{NH_3} gradients, plasma ammonia concentrations stabilized during HEA exposure. The stabilization of plasma T_{Amm} was likely the consequence of a stimulation of an outwardly directed J_{Amm} flux mechanism in combination with a possible decrease in the permeability of the gills and body surface to NH_3/NH_4^+. Reductions in the branchial permeability could arise from an increase in the diffusion distance (L) across the gill, or a decrease in the abundance of Rhcg in the apical epithelium of the gill ionocytes, where this protein is localized (Braun and Perry, 2010). Reductions in branchial blood-water diffusion distance have been reported to occur in rainbow trout to facilitate ammonia excretion during exposure to alkaline (pH 9.5) water (Laurent et al., 2000).

Given the likely importance of Rhcg for facilitating NH_3 diffusion, another distinct possibility is that there was a reduction in Rhcg1 abundance in the gills and/or skin during HEA. This would have lowered branchial NH_3 permeability and restricted NH_3 entry down its ΔP_{NH_3} gradient. However, no changes in Rhcg protein abundance in gills during exposure to or recovery from HEA were observed, nor was the precise localization of Rhcg in the gills of hagfish established in the present study. Future studies using high resolution immunohistochemistry could be used to determine if the Rhcg is distributed in the apical membrane, and therefore functional, or re-packaged in cytoplasmic vesicles in a non-functional state during HEA exposure in the hagfish.

The first 16 h of HEA exposure resulted in a massive uptake of T_{Amm} by the hagfish. The magnitude of this disturbance was quantified by calculating the ammonia load experienced by the hagfish, which is the difference between the predicted ammonia excretion rate minus the observed ammonia flux, multiplied by time (Table 5.1). Over the first 16 h of HEA exposure, the hagfish accumulated approximately 85 mmol T_{Amm} kg^{-1} body mass. However, more than 80% of this accumulated ammonia load was cleared by the fish over the ensuing 32 h (Table 5.1), at which time plasma T_{Amm} concentrations stabilized and J_{Amm} was once again directed outward (excretion). During recovery in ammonia-free water, the remainder of the ammonia load, approximately 16 mmol T_{Amm} kg^{-1} body mass, was "washed-out" (Table 5.1) as the favorable ΔP_{NH_3} gradient was restored, leading to a near complete offloading of plasma and muscle ammonia stores.

Consistent with other studies, only a small proportion of the ammonia load incurred by the hagfish during HEA exposure was retained in the extracellular fluid (sum of the plasma plus the interstitial fluid). The plasma and blood volume of the hagfish is approximately twice as large as in other vertebrates, which likely gives it reserve oxygen carrying capacity under hypoxic conditions (Forster et al., 2001). Not surprisingly, this greater plasma volume is accompanied by a higher extracellular fluid volume (ECFV ~0.338 L kg^{-1} body mass; Forster et al., 2001). Despite their greater ECFV however, the present findings suggest that only a small proportion of the whole body ammonia load was stored in this compartment. For instance, after 24 h the plasma T_{Amm} concentration was approximately 5.45 mmol L^{-1}, which equates to an ECF T_{Amm} load of 1.84 mmol kg^{-1} (assuming an ECFV of 0.338 L kg^{-1} body mass). At roughly the same time (16 h), when

the whole body ammonia burden was approximately 85 mmol kg^{-1} (see above), the difference between the whole body ammonia load and the ECF ammonia load was approximately 83.2 mmol kg^{-1}. This extra ammonia would therefore had to have been stored in the intracellular fluid (ICF) spaces of the body. Theoretically, this deduction is commensurate with previous studies that have shown that the majority of ammonia is shunted to the ICF, the muscle in particular, under conditions that lead to internal ammonia accumulation (*e.g.* Wang et al., 1994; Wang et al., 1996; Wilkie and Wood, 1995; Wright and Wood, 1988). Because the distribution of ammonia between the muscle ICF and the ECF is mainly determined by the NH_4^+ electrochemical gradient, the concentration of ammonia is 20-30 times greater in the ICF of the muscle (Wang et al., 1996; Wright and Wood, 1988). Given the persistence of the large inwardly directed ΔP_{NH_3} and $E_{NH_4^+}$ gradients during HEA, how then did the hagfish excrete ammonia during HEA exposure? Braun and Perry (2010) speculated that the resumption of J_{Amm} could be explained by Rhcg-mediated NH_3 diffusion and acid-trapping of NH_3 which would maintain an outwardly directed P_{NH_3} gradient between the plasma and gill boundary layers. However, they did not measure water or plasma P_{NH_3}. My results suggest that passive NH_3 excretion can be ruled-out because the sheer magnitude of the inwardly directed P_{NH_3} gradients would be far too large to be overcome by simply trapping NH_3 as NH_4^+. Unlike in fresh water fishes, it is questionable whether there could be NH_3 movement through the Rhcg followed by VHA- (Vacuolar H^+-ATPase) or NHE-mediated H^+ trapping in gill boundary layers in seawater fish (Wright and Wood, 2009). Seawater generally has a higher buffering capacity (total alkalinity of approximately

2100-2300 µmol L^{-1}) than fresh water (Lerman and Stumm, 1989; Millero et al., 1998), which could also preclude ammonia excretion in such a manner (Wilkie, 2002).

The possibility of NH$_4^+$ diffusion *via* paracellular pathways in hagfish seems even less likely, given the low cationic permeability of the hagfish body surface (Evans, 1984) and the persistent, positive $E_{NH_4^+}$ they faced in the present study. It should be noted that the true electrochemical gradient for ammonia movements across the gills is the difference between the transepithelial potential (TEP) and the Nernst potential. Because the fish used in the present study were not fitted with surgically-implanted catheters, it was not possible to measure TEP across the body surface of the animals for an exact determination of the NH$_4^+$ electrochemical gradient. Nevertheless, the provided measurements of the Nernst potential are likely indicative of a large inwardly directed electrochemical gradient for NH$_4^+$ because of the relatively low TEP across the hagfish body surface (–3 mV; Evans, 1984). Indeed, the measured Nernst potential for NH$_4^+$ of +40 to +60 mV across the body surface would oppose any significant outward NH$_4^+$ movement (excretion), unless it were countered by an increase in TEP across the gills that was greater than these values. Such an increase seems highly unlikely given that little change in TEP was observed when hagfish were transferred from sea water to Na$^+$-free sea water (Evans, 1984). Wood and Nawata (2011) reported that TEP increased by approximately +15 mV in rainbow trout exposed to 1 mmol L^{-1} HEA in fresh water, which they argued attenuated the inwardly directed electrochemical gradient favoring ammonia loading. It was also notable that they observed no change in TEP in trout exposed to HEA in sea water.

The most likely route of NH_4^+ diffusion in marine teleosts would be *via* "leaky" paracellular routes (Wilkie, 2002) through which Na^+ passes following its excretion by basolateral Na^+/K^+-ATPase pumps (Edwards and Marshall, 2013). Because hagfish are isosmotic to seawater, however, there is simply no need for them to use such pathways to unload Na^+ to the water as is common in most marine fishes (Edwards and Marshall, 2013). Indeed, the ionocytes of hagfish are intercalated between adjacent pavement cells, to which they are joined by deep intercellular ("tight") junctions, which is further suggestive that the gills of these isosmotic vertebrates have low cationic permeability (Bartels, 1988). Such an arrangement would not only preclude Na^+ movements *via* these pathways, but also NH_4^+ excretion.

The possibility that increases in renal J_{Amm} contributed to the stabilization of plasma T_{Amm} and the restoration of overall J_{Amm} cannot be discounted. But the very low urinary flow rates (UFR) of hagfish (Morris, 1965) suggest that the contribution of the kidneys to overall J_{Amm} under control or HEA conditions would be minimal. Moreover, the kidneys appear to be mainly involved in the excretion of divalents (Mg^{2+}; SO_4^{2-}; Ca^{2+}), with little or no water re-absorption taking place (Alt et al., 1981; Munz and McFarland, 1964).

Another possible route of ammonia excretion is the skin. Glover et al. (2011) reported that hagfish are capable of transporting amino acids across the gills and skin, which suits the hagfishes' propensity to burrow into decaying flesh of carrion, which is rich in nutrients. Given that the skin can act as a route of amino acid uptake, it seems logical that it could also act as a waste excretion route. Recent evidence has suggested that hagfish are indeed capable of skin J_{Amm} rates that are $10 - 30\%$ of total J_{Amm} (Clifford

et al., 2014); however, the role of the skin in recovery from HEA remains to be determined.

The most likely explanation to explain the restoration J_{Amm} by Pacific hagfish at HEA is that they used secondary active transport to excrete NH_4^+ *via* apical Na^+/NH_4^+ (H^+) exchange *via* the NHE. Although J_{Amm} was unaffected when Evans (1984) transferred hagfish to Na^+-free seawater, this treatment should not have been expected to eliminate J_{Amm} because outward P_{NH_3} diffusion gradients would still have been maintained, which would have promoted NH_3 excretion. In the present study, the outward P_{NH_3} gradient was eliminated (reversed), which would have forced the hagfish to increase their reliance on Na^+/NH_4^+ exchange. The presence of basolateral NKA in the hagfish ionocytes (Choe et al., 2002; Edwards et al., 2001; Tresguerres et al., 2006a) would likely have been more than sufficient to maintain the low cytoplasmic Na^+ concentrations needed to drive inward Na^+ movement *via* the NHE1, NHE2 or NHE3, each of which has been described in Atlantic and/or Pacific hagfishes (Choe et al., 2002; Edwards et al., 2001; Tresguerres et al., 2006a).

Taken together, my results suggest that J_{Amm} in the Pacific hagfish is likely a combination of Na^+/NH_4^+ exchange and passive NH_3 diffusion *via* the Rh glycoprotein metabolon (Wright and Wood, 2009). Such an arrangement would provide the hagfish with a flexible means to unload ammonia, depending upon the local conditions and/or their internal ammonia load (*e.g.* following feeding). I therefore propose that the contribution of apical Na^+/NH_4^+ exchange would normally be of secondary importance because it would be more energetically expensive than passive NH_3 diffusion, due to its dependency on NKA-mediated Na^+ export from the cytoplasm of ionocytes. However,

the secondary active transport of NH_4^+ would take on added importance when the fish were trying to maintain nitrogen or pH homeostasis when exposed to high levels of environmental ammonia or when trying to correct acid/base disturbances (*e.g.* Clifford et al., 2014; Edwards et al., 2001; McDonald et al., 1991; Tresguerres et al., 2007a). Further studies using radiolabelled Na^+ (*e.g.* $^{22}Na^+$), pharmacological approaches, or Na^+-free seawater could be used to further test such hypotheses.

Mechanisms of acid/base regulation in hagfish during HEA exposure

The pronounced alkalosis observed over 0 – 4 h was solely metabolic in nature, with a relatively stable P_{CO_2} (Figure 5.5). Its origin was clearly the result of the high rates of NH_3 uptake observed, which would have led to the metabolic acid consumption (acid deficit = base load) through the conversion of NH_3 to NH_4^+ as ammonia entered the fish. The stepwise correction of the alkalosis was likely due to a counterbalancing increase in the addition of metabolic acid to the blood. This conclusion is borne-out by the pronounced metabolic acidosis that resulted following the return of the hagfish to nominally ammonia-free water (Figure 5.4). In rainbow trout and Lahontan cutthroat trout (*Oncorhynchus clarki henshawi),* metabolic and respiratory alkalosis arising from exposure to alkaline (pH 9.5 – 10.0) water are offset by the generation of metabolic acid arising from increased lactate production (Wilkie and Wood, 1991; Wilkie and Wood, 1995; Wilkie et al., 1993). However, there was no evidence of such a counterbalancing lactacidosis in the Pacific hagfish exposed to HEA. While the resting lactate levels were very low in hagfish, likely a reflection of their low basal metabolic rates and correspondingly low rates of glycolytic flux, they are capable of generating large

amounts of lactate and ΔH^+_m under hypoxic/anoxic conditions (Cox et al., 2011), and following strenuous exercise (Davison et al., 1990).

More likely, the metabolic base load was corrected through a combination of apical anion exchange (*e.g.* Cl^-/HCO_3^- exchange) on the ionocytes, accompanied by increased H^+ extrusion to the plasma *via* a basolateral VHA. Such an arrangement was proposed to help correct blood pH in hagfish experiencing metabolic alkalosis following repeated $NaHCO_3$ injection, where immunohistochemical analysis revealed that there was an increase in basolateral VHA abundance (Tresguerres et al., 2007a). Unfortunately, there is presently no direct evidence of the anion exchange in the hagfish gill. Earlier work by Evans (1984) and McDonald et al. (1991), and more recently Clifford et al. (2014) clearly indicates that hagfish are capable of rapidly modulating acid and base equivalent excretion to correct metabolic acid/base disturbances. Learning more about the underlying mechanisms of acid/base regulation in these ancient craniates could shed considerable light on this subject, and how and when ion and acid/base regulatory strategies first appeared in the vertebrate lineage.

Tables

Table 5.1 Ammonia budget of Pacific hagfish exposed to high external ammonia (HEA; nominal [T_{Amm}] ~20 mmol L^{-1}) and following recovery in nominally ammonia-free water for 24 h.

Duration	Duration (h)	Duration (μmol kg^{-1})
Predicted (non-exposed)	0–48	−2,395
Observed (during HEA)	0–8	+51,223
	8–16	+34,156
	16–24	−25,107
	24–35	−38,400
	35–48	−8,212
Gross ammonia load (at 48 h HEA)		+13,670
Net ammonia balance (Observed – Predicted)		+16,055
Wash-out (Recovery)	0–8	−16,215

Note: Positive values denote net accumulation of ammonia due to ammonia uptake (gain), and negative values denote net ammonia excretion (loss) over each time period. Ammonia load calculations based on the ammonia excretion rates (μmol $kg^{-1} h^{-1}$) depicted in Figure 5.1A multiplied by the duration of each measurement period (h). Period of ammonia washout was determined following re-introduction of fish into nominally ammonia-free water following 48 h of HEA exposure.

Figures
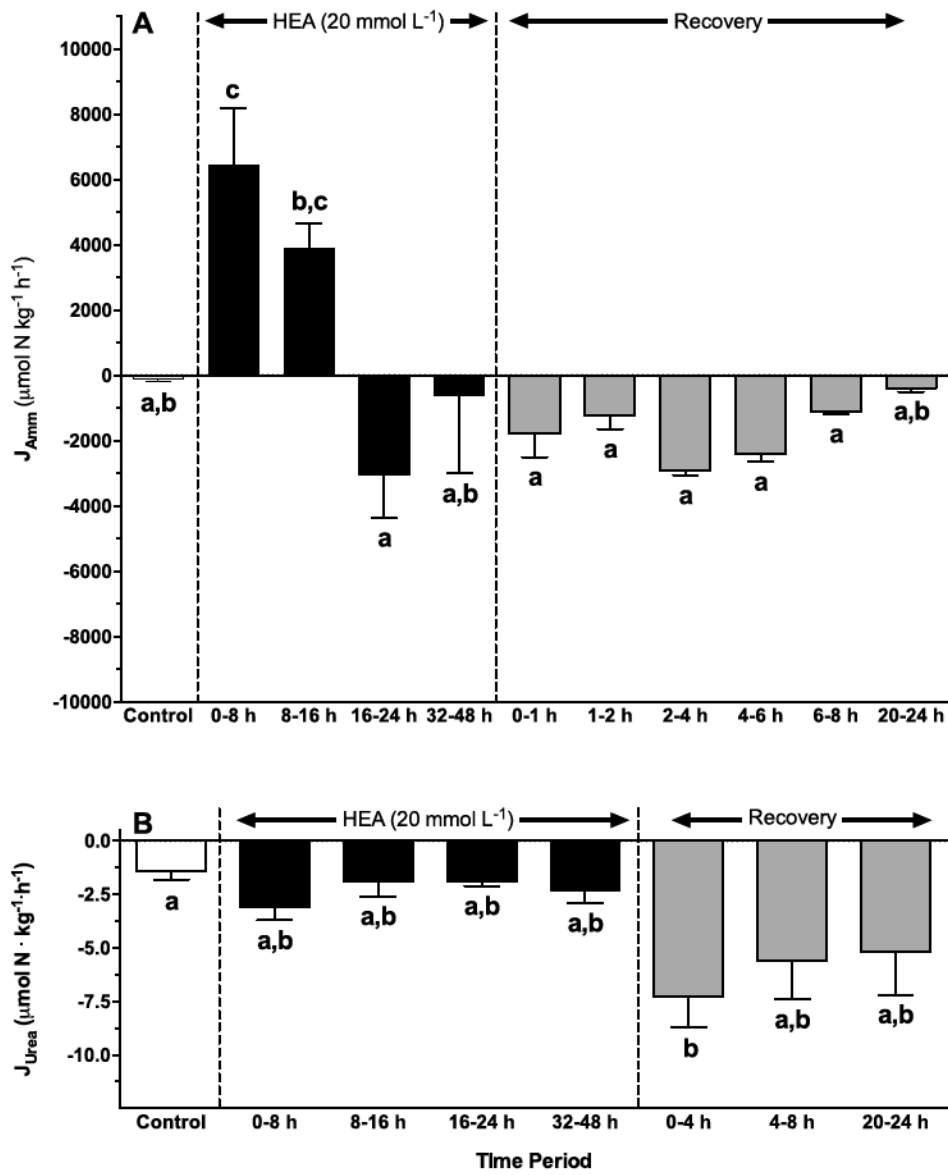
Figure 5.1 Nitrogen excretion patterns during and following HEA exposure.

Changes in the (A) ammonia excretion rate (J_{Amm}) and (B) urea excretion rate (J_{Urea}) of Pacific hagfish during exposure to high external ammonia (HEA; nominal T_{Amm} = 20 mmol L^{-1}) and following recovery in nominally ammonia-free seawater following 48 h exposure to HEA. Data presented as the mean ± 1 s.e.m.; n = 6 under during each measurement period. Bars sharing letters are not significantly different ($p < 0.05$).
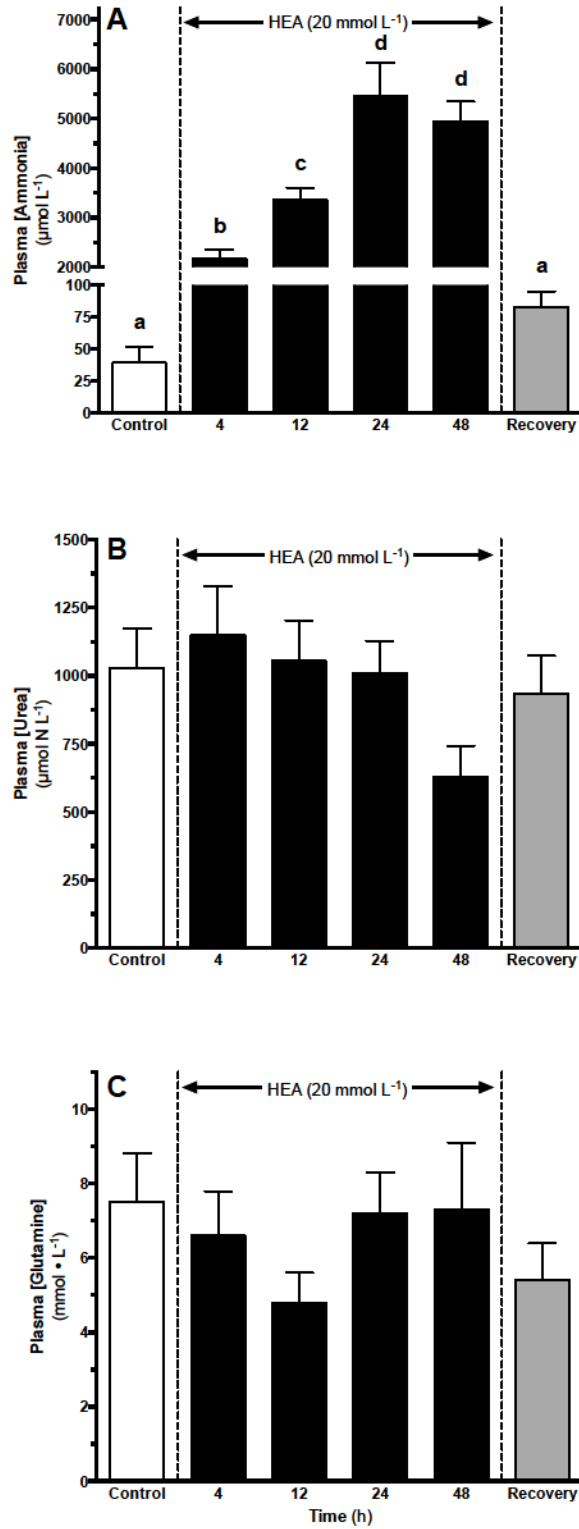
Figure 5.2 Plasma concentrations of nitrogen-based compounds during and following HEA exposure.

Changes in (A) total ammonia (T_{Amm}), (B) urea-N, and (C) glutamine concentration in the plasma of Pacific hagfish exposed to high external ammonia (HEA; nominal concentration = 20 mmol L^{-1}) for 48 h, and after re-introduction into nominally ammonia-free, full strength seawater. Data presented as the mean ± 1 s.e.m.; n = 10 – 12 under control (nominally ammonia-free) conditions, and after 4 h, 12 h and 24 h of HEA, and n = 6 after 48 of HEA and following the 24 h recovery period in nominally ammonia-free water. Bars sharing letters are not significantly different ($p < 0.05$).
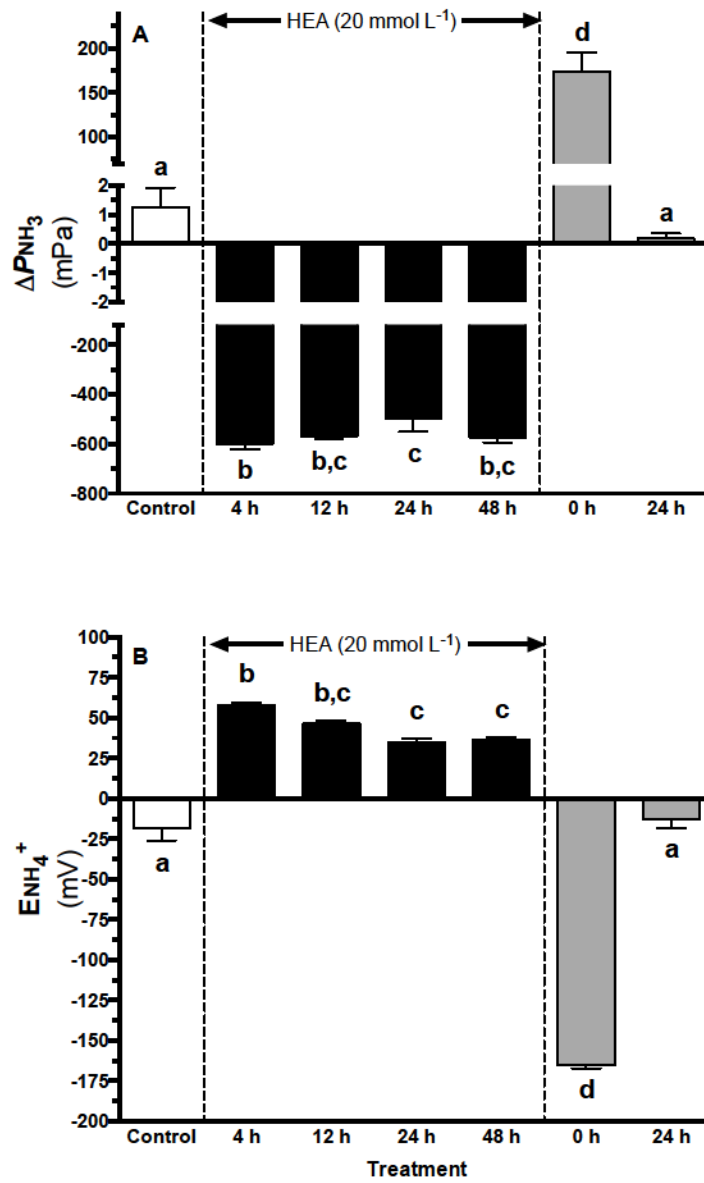
Figure 5.3 Calculated ΔP_{NH_3} and $E_{NH_4^+}$ values during and following HEA exposure.

Effect of high environmental ammonia (HEA; nominal $T_{Amm} = 20$ mmol L^{-1}) exposure on the (A) ΔP_{NH_3} and (B) Nernst Equilibrium for NH_4^+ ($E_{NH_4^+}$) in Pacific hagfish during exposure to high external ammonia (HEA; nominal T_{Amm} concentration of 20 mmol L^{-1}), and following recovery in nominally ammonia-free seawater for 24 h. Asterisks denote significant differences ($p < 0.05$) from control values. A positive ΔP_{NH_3} denotes an outwardly directed, blood-to-water P_{NH_3} gradient, and negative $E_{NH_4^+}$ denotes outwardly directed NH_4^+ gradient. $n = 10 - 12$ under control (nominally ammonia-free) conditions, and after 4 h, 12 h and 24 h of HEA, and $n = 6$ after 48 of HEA and following the 24 h recovery period in nominally ammonia-free water. Bars sharing letters are not significantly different ($p < 0.05$).
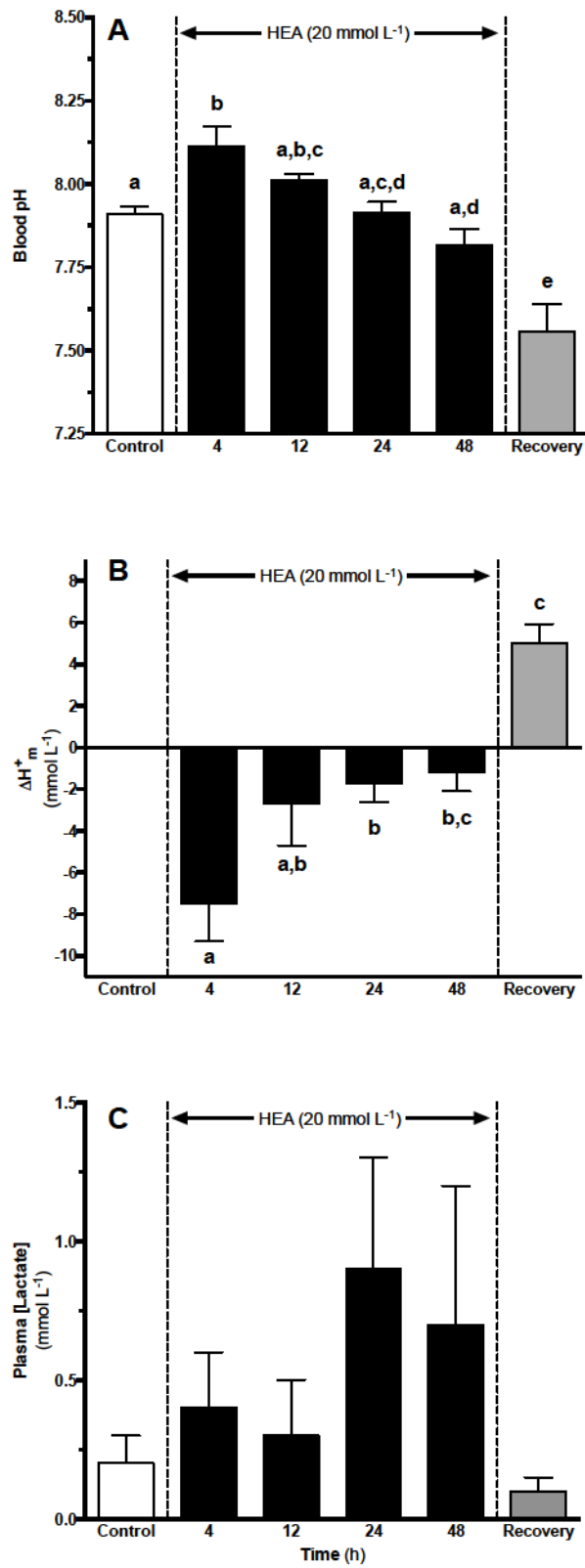
Figure 5.4 Blood pH and plasma lactate values during and following HEA exposure.

Changes in (A) sinus blood pH, (B) metabolic acid load (ΔH^+_m), and (C) lactate concentration in the plasma of Pacific hagfish exposed to high external ammonia (HEA; nominal concentration = 20 mmol L^{-1}) for 48 h, and after re-introduction into nominally ammonia-free, full strength seawater. Data presented as the mean ± 1 s.e.m.; $n = 10 - 12$ under control (nominally ammonia-free) conditions, and after 4 h, 12 h, 24 h and 48 h of HEA exposure, and $n = 6$ after following the 24 h recovery period in nominally ammonia-free water. Bars sharing a common letter denote mean values that are not significantly different from one another ($p < 0.05$). Note that a negative ΔH^+_m is indicative of a negative metabolic acid deficit (equals base load).
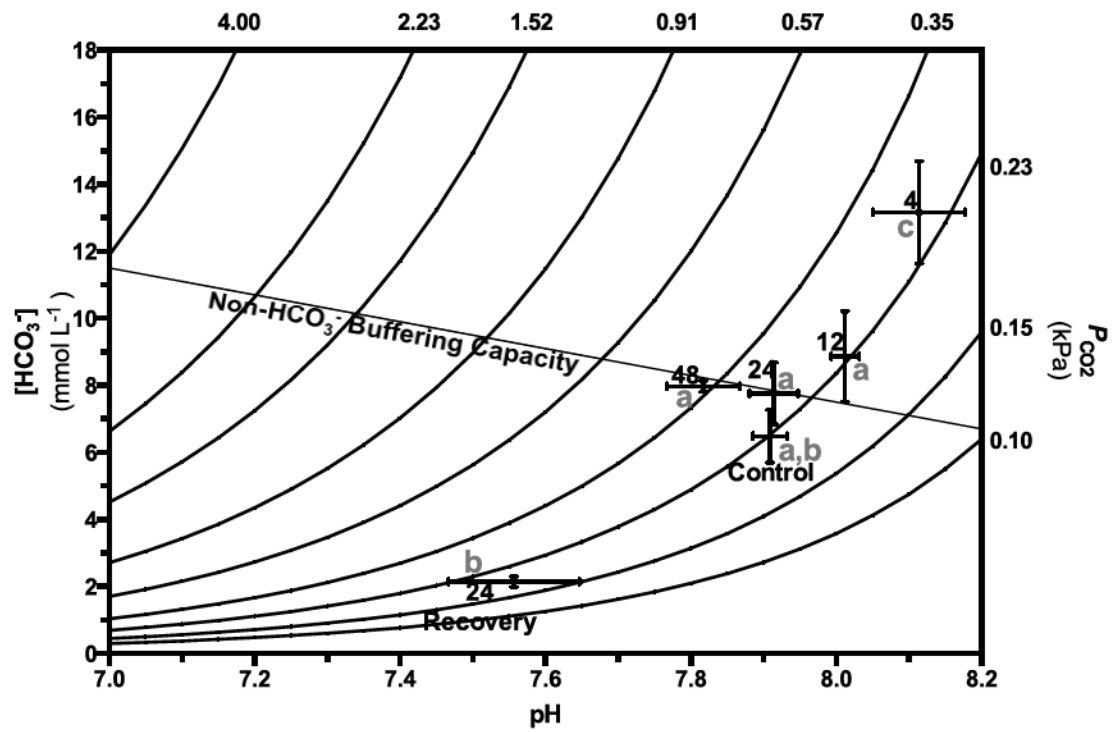
Figure 5.5 Blood and plasma acid/base status during and following HEA exposure.

Blood pH/[HCO$_3^-$] diagram, or Davenport diagram (Davenport, 1974) depicting the acid–base status of the blood of hagfish during exposure to high external ammonia (HEA; nominal concentration = 20 mmol L^{-1}) for 48 h and after re-introduction into nominally ammonia-free, full strength seawater. Data presented as the mean ± 1 s.e.m.; $n = 10$ under control (nominally ammonia-free) conditions, and after 4 h, 12 h, 24 h and 48 h of HEA, and $n = 6$ after following the 24 h recovery period in nominally ammonia-free water. The solid straight line is the non-bicarbonate buffer line determined by Wells et al. (1986). Asterisks denote significant ($p < 0.05$) differences in [HCO$_3^-$]. Bars sharing letters are not significantly different ($p < 0.05$) with respect to plasma [HCO$_3^-$]. No differences were observed in P_{CO_2}. For differences in blood pH please see Figure 5.4A.
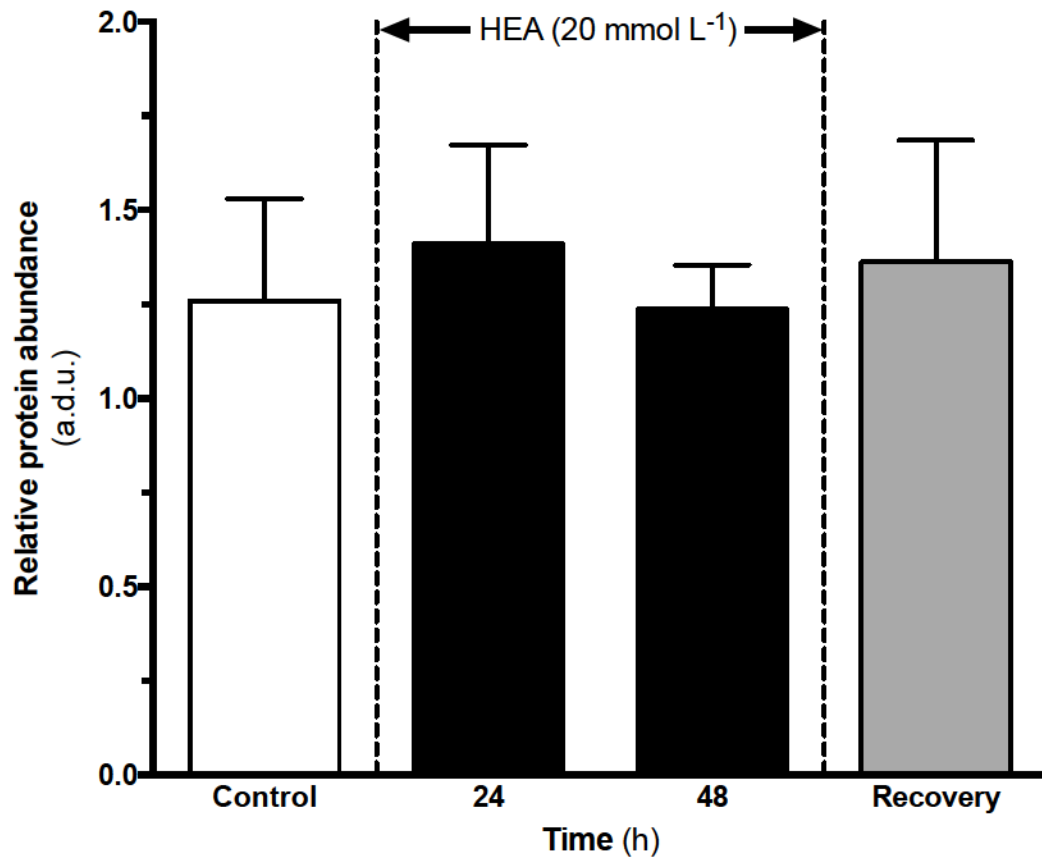
Figure 5.6 Western blot analysis of hagfish gill Rhcg abundance

Relative abundance of Rhcg in hagfish gill following exposure to high external ammonia (HEA; nominal concentration = 20 mmol L^{-1}) for 48 h and after re-introduction into nominally ammonia-free, full strength seawater. $n = 6$ for all groups except recovery group where $n = 5$.

Chapter 6: Flexible ammonia handling strategies using the skin and gill contribute to the high ammonia tolerance of the Pacific hagfish

Introduction

Hagfishes are distributed throughout the world's oceans, and along with the lampreys, are one of two families of extant jawless fishes that diverged from the vertebrate lineage approximately 500 million years ago (Bardack, 1991). Hagfishes are also well-known scavengers, feeding on carrion that falls to the ocean bottom (Martini, 1998). Such food drops may include marine mammals (Smith and Baco, 2003) and more commonly, fishes, including commercial by-catch (Collins et al., 1999). Adaptations for this mode of feeding include a protrusible dental plate capable of burrowing into and tearing flesh from carrion (Clark and Summers, 2007), high tolerance to anoxic and hypoxic conditions (Cox et al., 2011), and the ability to acquire amino acids (Glover et al., 2011) and phosphate (Schultz et al., 2014) across the skin and gill epithelia, in addition to the intestine (For review see Clifford et al., 2015b). My recent work suggests that high tolerance to ammonia is also strongly related to the scavenging lifestyle of hagfishes, which may routinely encounter extremely high concentrations of ammonia while burrowing into the decomposing carcasses of fishes and large marine mammals (Clifford et al., 2015b; Clifford et al., 2015a). While few, if any, studies have demonstrated that decomposing carcasses of marine animals generate ammonia, forensic studies on terrestrial mammals have demonstrated that the putrefactive processes occurring during decomposition generate millimolar concentrations of ammonia and other waste products such as methane and hydrogen sulfide (Carter et al., 2007).

In most teleost fishes, ammonia toxicity arises when plasma ammonia concentrations exceed 1 mmol L^{-1}, leading to gill damage, metabolic disturbances, and disruption of the central nervous system as characterized by pronounced swelling of the

brain (Wilkie et al., 2015), hyperexcitability, coma, and eventually death (see Smart, 1976, Ip et al., 2001b, Walsh et al., 2007 for reviews). A number of tropical fishes however, including the weatherloach (*Misgurnus anguilla caudatus*; Chew et al., 2001; Tsui et al., 2002), mudskipper (*Periophthalmodon schlosseri*; Ip et al., 2004), and snakehead (*Channa asiatica*; Chew et al., 2003) can withstand exposure to ammonia concentrations ranging up to 100 mmol L^{-1}. The Pacific hagfish (*Eptatretus stoutii*) too is highly ammonia tolerant, readily surviving 48 h exposure to 20 mmol L^{-1} total ammonia (T$_{Amm}$), which results in plasma ammonia concentrations of 5700 µmol L^{-1}, the highest amounts reported in any chordate. It is also able to excrete ammonia against large, inwardly directed gradients during HEA exposure through active excretion (Clifford et al., 2015a).

The overarching goal of the present study was to investigate the relative roles of the gill and skin of Pacific hagfish in ammonia uptake and excretion during and following exposure to HEA. In the teleost gill, Rhcg (Rhesus glycoprotein type c) acts as a facilitated ammonia transporter (SLC 42 transporter family) (Wright and Wood, 2009) and has been recently localized to the gill and skin of Atlantic hagfish (*Myxine glutinosa*; Edwards et al., 2015), Similarly, the Pacific hagfish gill also expresses Rhbg and Rhcg (Braun and Perry, 2010). The presence of Rhcg in both gill and skin of hagfishes suggests that it likely plays an important role in modulating J$_{Amm}$ *via* the gills, but perhaps also the skin.

In the present study, the sites of ammonia flux (J$_{Amm}$) before, during and following exposure to HEA (20 mmol L^{-1}) were determined in Pacific hagfish using divided chambers. Isolated skin flux studies, Western blotting and immunohistochemistry

where then used to characterize and localize Rh glycoproteins to determine if the skin facilitates J_{Amm} in these ancient, highly ammonia-tolerant fishes.

Materials and methods

Experimental animals and holding

Pacific hagfish (*E. stoutii;* N = 78; average mass = 139.03 g; range = 95.85 – 199.45 g) were captured from Trevor channel near Bamfield, BC, Canada and held at Bamfield Marine Sciences Centre (BMSC) as previously described (Clifford et al., 2014). Hagfish were fasted for one week prior to experimentation to minimize the effects of postprandial nitrogenous waste production and excretion, and defecation on experiments. All animals were used under licenses of the Department of Fisheries and Oceans Canada (permit # XR-223 2013; XR-192 2014) and approved animal care protocol from BMSC (RS-13-24) and University of Alberta (00001126).

Chemicals

All chemicals, reagents and enzymes were purchased from Sigma-Aldrich Chemical Company (St. Louis, MO), unless otherwise noted.

Experimental protocols

Series 1: Sites of ammonia excretion following exposure HEA

Hagfish were transferred to 10 L, darkened buckets receiving continuously flowing seawater for overnight acclimation. The following morning, hagfish were removed, anaesthetized (0.5 g L^{-1} tricaine methanesulfonate [TMS; Syndel Laboratories Ltd., Nanaimo, British Columbia, Canada] neutralized with NaOH (0.15 g L^{-1}) and a pre-exposure blood sample (200 µL) was drawn from the subcutaneous sinus using a

heparinized 21G needle for blood and plasma acid/base/ammonia analysis. Following blood sampling, hagfish were exposed to HEA (nominal $[NH_4Cl] = 20$ mmol L^{-1}) in 5.0 L aerated seawater for 48 h. Simultaneous control (no HEA) animals were held in the same manner. After 48 h, both the control and HEA-exposed hagfish were anaesthetized, weighed and blood collected as described above with the puncture wound sealed using cyanoacrylate glue and a small square (~4 mm^2) of nitrile rubber.

To evaluate the potential contribution of the cloaca to ammonia excretion, the cloaca was sealed in a subset of experimental animals ($n = 8$) with a rubber bandage and cyanoacrylate glue. No differences were detected in ammonia efflux in the posterior compartment in animals with or without this seal, so this practice was discontinued for remaining experiments.

Immediately following blood sample collection, hagfish were placed into divided chambers that isolated the posterior body region from the anterior region containing the gill pores (see Clifford et al., 2014 for apparatus and protocol details). Nominally ammonia-free seawater was then added to the anterior compartment only, and seal efficacy checked by monitoring water appearance in the posterior compartment. Ammonia-free seawater was then added to the posterior compartment and a lid secured. The chamber was placed in a wet table receiving flowing seawater for temperature control (10 ˚C). Water samples (1 mL) for ammonia quantification were collected and immediately frozen following placement of hagfish into the chamber and following the 4 h recovery period. After final sample collection, the patency of the seal was visually inspected, the hagfish removed from the apparatus, killed by TMS overdose (5 g L^{-1} TMS neutralized with 1.5 g L^{-1} NaOH), and a final blood sample collected (as above).

Series 2: Variation in the routes of ammonia excretion following HEA

The effects of localized HEA exposure in anterior vs. posterior body regions were determined by exposing each region individually to HEA and measuring ammonia flux in the other compartment. Hagfish were sampled for blood and placed in the divided chambers, followed by addition of sufficient NH_4Cl stock solution (1 M prepared in autoclaved seawater) to either the anterior or posterior compartment to yield a $[T_{Amm}]$ of 20 mmol L^{-1}. Water samples were taken immediately in the opposing compartment, and again after 4 h. The animals were then removed and blood samples collected for pH and T_{Amm} measurement.

To rule out artifacts, the separating chamber apparatus was leak-tested by measuring Mg^{2+} flux as a proxy for leakage. Hagfish were fitted into the chambers (as above), and artificial seawater (ASW; in mmol L^{-1} NaCl, 415; KCl, 10.2; Na_2SO_4, 28; $CaCl_2$, 10; [pH = 8.0]) containing 50 mmol L^{-1} $MgCl_2$ was added to the anterior compartment, and ASW containing 75 mmol L^{-1} $C_5H_{14}ClNO$ (choline chloride) to the posterior compartment for osmotic balancing. An additional group of hagfish were also placed into undivided chambers filled with Mg^{2+}-free seawater containing 75 mmol L^{-1} $C_5H_{14}ClNO$ to determine endogenously derived branchial, cutaneous and cloacal Mg^{2+} flux into the Mg^{2+}-free solution. All solutions were osmotically balanced with mannitol (± 1.0 mOsm kg^{-1}; VAPRO® vapor pressure osmometer, model 5520; Wescor Inc, Logan, Utah, USA). No detectable movement of Mg^{2+} from the anterior-to-posterior chamber over 4 h was observed, which ruled out any leakage between compartments (Mg^{2+} detection limit of 0.5 µmol L^{-1}; $n = 6$).

Series 3: The skin as a route of ammonia excretion

Measurements of skin J_{Amm} were conducted using the approach described by Glover et al. (2011). Hagfish were held in ammonia-free seawater or exposed to HEA (20 mmol L^{-1} NH$_4$Cl) for 48 h, then killed by TMS overdose (as above). The skin dorsal to slime glands running the length of the body from the ~5th branchiopore to the tail was removed, and 5 skin patches bisected by the dorsal midline (~3 cm X ~3 cm) were prepared. Samples of skin were also fixed for immunohistochemistry (see below). Skin patches were maintained in aerated saline (in mmol L^{-1}: NaCl, 474; KCl, 8; MgCl$_2$, 9; MgSO$_4$, 3; NaH$_2$PO$_4$, 2.06; NaHCO$_3$, 5; HEPES, 20; glucose, 5; [pH = 7.8]) and used within 1 h of excision. Each individual patch was placed over the top of the flux vial, and secured in place with the serosal (basal) side of the skin facing outward. The inverted chamber was then placed in a small plastic bottle (serosal bath) containing 20 mL of hagfish saline. The inner chamber of the vial served as the mucosal bath and was comprised of filtered, autoclaved seawater containing different [T_{Amm}] (0.05, 0.1, 0.5, 1.0, 5.0 mmol L^{-1}). Serosal and mucosal solutions were independently mixed using a pipette and continual aeration provided throughout the flux period. Mucosal water samples (1 mL) were drawn at the beginning and end of each flux measurement period (0, 2 h). Water samples were then acidified with 1 µL of 1 N HCl to prevent NH$_3$ volatilization and stored at -20° C.

In a second set of experiments, the ammonia excreting capacity of the skin was determined along the length of the hagfish. Six patches of skin (~3 cm X ~3 cm) were excised as above at regular intervals along the longitudinal axis of the body and tested for differences in J_{Amm}.

Series 4: Determination of cutaneous Rhcg abundance along the length of the animal

Hagfish that were naïve to experimental HEA were terminally anaesthetized (as above). Animals were then weighed and total animal length was recorded. Skin was excised at three locations at measured lengths from the anterior of the animal. Excised skin was immediately transferred to a 2 mL eppendorf tube containing RNAlater. Samples were then stored at -20 ˚C until protein expression analysis could be determined.

Series 5: Role of Rh glycoproteins in ammonia excretion by Pacific hagfish

Multi-species alignments for Rh glycoprotein were constructed (15 Rhbg and 13 Rhcg homologues; Table 5.1) using MUSCLE (ebi.ac.uk/Tools/msa/muscle/) and an HMM (Hidden Markov Model) profile for each isoform was determined using HMMER3 (v3.0; Janelia Farm; hmmer.janelia.org). With these profiles, HMMER searches were conducted through a translated hagfish gill/slime gland Illumina transcriptome and results were BLAST analyzed on NCBI to verify Rh family homology. Searches resulted in a full-length sequence for EsRhcg (*Eptatretus stoutii* Rhcg; including 5' and 3' untranslated regions [UTRs]) and two partial sequences for EsRh-like (*Eptatretus stoutii* Rh-like; sequence 1 containing 5' UTR and sequence 2 containing 3'UTR). Using this sequence information, PCR primers were constructed based off of the UTRs (Table 5.2) to confirm full-length coding sequence (CDS) *via* cloning (see below).

Analytical methods

Blood sample analysis

Immediately following blood collection, blood pH was measured using a thermojacketed (10 ˚C) Orion ROSS Micro pH electrode (Fisher Scientific, Ottawa, ON). The blood samples were then centrifuged (12,000 g for 30 seconds), and the plasma stored at -80 ˚C for T_{Amm} analysis. Plasma T_{Amm} concentration was quantified enzymatically using a commercial kit (Sigma-Aldrich Procedure A001) at 340 nm.

Water chemistry

Water ammonia concentrations were determined colorimetrically using the salicylate-hypochlorite assay at 650 nm (Verdouw et al., 1978), with a microplate spectrophotometer (Spectramax 190, Molecular Devices, Sunnyvale, CA) as previously described (Clifford et al., 2015a). Samples for Mg^{2+} quantification (Series 2) were analyzed using an atomic absorption spectrophotometer (Thermo Scientific model iCE 3300).

Molecular determination of EsRhcg and EsRh-like transcripts

Total RNA was obtained from the hagfish gill (~100 mg) using TRIzol extraction. DNase I (Ambion/Life Technologies, Carlsbad, CA, USA) treated RNA was used to synthesize cDNA using RevertAid H-minus M-MuLV reverse transcriptase (Fermentas/Thermo Scientific, Pittsburgh, PA, USA). PCR reactions targeting full-length CDS were conducted using Phusion DNA polymerase (Thermo Scientific, Pittsburgh, PA, USA) with species-specific primers (Table 6.2) for 35 cycles. Amplicons were

analyzed by gel electrophoresis, imaged using Alpha Imager 2200, and gel purified using QIAquick Gel Extraction Kit (Cat. #28704). Products were cloned into *E.coli* (dh5-α) using the CloneJet PCR cloning kit (Thermo scientific, Pittsburgh, PA, USA). Plasmid DNA was isolated and sequenced.

Phylogenetic sequence analysis of cloned EsRhcg and EsRh-like transcripts

An alignment of the sequenced hagfish Rh glycoprotein homologues against Rh homologues from other species was conducted using MUSCLE (Edgar, 2004) in SeaView (Galtier et al., 1996; Gouy et al., 2010) for MacOS. The resulting alignment was then refined using GBlocks (Castresana, 2000) to subtract gaps and residues of low/noisy homology with parameters selected to allow for more relaxed stringency (Talavera and Castresana, 2007). Phylogenetic analysis was conducted on the Cyberinfrastructure for Phylogenetic Research (CIPRES) Science Gateway servers (Miller et al., 2010) using RAxML version 8.0.9 (Stamatakis, 2014) utilising the LG evolutionary model (Le and Gascuel, 2008). Branch support was estimated by bootstrap with 300 replications (auto cutoff set at 1000 bootstraps). For phylogenetic analysis, base frequencies were model-determined and the proportion of invariable sites was determined using the GTRGAMMA model. A total of 85 protein sequences from the Rh glycoprotein family were collected from different species (including hagfish EsRhcg and EsRh-like protein sequences) and used in the analysis.

Histology and immunohistochemical detection of Rhcg in skin tissue

Skin from non-HEA exposed hagfish (Series 3 experiments) was placed in fixative (4% paraformaldehyde in 10 mmol L^{-1} phosphate-buffered saline, pH 7.4) for 24

h at 4°C, rinsed (3X) in PBS then paraffin processed. Tissue sections were then processed for immunohistochemistry using Atlantic hagfish *Myxine glutinosa* Rhcg antibody (*h*Rhcg; Edwards et al., 2015) and visualized using a Zeiss LSM510 Confocal Microscope.

Negative staining controls for *h*Rhcg were processed in the absence of primary antibody and using pre-absorbed antibody incubations. In pre-absorbed controls, *h*Rhcg was diluted to 1.25 µg mL^{-1} in blocking solution containing 2.5 µg mL^{-1} of *h*Rhcg antigen. The antibody and peptide mixture was incubated at RT for 30 min before addition to tissue sections. Routine heamatoxylin and eosin staining was used for structural reference, using methods described by Weinrauch et al. (2015).

Electrophoresis and Western blot analysis

Skin samples stored in RNAlater were pulverized under liquid nitrogen then transferred (~100 mg) to a centrifuge tube containing 1:10 w/v of ice-cold homogenization buffer (250 mmol L^{-1} sucrose, 1 mmol L^{-1} EDTA, 30 mmol L^{-1} Tris, 100 mg/mL PMSF, and 5 mg mL^{-1} protease inhibitor cocktail). Samples were then homogenized on ice using a hand-held motorized mortar and pestle (Gerresheimer Kimble Kontes LLC, Dusseldorf, Germany) for 45 seconds. Homogenates were then centrifuged at 3000 × *g* for ten minutes at 4 ˚C and the supernatant drawn off. A subsample of the supernatant was assayed for protein determination *via* the BCA (bicinchoninic) technique (Thermo Scientific, Rockford, IL, USA).

Processed gill samples were diluted with 3X Laemmli buffer (Laemmli, 1970) and 25 µg of total protein was loaded in Criterion-TGX 20% acrylamide gels (Bio-Rad,

Hercules, CA) and separated by SDS-PAGE (sodium dodecyl sulfate, polyacrylamide gel electrophoresis).

Protein was transferred to a nitrocellulose membrane (Millipore, Billerica, MA). Protein transfer was confirmed by soaking membranes in Ponsceau S staining solution (0.1% (w/v) Ponceau S in 1% (v/v) acetic acid). Membranes were washed (2 min in distilled water followed by 3 x 1min in 0.5 M Tris-Buffered Saline [TBS; pH=8.0] containing 0.2% Tween-20 [TBST]) and then blocked in 5% blotto (5% skim milk powder in TBST) on a shaking carousel overnight at 4 ˚C.

Membranes were then washed (3x15 min in TBS and then 3 x 15 min in TBST) before overnight incubation in blocking buffer containing 1˚ antibody (1:5000 rabbit anti-*h*Rchg) at room temperature. Membranes were then washed 3 times (15 min in TBST) then incubated with 2˚ antibody (1:10,000 goat anti-rabbit HRP; Santa Cruz Biotechnologies Inc., Dallas, TX, USA) and Precision Protein StrepTactin-HRP conjugate (Bio-Rad) in TBST at room temperature for 1 h. Membranes were washed 3 times (15 min) in TBST followed by a final wash in TBS. Labeled protein bands were detected *via* enhanced chemiluminescence (ECL; Pierce; SuperSignal West Pico Chemiluminescent Substrate; Rockford, Il, USA). Visualization was done using Bio-Rad Chemidoc system with densitometry analysis completed using image analysis software (Bio-Rad). Standardization for protein concentration was quantified on the basis of 25 μg of total protein loaded into each well.

Calculations and statistical analysis

J$_{Amm}$ calculations were based on the T$_{Amm}$ accumulation in the water in either the anterior and/or posterior compartments using the following equation:

$$J_{Amm} = \left([T_{Amm}]_{initial} - [T_{Amm}]_{final} \cdot V\right) \cdot \frac{1}{m} \cdot \frac{1}{\Delta t} \qquad (1)$$

where [T$_{Amm}$] is the initial or final concentration of ammonia in the water (μmol L^{-1}); V is the volume of water (mL); m is the animal mass (g) and Δt the duration of the flux period.

J$_{Amm}$ across excised hagfish skin was determined by measuring ammonia appearance in the mucosal bath of the miniature flux chambers using the following equation:

$$J_{Amm}^{Skin} = \left([T_{Amm}]_{initial} - [T_{Amm}]_{final} \cdot V\right) \cdot \frac{1}{SA} \cdot \frac{1}{\Delta t} \qquad (2)$$

where SA is the measured mucosal surface area of hagfish skin exposed to seawater (cm^2), and other notations are as stated above.

All data are presented as the mean ± s.e.m. Differences between groups with respect to plasma T$_{Amm}$ and blood pH were tested using one-way analysis of variance followed by Sidak's multiple comparison *post-hoc* tests with pre-planned comparisons. Differences in J$_{Amm}$ for the divided chamber studies and measurement of J$_{Amm}$ across sections of skin (skin from HEA vs. non-HEA hagfish) were compared using Student's t-test. Linear regression tested for differences in skin J$_{Amm}$ along the hagfish length. Differences in *h*Rhcg abundance along the length of the skin was tested using one-way

ANOVA followed by Holm-Sidak multiple comparision *post-hoc* test. The fiducial limit of statistical significance was $p < 0.05$. All statistical analyses were completed using GraphPad Prism 6.0 (GraphPad Software, San Diego, USA).

Results

Series 1: Sites of J_{Amm} following HEA exposure

Plasma T_{Amm} averaged 554.8 ± 38.0 µmol L^{-1} in Pacific hagfish prior to HEA exposure and remained unchanged in parallel non-HEA exposed hagfish following the 48 h exposure (614.2 ± 116.9 µmol L^{-1}) and 4 h recovery period (603.2 ± 69.1 µmol L^{-1}; Figure 6.1A). The group exposed to 20 mmol L^{-1} HEA for 48 h exhibited no mortalities during either exposure or recovery and had significant plasma T_{Amm} accumulation (3751.2 ± 111.8 µmol L^{-1}) after 48 h. Following 4 h of recovery in ammonia-free water, plasma T_{Amm} was reduced to 2820.2 ± 213.4 µmol L^{-1} (Figure 6.1A).

Prior to HEA exposure, blood pH was 7.92 ± 0.02 (Figure 6.1A), and not significantly different from animals held in ammonia-free seawater. Following 48 h HEA exposure, blood pH was unchanged compared to the parallel controls in ammonia-free seawater (pH 7.95 ± 0.06). However, following 4 h recovery in ammonia-free seawater, there was a significant 0.4 unit drop in blood pH to pH 7.63 ± 0.05 in HEA exposed hagfish (Figure 6.1B).

When control hagfish, not exposed to ammonia, were placed in divided chambers, routine J_{Amm} averaged 40.0 ± 25.9 µmol kg^{-1} h^{-1} (Figure 6.2A) in the anterior compartment and 4.9 ± 1.4 µmol kg^{-1} h^{-1} in the posterior compartment (Figure 6.2B), totaling ~45 µmol kg^{-1} h^{-1} for the whole animal. However, anterior J_{Amm} in the ammonia-loaded animals increased approximately 15-fold (590.7 ± 91.5 µmol kg^{-1} h^{-1}; Figure 6.2A). Excretion in the posterior compartment however, increased nearly 26-fold to 129.1 ± 14.3 µmol kg^{-1} h^{-1} representing approximately 20% of combined J_{Amm} from anterior

and posterior compartment (~720 μmol kg^{-1} h^{-1}) in HEA-exposed animals compared to approximately 11% in the non-exposed controls (Figure 6.2B).

Series 2: Variation in the routes of J_{Amm} following HEA

Exposure of the anterior region of the hagfish to HEA for 4 h resulted in a plasma T_{Amm} load of 1273.6 ± 106.4 μmol L^{-1}, which was not significantly greater than the concentrations measured in control (no HEA) animals (603.2 ± 69.1 μmol L^{-1}; Figure 6.3A). Notably, when the posterior end of the hagfish was exposed to HEA, animals experienced a substantial accumulation in plasma T_{Amm} (3081.7 ± 368.3 μmol L^{-1}) suggesting that the posterior zones of the body were more permeable to external ammonia than the anterior region (Figure 6.3A).

Control animals, not exposed to HEA, had an average blood pH of 7.77 ± 0.06 (Figure 6.3B) in agreement with previous experiments. While no differences in blood pH were observed following 4 h exposure of the anterior body to HEA (7.80 ± 0.05 pH units), exposure of the posterior body regions to HEA resulted in a significant acidosis characterized by drop in blood pH to 7.56 ± 0.08 (Figure 6.3B).

When the route of HEA exposure was *via* either the anterior or posterior chamber, J_{Amm} was measured in the opposing HEA-free compartment. When HEA exposure was *via* the anterior compartment, posterior J_{Amm} averaged 121.7 ± 40.9 μmol kg^{-1} h^{-1}, which was 5-fold greater than rates in control animals (Figure 6.4A). When the route of HEA was *via* the posterior compartment, J_{Amm} averaged 151.7 ± 49.8 μmol kg^{-1} h^{-1} in the anterior compartment, ~4-fold greater than measured in controls (Figure 6.4B).

Series 3: Ammonia flux across excised skin tissue

To further investigate the skin's role in ammonia handling, skin sections were excised from the dorsal region of hagfish pre-exposed to HEA (20 mmol L^{-1}) or control animals held in ammonia-free seawater for 48 h. In both cases J_{Amm} was concentration-dependent over the range of serosal T_{Amm} concentrations tested (Figure 6.5A). However, J_{Amm} across the skin excised from HEA-exposed animals was up to 8-fold greater at a serosal $[T_{Amm}]$ of 0.05 mmol L^{-1} and 1.3-fold greater at a serosal $[T_{Amm}]$ of 5 mmol L^{-1} (Figure 6.5B).

The skin contribution to J_{Amm} also appeared to be greater in posterior relative to anterior body regions, with J_{Amm} increasing linearly in skin sections sampled sequentially from anterior to posterior (R^2= 0.88) with a slope of 0.1307 ± 0.024 ([nmol cm^{-1} h^{-1}]/ [% distance from snout]; $F_{1,4}$ = 30.30, *p*=0.00531; Figure 6.5C).

Series 4: Determination of cutaneous Rhcg abundance along the length of the animal

Skin tissue excised sequentially from anterior to posterior was distributed on a percentage distance from snout basis (Anterior: 27.58 ± 0.9 %; Middle: 57.21 ± 1.40 %; Posterior: 84.19 ± 1.08 %). Western blot analysis on skin tissue using *h*Rhcg antibody (Edwards et al., 2015) yielded a single immunoreactive protein band at ~50 kDa (Figure 6.6a). Rhcg abundance was variable across the length of the skin and was statistically greater in skin sections excised from the middle on the animal compared to sections from the anterior of the animal. Arguably, there was also greater abundance of Rhcg in the posterior region compared to the anterior region; however, this was not statistically

significant. No significant differences were observed between the middle and posterior sections.

Series 5: Detection and distribution of Rhcg in cutaneous tissue

Using an Illumina transcriptomes for combined gill/slime gland, a full-length sequence for *Es*Rhcg and a partial *Es*Rh-like was isolated. Using species-specific primers based off transcripomic data, full-length amplicons were amplified using PCR. Sequencing following subsequent cloning identified a 1386 bp ORF (open reading frame) encoding a 462 amino acid residue protein for EsRhcg sequence and a 1443 bp ORF encoding a 481 amino acid protein for EsRh-like sequence. These sequences share high homology (>98% at amino acid level) with previously identified homologues from Atlantic hagfish (Edwards et al., 2015). Maximum-likelihood phylogenetic analysis of these sequences against subfamilies of the Rh glycoprotein family demonstrated that the cloned *Es*Rhcg and *Es*Rh-like are members of the Rh glycoprotein family (Figure 6.7). Full-length sequences for cloned *Eptatretus Stoutii* Rhcg and Rh-like sequences are found on the NCBI database (accession numbers KT943755, KT943754 respectively).

H&E staining highlighted the cellular composition of the capillary-rich (Cp) dermis (d), as well as the prominent mucous cells (MC) in the basal aspect of the epidermis (E; Figure 6.8A). Immunohistochemical analysis, using *h*Rhcg antibody (Edwards et al., 2015), demonstrated that *h*Rhcg immunoreactivity was localized to the basal aspect of the skin epidermis (Figure 6.8B). Peptide competition eliminated this staining in the basal aspect (Figure 6.8B inset). The Pacific hagfish *Es*Rhcg sequence

exhibited 90% (18/20 a.a.) similarity with antigenic peptide sequence used to create

*h*Rhcg antibody (Table 6.3).

Discussion

Overview

Previous reports have demonstrated the impressive ammonia handling capabilities of hagfish in relation to tolerance of exposure, tolerance of uptake and excretory capacity (Braun and Perry, 2010; Clifford et al., 2015a; Edwards et al., 2015; Evans, 1984; McDonald et al., 1991). The goal of this study was to extend these observations by: 1) identifying *in vivo* if hagfish can utilize cutaneous excretion to counteract HEA-induced ammonemia 2) determining if ammonia handling is altered in response to internal and external ammonia loads and 3) determining if hagfish possess the necessary ammonia transporters in cutaneous tissue. The findings presented herein clearly demonstrate that hagfish have the capacity to differentially handle ammonia by modulating J_{Amm} across the gills and skin. These findings confirm previous observations that hagfish routinely excrete nitrogenous wastes from skin at rates 10-30% of whole animal rates (Clifford et al., 2014), and reaffirm the extraordinarily high tolerance of the hagfish both to HEA and high plasma T_{Amm} (Braun and Perry, 2010; Clifford et al., 2015a). Furthermore, following ammonia loading *via* HEA exposure, J_{Amm} increased across both gill (~15-fold) and skin (~26-fold) epithelial tissue in comparison to routine rates in the whole animals. These findings are supported by my skin flux studies, which demonstrate that following HEA exposure, ammonia transport rates across excised skin tissue increases along the length of the animal from anterior to posterior. Moreover, based on the serosal T_{Amm} concentration, greater fold-changes were observed at lower, and likely more environmentally relevant, T_{Amm} concentrations. Finally, two Pacific hagfish Rh orthologs were identified and, using immunohistochemistry, I demonstrate Rhcg localization in the epidermal area near the

basement membrane, thus providing a mechanistic route for ammonia transfer across the skin.

Cutaneous adaptations to adverse feeding conditions

Hagfish partially burrow into carrion and feed on the soft tissues of the decaying carcass (Martini, 1998). This feeding behaviour immerses the branchial region in an area likely containing high amounts of putrefactive products (see Introduction) leaving the posterior region of the animal exposed to seawater where the gradients of these substances are diminished and likely favour excretion, provided that the transport mechanisms are present. Interestingly, anterior HEA exposure resulted in lower accumulations of ammonia in the blood compared to an equivalent HEA exposure in the posterior region. I hypothesize that this may be an adaptation to reduce ammonia loading during feeding bouts where the anterior region of the animal is in closer proximity to the decaying carcass.

A recent study on Atlantic hagfish (*Myxine glutinosa*) demonstrated that Rhcg was present in the gills, a common site for ammonia excretion, but also in skin (Edwards et al., 2015). The presence of a dermal capillary network in hagfish skin is also postulated to be an important site of gas exchange (Potter et al., 1995). It may be that the dermal capillary network in of Pacific hagfish skin is used to facilitate ammonia excretion provided ammonia gradients are outwardly directed. Immunohistochemistry has demonstrated that Pacific hagfish express the Rhcg protein in the basal region of the skin epidermis; thus providing a route by which ammonia can be transported across the skin. The Rhcg staining is most prominent in close proximity to the dermal/epidermal interface

and immediately adjacent to the dermal capillary network. I propose that Rh proteins provide an increased directional permeability facilitating ammonia transport across the skin to the environment.

The results of increasing skin permeability from the anterior to posterior regions of the hagfish (Figure 6.3C) also support this adaptive hypothesis. Presumably while feeding, more posterior regions of hagfish skin have more favourable excretory gradients due to the diminishment of putrefactive products including ammonia in the adjacent water more distal to the carrion. These results also demonstrate that pre-exposure to HEA causes significant increases in cutaneous permeability presumably as a mechanism to increase excretion in the posterior (cutaneous) regions. Unfortunately, reliable protein extracts were unable to be obtained from frozen skin tissue from HEA and control fish. Updated collection methods with RNAlater however, did yield successful protein extractions from skin tissues taken along the length of control animals. There does appear to be differences in Rhcg expression across the length of the animal with lower expression from anterior tissue and higher expression in skin excised from the middle and the posterior sections of the animal. Thus, expression analysis of Rhcg does provide some support for the increased flux along the length of the animal. Future research should examine how cutaneous Rhcg expression is modulated during HEA exposure and recovery.

Regional differences in J$_{Amm}$ following HEA exposure

During recovery, both the gill and skin contributed to J$_{Amm}$ in the anterior compartment, while cutaneous and cloacal (intestinal and renal combined) constituents contributed to J$_{Amm}$ in the posterior compartment. Preliminary experiments revealed that

a cloacal seal did not impact J_{Amm} in the posterior chamber in either control or HEA exposed animals, demonstrating that cloacal efflux does not play a prominent role in J_{Amm}. Given the low urine flow-rate of the hagfish (227 μl kg^{-1} h^{-1}; Morris, 1965), the urine would have to be concentrated to >800 mmol L^{-1} to account for the measured J_{Amm}. This would be ~2 orders of magnitude greater than the hagfish plasma T_{Amm} following HEA exposure. Given that hagfish do not ionoregulate (Currie and Edwards, 2010), have rudimentary kidneys without a multiplying loop of Henle (Weinrauch et al., 2015) and have a urine composition similar to plasma (Alt et al., 1981), it is unlikely that hagfish concentrate ammonia within their urine as a means of excretion. Thus posterior flux rates are interpreted as being primarily cutaneous.

When in the divided chambers, ~40% of the hagfish skin was in the anterior compartment whilst ~60% was in the posterior compartment. I have previously reported that basal cutaneous ammonia excretion rates in hagfish are in the range of 10-30% of whole animal rates (Clifford et al., 2014) corroborating with results in the present study (~18% of routine rates and ~30% following exposure to HEA). Cutaneous ammonia excretion has been observed in several fish species including dab (*Limanda limanda*; Sayer and Davenport, 1987), rainbow trout (*Oncorhynchus mykiss*; Zimmer et al., 2014) and the mangrove killifish (*Kryptolebias marmoratus*; Frick and Wright, 2002). In trout, cutaneous ammonia excretion accounted for 4.5% of total J_{Amm} under routine conditions and mildly increased to 5.7% following HEA exposure (12 h; 2 mmol L^{-1}; Zimmer et al., 2014)) while in the dab, cutaneous ammonia excretion accounted for 47% under routine conditions; however, the effect of ammonia loading *via* HEA exposure has yet to be determined (Sayer and Davenport, 1987).

Acid/base response during exposure, recovery and localized exposure.

The acidosis observed following 4 h recovery in ammonia-free seawater agrees with previous studies (Clifford et al., 2015a) and is the result of a compensatory metabolic acid load associated with NH_3 excretion. However, a perplexing ~0.2 pH unit acidosis was observed associated only with posteriorly-applied HEA and not anteriorly-applied HEA. While posterior entry of NH_4^+ would account for this result, the entry of ammonia as NH_4^+ seems unlikely given the relatively low cationic permeability of the hagfish body surface (Evans, 1984). One possibility is that there is a differential response to anteriorly-vs. posteriorly-applied HEA and this bears further investigation.

Ammonia permeability in the branchial region

Interestingly, localized ammonia exposures demonstrated anterior (i.e. branchial) HEA exposure does not result in an equal rate of increase in plasma T_{Amm}, as does equivalent posterior HEA exposure. This hysteresis in response to localized HEA not only suggests that ammonia loading *via* cutaneous means may be a major route of ammonia uptake in hagfish, but also that the anterior regions (gills and/or anterior skin) possess the ability to reduce ammonia uptake when exposed to HEA, even in the face of massive inwardly-directed ammonia gradients. In contrast, the rise in plasma ammonia when the route of exposure is *via* the posterior chamber indicates that hagfish are unable to limit posterior cutaneous ammonia uptake, at least acutely. Reduced plasma T_{Amm} loading during localized HEA exposure provides further evidence that hagfish have adapted novel ammonia handling strategies to overcome the challenges associated with feeding on putrefying carrion.

While the mechanisms behind this hysteresis are unknown, changes in gill ammonia permeability due to changes in hRhcg abundance can be ruled out. Western blots of gill tissue demonstrated that prolonged exposure of hagfish to identical ammonia concentrations were not accompanied by changes of branchial hRhcg protein abundance (Clifford et al., 2015a).

In the absence of any changes in Rhcg abundance, it may be that the hagfish were able to restrict ammonia uptake by either alteration of other Rh protein expression and function, alteration in Rhcg function, or perhaps by reducing branchial ventilation rate and/or flow. Further investigation is warranted in these aspects to identify the underlying mechanism responsible for this remarkable ability to essentially 'block' ammonia uptake. This study demonstrates that hagfish have the capacity to spatially regulate ammonia excretion across multiple epithelia and that there exists a capacity to adjust ammonia permeability in response to localized environmental ammonia.

Conclusions

This study is the first to demonstrate localized ammonia transport with increased ammonia permeability occurring more posteriorly. HEA-induced plasma ammonia loading results in a higher cutaneous permeability in excised skin suggesting regulation of ammonia permeability. These findings also demonstrate that hagfish can actively regulate ammonia handling in response to an environmental ammonia stress; an adaptation appropriately suited for the carrion scavenging behaviour of the hagfish.

Tables

Table 6.1 List of Rh sequences used for HMMER search

Rh glycoprotein sequences used to construct HMM profiles for HMMER search querying hagfish illumina transcriptomes. Sequences were acquired from NCBI GenBank repository

Isoform	Species	Accession #
Rhbg	*Takifugu rubripes*	AAM48577.1
	Alcolapia grahami	AFZ78445.1
	Cyprinus carpio	AGM46574.1
	Porichthys notatus	AGA93879.1
	Opsanus beta	AEA77168.1
	Bos Taurus	AAI33319.1
	Rattus norvegicus	AAH79365.1
	Oryzias latipes	NP_001098561.1
	Danio rerio	NP_956365.2
	Takifugu rubripes	AAM48577.1
	Porichthys notatus	AGA93879.1
	Ophiophagus hannah	ETE58616.1
	Xenopus tropicalis	AAU89493.1
	Pan troglodytes	AAX39716.1
	Tetraodon nigroviridis	Q3BBX8.1
Rhcg	*Takifugu rubripes*	Q18PF5.1
	Danio rerio	NP_001083046.1
	Oncorhynchus mykiss	NP_001117995.1
	Oreochromis niloticus	XP_003442301.1
	Opsanus beta	AEA77169.1
	Gallus gallus	NP_001004370.1
	Monodelphis domestica	XP_001369976.1
	Xenopus tropicalis	NP_001003661.1
	Sus scrofa	NP_001038042.1
	Anolis carolinensis	XP_003227100.1
	Canis lupus familiaris	NP_001041487.1
	Pan troglodytes	NP_001030600.1
	Homo sapiens	NP_057405.1

Table 6.2 List of primers used for PCR amplification.

Application		Sequences
		*Es*Rhcg
PCR set	sense:	5'- CCTGCTGTATAACCGGTCGATATT -3'
Full CDS	antisense:	5'- CCAATGGAGCTTGCACCAAATAG -3'
		*Es*Rh-like
PCR set	sense:	5'-CAACTCCGAGCTTCGCAA-3'
Full CDS	antisense:	5'-TGCCTGTATGTCTGCTTGTATG-3'

Table 6.3 Comparison of hagfish Rhcg antibody binding domain

Species	Peptide sequence
Myxine glutinosa	5'-CYEDRAYWEVPEEEVTY-3'
Eptatretus stoutii	5'-CYEDEAYWEVPEEEVTL-3'

Figures
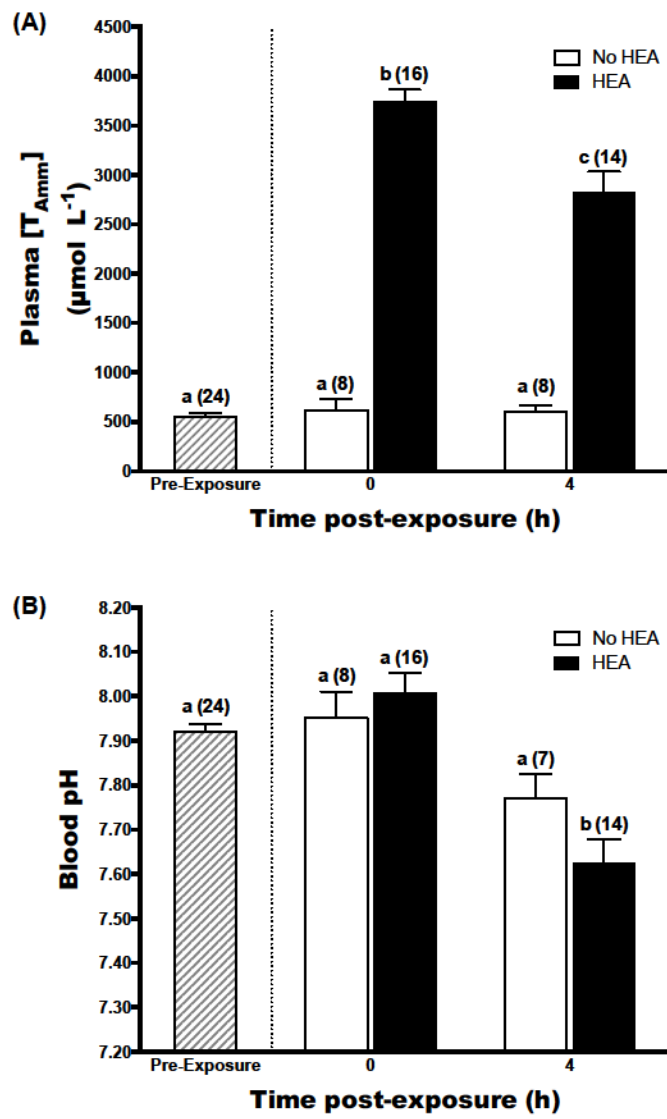
Figure 6.1 Plasma [T$_{Amm}$] and blood pH during recovery from HEA.

Changes in (A) plasma [T$_{Amm}$] and (B) blood pH of Pacific hagfish exposed to HEA (20 mmol L^{-1}) for 48 h and following a 4 h recovery in ammonia-free, full strength seawater within divided chambers. Control fish (open bars) were housed in ammonia-free seawater for the exposure period. Blood was drawn immediately prior to HEA exposure (Pre-exposure; hashed bars), following HEA exposure (0 h) and following a 4 h recovery period (4 h). Data are presented as mean + s.e.m. (n). Bars with same letter are not statistically different ($p < 0.05$) as determined by one-way ANOVA followed by Sidak's multiple comparisons test
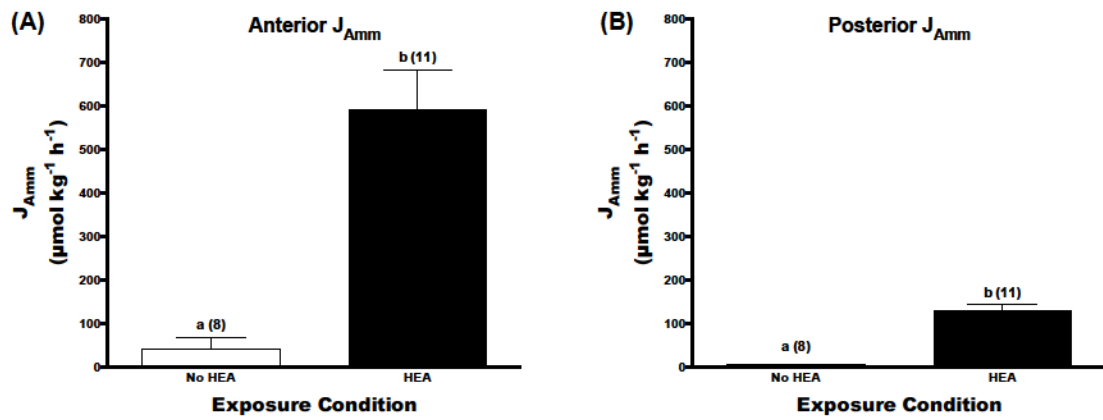
Figure 6.2 Partitioning of ammonia excretion during recovery from HEA.

During recovery from HEA (20 mmol L^{-1}) for 48 h in divided chambers, (A) anterior and (B) posterior net outward J_{Amm} was measured. Data are presented as mean + s.e.m. (n). Bars with same letter are not statistically different ($p < 0.05$) as determined by Student's two-tailed t-test
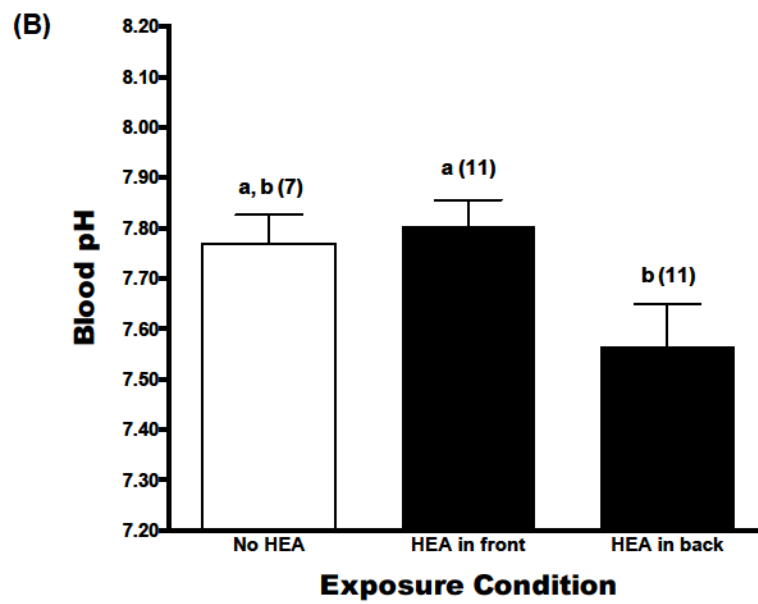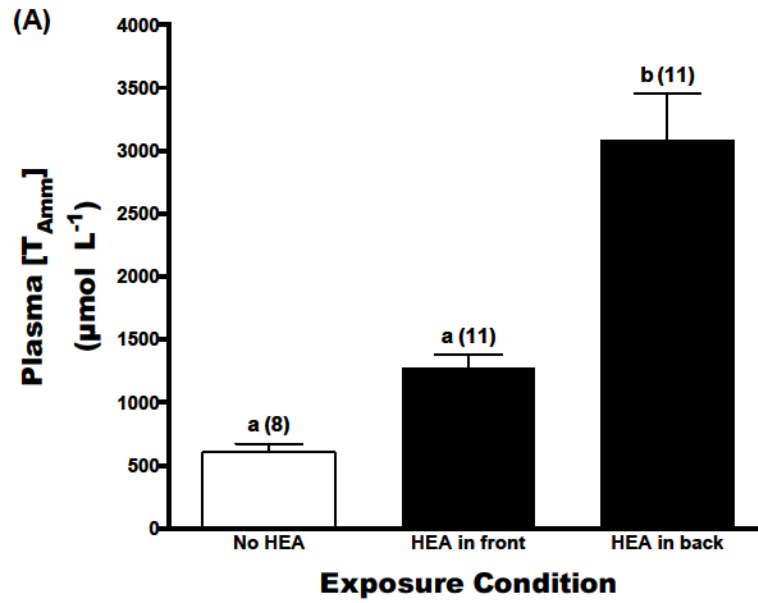
Figure 6.3 Plasma [T$_{Amm}$] and blood pH during localized HEA exposure.

Hagfish (A) plasma [T_{Amm}] and (B) blood pH following compartmentalized HEA exposure. Hagfish were placed into divided chambers containing either ammonia-free seawater (no HEA; open bars) or 20 mmol L^1 T_{Amm} in either the anterior (HEA in front) or posterior (HEA in back) 20 mmol L^{-1} HEA chamber for 4 h (closed bars). Blood samples were drawn immediately following exposure. Data are presented as mean + s.e.m. (n). Bars with same letter are not statistically different ($p < 0.05$) as determined by one-way ANOVA followed by Sidak's multiple comparisons test.
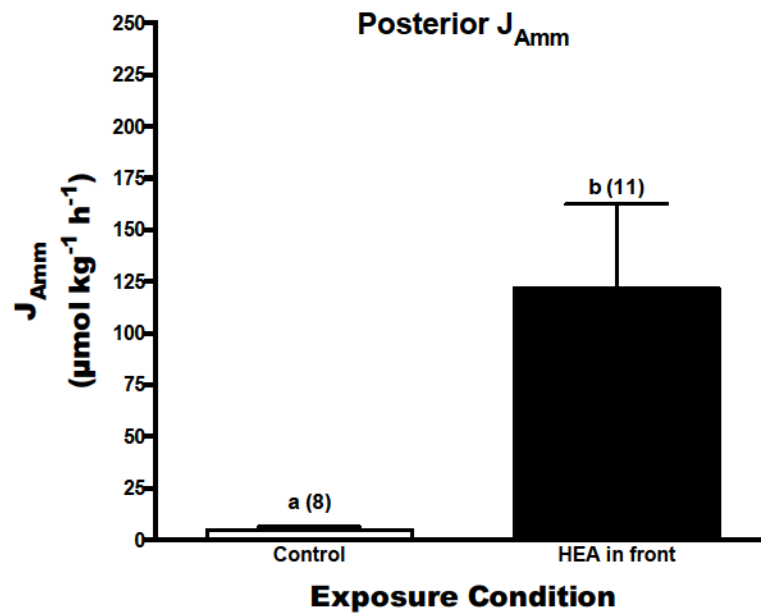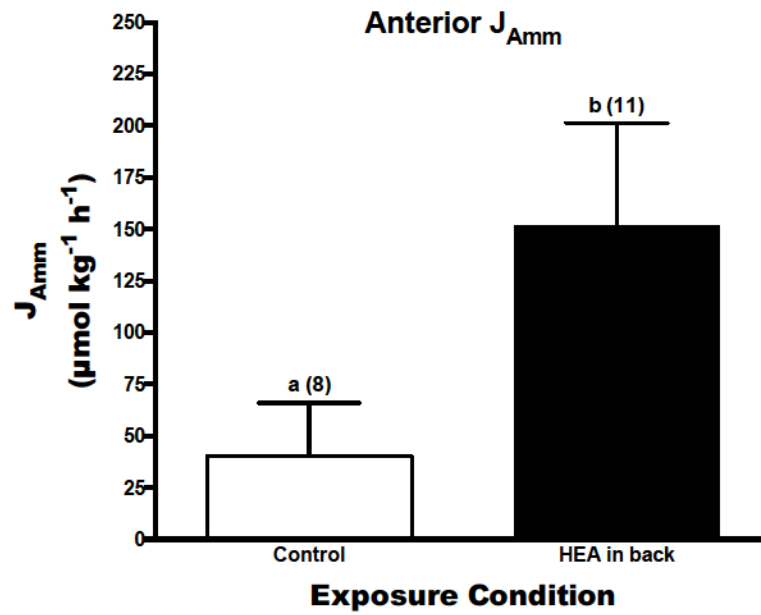
Figure 6.4 Ammonia excretion during localized HEA exposure.

Net outward (A) anterior and (B) posterior J_{Amm} from hagfish during acute localized HEA exposure was determined in the compartment opposite to the HEA-containing compartment. Data are presented as mean + s.e.m. (n). Bars with same letter are not statistically different ($p < 0.05$) as determined by Student's two-tailed t-test.
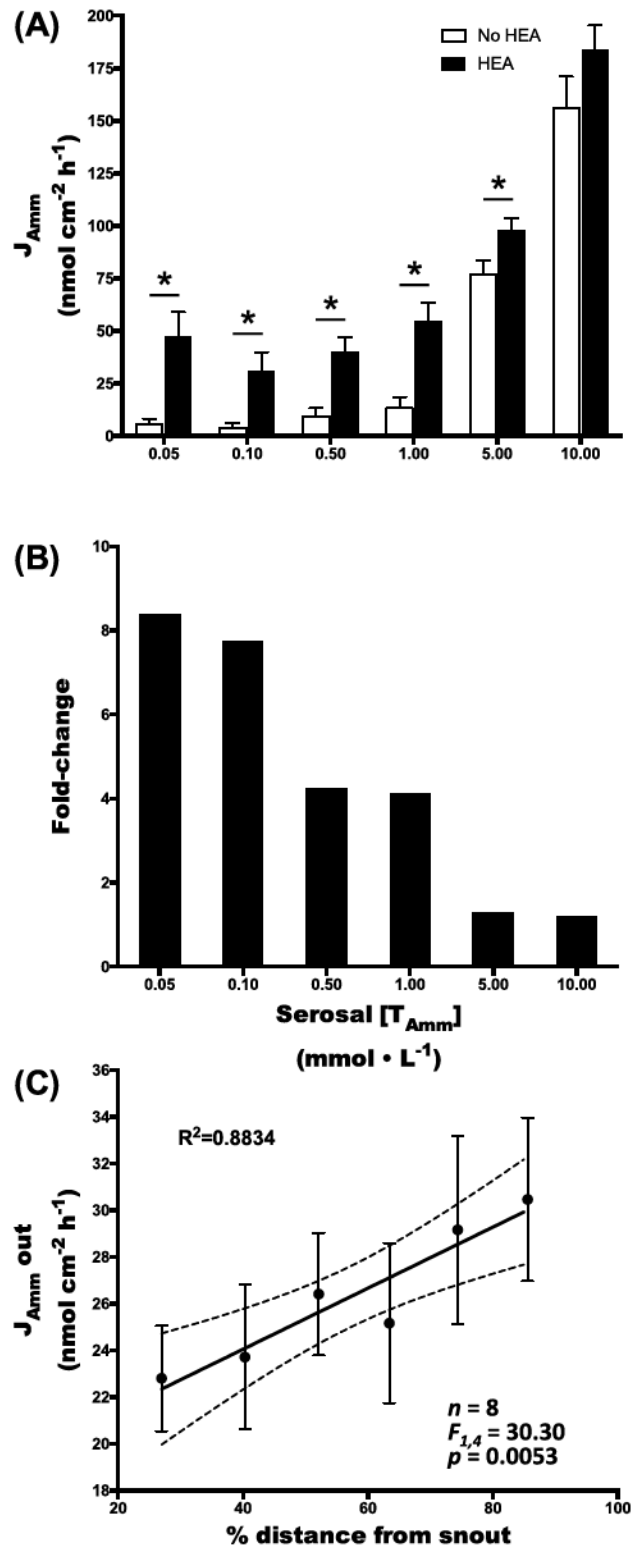
Figure 6.5 Ammonia flux across excised skin.

Total ammonia flux across excised skin as determined by appearance of ammonia in mucosal medium following introduction to serosal HEA ($0.05 – 10.0$ mmol L^{-1} in hagfish saline). Concentration-dependent flux (A) was determined in excised skin from hagfish either pre-exposed to HEA (20 mmol L^{-1}) for 48 h (closed bars) or non-exposed controls (open bars). Concentration dependent fold-changes (B) were calculated based on mean J_{Amm} rates from excised skin tissue from HEA and non-HEA exposed animals presented in (A). Skin J_{Amm} was measured in skin excised from serial sections along the length of non-HEA exposed animals. The serosal side of skin sections were then exposed to 5 mmol L^{-1} ammonia in hagfish saline, and the appearance of ammonia measured on the mucosal side of the chamber. Data are presented as mean + s.e.m. in (A) and mean $\pm$ s.e.m. (n) in (C). Statistical differences in (A) are denoted by asterisks (*; $p < 0.05$) as determined by Student's two-tailed t-test. Solid line in (C) represents line of best fit as determined by linear regression analysis; broken lines represent 95% confidence limits for line of best fit.

(A)

50kDa

(B)
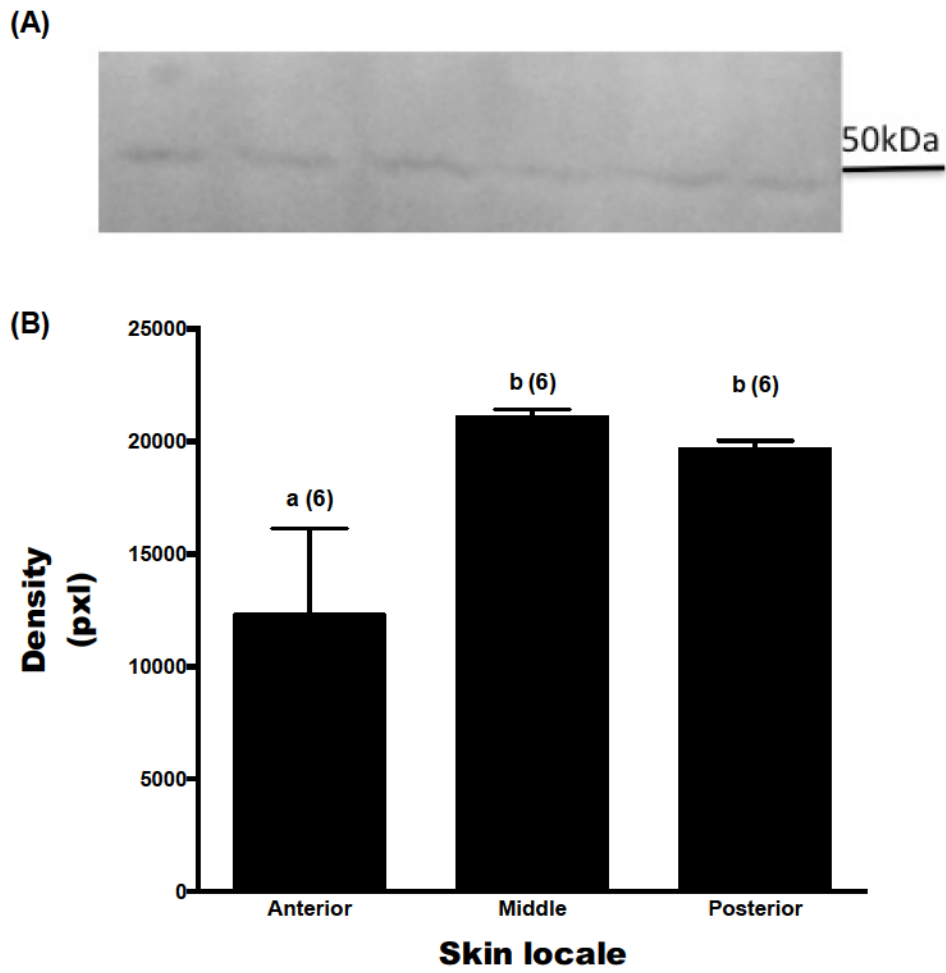
Figure 6.6 Cutaneous distribution of Rhcg abundance in hagfish.

Hagfish skin was excised in sequential sections (Anterior, Middle, Posterior) from along the length of the animal. Skin sections were distributed by percentage distance from the snout (Anterior: 27.58 ± 0.9 %; Middle: 57.21 ± 1.40 %; Posterior: 84.19 ± 1.08 %). (A) Representative blot from posterior skin sections. (B) Relative abundance of cutaneous hRhcg expression from sequential skin sections. Data are presented as mean + s.e.m (n). Bars with same letter are not statistically different ($p < 0.05$) as determined by one-way ANOVA followed by Holm-Sidak multiple comparisions *post-hoc* test.

Figure 6.7 Phylogenetic analysis of 2 cloned hagfish Rh glycoprotein sequences.

Phylogenetic analysis of 2 cloned Rh glycoprotein sequences showed phylogenetic relationships of EsRhcg and EsRh-like peptide sequences. Analysis was completed using RAx-ML with methods previously described on the Cyberinfrastructure for Phylogenetic Research (CIPRES) Science Gateway servers. Branch support was estimated by bootstrap with 300 replications with auto-cutoff threshold set to 1000. Cloned sequences are denoted with an arrow. Numbers in square brackets are the GenBank accession numbers of the sequences.
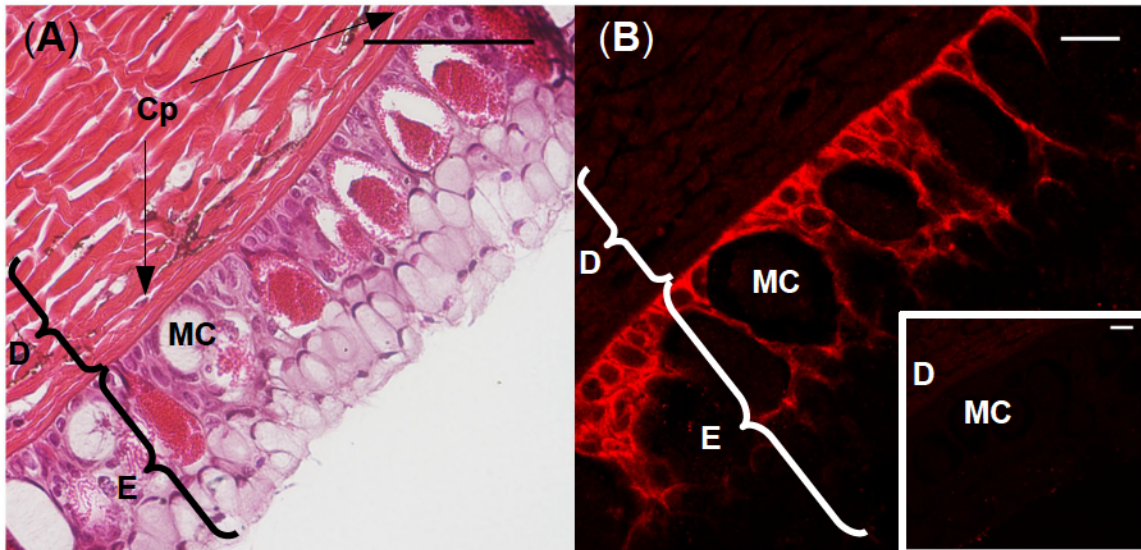
Figure 6.8 Representative micrographs depicting Pacific hagfish cutaneous cellular organization and Rhcg localization.

H&E staining (A) highlighting the large mucous cells (MC) and clearly defined basement membrane separating the epidermis (E) from the capillary-rich (Cp) dermis (D). Scale bar = 20 μm. Immunohistochemistry representative confocal images showing localization of the EsRhcg using myxinid-derived antibodies (red) to the basal aspect of the epidermis (B). Immunoreactivity clearly observed along the length of the basement membrane of the epidermis, extending up to surround the large mucous cells (MC). Scale bar = 20 μm. Pre-absorbed antibody control micrograph (inset) demonstrating no evidence of Rhcg staining. Scale bar = 20 μm.

SECTION 3:

IONOREGULATION

Chapter 7: Regulation of plasma glucose and sulfate excretion in Pacific hagfish, *Eptatretus stoutii* is not mediated by 11-deoxycortisol

Introduction

There has long been debate on the true phylogenetic relationship between the two extant groups of cyclostomes, the lamprey and hagfish (Janvier, 2010). Past morphology-based approaches suggested paraphyly with the lamprey being more closely related to the jawed vertebrates, gnathostomes, than the hagfish (Janvier, 2010). Contrarily, current molecular evidence provides support for monophyly with both groups forming a single clade separating from the vertebrate lineage evolution (Heimberg et al., 2010) although, the strength of these assumptions have recently been questioned (Thomson et al., 2014). A monophyletic cyclostome clade would indicate that the ancestral vertebrates were more complex than originally thought with the lamprey retaining a number of features that are present in gnathostomes and the hagfish undergoing an unprecedented loss of vertebrate features. Alternatively, the lamprey would have had to develop key physiological traits in a convergent evolutionary context with the gnathostomes, but also possess the genetic features at divergence to allow for this parallel evolution, suggesting that hagfish and lamprey diverged early on following the emergence of the cyclostome clade around 525MYA (Near, 2009).

Two examples of physiological and endocrinological processes that have either been lost, or appear more primitive in hagfish are ionoregulation and the hypothalamic-pituitary axis (HPA). When comparing ionoregulatory strategies of lamprey and hagfish, lamprey are euryhaline with blood ion concentrations similar to the rest of the vertebrate lineage at $\sim 1/3$ seawater (Smith, 1932), while hagfish are strictly marine in their evolutionary history (Bardack, 1991). Hagfish are particularly unique within the vertebrates as their blood plasma is similar to seawater with respect to Na^+ and Cl^-

concentrations (Bellamy and Chester Jones, 1961). Furthermore, hagfish are stenohaline and thus cannot regulate Na^+ and Cl^- when placed in media differing in salt composition from seawater (Robertson, 1954; Sardella et al., 2009). Hagfish do, however, regulate the divalent ions sulfate (SO_4^{2-}), magnesium (Mg^{2+}) and calcium (Ca^{2+}), giving support to the hypothesis that these divalent cations were among the first ions to be actively regulated in vertebrates (Bellamy and Chester Jones, 1961; Clifford et al., 2015b). It has been proposed that the early steroids and receptors used for this mineral regulation have been adopted for regulation of the monovalent ions (Na^+, Cl^-, K^+; Sardella et al., 2009)

The emergence of the hypothalamic-pituitary axis (HPA) is specific to vertebrates and is a key event in the evolution of divergent physiological processes (*e.g.* reproduction, growth, metabolism, stress response and osmoregulation; Bury et al., 2015). Current evidence suggests that hagfish possess a far less morphologically distinct HPA compared to lamprey (Uchida et al., 2010) in that there is no apparent partitioning of the pars distalis and pars intermedia of the pituitary gland as observed for lamprey and all the gnathostomes (*e.g.* Nozaki et al., 2007). A number of the corticotropins, melanotropins and gonadotropins that are released from the pituitary to stimulate steroid hormones synthesis have been described in lamprey (Sower et al., 2006; Takahashi et al., 1995) but have yet to be definitively identified in hagfishes (Uchida et al., 2010).

The HPA controls the synthesis of a number of steroid hormones that circulate the body and bind to nuclear hormone receptors to act as ligand inducible transcription factors, examples of which are the sex [estrogen (ER), androgen (AR) and progesterone receptors (PR)] and adrenal hormone receptors [the two corticoid receptors (CR); glucocorticoid (GR) and mineralocorticoid receptors (MR)] of the gnathostomes. The

origins of these groups of receptors can be traced back to the estrogen "like" receptor (ERR) present in some groups of Protosomes, *e.g.* the molluscs and annelids (Keay and Thornton, 2009; Keay et al., 2006). These early ERR receptors are constitutively active and their mode of regulation remains unclear (Keay and Thornton, 2009; Keay et al., 2006). In the cephalochordate *Branchiostoma floridae*, an ERR (Paris et al., 2008), ER and steroid receptor (SR) have been reported (Bertrand et al., 2011). The SR is expressed in the gonads (Callard et al., 2011) and is activated by estrogens (Katsu et al., 2013), and negatively regulated by the ER (Callard et al., 2011), this suggests that the ancestral role of the SR may be to regulate reproduction.

Whole genome duplication (WGD) events in the early vertebrate lineage has lead to the emergence of 3 distinct hormone receptors, the CR, ER and PR, in cyclostomes (Bridgham et al., 2006; Rossier et al., 2015). The cloning of these receptors and *in vitro* assays has identified the receptors hormone binding and transactivation profiles. The CRs of lamprey and Atlantic hagfish are promiscuous, being activated by a number of different corticoids including cortisol, 11-deoxycorticosterone (DOC), 11-deoxycortisol (11-DOC) and corticosterone (Bridgham et al., 2006). However, even though these *in vitro* assays have proven invaluable in identifying potential mechanisms of protein evolution at a molecular level (Bridgham et al., 2009), they do not provide information on the actual active hormones *in vivo* or the evolution of their physiological role (Close et al., 2010). For example, even though the lamprey CR is activated by a wide range of corticoids *in vitro,* Close et al. (2010) recently identified that only 11-DOC is elevated in the plasma of lamprey and that this hormone performs both a classical glucocorticoid

role, controlling gluconeogenesis, and a mineralocorticoid role, regulating ion homeostasis.

The clear divergence in ionoregulatory strategies between these two agnathan taxa and the knowledge that steroid hormones regulate ion balance in lamprey and more derived vertebrates provides the impetus to reevaluate steroid function in hagfish. This study aims to identify the presence of classical corticosteroid hormone responses in the Pacific hagfish (*Eptatretus stoutii*) through either *in vivo* perturbations (handling or elevation of plasma sulfate *via* injection) or *via* hormonal implants followed by monitoring of classical glucocorticoid (plasma glucose) and mineralocorticoid (gill ATPase activity and plasma sulfate regulation) responses. Sulfate is one of the three divalent ions that hagfish regulate (Bellamy and Chester Jones, 1961) therefore it was hypothesized that a mineral stress may elicit a measurable hormonal response. Specifically, I sought to characterize the effects of sulfate loading on hagfish plasma glucose and 11-DOC levels. I also characterized recovery from sulfate loading by examining both glomerular filtration rate and sulfate excretion rate following sulfate plasma loading. Administration of cortisol, DOC, and corticosterone *via* coconut oil implants allowed for the investigation into the potential for each of these steroids to serve as either direct activators of the CR or precursors for the biosynthesis pathway for the CR ligand. Plasma 11-DOC levels were measured following *in vivo* perturbations. Furthermore, analysis of a hagfish transcriptome allowed me to identify the presence of specific enzymatic elements of the corticosteroid biosynthesis pathway.

Material and Methods

Experimental animals and holding

Pacific hagfish (*Eptatretus stoutii;* 65 – 227 g) were captured near Bamfield, BC, Canada and held at Bamfield Marine Sciences Centre (BMSC) as previously described (Clifford et al., 2015a; Schultz et al., 2014). Fish remained unfed during captivity and were used for experimentation within 2 weeks of capture. All animals were used under the licenses of Department of Fisheries and Ocean Canada collection permits XR 214 2007, XR 214 2010, XR 214 2011 and XR 214 2013 and Bamfield Marine Science Centre Animal Care protocol numbers BMSC RS 10-42, RS 11-26, and RS-13-24.

Chemicals

Unless noted, reagents and enzymes were supplied by Sigma-Aldrich (St. Louis, MO). Cortisol, 11-DOC, DOC, and corticosterone were obtained from commercial suppliers (Stereloids, USA). Coconut oil was purchased from a local health food store. Tricaine methanesulfonate (TMS) was obtained from Syndel laboratories (Nanaimo, BC, Canada).

Experimental protocol

Experiment 1 - Exogenous elevation of plasma hormone concentrations

To induce elevated plasma hormone concentrations, hagfish were administered molten coconut oil (kept at 27 ˚C prior to injection) impregnated with cortisol, corticosterone or DOC at dose of 20, 100 or 200 mg kg^{-1}. Briefly, animals were lightly

anaesthetized in seawater containing TMS (0.75 g L^{-1}) buffered with 1.5 g L^{-1} sodium bicarbonate for 3 – 5 min. The animals were then removed from the water and were held vertically causing pooling of blood in the caudal subcutaneous sinus within 20 sec. A 200 μL control blood sample was removed from the sinus with a heparinized 21G needle and 1 mL disposable syringe, centrifuged briefly (30 sec, 14,000g) and the plasma was removed and rapidly frozen on liquid nitrogen (-80 ˚C) for later analysis. The animals were then laid on a flat surface and steroidal implants were placed in the body cavity approximately 3 inches caudal to the last branchial pore using a warm (27 ˚C) 18 g needle and 3 mL syringe. All implant concentrations were administered at a dose equivalent to 2% of body mass. Coconut oil injections without steroid served as a control for all experiments. Blood samples were also removed 4 and 7 days post-implantation. Confirmation of successful placement of the implant was evaluated visually upon termination and dissection. Plasma cortisol and glucose concentrations were measured 4 and 7-days post-implantation, whereas total gill ATPase activities were only measured 7-days post-implantation and these results have been reported elsewhere (Bury et al., 2015). To confirm the efficacy of the implant at achieving the desired nominal concentrations, a commercial cortisol RIA (MP Biomedical, Orangeburg, NY) was used as a surrogate for the efficacy of the DOC and corticosterone injections (see Figure 7.2).

Experiment 2 – Effects of handling stress on hagfish plasma glucose and 11-DOC levels

In order to determine the effects of handling stress on potential candidates of hagfish stress hormones, hagfish were subjected to an extended handling stress. Hagfish ($n = 6$) were acclimated in a darkened, aerated box with flowing ambient seawater overnight (> 10 h) prior to any experimentation. Hagfish were then lightly anaesthetized

243

(0.75 g L^{-1} TMS) in the dark without handling to allow for control blood samples (200 µL) to be taken. Following recovery from anesthesia (~1 h), hagfish were agitated by continual manual grasping for 30 min. They were then allowed to recover for 6, 12, 24 and 48 h and blood samples collected as described above. Blood was centrifuged and then the plasma was snap frozen in liquid nitrogen (-80 ˚C) for later determination of plasma glucose and 11-DOC concentrations.

Experiment 3 - Effect of sulfate loading

Hagfish were anaesthetized and individually weighed (range 115 – 192 g, $n = 6$ for each treatment). To chronically elevate plasma SO_4^{2-}, hagfish were administered a daily load of 2 µL g^{-1} of a stock 200 mmol L^{-1} Na$_2$SO$_4$/300 mmol L^{-1} NaCl solution (400 µmol SO_4^{2-} kg^{-1} body mass) for 3 days. Assuming a blood volume of 18% (Forster, 1989; McCarthy and Conte, 1966), this dose was designed to elevate plasma SO_4^{2-} by a nominal amount of ~3 mmol L^{-1} injection^{-1}. Controls consisted of an equivalent injected volume (2 µL g^{-1}) of 500 mmol L^{-1} NaCl. On day 4, both sulfate-loaded and saline-loaded hagfish were then injected with 200 µL of either 200 mmol L^{-1} Na$_2$SO$_4$ /300 mmol L^{-1} NaCl or 200 µL of 500 mmol L^{-1} NaCl solution as appropriate. Each solution on day 4 also contained 5 µCi of radiolabelled sulfate ($^{35}SO_4^{2-}$: Perkin Elmer as Na^{35}SO$_4^{2-}$: 3000 µCi mmol^{-1}) and 1 µCi of ^{3}H- inulin as a GFR marker (Perkin Elmer as ^{3}H-inulin: 3000 µCi mmol^{-1}; Munger et al., 1991). Given the high specific activity (SA) of the injected $^{35}SO4^{2-}$ this would only amount to a nominal dose (~0.0017 mmol) of SO_4^{2-} in the control hagfish and not be expected to increase plasma [SO_4^{2-}]. Hagfish were then placed into individual flux chambers and ^{3}H-inulin and $^{35}SO_4^{2-}$ activity allowed to equilibrate in the plasma for 6 h. Preliminary experiments determined that plasma concentrations were

fully mixed and stable in the 6 – 12 h post-injection period. To start the experimental period, blood samples were withdrawn from lightly anesthetized hagfish at 6 h post-radiolabeled sulfate/inulin injection. To determine SA of plasma, 25 μl (0.025 mL) of plasma was added to 4 mL of ACS scintillation fluid (Fisher chemical) and ^{3}H and ^{35}S radioactivity determined using a Beckman LS-6000 with appropriate energy windows used for counting of each ion independently. The remaining plasma was then snap frozen in liquid nitrogen (-80 ˚C) for later analysis of plasma sulfate, glucose and 11-DOC. The flux chambers were weighed at the beginning and end of the flux period to determine the flux volume (minus the weight of the fish). To begin the flux period, water samples (4 mL) were collected from the flux chamber (T$_1$) and each flux was terminated after 2 h (8 h post injection) by withdrawing final water samples (T$_2$). The T$_1$ and T$_2$ water samples were mixed with 8 mL of ACS fluor and ^{3}H and ^{35}S radioactivity measured using a Beckman LS-6000 beta counter. At the completion of each flux period, plasma samples were collected from the hagfish and analyzed as described above.

Analytical methods

Calculation of GFR and sulfate excretion rate

Glomerular filtration rate was calculated based on ^{3}H excretion rate using the following equation:

$$GFR = [(CPM^{T_2}_{water} - CPM^{T_1}_{water}) \cdot Weight^{-1} \cdot Time^{-1}] \cdot Volume_{Flux} \cdot SA \qquad (1)$$

where SA was calculated as:

$$SA = \frac{\left(\frac{volume}{CPM_{plasma}^{T2}} + \frac{volume}{CPM_{plasma}^{T1}}\right)}{2} \qquad (2)$$

Sulfate excretion rate in both saline loaded (control) and sulfate-loaded animals was calculated according to the following equation:

$$J_{SO_4^{2-}} = [(CPM_{water}^{T2} - CPM_{water}^{T1}) \cdot Weight^{-1} \cdot Time^{-1}] \cdot Volume_{Flux} \cdot SA \qquad (3)$$

where SA was calculated as:

$$SA = \frac{\left(\frac{\mu mol}{CPM_{plasma}^{T2}} + \frac{\mu mol}{CPM_{plasma}^{T1}}\right)}{2} \qquad (4)$$

and plasma [SO_4^{2-}] (mmol mL^{-1}) was measured at 600 nm on a microplate spectrophotometer (Spectramax 190 Molecular Devices, Sunnyvale, CA) using a commercially available assay kit (Quantichrom Sulfate Assay Kit, DSFT-200, BioAssay Systems, Hayward, CA).

Plasma sample analysis

Plasma glucose concentrations were measured at 340 nm using a microplate spectrophotometer (Spectramax 190 Molecular Devices, Sunnyvale, CA) with a hexokinase assay utilizing glucose-6-phosphate as a coupling enzyme (Bergmeyer, 1983). Plasma 11-DOC concentrations were analyzed with a commercially available RIA kit (11-DOC RIA, 38-DESHU-R96, Alpco Diagnostics, Salem, NH) and plasma cortisol

concentrations were measured using a commercially available RIA (MP Biomedical, Orangeburg, NY).

Production and analysis of hagfish transcriptome

A hagfish combined gill/slime gland transcriptome was commercially produced by BGI (Shenzhen, China). Pacific hagfish ($n = 3$ for each treatment) from either no stress, stress by acid or base injection, or stress *via* handling as above. For the acid and base stress, hagfish were lightly anaesthetized in seawater containing 0.75 g L^{-1} TMS buffered with 1.5 g L^{-1} sodium bicarbonate for 3 – 5 minutes, weighed and then held vertically causing pooling of the blood in the caudal subcutaneous sinus. The animals were then injected (3 mL syringe and 23g needle) with either acid saline (250 mmol L^{-1} HCl [pH=0.60], 250 mmol L^{-1} NaCl) or alkaline saline (250 mmol L^{-1} NaHCO$_3$, 250 mmol L^{-1} NaCl, [pH~8.43]) at a standard volume of 2.4 μL g^{-1} to induce an acid/alkaline/saline load of 6000 μmol kg^{-1}; similar to injection protocols that have been employed in previous studies (Clifford et al., 2014; McDonald et al., 1991; Parks et al., 2007b; Tresguerres et al., 2007a). Following a 3 h recovery period, animals were then euthanized with an overdose of TMS (2 g L^{-1}) buffered with 1.5 g L^{-1} sodium bicarbonate and the gills and slime glands were rapidly excised and freeze-clamped in liquid nitrogen (-80 ˚C, within 30 s). Total RNA was obtained from tissues (~100 mg) using a TRIzol extraction protocol. RNA samples were then cleaned of genomic contents using DNAse I (Ambion/Life technologies, Carlsbad, CA) after which, isolated RNA from the 24 samples (12 gill +12 slime gland) were mixed into one sample to specifications set forth by BGI. With this combined sample, a transcriptome was generated using Illumina technologies by BGI. Transcriptome annotation was performed by BGI *via* BLAST

cross-referencing with NCBI non-redundant, Swiss-Prot, Kyoto Encyclopedia of Gene and Genome (KEGG) and COG (Clusters of Orthologous Groups) databases. I utilized KEGG pathway analysis provided by BGI to determine the presence of transcripts for specific enzymes involved in steroid biosynthesis.

Statistical analysis

All data are presented as the mean ± s.e.m.. Differences in plasma concentrations of glucose, sulfate and 11-DOC were analyzed using one-way analysis of variance (ANOVA). When significant differences were observed, differences between the means were quantified using a Dunnet's *post-hoc* test at the $p < 0.05$ level. When the assumptions for ANOVA were not satisfied, a nonparametric ANOVA, followed by Dunn's test by ranks was used where appropriate. All statistical analyses were completed using Prism 6 for Mac (Graphpad Software Inc, La Jolla, CA).

Results

Identified elements of hagfish corticosteroid biosynthesis pathway

Analysis of a hagfish gill/slime gland transcriptome revealed the presence of homologous enzymes required to transform cholesterol sulfate to progesterone including steryl sulfatase/alcohol sulfotransferase, CYP11a1, and 3b-HSD (Figure 7.1). However, transcripts for important enzymes necessary for the synthesis of 17-OH-progesterone, androstenedione and testosterone (CYP17), DOC (CYP21) cortisol (CYP11B1), or estradiol (CYP19) were not found in the hagfish transcriptome.

Efficacy of steroid delivery via coconut oil implants

Cortisol implants and a cortisol RIA were used to determine the efficacy of the coconut oil implants at delivering the nominal doses of each steroid, assuming equivalency of release for each of the steroids from the coconut oil implant. To confirm that the RIA could detect cortisol in the presence of hagfish plasma, Radioimmunoassays were initially conducted using hagfish control plasma spiked with varying concentrations of cortisol. The % recovery of cortisol from the spiked hagfish plasma was 98% and the interassay variation was found to be < 6.9% suggesting that the RIA was effective.

Plasma cortisol concentrations were elevated in fish that received the coconut oil implanted with cortisol, but were unaffected in those that received the sham injection or an implant with either DOC or corticosterone (Figure 7.2). Moreover, the target concentrations in the cortisol treated animals 4 days after injection were ~10, 100 and 150 μg dL^{-1} for the nominal 20, 100 and 200 mg kg^{-1} dose groups, respectively, demonstrating that the implants were relatively effective at delivering their intended dose.

Effects of steroidal implants

As published previously (Table 7.1, adapted from Bury et al. 2015), a significant increase in plasma glucose levels from 0.74 ± 0.17 mmol L^{-1} (control) to 1.88 ± 0.45 mmol L^{-1} was observed in hagfish 4 days post-implantation with 200 mg kg^{-1} DOC (Table 7.1). There were also small but statistically significant increases at day 7 for the 20 mg kg^{-1} DOC (0.70 ± 0.09 mmol L^{-1}, $n = 6$) and 100 mg kg^{-1} corticosterone (0.84 ± 0.13 mmol L^{-1}) implanted hagfish compared to hormone-free implanted controls (0.28 ± 0.07 mmol L^{-1} values. No changes in total gill-ATPase activity were detected 7 days post-implantation with any of the tested hormone implants at any dosage (Table 7.1).

Effects of desliming stress on hagfish physiology

Thirty minutes of continuous handling stress induced a significant gluconeogenic response in the hagfish. At 6 h post-handling stress, plasma glucose levels significant increased from 0.27 ± 0.16 mmol L^{-1} (control) to 1.65 ± 0.46 mmol L^{-1} (Figure 7.3a). Plasma glucose levels were reduced by 12 h (1.59 ± 0.44 mmol L^{-1}) and returned to control levels at 24 h post-handling stress (0.96 ± 0.36 mmol L^{-1}). Hagfish plasma 11-DOC levels were also measured post-handling stress. Under control conditions, 11-DOC concentrations were extremely low, near the detection limit for the assay (0.08 ng mL^{-1}) and they remained unchanged from control values for the duration of the 48 h recovery period (Figure 7.3b).

Effects of sulfate loading on hagfish

To test for the presence of a glucogenic response as a result of divalent ion plasma loading, hagfish were acutely injected with 2 μL g^{-1} body mass of a 0.2 M Na_2SO_4

solution, which was a dosage designed to elevate plasma SO_4^{2-} by ~3 mmol L^{-1} over the resting plasma value of ~2 – 3 mmol L^{-1}. However, acute elevation of plasma SO_4^{2-} did not result in any increases in plasma glucose at either 6 or 8 h post-injection (data not shown). Therefore, to stimulate a glucogenic response, a chronic sulfate elevation protocol was instituted where hagfish were injected with a daily load of 2 μL g^{-1} 200 mmol L^{-1} Na_2SO_4 /300 mmol L^{-1} NaCl, equaling a nominal dose of 400 μmol SO_4^{2-} kg^{-1} body mass. An equivalent volume of 500 mmol L^{-1} NaCl was also injected in a group of hagfish for 3 days and served as a paired control. On day 4, both sulfate loaded and saline loaded hagfish were injected with the same solutions with added radiolabelled $^{35}SO_4^{2-}$ and ^{3}H-inulin as described in the methods to measure the sulfate excretion rate and GFR.

Plasma SO_4^{2-} levels in the hagfish 4 days post-injection with NaCl did not deviate from the pre-injected controls (4.01± 0.47 mmol L^{-1}), whereas, plasma SO_4^{2-} levels significantly increased greater than two-fold in chronically (4 day) SO_4^{2-}-loaded hagfish at both 6 and 8 h post-injection (9.65 ± 1.38 mmol L^{-1} and 9.25 ± 1.11 mmol L^{-1}, respectively; Figure 7.4a).

Plasma glucose levels in NaCl-injected hagfish (control), remained stable at 6 and 8 h post-4th injection (1.71 ± 0.35 mmol L^{-1} and 2.04 ± 0.58 mmol L^{-1}, respectively) compared to control levels (1.09 ± 0.19 mmol L^{-1}, Figure 7.4b). In contrast, chronic-injection of Na_2SO_4 resulted in a significant 3 to 5-fold increase in hagfish plasma glucose levels at both 6 h (3.16 ± 0.19 mmol L^{-1}) and 8 h post-injection (5.08 ± 1.12 mmol L^{-1}; Figure 7.4b).

To investigate if 11-DOC played a role in the hagfish gluconeogenic stress response, plasma 11-DOC concentrations were also measured after sulfate loading.

Interestingly, no changes in plasma 11-DOC were detected and hagfish plasma 11-DOC

levels were approximately an order of magnitude lower than reported in Figure 7.4 and

were at or below detectable limits of the assay (Figure 7.4c).

SO_4^{2-} excretion rates were calculated for both chronic NaCl and SO_4^{2-} loaded

hagfish and I determined that SO_4^{2-} loading resulted in a significantly greater SO_4^{2-}

excretion rate (1.29 ± 0.39 μmol kg^{-1} hr^{-1}) compared to NaCl injected controls ($0.29 \pm$

0.13 μmol kg^{-1} hr^{-1}; Figure 7.5a). To ensure that the increased SO_4^{2-} excretion rate was

not associated with volume loading and a subsequent increase in GFR, ^{3}H-inulin

excretion rate was used as an indicator of GFR. Hagfish GFR was similar in chronic

NaCl injected animals (0.15 ± 0.03 mL kg^{-1} hr^{-1}) compared to the SO_4^{2-} injected animals

(0.14 ± 0.05 mL kg^{-1} hr^{-1}; Figure 7.5b) demonstrating that no changes in GFR occurred

during the SO_4^{2-} loading experiments.

Discussion

Overview

The findings presented herein demonstrate that Pacific hagfish are able to generate both a glucocorticoid response (as demonstrated by an increased plasma glucose following hagfish handling and mineral/SO_4^{2-} loading) and a mineralocorticoid response (as demonstrated by increased active secretion of SO_4^{2-} following SO_4^{2-} loading). These responses are not mediated by either cortisol or corticosterone, as implants failed to elevate these responses above basal values; while DOC did illicit small but statistically significant increases in plasma glucose at both 4 days (200 mg kg^{-1}) and 7 days (20 mg kg^{-1}). However, ATPase activity remained unchanged regardless of steroidal implant type, dose or time. 11-DOC levels remained near or below detection limits following either exhaustive handling stress or chronic sulfate loading, suggesting 11-DOC, thought to be the active steroid in lamprey (Close et al., 2010), is not active in Pacific hagfish. While there have been numerous studies examining the steroidogenesis of the sex steroids (*e.g.* Kime and Hews, 1980; Kime et al., 1980; Nozaki et al., 2007; Weisbart et al., 1980), to my knowledge, this is the first study to demonstrate that both glucogenic and mineralocorticoid responses are present in hagfish and to further investigate the steroids responsible for eliciting of these physiological responses.

Validation injection and dosing techniques

Weisbart an Idler (1970), using RIA suggested that cortisol in plasma of Pacific hagfish was near or below the detectability limit of their assay. Assaying hagfish plasma did not yield any detectable cortisol as levels were below the limits of detection of the

commercial RIA kit. This suggests that the cortisol is also not a candidate for hagfish steroidal control of either mineralocorticoid or glucocorticoid responses. Injection of cortisol did provide validation of the injection and dosing technique by a demonstrated elevation of plasma cortisol to values close to the nominal target dose. However, since the elevation in plasma cortisol did not increase either plasma glucose (at either 4 or 7 d post-injection) or gill ATPase activity (at 7 d post-injection), the absence of a steroidal role for cortisol in either response was confirmed. This lack of effect of cortisol then allows cortisol to be used as a tracer for the efficacy of the implant protocol for other steroids since cortisol is readily measured by RIA. This method demonstrated that for cortisol, ~100 ng mL^{-1} was achieved for plasma cortisol at 4 days post-implantation for the 100 mg kg^{-1} nominal group and ~150 ng mL^{-1} for the 200 mg kg^{-1} nominal group. I am therefore confident that hagfish were appropriately dosed with either corticosterone or DOC.

Transcriptomic analysis reveals details of hagfish steroid biosynthesis

Transcriptome analysis revealed the presence of mRNA transcripts corresponding to key steroidogenic enzymes CYP11A1 and 3β-HSD necessary for the conversion of cholesterol to progesterone. Other studies have reported the presence of the sex steroids in the plasma of hagfish and thus, the enzymes CYP17 and 17β-HSD and CYP19 must be present in hagfishes (Nishiyama et al., 2013). However, I was unable to identify the enzymes necessary for the synthesis of 11-DOC (CYP21) and conversion of 11-DOC (CYP11B1) to cortisol, respectively. An absence of these enzymes would explain the inability of Pacific hagfish to convert steroid precursors to cortisol even with long-term (4 – 7 days) supraphysiological doses in the plasma.

Idler and Burton (1976) identified "presumptive interrenal" cells in the pronephron of the Atlantic hagfish (*M. glutinosa*) and presumed them analogous to the cortisol synthesizing tissues of the teleosteii, however, the capability of synthesizing cortisol in these tissues has never been definitely addressed and therefore the location of primary corticosteroid tissue(s) in hagfishes remains to be determined. Supporting my hypothesis that hagfish lack key biosynthesis enzymes is the fact that implants of 11-dexoxycorticosterone, corticosterone or cortisol also failed to induce either an increase in plasma glucose or total ATPase activity, common indicators of glucocorticoid or mineralocorticoid responses (Close et al., 2010). In this study, only total ATPase activity was able to be measured rather than Na^+/K^+ ATPase activity due to the lack of inhibition of hagfish Na^+/K^+ ATPase by the common inhibitor ouabain. The reasons for the lack of ouabain inhibition are unknown but similar reduced sensitivities have been observed in the goldfish brain (Chasiotis and Kelly, 2008).

In lampreys, the other extant vertebrate in the agnathan lineage, cortisol is not detectable in plasma and thus not considered to be a functional steroid. In lamprey, 11-DOC has been demonstrated to be the active steroid for both mineralocorticoid and glucocorticoid responses (Close et al., 2010). Progesterone has been demonstrated to be present in hagfish plasma (Nishiyama et al., 2013) and it has been suggested that 11-DOC can be produced at very low conversion efficiency by bathing hagfish follicular tissue with pregnenolone (Hirose et al., 1975), suggesting the presence of CYP21 activity in the ovary. But, circulatory 11-DOC concentrations (Figure 7.3b) are exceptionally low and are arguably at levels that are unlikely to be biologically active.

I was also able to identify the presence of transcripts for enzymes necessary to allow for conversion of cholesterol sulfate to pregnenolone (sterol sulfatase/3β-HSD, and CYP7A1) and progesterone (3β-HSD). However, despite extensive efforts, I was unable to identify the necessary biosynthesis enzymes required for further conversion of progesterone or pregnenolone to downstream steroids (CYP21a, CYP17a; see Figure 7.1). In *M. glutinosa*, progesterone was able to be converted to testosterone at a nominal rate (3% conversion efficiency; Kime et al., 1980) suggesting CYP17a is present in *Myxine* species, however, further conversions requiring CYP 21 did not occur. Bearing in mind that the hagfish transcriptome were obtained from gill and slime gland tissues, it is possible that this transcriptome does not contain transcripts for CYP21a and CYP17a since the tissues used for transcriptome creation are not specific for glucocorticoid and mineralocorticoid regulation. Steroidogenic tissues responsible for sex steroid metabolism have been identified in the gonads (Nozaki and Sower, 2015) but corticosteroidogenic tissues have not, as yet, been identified in hagfishes.

Hagfish elicit glucogenic and mineralogenic responses

Elevations in plasma glucose are indicative of a glucogenic stress response, typically resulting from activation of GR receptors. I have demonstrated that hagfish can indeed generate a strong glucogenic response to either handling stress or repeated SO_4^{2-} injections. Hagfish possess only single CR that has been demonstrated to bind DOC, cortisol, 11-DOC and corticosterone by stimulating reporter activity (at 100 nmol L^{-1}) in a heterologous expression system (Bridgeham et al, 2006). However, assuming the measured cortisol concentrations yield similar dosing for other steroidal implants, other plasma steroids would range from ~300 nmol L^{-1} in the 20 mg kg^{-1} dose to ~4500 nmol L^{-}

[1] in the 200 mg kg^{-1} dose. Since only small increases in plasma glucose were measured following implant with 200 mg kg^{-1} DOC or 100 mg kg^{-1} corticosterone, even at the highest dose, this suggests that either DOC or corticosterone are not the endogenous glucocorticoids.

Hagfish are considered ionoconformers for plasma Na^+ and Cl^- (Smith, 1930). However, they are capable of regulating the divalent ions Ca^{2+}, Mg^{2+} and SO_4^{2-}. I elicited an ionoregulatory challenge through injection of Na_2SO_4 to elevate plasma $[SO_4^{2-}]$. This allows both the use of radiotracers (^{35}S) and also avoids the known physiological impairments that would result from manipulation of either plasma Ca^{2+} or Mg^{2+}. I demonstrate that hagfish are clearly able to increase SO_4^{2-} excretion rates in response long-term elevations in plasma $[SO_4^{2-}]$. This was accomplished without concomitant increases in GFR suggesting up-regulation of active secretion mechanisms. This can be considered evidence of an active mineralocorticoid response. Slc26a1 is a known SO_4^{2-} transporter in teleost fish (Katoh et al., 2006). I identified an slc26a1-like homologue in the hagfish transcriptome but was unable to demonstrate any changes in expression in kidney tissue response to plasma SO_4^{2-} elevation (results not shown) so the molecular mechanism for sulfate excretion remains to be identified. This is the first measurement of whole-animal GFR in hagfishes although previous estimates of single nephron GFR have been made (Riegel, 1978). Interestingly, GFR in hagfishes is relatively high (~0.150 mL kg^{-1} h^{-1}, approx. ½ of that measured in more derived vertebrates) which agrees with a previously measured urine flow rate of 0.227 mL kg^{-1} h^{-1} in *M. glutinosa* (Morris, 1965) suggesting little resorpative capacity of the hagfish kidney.

Conclusions

In summary, I show that hagfish are able to mount plasma glucogenic responses and increased mineral excretory capacity in response to specific stimuli. However, this study rules out cortisol, DOC, 11-deoxycortisol and corticosterone as candidate endogenous CR ligands. The steroid responsible for eliciting these responses remains elusive and bears further investigation. Finally, given the relatively conserved nature of steroids in evolutionary history, understanding hagfish stress endocrinology will be important in resolving the relationships within the agnathans (hagfishes and lampreys) and also between the agnathans and the other clades in the vertebrate lineage.

Table 7.1 Plasma glucose and total gill-ATPase activity

Hagfish plasma glucose concentrations (mmol L^{-1}) at 4 and 7 days post-implantation and total gill ATPase activity (μmol mg protein^{-1} hr^{-1}) at 7 days post-implantation with coconut oil (control) or coconut oil infused with steroid (cortisol, DOC, or corticosterone) at a dose of 20, 100, and 200 mg kg^{-1}. Data is reported as mean ± s.e.m. ($n = 6$ unless otherwise noted). Asterisk (*) denotes significant difference compared to control ($p \leq 0.05$, ANOVA).

Injected steroid	Dose (mg kg^{-1})	Plasma Glucose (mmol L^{-1})		Total gill-ATPase activity (μmol ADP mg protein^{-1} h^{-1})
		Day 4	Day 7	Day 7
Control	-	0.74 ± 0.17	0.28 ± 0.07	10.44 ± 1.40
Cortisol	20	0.93 ± 0.16	0.51 ± 0.12	7.87 ± 0.81
	100	0.64 ± 0.10	0.64 ± 0.08	7.81 ± 0.79
	200	0.64 ± 0.08	0.60 ± 0.09	7.84 ± 0.40
DOC	20	0.83 ± 0.12 (5)	0.70 ± 0.09*	11.45 ± 1.59
	100	0.95 ± 0.45	0.63 ± 0.08	9.15 ± 1.09 (5)
	200	1.88 ± 0.64*	0.48 ± 0.12 (5)	10.45 ± 1.94 (5)
Cortico-sterone	20	0.52 ± 0.08	0.64 ± 0.12 (4)	9.70 ± 1.46 (4)
	100	0.86 ± 0.16	0.84 ± 0.13*	10.64 ± 0.79
	200	0.52 ± 0.09	0.60 ± 0.05	10.85 ± 1.56 (5)

Adapted from Bury et al. 2015

Figure 7.1 Steroid biosynthesis pathway in hagfish.

Proposed steroid synthesis pathway in hagfish, *Eptatretus stoutii*. Next-Gen Illumina sequencing of hagfish gill and slime gland tissues followed by KEGG analysis revealed complete elements of the steroid biosynthesis pathways leading to pregnenolone and progesterone. Sequence information for several other important enzymes necessary for steroid biosynthesis (highlighted in grey) were not detected in the hagfish gill and slime gland transcriptome.
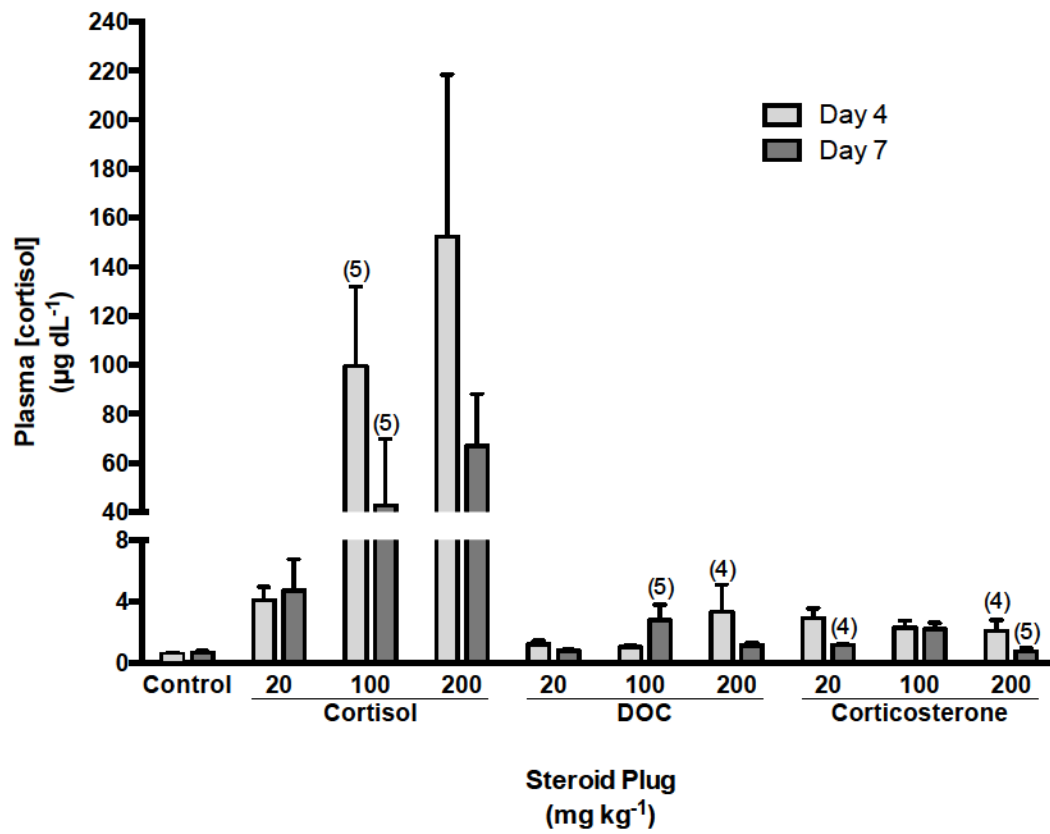
Figure 7.2 Effect of steroidal implants on circulating plasma cortisol levels.

Plasma cortisol concentrations (μg dL^{-1}) measured in hagfish 4 and 7 days post-implantation with coconut oil (control), cortisol, 11-deoxycorticosterone (DOC), and corticosterone. Cortisol, DOC, or corticosterone were dissolved in warm coconut oil and injected into hagfish to achieve nominal plasma concentrations of 0 (control), 20, 100 and 200 mg kg^{-1}. Measurement of cortisol at 4 and 7 days post-implantation were used to confirm loading rates. Data is reported as mean $\pm$ s.e.m. (*n*). Unless otherwise noted *n* = 6.
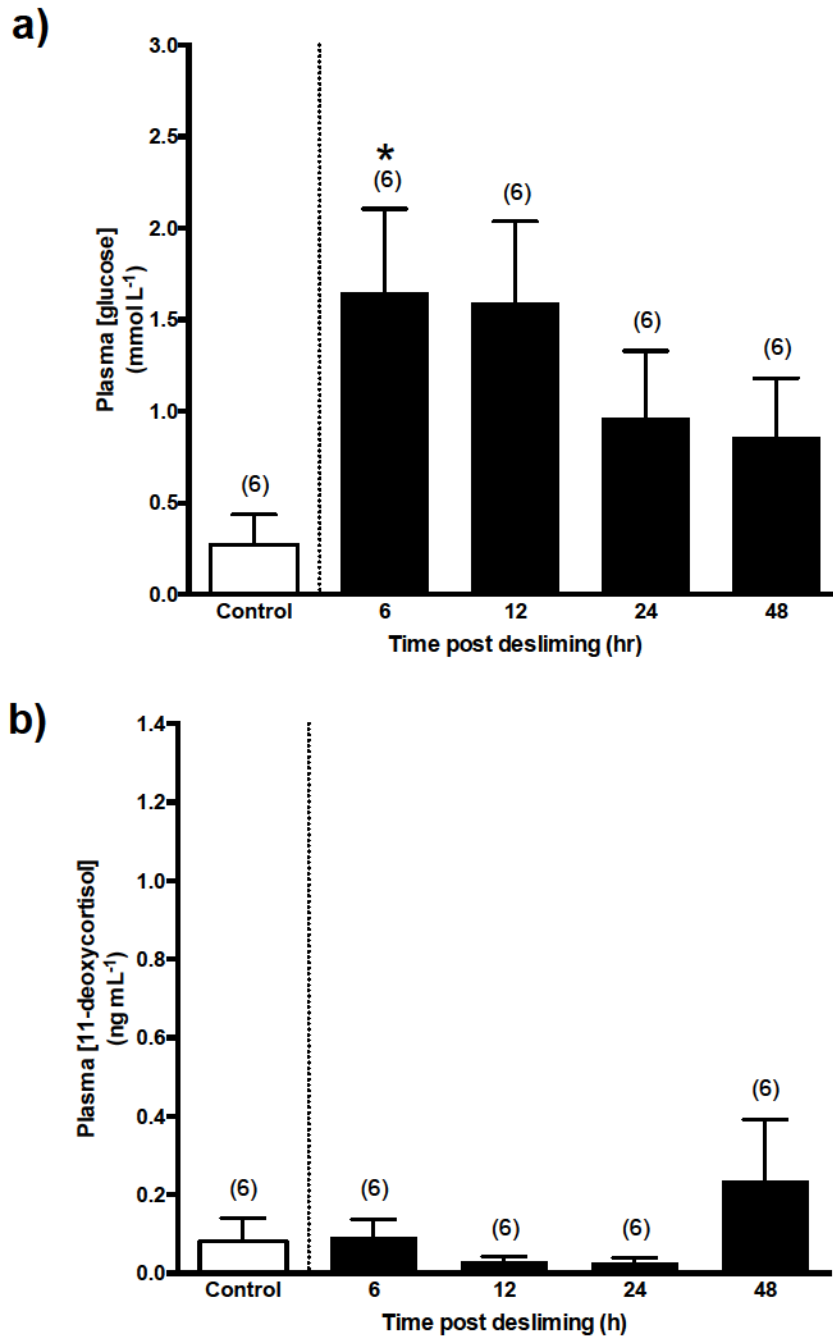
Figure 7.3 Effects of de-sliming stress on plasma glucose and 11-deoxycortisol.

Hagfish plasma glucose concentrations (mmol L^{-1}; a) and 11-deoxycortisol (11-DOC) concentrations (ng mL^{-1}; b) pre- (control) and 6, 12, 24, and 48 h post-desliming stress. Data is reported as mean ± s.e.m. (n = 6). Asterisk (*) denotes significant difference compared to control ($p \leq 0.05$, ANOVA).
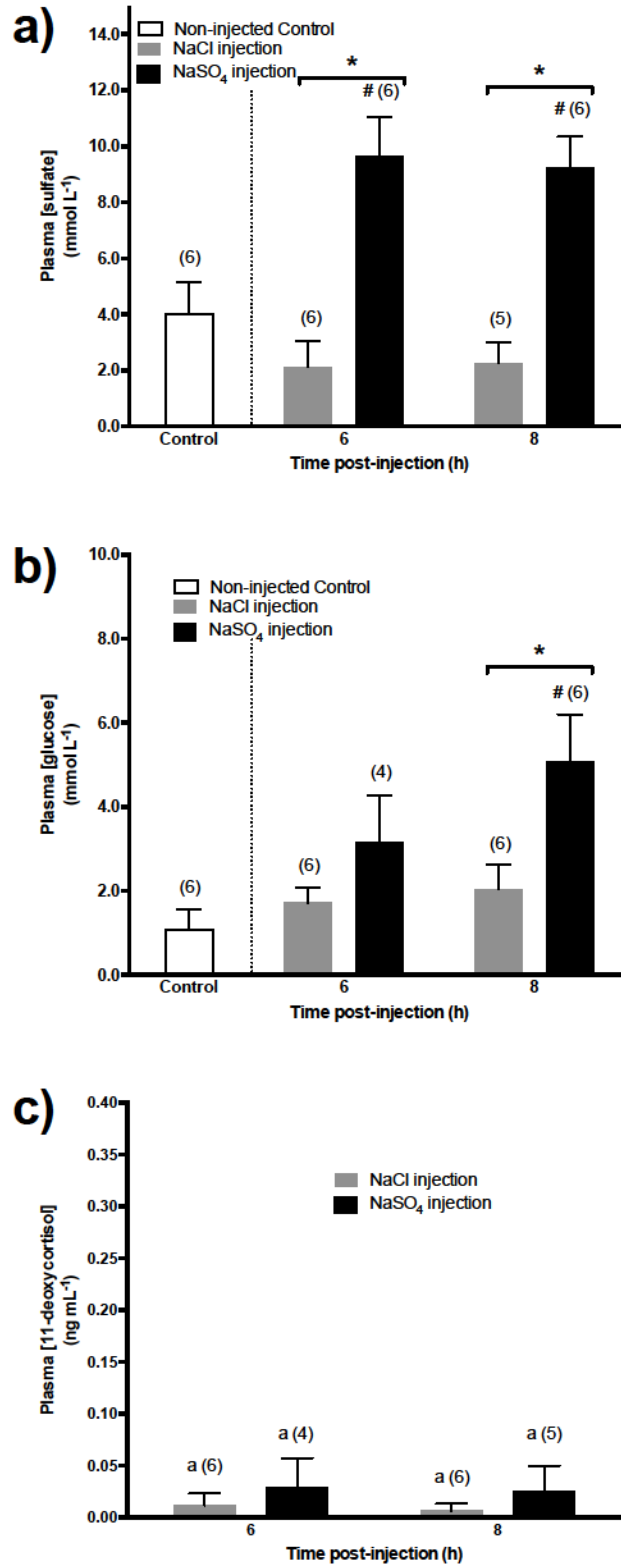
Figure 7.4 Plasma [sulfate], [glucose] and [11-deoxycortisol] following repeated mineral loading.

Plasma sulfate concentrations (mmol L^{-1}; a), glucose concentrations (mmol L^{-1}; b) and 11-DOC concentrations (ng mL^{-1}; c) in non-injected hagfish (white bars; control), and hagfish 6 and 8 h post-injection with NaCl (grey bars) or NaCl/Na_2SO_4 (black bars). Hagfish were injected daily for 3 days with 0.5 M NaCl (3000 μmol kg^{-1}) or 0.5 M Na_2SO_4 (3000 μmol kg^{-1}) and were then injected with 0.5 M NaCl (3000 μmol kg^{-1}) or 0.5 M NaCl/Na_2SO_4 (6000 μmol kg^{-1}) on day 4. Data is reported as mean ± s.e.m. ($n = 6$ unless otherwise noted above bars). In (a) and (b), an asterisk (*) denotes a significant difference between groups ($p \leq 0.05$, ANOVA), and a hash tag (#) denotes a significant difference compared to control ($p \leq 0.05$, ANOVA). Note, in (c) plasma 11-DOC concentrations were not measured in control hagfish samples.
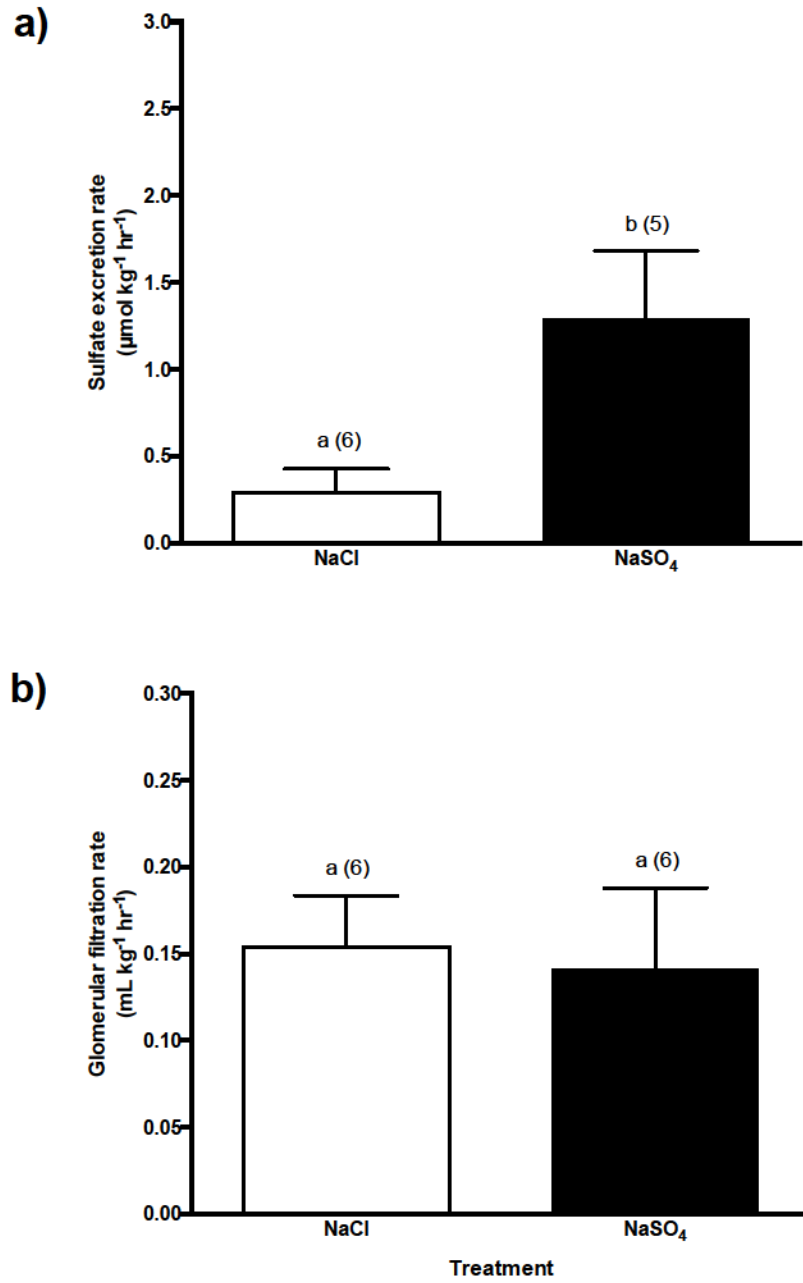
Figure 7.5 Sulfate excretion and glomerular filtration rates following repeated mineral loading.

Sulfate excretion rates (μmol kg^{-1} h^{-1}) and glomerular filtration rates (mL kg^{-1} h^{-1}) of hagfish 8 h post-injection with 0.5 M NaCl (white bars) or 0.5 M Na$_2$SO$_4$ (black bars). Data is reported as mean $\pm$ s.e.m. ($n = 6$ unless otherwise noted above bars). Different lower case letters denotes a significant difference between groups ($p \leq 0.05$, ANOVA).

SECTION 4:

RESPIRATION

Chapter 8: It's all in the gills: Evaluation of O₂ uptake in Pacific hagfish refutes a major respiratory role for the skin

Introduction

Recent studies have highlighted the importance of cutaneous transport in hagfish for nutrient acquisition (Glover et al., 2011; Schultz et al., 2014), ammonia and base excretion (Clifford et al., 2014), and trace metal uptake (Glover et al., 2015); however, the role of hagfish skin in O_2 uptake (M_{O_2}) is contentious. Cutaneous respiration has been demonstrated in the phylogenetically-related lampey (*Geotria australis*) in larval form (Potter et al., 1996), European eel (*Anguilla anguilla*) (Nonnotte and Kirsch, 1978) both of which share similar body plans to the hagfish, and several species of fish such as the inanga (*Galaxias maculatus*) (Urbina et al., 2012; Urbina et al., 2014), flounder (*Platichthys flesus*) and sole (*Solea solea*) (Nonnotte and Kirsch, 1978). Steffensen et al. (1984) proposed that hagfish ventilation can theoretically satisfy only ~20% of whole-animal M_{O_2} and that the skin is well suited for cutaneous respiration due to prominent dermal capillary networks. Moreover, when gill apertures were sutured shut, hagfish retained 89% of M_{O_2} lending support for this hypothesis (Lesser et al., 1996). Contrarily, Malte and Lomholt (1998) argued against the capacity for cutaneous O_2 uptake in the hagfish, citing the impracticality for O_2 exchange across the 70-100 μm epidermal layer, perfusion of capillaries with arterial blood of high P_{O_2} (partial pressure of oxygen), and the impact of skin boundary layers on diffusion.

Here, I used custom-designed respirometry chambers to isolate anterior (branchial+cutaneous) and posterior (cutaneous) regions of the hagfish to partition whole-animal M_{O_2} and ammonia excretion (J_{Amm}). Exercise in animals typically increases M_{O_2} and J_{Amm} during post-exercise recovery; therefore exhaustive exercise was employed to

determine the relative contribution of the gills and skin to elevations in metabolic demand. Given that skin is proposed as the primary site for M_{O_2} in hagfish (Steffensen et al., 1984), while J_{Amm} is gill-dominant (Clifford et al., 2014; Chapter 6), I hypothesized that exercise would yield increases primarily in cutaneous M_{O_2} and branchial J_{Amm} during recovery.

Hagfish often partially burrow into decaying carcasses (Hardisty, 1979) where conditions are hypoxic (Clifford et al., 2015b). I further hypothesized that under such conditions, cutaneous O_2 exchange would become more important. Thus, hagfish were exposed to anteriorly-localized hypoxia to examine if they can compensate for reduced branchial O_2 availability by elevating cutaneous O_2 uptake. This represents the first direct assessment of the cutaneous contribution to O_2 uptake in hagfish under resting and metabolically challenging conditions.

Materials and methods

Experimental animals

Pacific hagfish (*Eptatretus stoutii;* N = 32, 86.53 ± 4.13 g; mean ± s.e.m) were captured near Bamfield, BC, Canada and held at Bamfield Marine Sciences Centre (BMSC) as previously described (Clifford et al., 2014) under licenses from Department of Fisheries and Oceans Canada (permit # XR-310 2015) and animal care protocols from BMSC (RS-15-31) and University of Alberta (AUP00001126).

Experimental series

Series 1: Post-exercise metabolism in hagfish

Hagfish were transferred from holding tanks to 200 L wet-tables receiving flowing seawater. Hagfish were subjected to either 25 min of exercise induced by chasing and tail-pinching while control animals were left undisturbed for the same duration.

Following exercise or control protocols, hagfish were immediately transferred to individual 1.5 L respirometers containing magnetic stir-bars and filled with normoxic seawater. An initial 10 mL sample was drawn for analysis of oxygen tension (P_{O_2}) *via* a Clarke electrode and total ammonia (T_{Amm}) concentration using the colorimetric salicylate-hypochlorite method (Verdouw et al., 1978). Immediately following sampling, respirometers were sealed. After 2 h, each respirometer was stirred to ensure complete mixing, a final water sample was drawn and analyzed as above, and respirometer volume and hagfish weight were recorded.

In a second protocol, hagfish were exercised as above. However, following exercise, they were anaesthetized (MS-222; 0.5 g L^{-1} neutralized with NaOH; 0.15 g L^{-1}), and fitted into separating chambers as previously described (see Clifford et al. 2014 for apparatus details) with the separation occurring ~2 cm posterior to the last branchiopore. Magnetic stir-bars were added to both the anterior and posterior chambers to ensure adequate mixing. The animal's body length in each chamber was measured. Normoxic seawater (~500 mL) was added to both anterior and posterior chambers and initial water samples were drawn before sealing as above. After 2 h, chambers were stirred, final water samples taken, and anterior and posterior chamber volumes and hagfish weight were recorded.

Series 2: Effects of hypoxia on whole-animal and partitioned metabolic rate

O$_2$ uptake was characterized during whole-animal and anteriorly-localized hypoxia. Hagfish were transferred into 1.5 L respirometers containing hypoxic seawater (P_{O_2}~3.9 kPa; bubbled with 100% N$_2$ gas for 20 min) and experiments were performed as above. In a second protocol, hagfish were fitted into separating chambers as above. Hypoxic seawater (P_{O_2}~4.6 kPa) was added to the front compartment while the rear compartment contained normoxic seawater. Sample collection and respirometry trials were conducted as above.

Calculations and statistical analysis

Calculation of M_{O_2} was done as previously described (Guffey and Goss, 2014) based on measured P_{O_2} values using the following equation:

$$M_{O_2} = \left(\left(P_{O_2 \, initial} - P_{O_2 \, final}\right) \cdot \alpha_{O_2} \cdot V\right) \cdot \frac{1}{m} \cdot \frac{1}{\Delta t} \qquad (1)$$

where P_{O_2} is the initial or final O_2 content in the water (Torr), α_{O_2} is the solubility

constant for O_2 (μmol O_2 L^{-1}.Torr^{-1}) derived by (Boutilier et al., 1984), V is the volume of

water (L), m is the animal mass (g), and Δt the duration of the flux period.

J_{Amm} was calculated as previously described (Clifford et al., 2015a) based on the

T_{Amm} accumulation in the water using the following equation:

$$J_{Amm} = \left([T_{Amm}]_{initial} - [T_{Amm}]_{final} \cdot V\right) \cdot \frac{1}{m} \cdot \frac{1}{\Delta t} \qquad (2)$$

where [T_{Amm}] is the initial or final concentration of ammonia in the water (μmol L^{-1}).

Anterior and posterior M_{O_2} rates ($M_{O_2}^{ant}$ and $M_{O_2}^{post}$) were converted to branchial

and cutaneous rates ($M_{O_2}^{branc}$ and $M_{O_2}^{cutan}$) as follows:

$$M_{O_2}^{cutan} = M_{O_2}^{post} + \left(\left(\frac{M_{O_2}^{post}}{L^{post}}\right) \cdot L^{ant}\right) \qquad (3)$$

$$M_{O_2}^{branc} = M_{O_2}^{ant} - \left(\left(\frac{M_{O_2}^{post}}{L^{post}}\right) \cdot L^{ant}\right) \qquad (4)$$

where L^{ant} and L^{post} are the measured body lengths (cm) in the anterior and posterior

compartments. Equation (3) and (4) were used similarly to calculate branchial and

cutaneous J_{Amm} (J_{Amm}^{branc} and J_{Amm}^{cutan} respectively). All data are expressed as the mean $\pm$ 1

standard error (s.e.m.). Whole-animal, and combined branchial and cutaneous rate comparisons were made using unpaired t-tests while comparisons between anterior and posterior rates within the same group were made using paired t-tests. The fiducial limit of significance was $p < 0.05$.

Results and discussion

Routine M_{O_2} in the current study (583.4 $\pm$ 162.3 µmol kg^{-1} h^{-1}; Figure 8.1A) was consistent with other reported values for *E. stoutii* (Cox et al., 2011; Munz and Morris, 1965). To my knowledge, this study is the first to describe M_{O_2} and J_{Amm} in hagfish following exercise. Excess post-exercise O$_2$ consumption (EPOC; Wood, 1991), whereby M_{O_2} nearly doubled (1085.0 $\pm$ 148.0 µmol kg^{-1} h^{-1}) compared to routine rates ($p = 0.03$; Figure 8.1A) and likely served to replenish phosphagen stores and oxidize lactate (Wood, 1991). Increased M_{O_2} in post-exercised hagfish was accompanied by a ~4-fold increase in J_{Amm} (126.1 $\pm$ 17.4 versus 33.2 $\pm$ 6.4 µmol kg^{-1} h^{-1} µmol kg^{-1} h^{-1} under resting conditions, $p < 0.01$); Figure 8.1C), a response associated with post-exercise recovery (Wood, 1991; Wood, 2001) as a result of adenylate deamination (Dobson and Hochachka, 1987).

Whole-animal metabolic metrics did not statistically differ from combined partitioned rates for either control (M_{O_2} = 583.3 $\pm$ 162.3 vs. 604.0 $\pm$ 107.26 µmol kg^{-1} h^{-1}, $p = 0.92$; J_{Amm} = 33.2 $\pm$ 6.4 vs. 39.6 $\pm$ 7.8 µmol kg^{-1} h^{-1}, $p = 0.54$) or post-exercised (M_{O_2} = 1085.0 $\pm$ 148.0 vs. 1001.6 $\pm$ 139.8 µmol kg^{-1} h^{-1}, $p = 0.69$) hagfish with the exception of J_{Amm} in post-exercised animals, which was slightly elevated in partitioned experiments (199.8 $\pm$ 19.7 vs. 126.1 $\pm$ 17.4 µmol kg^{-1} h^{-1}, $p = 0.03$). Thus, use of the separating chambers did not interfere with normal hagfish metabolism.

In control animals, branchial M_{O_2} averaged 521.7 $\pm$ 123.8 µmol kg^{-1} h^{-1}, while cutaneous rates were much lower (82.3 $\pm$ 22.2 µmol kg^{-1} h^{-1}, $p = 0.04$; Figure 8.1B). Following exercise, the increase in O$_2$ uptake was solely a function of branchial

exchange, nearly doubling to 935.1 ± 160.8 µmol kg^{-1} h^{-1} ($p = 0.04$) comprising $92 \pm 3.1\%$ (Table 8.1) of total M_{O_2}, and further confirming the dominant role of hagfish gills over skin in O_2 uptake. Cutaneous M_{O_2} remained unchanged at 66.5 ± 27.5 µmol kg^{-1} h^{-1}, ($p = 0.33$). Interestingly, while ~30% of total resting J_{Amm} in control hagfish was cutaneous, post-exercise animals exhibited a 6-fold increase ($p < 0.01$) in branchial J_{Amm}, comprising $99.3 \pm 0.7\%$ of total ammonia excretion (Figure 8.1D, Table 8.1). Hagfish did not demonstrate an important capacity for cutaneous O_2 uptake in either control ($19 \pm 7.3\%$) or post-exercise ($8.0 \pm 3.1\%$) animals in contrast to previous reports ($75 - 89\%$; Lesser et al., 1996; Steffensen et al., 1984).

While feeding on decaying carrion, hagfish immerse their heads in the flesh (Hardisty, 1979), subjecting the gills to a localized environment that is hypoxic, hypercapnic and high in [T$_{Amm}$] (Clifford et al., 2015b), while the tail remains outside. I hypothesized that significant cutaneous M_{O_2} might only occur when branchial M_{O_2} was impaired. Indeed, Lesser et al. (1996) found that whole body M_{O_2} was maintained when branchial pores of hagfish were sutured shut, and therefore concluded that hagfish must recruit the skin to maintain M_{O_2} in the absence of branchial contribution. Based on these observations, it was predicted that anteriorly-localized hypoxia would have minimal effects on whole-body M_{O_2}. Note that given the asymmetric conditions of this experiment, it was inappropriate to apply a correction to cutaneous data. In response to non-localized hypoxia, whole-body M_{O_2} in hagfish decreased by 90%, as noted in previous reports (Forster, 1990). Summing anterior and posterior M_{O_2} during anteriorly-localized hypoxia yielded a total of 87.3 ± 9.8 µmol kg^{-1} h^{-1}, not significantly different from whole-animal M_{O_2} during non-localized hypoxic exposure (54.8 ± 61.4 µmol kg^{-1}

h^{-1}, $p = 0.67$; Figure 8.2) in accord with my hypothesis. Nevertheless, during anteriorly-localized hypoxia, posterior M_{O_2} was significantly elevated (81.8 ± 6.7 µmol kg^{-1} h^{-1}) compared to control posterior M_{O_2} rates (44.0 ± 11.5 µmol kg^{-1} h^{-1}; $p < 0.01$), thereby accounting for ~94% of summed anterior and posterior M_{O_2} in animals exposed to anteriorly-localized hypoxia. The increase in posterior M_{O_2} likely occurred due to reduced arterial P_{O_2} augmenting the driving gradient for O_2 transport. Indeed, measurements in the anterior chamber during anteriorally-localized hypoxia revealed increases in P_{O_2} from baseline hypoxia for some (3 of 6) experimental trials suggesting loss of O_2 across the gills. Importantly, on an absolute basis, this posterior increase was small, so these data clearly demonstrate that even when branchial O_2 acquisition is greatly impaired and transcutaneous water-blood P_{O_2} gradients are likely optimal, the skin is not recruited to any great extent to maintain whole-body M_{O_2} at control rates contrary to previous reports (Lesser et al., 1996).

The contrasting cutaneous O_2 exchange contributions presented here versus those reported previously (Steffensen et al., 1984; Lesser et al., 1996) are likely explained by procedural differences. For instance, Steffensen et al. (1984) concluded that over 80% of M_{O_2} occurred cutaneously in hagfish based on measuring branchial ventilation rates and assuming that gill oxygen extraction could not account for the whole-body M_{O_2} measured in their study. Malte and Lomholt (1998) have since argued against these findings, claiming that these authors had underestimated gill oxygen extraction. Lesser et al. (1996) similarly did not directly assess branchial and cutaneous M_{O_2} but rather estimated cutaneous M_{O_2} by measuring M_{O_2} in hagfish whose branchial pores had been sutured shut.

However, these authors did not report any methods to check for leaks in the suturing technique and also did not account for the phenomenon of "sneezing" (Steffensen et al., 1984), which may allow for oxygenated water to be taken in *via* the nasopharyngeal duct. The present study is the first to truly measure branchial and cutaneous M_{O_2} in hagfish using a direct method. Indeed, separating chambers have been effectively utilized previously (Clifford et al., 2014; Urbina and Glover, 2015; Urbina et al., 2014; Urbina et al., 2012; Zimmer and Wood, 2015; Zimmer et al., 2014) and this technique is considered the "gold standard" for estimating branchial and cutaneous contributions to osmorespiratory exchanges (Brauner and Rombough, 2012). Thus, contrary to previous reports, my results clearly refute a major role of the hagfish skin in gas exchange, which have been over-estimated. While the skin does have some other important transport functions (Clifford et al., 2014; Glover et al., 2011; Glover et al., 2015; Schultz et al., 2014), the gills are the dominant site for both M_{O_2} and J_{Amm}.

Table 8.1 Calculation of skin-specific rates and corrected distribution of M_{O_2} and J_{Amm} in branchial and cutaneous components.

Measured anterior and posterior oxygen consumption (M_{O_2}) and ammonia excretion (J_{Amm}) from series 1 experiments were converted to corrected branchial (Bran.) and cutaneous (Cut.) rates (Figure 8.1). Rates were calculated assuming similar M_{O_2} cm^{-1} and J_{Amm} cm^{-1} and based on individual animal skin lengths (displayed above as both length in centimeters and as % length) using equations (3) and (4). N=5.

	Uncorrected rate		Skin length in chamber		Skin length-specific rate	Corrected rate		
	Anterior	Posterior	Anterior	Posterior		Bran.	Cut.	s.e.m.
	μmol kg^{-1} h^{-1}				μmol kg^{-1} h^{-1} cm^{-1}		%	
M_{O_2}			In centimeters					
Control	560.0 ± 116.1	44.0 ± 11.5	18.74 ± 7.05	22.14 ± 15.07	2.0 ± 0.59	81.0	19.0	± 7.3
Post-Exercise	966.3 ± 150.7	35.3 ± 14.7	17.96 ± 10.59	20.24 ± 12.52	1.66 ± 0.70	92.0	8.0	± 3.1
J_{Amm}			As %					
Control	33.3 ± 6.4	6.3 ± 2.2	41.7 ± 1.1	49.0 ± 1.4	0.30 ± 0.12	70.7	29.3	± 6.9
Post-Exercise	199.7 ± 23.3	0.04 ± 2.8	42.1 ± 0.7	47.4 ± 1.0	-0.01 ± 0.14	99.3	0.7	± 2.4
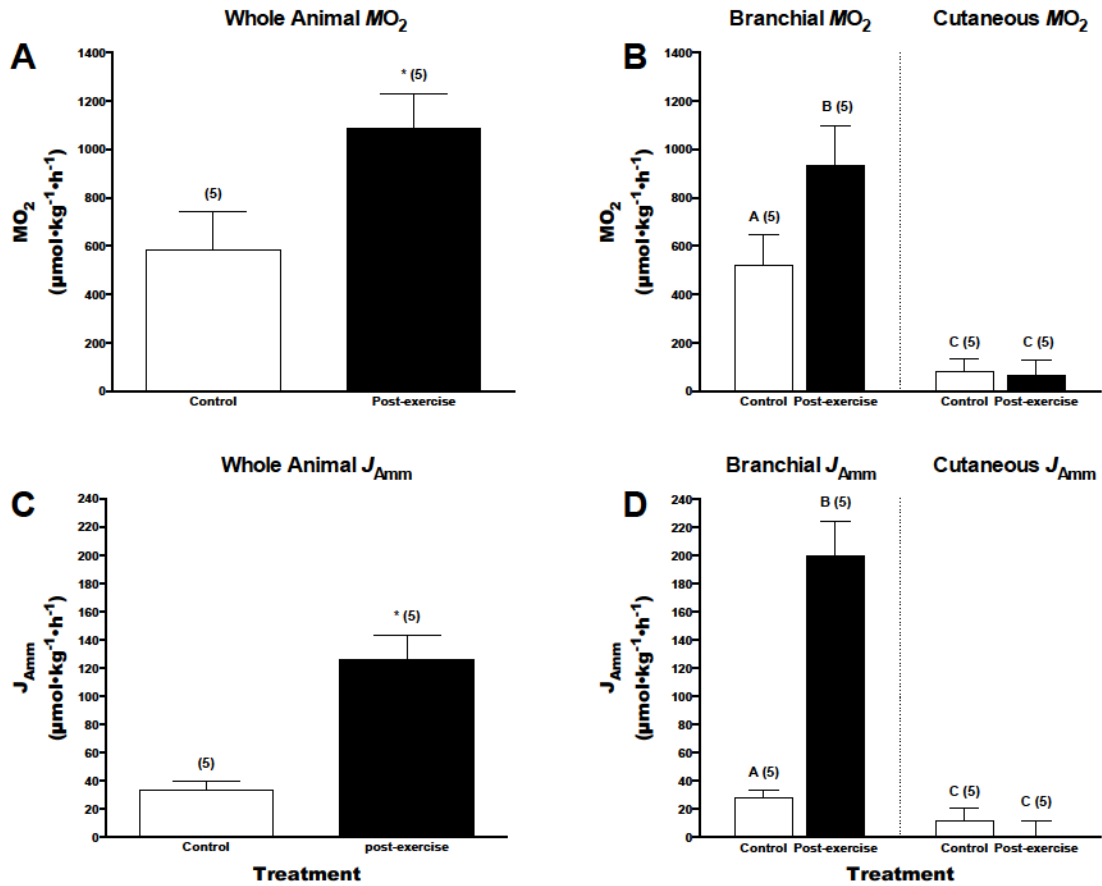
Figure 8.1 Whole-body and partitioned M_{O_2} and J_{Amm} in during post-exercise recovery.

Whole-body (A,C), and partitioned branchial and cutaneous (B,D) M_{O_2} (A,B) and J_{Amm} (C,D) of hagfish following exhaustive exercise (25 min; closed bars). Rates were measured over 2 h. Data are presented as mean + s.e.m. (n). Asterisks (*) denote significant differences ($p < 0.05$) from routine rates (open bars) in whole-body exposure while bars sharing common letters are not significantly different ($p < 0.05$).
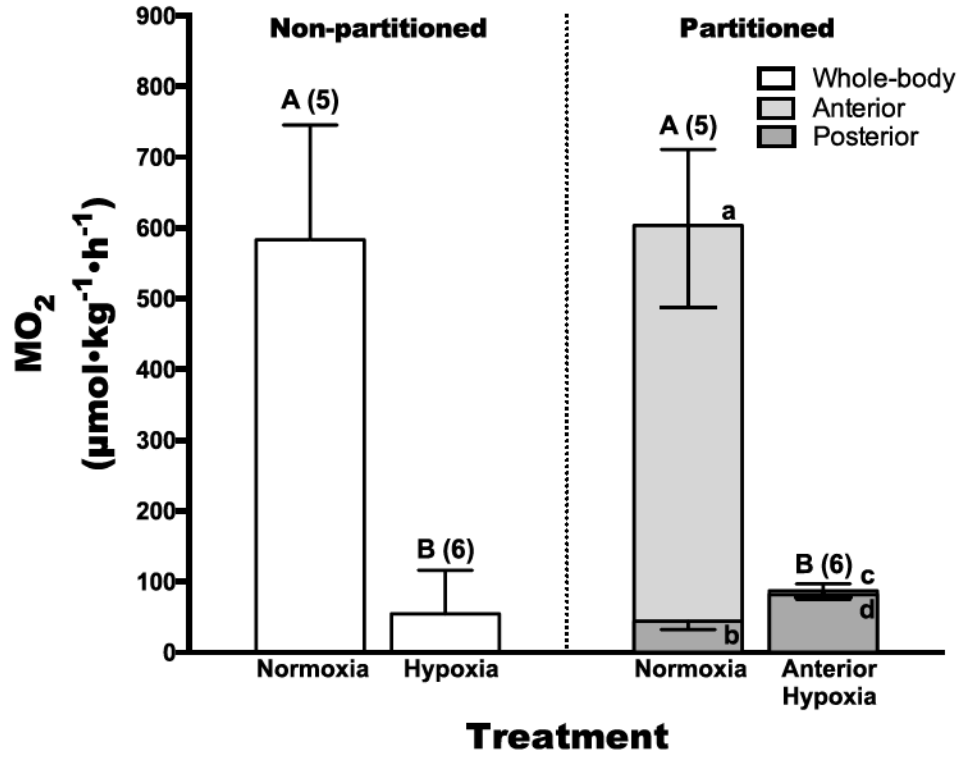
Figure 8.2 Measured M_{O_2} in hagfish exposed to either normoxia or hypoxia.

Measured M_{O_2} in hagfish exposed to either normoxia or hypoxia in non-partitioned chambers (open bars) or normoxia and anteriorly-localized hypoxia in separating chambers. Non-partitioned bars presented as mean + s.e.m. (*n*). Combined anterior (light grey) and posterior (dark grey) bars presented as mean + s.e.m. (*n*). Partitioned anterior and posterior bars presented as mean − s.e.m. Bars sharing common letters are not statistically different ($p < 0.05$). Upper-case letters denote statistical differences for whole-body/combined anterior and posterior measurements. Lower-case letters denote statistical differences for partitioned rates

Chapter 9: General Conclusions

General summary

Since Homer Smith's (1932) review contrasting the osmotic condition of hagfish to other aquatic species, hagfish have become an exciting organismal model for zoologists with respect to osmoregulation, ionoregulation and acid/base physiology. Furthermore, the phylogenetic placement of hagfish at the base of the vertebrate lineage reinforces these peculiar animals' usefulness as a model for study on the evolution of not just the aforementioned physiological processes, but also for the evolution of endocrine systems, feeding and digestion and respiration. This thesis represents a substantial contribution to each of these areas regarding the physiology of this phyletically ancient organism and insights drawn from my thesis will serve to inform future comparative/evolutionary physiological studies.

A common topic throughout my thesis pertains to the feeding lifestyle of the hagfish, or rather the extreme environment hagfish encounter when feeding. For most other aquatic vertebrates this environment would be considered physiologically aggravating; however, hagfish are capable of surviving and thriving these noxious conditions. In this thesis, I have provided insights on the mechanisms and adaptations, which allow the Pacific hagfish (*Eptatretus stoutii*) to tolerate these stresses and describe how post-exposure recovery is mediated. This discussion chapter serves as a general summary of findings, where I highlight trends between chapters and point out new lines of research.

Acid/base regulation

Hagfish are champions in the acid/base world, capable of surviving and recovering from extreme deviations in blood acid/base status. Such a tolerating ability seems logical given that hagfish likely frequently experience hypercapnic conditions while feeding. When exposed to high levels hypercapnia, hagfish offset blood acidosis by raising plasma $[HCO_3^-]$ to the highest levels ever reported in any animal (Baker et al., 2015). Section I of this thesis focuses on describing the physiological strategies that hagfish employ to mitigate the effects from acid/base perturbations and further characterize the adaptations and mechanisms employed to recover when stress is removed.

Sites of acid and base excretion

In Chapter 2, I demonstrated that following acid loading with HCl, the resultant acid load is excreted from the anterior section of the hagfish, likely the gills, as no other acid equivalent flux was realized in the posterior (skin or skin + cloaca) chamber. When recovering from acute base loading with $NaHCO_3$ however, hagfish excrete the alkaline load predominantly from the posterior region of the animal. Hagfish lack concentrating abilities (Alt et al., 1981) in their rudimentary kidney, producing only low rates of urinary flow (Morris, 1965). The low glomerular filtration rate (GFR) in hagfish which I measured in hagfish in Chapters 3 and 7 combined with the fact that cloacal constituents to total flux were inhibited by cloacal seals leads me to conclude that the skin of the hagfish is capable of functioning in the excretion of base equivalents when necessary. Furthermore, results from this thesis also provide evidence that hagfish utilize their skin

to offload ammonia into the environment. Previous studies examining nutritive uptake in hagfish *via* cutaneous mechanisms demonstrate uptake of amino acids L-alanine and L-glycine (Glover et al., 2011) and uptake of phosphate (Schultz et al., 2014). The thickness of the epidermal tissue in relation to the dermal capillaries is too great (70-100 μm thick; Weinrauch et al., 2015; Welsch and Potter, 1998) to allow simple diffusion of these constituents; thus molecular transporters must exist within the skin in order to facilitate movement of these ions. The likely molecular identity of the cutaneous ammonia excreting mechanism is discussed below; however, the identity of the transporter(s) responsible for excretion of bicarbonate remains to be realized. Based on plasma [Cl⁻] data from Chapter 3 and 4, the transporter involved is likely an isoform from the SLC26 family (Cl^-/HCO_3^- exchanger; CBE) or the SLC4 related family members (AE family of transporters); which are Cl^- linked HCO_3^- transfer proteins (Alper, 2006; Alper and Sharma, 2013). Future research should focus on identifying the molecular mechanisms for bicarbonate transfer across the skin of hagfish.

Based on observing acid excretion only in the anterior compartments following infusion, I had initially hypothesized that the single type of mitochondrion rich cells (MRCs) that hagfish possess (Tresguerres et al., 2006a) were acid secreting cells only. In all other fishes studied there are at least two or more types of MRCs with at least one population capable of acid secretion and another capable of base secretion (Dymowska et al., 2012; Hwang and Lee, 2007). However, my results from Chapter 4 force reconsideration of this hypothesis, since hagfish that were hypercarbic (*via* hypercapnia exposure; 72 h; 0.6% CO_2) excreted base equivalents across both posterior and anterior sections. While it is possible that the anterior skin was also excreting base equivalents,

equally likely is that this anterior flux is truly representative of branchial base equivalent efflux. To date, only NHE (Na$^+$/H$^+$ Exchanger), NKA (Na$^+$-K$^+$-ATPase) and VHA (Vacuolar H$^+$-ATPase) have been co-localized to hagfish gill MRCs. Careful experimentation involving base infusions/hypercapnia exposure and molecular analysis/co-localization studies involving the CBEs and/or NBCs in the gill will allow for definitive conclusions to be made on the base secreting ability of hagfish MRCs. Regardless, it appears that anterior (branchial) mechanisms of base equivalent excretion must be up-regulated or activated in order to function and this is supported by results in Chapter 3 demonstrating that Cl$^-$/HCO$_3^-$ transporting mechanisms must be up-regulated or activated which occurs at least 2 h after egress from hypercapnia.

Modulation of base excretion mechanisms

How these branchial base excretion mechanisms are modulated is a topic of interest and comparison of mechanisms and results between the extrabranchial infusion and extrabranchial hypercapnia studies yield several possible explanations. One noted difference is the method of stimulating/generating hypercarbia. During hypercapnia, CO$_2$ diffuses into the hagfish across epithelia either passively or possibly facilitated by Rh-like (Rhesus-like) glycoprotein (SLC42 transporter family) (Chapter 6; see below) or aquaporins (AQPs) (Endeward et al., 2006; Musa-Aziz et al., 2009; Perry et al., 2010). Upon entry into the animal, P_{CO_2} (partial pressure of CO$_2$) gradients are rapidly equilibrated by CA (carbonic anhydrase) conversion into HCO$_3^-$ and H$^+$ whereas direct infusion of NaHCO$_3$ causes a HCO$_3^-$ load without a CO$_2$ signal. In the gill, sAC is thought to work as an HCO$_3^-$ sensor that when activated, generates cAMP (Cyclic AMP) to mediate microtubule-dependent translocation of VHA. However, sAC can also

associate with CA and other acid/base related proteins, which together can allow sAC to act as a *de facto* CO_2 and pH sensor (Tresguerres et al., 2014). Perhaps a CO_2 signal is needed in order to activate compensation and recovery pathways *via* sAC (soluble adenylyl cyclase) signaling. Localized hypercapnia experiments in Chapter 4 further suggest that CO_2 sensing may be responsible for mounting compensatory responses during hypercapnia (see below).

Another explanation could be that TCO_2 (total CO_2 content)/$[HCO_3^-]$ thresholds must be met in order for branchial mechanisms to be up-regulated/activated. Infusion of $NaHCO_3$ likely only yielded a TCO_2 load of ~22 mmol based on Tresguerres et al. (2007) while hypercapnia exposure (0.6% CO_2; 72 h) generated TCO_2 responses approximately double that. Thus basal cutaneous excretion mechanisms may have been sufficient to offload the resultant hypercarbia from infusion but not from hypercapnia where TCO_2 loads were greater.

Finally, the noted differences may also be due to how hypercarbia was achieved as recovery immediately followed hypercarbia induced by acute infusions while hypercapnia persisted for 72 h prior to recovery. Molecular analysis of gill tissue from hagfish exposed to acute or chronic hypercapnia or repeated alkaline infusion will help determine which of the above are responsible for differences between studies.

Mechanisms of hypercarbia recovery

The purpose of alkaline infusions in Chapter 2 was to generate hypercarbia loads within hagfish and describe mechanisms of hypercarbia recovery. In Chapter 3, I utilized hypercapnia (4% CO_2) to mount similar compensatory plasma $[HCO_3^-]$ responses, but

with greater effect. Chapter 3 yields a considerable amount of insight regarding the mechanisms by which hagfish rapidly restore plasma $[HCO_3^-]$ to basal levels upon egress from hypercapnia. First, hagfish re-equilibrate CO_2 according to the partial pressure gradients, either by passive diffusion across epithelia or perhaps *via* Rh-protein or AQP facilitated diffusion (Musa-Aziz et al., 2009; Perry et al., 2010; see below). Direct Cl^-/HCO_3^- exchange *via* HCO_3^- flux does not appear to occur to a measurable degree within the first 2 h of recovery; however, between 2 – 6 h, mechanisms of HCO_3^- equivalent excretion appear to be up-regulated/activated. Despite these increases, HCO_3^- equivalent excretion cannot account for the total plasma TCO_2 recovery observed, nor can the increases in GFR observed throughout recovery. Rather, a large proportion of plasma TCO_2 correction is facilitated by an up-regulated CA-mediated dehydration of HCO_3^- into CO_2, which again can be lost diffusively with the mechanisms listed above. This process leaves many avenues to be further explored and will be a focal point of my future research program.

Insights from localized hypercapnia exposure

In Chapter 4, perhaps my most intriguing results stem from interpretation of my localized hypercapnia (0.6% CO_2; 4 h) experiments. Hagfish displayed acidosis regardless of whether they were anteriorly- or posteriorly-exposed; however, a compensation response was only present in anteriorly-exposed animals. Two important realizations came be made from this: 1) This indicates that CO_2 can readily permeate into the organism *via* both branchial and cutaneous epithelia and 2) the selective compensation suggests that hagfish may utilize an anteriorly-mediated sensor to respond to hypercapnia induced acid/base disturbances.

Evidence for facilitated epithelial CO$_2$ exchange

Given results presented in Chapter 8 demonstrating that hagfish have limited oxygen uptake across cutaneous epithelia (discussed below), it's logical to assume that one of the main arguments against cutaneous oxygen uptake (i.e. thick epidermal layer between environment and dermal capillaries) should also apply for CO$_2$ exchange. However, given the degree of blood acidification during posteriorly-localized hypercapnia exposure, such an assumption appears false. How then is CO$_2$ able to permeate across the skin into the blood space while O$_2$ exchange is physically impaired? A likely explanation may be that CO$_2$ diffusion into the hagfish may be facilitated by AQP or Rh-like glycoprotein transport. I have demonstrated that hagfish express an Rhcg-like protein in epidermal tissue of the skin (Chapter 6). Rh proteins have been demonstrated to not only facilitate transport of ammonia (Hung et al., 2007; Nakada et al., 2007; Nawata et al., 2007; Tsui et al., 2009), but also CO$_2$ (Endeward et al., 2006; Musa-Aziz et al., 2009; Perry et al., 2010). Thus, it stands to reason that Rh proteins located in the skin may also function in cutaneous exchange of CO$_2$ and this will be a focus of my research going forward. I have not specifically investigated a role for AQP in facilitated CO$_2$ diffusion and future research aspects could examine the involvement of this protein family in these processes.

Evidence for CO$_2$ sensing

The difference in activating a compensatory hypercarbia-response between hagfish exposed to hypercapnia (0.6% CO$_2$; 4 h) either anteriorly and posteriorly provide preliminary evidence that an anteriorly-mediated CO$_2$ sensor, rather than a proximal

blood pH-mediated sensor, is responsible for activating bicarbonate compensation. While speculative at this time given the limited evidence, I suggest that the molecular identity of this sensor is sAC, a known physiological HCO_3^- sensor (Rahman et al., 2013; Tresguerres et al., 2014; Tresguerres et al., 2010). However, further validation of my experimental protocols is required to definitively rule out mixing effects (*e.g.* accounting for low circulatory rate in hagfishes; Forster et al., 2011). Following this, the identity of the CO_2 sensor will be investigated using know sAC inhibitors (KH7 and/or 4CE) to elucidate the potential pH/CO_2 sensing mechanism(s) in hagfish.

Nitrogen handling

Hagfish are tolerant of high levels of internal and external ammonia concentrations (Braun and Perry, 2010; Clifford et al., 2015a). Similar to their tolerance to hypercapnia (see above), the ability of the hagfish to withstand high environmental ammonia is likely adaptive to their feeding lifestyle. Microorganisms feeding on the same carrion as hagfish will likely cause increases in water [ammonia]. This environment would subsequently cause buildups in plasma [ammonia], which can be toxic if left unchecked. Furthermore, the high protein diet of the hagfish (Auster and Barber, 2006; Collins et al., 1999; Martini, 1998; Smith, 1985) results in the catabolism of ingested amino acids which also contribute to the net nitrogen load of the fish and thus must be excreted (Nelson et al., 2008). Prior to starting this thesis project, little was known regarding how hagfish handle nitrogen excretion, both normally and during times of hyperammonemia. Section II of this thesis focused on describing the physiological strategies and adaptations hagfish possess to withstand and recover from ammonia related perturbations.

Tolerance to HEA and hyperammonemia

In Chapter 5, I have identified and ruled out some of the obvious potential physiological mechanisms by which ammonia tolerance feats are possible by the hagfish. When exposed to high environmental ammonia (HEA; 20 mmol L^{-1}; 48 h) hagfish initially gained high amounts of ammonia at high rates of uptake. Under this condition, hagfish reached peak plasma total [ammonia] ([T_{Amm}]; 5450 µmol L^{-1}) within 24 h of exposure, after which time plasma [T_{Amm}] plateaued. These levels are the highest plasma

[T_Amm] reported in any organism following HEA exposure. Using plasma as a surrogate for other tissues such as liver and muscle, it was clear that hagfish did not rely on bio-conversion of ammonia to less toxic end-products such as urea or glutamine. However, brain tissues were not collected in this study and there is evidence in other fishes that brain [glutamine] increase markedly in response to HEA exposure (Ip et al., 2001b; Sanderson et al., 2010; Sinha et al., 2013; Tay et al., 2003; Veauvy et al., 2005; Wilkie et al., 2011) and following feeding (Wicks and Randall, 2002).

Hagfish are adapted to feed on decaying carrion

During HEA exposure, ammonia enters *via* passive diffusion of NH_3 likely facilitated by Rhcg which have been localized to the apical regions of pacific hagfish pavement cells (Braun and Perry, 2010) and to epidermal regions of hagfish skin tissue (Edwards et al., 2015; Chapter 6). Interestingly, in my study where I locally exposed hagfish to HEA either anteriorly or posteriorly (Chapter 6), hagfish that were posteriorly-exposed experienced greater ammonemic effects than those exposed anteriorly. These results highlight two important findings: 1) It suggests that the primary route of ammonia loading is *via* cutaneous means rather than branchially and 2) stemming from this, hagfish possess the ability to reduce ammonia uptake when branchially (but not cutaneously, at least within 4 h) exposed to HEA, even in the face of massive inwardly-directed ammonia gradients. As mentioned throughout the thesis, the local environment surrounding decaying carrion would likely contain high amounts of ammonia. Given the propensity of the hagfish to partially burrow into putrefying carrion to consume the soft tissue (Strahan, 1963), an ability to somehow impair entry of ammonia would be highly advantageous. During my whole animal HEA study (Chapter 5), I also noted an ability of

the hagfish to reduce ammonia uptake as plasma [T_{Amm}] stabilized around ~5000 µmol L⁻¹ within 24 – 48 h of exposure, despite considerable inwardly directed P_{NH_2} and $E_{NH_4^+}$ gradients. The directional reversal of ammonia flux (inward to outward) by 16 – 24 h likely aided in this stabilization; however, the length of time needed to generate this reversal cannot account for the impairment of ammonia uptake on the acute scale used in localized exposure studies (4 h). The mechanism of this impairment remains elusive and does not seem to be related to alterations of branchial hRhcg abundance as no differences in this metric were observed during HEA exposure or recovery (Chapter 5). However, it may be that permeability is reduced by a reduction of hRhcg on the membrane by a re-packaging into cytoplasmic vesicles. Furthermore relative abundance of other hagfish Rh proteins was not quantified.

Alternatively, alterations in branchial ventilation rate and/or flow may account for this reduction whereby hagfish simply 'hold their breath' to prevent uptake. This possibility could be investigated utilizing previously described methods similar to those used to look at ventilation in hagfish during hypoxia and hypercapnia (Perry et al., 2009). One final possibility could be that hagfish reduce the permeability of the gills by increasing the diffusion distance across the gills as has been observed previously in other fish species (Sinha et al., 2014). Overall, these findings provide convincing evidence that hagfish have adapted novel strategies to feed on putrefying carrion, and remain in a feeding environment containing high T_{Amm} for extended periods of time.

Routes of nitrogen excretion during exposure

In Chapter 5, despite taking up an impressive 85 mmol kg^{-1} within the first 16 h of exposure, hagfish readily offloaded ~80% of this ammonia load during the remainder of the 48 h exposure period. Again, this feat was accomplished against impressive inwardly directed P_{NH_3} and $E_{NH_4^+}$ gradients. I conclude that the most likely mechanisms by which this occurs is *via* secondary active transport whereby basolateral NKA (Na$^+$/K$^+$-ATPase drives an apical Na$^+$/NH$_4^+$(H$^+$) exchange *via* an NHE. Due to the high buffering capacity of seawater and the large inwardly directed gradients, it is unlikely that ammonia trapping (facilitated by a combination of Rh protein and VHA) can contribute to the restoration of J$_{Amm}$.

Interestingly, within 4 h of anteriorly-localized HEA exposure, hagfish were able to use cutaneous mechanisms to excrete ammonia, likely through Rhcg-mediated transport (see below). Furthermore, Western blot analysis suggests that there does appear to be some differential abundance of Rhcg along the length of the animal, which may explain the increase in flux rate observed along the length of hagfish in *in vitro* flux studies in Chapter 6. Localized HEA exposure likely better approximates the condition of the animal during feeding (except when hagfish fully burrow into carrion). Thus this experiment shows that hagfish have a means to excrete ammonia during exposure whereby the limited ammonia that does permeate into the organism in the branchial region is passively excreted cutaneously in the posterior region, facilitated by Rh-protein. This would then allow for longer feeding bouts with negligible buildups of ammonia.

Routes of nitrogen excretion during recovery

Upon re-entry into nominally ammonia free seawater, hagfish rapidly offload ammonia due to the restorations of outwardly directed P_{NH_3} and $E_{NH_4^+}$ gradients. Possible routes of excretion include the aforementioned $Na^+/NH_4^+(H^+)$ exchange *via* an NHE and through facilitated transport mediated *via* Rh protein and these may work in combination with one another.

In my studies looking at extrabranchial transport of ammonia (Chapter 2, 6, 8) hagfish consistently demonstrated use of cutaneous tissue to excrete ammonia. Furthermore, with the exception of post-exercised hagfish where increases in J_{Amm} were only observed in the anterior chamber/branchially, the ratio of anterior to posterior contributions (branchial to cutaneous in the case of Chapter 8) was also fairly consistent.

During either routine or post-HEA conditions, ammonia is excreted primarily (70 – 80%) *via* the gill with the remaining excretion (20 – 30%) occurring across the skin. The same arguments against significant cutaneous exchange of O_2 and CO_2 across the skin into/out of the dermal capillaries hold true for ammonia as well (i.e. thickness of dermis). Transport across skin epithelia must be facilitated given the relatively large distance between the dermal capillaries and the external environment. Staining of Rhcg demonstrated that the transport was most prominently located in close proximity to the dermal/epidermal interface and immediately adjacent to the dermal capillary network. I propose that Rh proteins provide an increased directional permeability facilitating ammonia transport across the skin between the animal and the environment.

Using *In situ* Ussing-style protocols adapted from Glover et al. (2011) I directly determined the ammonia flux capabilities of excised hagfish skin. Excised skin from control hagfish demonstrated diffusional flux of ammonia over a wide range (0-20 mmol L^{-1}) of mucosal [ammonia], simulating efflux from the animal. Furthermore, excised skin from hagfish pre-exposed to HEA had up to 4-fold higher ammonia excretion rates than skin from control animals, suggesting that hagfish regulate ammonia flux across the skin. Unfortunately, reliable protein extracts were unable to be obtained from frozen skin tissue from HEA and control fish, thus the molecular basis for this increase cannot be determined at this time.

I also demonstrated that hagfish exhibit a differentiation in flux rate along the length of the animal as rates of ammonia flux increased significantly in skin from the posterior portions of the hagfish. In this series of experiments, protein extracts could be obtained and Western blot analysis revealed that, while variable, there was differentiation of Rhcg expression along the length of the animal. Taken together, these results demonstrate that hagfish possess, utilize and regulate mechanisms within their skin for regulating ammonia excretion. Future efforts should attempt to characterize if hagfish adjust Rh expression in the skin during HEA.

Ionoregulation

As a stenohaline osmoconformer, hagfish maintain their blood osmolarity by having a plasma composition that is quite similar to seawater. Thus, hagfish do not regulate plasma Na^+ and Cl^- (Sardella et al., 2009), similar to proto-vertebrate lineages (*e.g Ciona, Amphioxus*), but distinct from lamprey (sister group within the clade) and all other vertebrates (Robertson, 1954). While hagfish do not regulate Na^+ and Cl^-, they do actively regulate plasma concentrations of the divalent ions, Ca^{2+}, Mg^{2+} and SO_4^{2-} to 30 – 50% of seawater levels (Bellamy and Chester Jones, 1961). The hormone(s) responsible for regulating these divalent ions has been actively sought for many years; however, the identity remains elusive. The corticosteroid-signaling pathway in hagfish is poorly understood; however, strong evidence exists suggesting that hagfish only possess a single corticosteroid receptor. Furthermore, *in vitro* expression studies demonstrated that this hagfish CR can be activated by several common corticosteroids, namely cortisol, 11-deoxycortisol (11-DOC), 11-deoxycorticosterone (DOC), corticosterone (Bridgham et al., 2006). The primary goal of Section 3/Chapter 7 was to assess the glucocorticoid and mineralocorticoid responses of the hagfish and identify the role, if any, of the corticosteroids previously shown to act of hagfish CR.

In Chapter 7, I show that hagfish are indeed capable of generating both glucocorticoid (as demonstrated by increases in plasma [glucose] following physical handling and during mineral/SO_4^{2-} loading) and mineralocorticoid responses (as demonstrated by the increased SO_4^{2-} excretion capacity for hagfish that received repeated infusions of SO_4^{2-}). I also show that the above corticosteroids are largely not responsible for mediating the noted glucocorticoid and mineralocorticoid responses. It is interesting

that in lamprey, the sister group to hagfish, 11-DOC is thought to be the active stress steroid while in hagfish, 11-DOC is found in biologically insignificant quantities. Thus, the active signaling steroid remains elusive; however, my results provide some interesting insights and avenues for future research.

The analysis of the hagfish transcriptome revealed some interesting results with regards to steroidogenesis in hagfish. It appears that hagfish may only possess steroidogenesis conversion enzymes that allow for synthesis from cholesterol to pregnenalone (CYP11A1 / cholesterol momooxygenase) and further to progesterone (3β-Hydroxy-Δ5-steroid dehydrogenase; or 3β-HSD). The enzymes necessary to go further into the steroid biosynthesis pathway (i.e. steroid 21-monooxygenase / CYP21, steroid 17a monooxygenase / CYP17, and steroid 11β-monooxygenase / CYP11B1) did not appear in my KEGG analysis. These KEGG results may explain why glucocorticoid and mineralocorticoid responses were not observed when injected with DOC, cortisol or corticosterone or why 11-DOC levels remained below detectable limits during handing and mineral stresses. One caveat that must be stated however is that the hagfish transcriptome was constructed using RNA from hagfish gill and slime gland, which are not steroidogenic tissues. Interestingly, Bridgeham et al. (2006) did show activation of hagfish CR with 100 nmol L^{-1} progesterone; however, results for pregnenalone were not reported. Furthermore, progesterone has been demonstrated to be present in hagfish plasma (Nishiyama et al., 2013). Future research efforts should attempt to establish whether plasma [pregnenalone] and/or [progesterone] change during similar stress tests utilized in Chapter 7. Alternatively, steroidal implants with these steroids could also be

used in order to test whether changes in either plasma glucose or sulfate handling occur following loading.

Given that hagfish do not regulate plasma $[Na^+]$ and $[Cl^-]$, but do regulate the divalent ions Ca^{2+}, Mg^{2+} and SO_4^{2-} there are limited options in ions to study ionoregulation in hagfish. Use of Ca^{2+} may lead to physiological impairments as it is used extensively in signaling. Isotopes of Mg^{2+} have very short half-lives (longest half-life: ^{28}Mg, ~21 h). SO_4^{2-} is tightly regulated across biological systems and ^{35}S has a considerable half-life of ~87 days making this divalent ion useful in the study ion hormonal control of ionoregulation and the techniques described within Chapter 7 will undoubtedly be useful in determining the active corticosteroid in hagfish.

Respiration

Characteristics for what makes a tissue a 'good' respiratory epithelia are that it: 1) is thin, 2) has a high surface area, and 3) is well vascularized. On first glance, the skin of hagfish seems poised to be excellent respiratory epithelia. The cutaneous tissue itself is relatively thin and indeed the dermal capillaries that underlie the epidermis are extensive. Finally the long and thin body-plan of the hagfish results in the cutaneous tissue having a considerable amount of surface area. Previous research examining respiration in hagfish suggests that the primary means for O_2 uptake is *via* cutaneous respiration. This adaptation would likely prove advantageous for the hagfish given how it immerses it branchial region into decaying carrion, an area that is likely to be hypoxic. These studies however, used indirect methods to come to these conclusions; and Malte and Lomholt (1998) suggest that cutaneous respiration is impractical, citing that the distance between the dermal capillaries is too thick (70-100 μm; Weinrauch et al., 2015; Welsch and Potter, 1998) and perfusion of dermal capillaries with arterial blood with a high P_{O_2}. For studies examining the branchial and extrabranchial components of ionoregulation and respiration, usage of separating chambers has been described as the "gold-Standard" (Brauner and Rombough, 2012). Thus, I utilized separating chambers in an attempt to determine the role of the skin in O_2 uptake.

In the final data section of my thesis, I definitively show that hagfish indeed do not utilize cutaneous respiration as a primary means for oxygen uptake. This does not mean that hagfish do not utilize their skin for any O_2 uptake. In this study, ~80% of total respiration occurred across the gills under control conditions and following exercise, hagfish increased their reliance on the branchial respiration to 92%. What then, should

we make of the limited cutaneous O_2 uptake that was observed, and which increased

during anteriorly-applied hypoxia? Given the aforementioned physical barriers that

prevent O_2 from diffusing into the animal, and given that the increase in posterior M_{O_2}

was not enough to supplement whole-animal M_{O_2} to routine rates, I believe that the

observed cutaneous O_2 uptake was primarily consumed by the skin itself. Welsch and

Potter (1998) argue that the functional role of dermal capillaries is to supply the

abundance of mucous cells (Blackstad, 1963; Weinrauch et al., 2015; Chapter 6) found in

the epidermal tissue with O_2 as the production/secretion of mucus is energetically costly

(Feder and Burggren, 1985). Oxygen consumption by skin tissue has also been observed

in other fishes (Kirsch and Nonnotte, 1977; Nonnotte and Kirsch, 1978). When hagfish

were introduced to hypoxia anteriorly, this limited O_2 supply to the blood so the mucus

cells, which interface with the water aspect (Chapter 6) likely obtained the available

oxygen from the normoxic posterior compartment, thus causing the increase in O_2

consumption. Regardless, while throughout this thesis and the literature the skin of

hagfish has been demonstrated to have important transport function (Clifford et al., 2014;

Glover et al., 2011; Glover et al., 2015; Schultz et al., 2014), this chapter shows that the

gills are the dominant site for M_{O_2}.

Future directions

Any great research project will end in more questions than answers and this thesis is no exception. Here I suggest several ideas and projects which will further the field on hagfish physiology.

Characterization of cloned hagfish NHEs

It is known that hagfish possess at least three members of the Na^+/H^+ exchanger (NHE; encoded by the SLC9 gene family) family of proteins (Choe et al., 2002; Edwards et al., 2001; Tresguerres et al., 2006a). In higher vertebrates, members from this family of transporters differs in tissue and cellular localizations, kinetics and roles in volume regulation, Na^+ absorption, cell growth and pH_i/pH_e (intracellular/extracellular pH) homeostasis (Demaurex and Grinstein, 1994; Orlowski, 1997; Wakabayashi et al., 1997). Since hagfish are not known to regulate plasma $[Na^+]$, the presence of these NHEs are thought to be primarily for acid/base regulation (Mallatt et al., 1987). At both the mRNA level (Edwards et al., 2001) and the protein level (Parks et al., 2007b), NHE2 been shown to be involved with recovery from plasma acidification; however, the tissue distribution of NHE2 and the involvement of other hagfish NHEs in pH recovery are still in question. Furthermore, to date, no work examining the specific functional characteristics of these transporters in hagfish has been conducted.

I spent an extensive amount of time cloning several hagfish NHES, specifically hagfish NHE2 and NHE3. Both of these isoforms are ready to be expressed into AP1 (NHE deficient) cell lines. With these cell lines, pH_i imaging techniques with the pH sensitive dye (BCECF) can be used to characterize the kinetic properties of each of these

307

transporters (*e.g.* Guffey et al., 2015). By measuring recovery in the presence of varying concentrations of known Na^+ transporter inhibitors (Amiloride, Phenamil, HMA, MIBA, DAPI, and Diminazen, Cariporide; all currently available in the Goss lab), the pharmacological inhibitor profiles for each isoform can be determined which will allow identification of isoform specific inhibitors. Pharmacokinetic profiles for hagfish NHEs can be compared to NHEs from other species including trout and dogfish and human. Given the likely involvement of NHEs in acid/base handling, a kinetic/pharmacological characterization of these isoforms with pH_i imaging will provide valuable insight for use of these inhibitors in whole-animal acid/base experiments. Furthermore, creation of hagfish-specific NHE antibodies would be a high priority (see below).

Cloning and characterization of hagfish Cl^-/HCO_3^- transporters

In my thesis I show that hagfish utilize Cl^-/HCO_3^- exchange as a mechanism for base excretion. Likely mechanisms for this transport are the anion exchangers (AE; SLC4 family of proteins; Alper, 2006) and chloride bicarbonate exchangers (CBE; from the SLC26; Alper and Sharma, 2013) family of proteins. My searches of the hagfish gill and slime gland transcriptome (available in the Goss lab) reveal several transcripts belonging to the SLC4 and SLC26 families. Utilizing qPCR techniques and tissues taken from hagfish during recovery from hypercarbia-induced hypercapnia, qPCR primers designed off of transcriptomic results for Cl^-/HCO_3^- candidate isoforms will allow for confirmation of which isoforms may be differentially expressed at the RNA level, thus giving clues to the molecular identity of the transporter responsible for Cl^-/HCO_3^- exchange. As with the NHEs (above) full cloning and characterization of transporters could be carried out measuring pH_i (intracellular pH) recovery with Cl^- replacement and with known Cl^-

/HCO_3^- inhibitors (*e.g.* DIDS). CBE/AE deficient cell lines do not yet exist, so for characterization of these proteins, *Xenopus* oocyte heterologous expression should be used. This will involve cloning the transporters of interest into a *Xenopus* expression system (*e.g.* PxT7; available in the Goss lab), followed by the generation of capped RNA (cRNA) *via* mMessage mMachine and subsequent injection into oocytes. These oocytes can be used with the pH_i imaging system (as above) using Cl^- replacement and Cl^-/HCO_3^- exchange inhibitors (*e.g.* DIDS). Again, pharmacokinetics will reveal potential isoform specificity (if any). After confirmation of isoform involvement, development of hagfish specific antibodies would be a high priority (See below).

How do hagfish MRCs regulate excrete acid and base excretion?

An investigation looking at how the single hagfish MRC type (Tresguerres et al., 2006a) changes/is remodeled during hypercapnia to modulate acid secretion and during recovery from hypercapnia-induced hypercarbia to modulate base secretion would be highly valuable. My results suggest that these cells may function as acid secreting cells initially but I also show that up-regulation/activation of base secreting mechanisms is necessary in order for the gills to excrete base as I have demonstrated that there are large increases in rates of HCO_3^- loss from plasma within 2 – 6 h recovery. These increases are mediated through up-regulation in both Cl^-/HCO_3^- exchange and CA activity. The question remains "do these single population of cells indeed control acid and base function?" A first step will be to use qPCR to identify which isoforms of each (SLC4, SLC26, CA) are involved (as above). Then using hagfish-specific antibodies if possible, or heterologous antibodies, Western analysis for V-H⁺-ATPase, NKA, CA, CBE and/or AE (see above), would inform about changes in abundance in whole-gill and membrane

fraction protein expression. Immunohistochemical analysis would demonstrate cellular localization of these transporters/enzymes. Further experimentation could also detail changes following other types of acid/base challenges.

Is recovery from hypercapnia-induced hypercarbia via CA-mediated CO_2 loss common across lineages?

To my knowledge, the finding that hagfish primarily utilize a CA-mediated mechanism to facilitate loss of plasma HCO_3^- following severe hypercarbia is a novel finding that has not been described in any other animal. In hypercapnia studies, I have found that recovery time-points are infrequently measured and when used, there is only a single time-point at 24 h. I am curious to know if the primary CA-mediated mechanism that hagfish use to restore HCO_3^- levels is specific to hagfish or is commonly observed across species. The hypercapnia tolerance in hagfish is due in part to their ability to raise plasma $[HCO_3^-]$ to levels never observed before in any other organism (Baker et al., 2015). Other organisms demonstrated to raise plasma/hemolymph $[HCO_3^-]$ to a high degree are the blue crab (*Callinectes sapidu*) and the channel catfish (*Ictalurus punctatus*). The question that remains is "are the mechanisms employed by the hagfish for hypercarbic recovery common to other organisms that are capable of mounting effective HCO_3^- responses, or is this a general trait?" Studies similar to those conducted in Chapter 3 but using select model species will prove valuable in answering these questions. Similarly, the selective use of permeable/impermeable CA inhibitors will also identify if the CAs involved are intracellular or plasma accessible. Utilizing techniques described above in (*How do hagfish MRCs regulate excrete acid and base excretion?*)

further characterization of recovery responses will be possible across a broad selection of organisms.

How are hagfish capable of preventing ammonia uptake during localized ammonia exposure?

In Chapter 6, I provide evidence that hagfish are capable of preventing loading of ammonia across the gill epithelial during localized HEA exposure. This impairment of ammonia entry occurs despite considerable inwardly directed P_{NH_3} and $E_{NH_4^+}$ gradients (Chapter 5). The question that remains is "How are hagfish capable of preventing uptake of ammonia during HEA exposure?"

I suggest that this ability arises from a reduction in ventilation in that hagfish simply stop ventilating during HEA exposure. Given that hagfish are tolerant of hypoxia, "holding their breath" would come of little consequence in a physiological sense. In Chapter 8, I show that the gill is the primary route of oxygen uptake, ruling out previously held notions that cutaneous uptake was the main mode of oxygen acquisition. With this knowledge, respirometry studies with hagfish during control and HEA conditions could be conducted using oxygen uptake as a surrogate for ventilation. If ventilation is reduced, we would expect to see differences between hagfish during control and HEA conditions. An alternative and preferred approach would be to utilize pressure or flow transducers in a similar manner as (Perry et al., 2009) to capture true ventilation.

Platitudes

Hagfishology presents exciting opportunities to study evolution, adaptation and comparative physiology. The phyletically ancient hagfish holds many physiological peculiarities to study. Future research efforts involving these extraordinary and beautiful creatures should endeavor to further describe the adaptations and mechanisms they possess to survive and thrive in their demersal and challenging conditions.

References

Adam, H. (1960). Different Types of Body Movement in the Hagfish, Myxine glutinosa L. *Nature* **188**, 595–596.

Alper, S. L. (2006). Molecular physiology of SLC4 anion exchangers. *Experimental Physiology* **91**, 153–161.

Alper, S. L. and Sharma, A. K. (2013). The SLC26 gene family of anion transporters and channels. *Mol. Aspects Med.* **34**, 494–515.

Alt, J. M., Stolte, H., Eisenbach, G. M. and Walvig, F. (1981). Renal electrolyte and fluid excretion in the Atlantic hagfish *Myxine glutinosa*. *J. Exp. Biol.* **91**, 323–330.

Auster, P. J. and Barber, K. (2006). Atlantic hagfish exploit prey captured by other taxa. *J. Fish Biol.* **68**, 618–621.

Axelsson, M., Farrell, A. P. and Nilsson, S. (1990). Effects of hypoxia and drugs on the cardiovascular dynamics of the Atlantic hagfish *Myxine glutinosa*. *J. Exp. Biol.* **151**, 297–316.

Baker, D. W., Sardella, B., Rummer, J. L., Sackville, M. and Brauner, C. J. (2015). Hagfish: Champions of CO_2 tolerance question the origins of vertebrate gill function. *Sci. Rep.* **5**, 11182.

Baldwin, J. and Davison, W. (1989). Properties of the muscle and heart lactate dehydrogenases of the New Zealand hagfish, *Eptatretus cirrhatus*: Functional and evolutionary implications. *J. Exp. Biol.* **250**, 135–139.

Ballantyne, J. S. (2001). Amino acid metabolism. In *Fish Physiology: Nitrogen Excretion* (eds. Wright, P. A. and Anderson, P., pp. 77–107. Fish physiology.

Bardack, D. (1991). First fossil hagfish (Myxinoidea): a record from the Pennsylvanian of Illinois. *Science* **254**, 701–703.

Bartels (1984). Orthogonal arrays of particles in the gill epithelium of the Atlantic hagfish, Myxine glutinosa. *Cell. Tissue. Res.* **238**, 657–659.

Bartels (1988). Intercellular junctions in the gill epithelium of the Atlantic hagfish, *Myxine glutinosa. Cell. Tissue. Res.* **254**, 573–583.

Bartels, H. (1985). Assemblies of linear arrays of particles in the apical plasma membrane of mitochondria-rich cells in the gill epithelium of the Atlantic hagfish (*Myxine glutinosa*). *Anat. Rec.* **211**, 229–238.

Bellamy, D. and Chester Jones, I. (1961). Studies on *Myxine glutinosa*—I. The chemical composition of the tissues. *Comp. Biochem. Physiol. A* **3**, 175–183.

Bergmeyer, H. U. ed. (1983). *Methods of Enzymatic Analysis*. New York: Academic Press.

Bertrand, S., Belgacem, M. R. and Escriva, H. (2011). Nuclear hormone receptors in chordates. *Mol. Cell. Endocrinol.* **334**, 67–75.

Blackstad, J. W. (1963). The skin and the slime glands. In *The Biology of Myxine* (eds. Brodal, A. and Fänge, R., pp. 195–230. Oslo: Universitetsforlaget.

Boron, W. F. (2004). Regulation of intracellular pH. *Advances in Physiology Education*

28, 160–179.

Boutilier, R. G., Heming, T. A. and Iwama, G. K. (1984). Appendix: Physicochemical parameters for use in fish respiratory physiology. In *Gills - Anatomy, Gas Transfer, and Acid-Base Regulation* (eds. Hoar, W. S. and Randall, D., pp. 403–430. Orlando: Elsevier.

Braun, M. H. and Perry, S. F. (2010). Ammonia and urea excretion in the Pacific hagfish *Eptatretus stoutii*: Evidence for the involvement of Rh and UT proteins. *Comp. Biochem. Physiol. A* **157**, 405–415.

Brauner, C. J. and Baker, D. W. (2009). Patterns of Acid–Base Regulation During Exposure to Hypercarbia in Fishes. In *Cardio-Respiratory Control in Vertebrates*, pp. 43–63. Berlin, Heidelberg: Springer Berlin Heidelberg.

Brauner, C. J. and Berenbrink, M. (2007). Gas Transport and Exchange. In *Fish Physiology: Primitive Fishes*, pp. 213–282. Elsevier.

Brauner, C. J. and Rombough, P. J. (2012). Ontogeny and paleophysiology of the gill: New insights from larval and air-breathing fish. *Respir. Physiol. Neurobiol.* **184**, 293–300.

Bridgham, J. T., Carroll, S. M. and Thornton, J. W. (2006). Evolution of hormone-receptor complexity by molecular exploitation. *Science* **312**, 97–101.

Bridgham, J. T., Ortlund, E. A. and Thornton, J. W. (2009). An epistatic ratchet constrains the direction of glucocorticoid receptor evolution. *Nature* **461**, 515–519.

Bucking, C. and Wood, C. M. (2008). The alkaline tide and ammonia excretion after voluntary feeding in freshwater rainbow trout. *J. Exp. Biol.* **211**, 2533–2541.

Bucking, C., Fitzpatrick, J. L., Nadella, S. R. and Wood, C. M. (2009). Post-prandial metabolic alkalosis in the seawater-acclimated trout: the alkaline tide comes in. *J. Exp. Biol.* **212**, 2159–2166.

Bucking, C., Glover, C. N. and Wood, C. M. (2011). Digestion under duress: Nutrient acquisition and metabolism during hypoxia in the Pacific hagfish. *Physiol. Biochem. Zool.* **84**, 607–617.

Burggren, W., Johansen, K. and McMahon, B. (1985). Respiration in Phyletically Ancient Fishes. In *Evolutionary Biology of Primitive Fishes*, pp. 217–252. Boston, MA: Springer US.

Bury, N. R., Clifford, A. M. and Goss, G. G. (2015). Corticosteroid signalling pathways in hagfish. In *Hagfish Biology* (eds. Edwards, S. L. and Goss, G. G., pp. 257–276. Boca Raton: CRC press.

Callard, G. V., Tarrant, A. M., Novillo, A., Yacci, P., Ciaccia, L., Vajda, S., Chuang, G. Y., Kozakov, D., Greytak, S. R., Sawyer, S., et al. (2011). Evolutionary origins of the estrogen signaling system: Insights from amphioxus. *J. Steroid Biochem. Mol. Biol.* **127**, 176–188.

Cameron, J. N. (1978). Effects of hypercapnia on blood acid-base status, NaCl fluxes, and trans-gill potential in freshwater blue crabs, *Callinectes sapidus*. *J. Comp. Physiol. B* **123**, 137–141.

Cameron, J. N. and Heisler, N. (1983). Studies of ammonia in the Rainbow trout: Physico-chemical parameters, acid-base behaviour and respiratory clearance. *J. Exp. Biol.* **105**, 107–125.

Cameron, J. N. and Iwama, G. K. (1987). Compensation of progressive hypercapnia in channel catfish and blue crabs. *J. Exp. Biol.* **133**, 183–197.

Carter, D. O., Yellowlees, D. and Tibbett, M. (2007). Cadaver decomposition in terrestrial ecosystems. *Naturwissenschaften* **94**, 12–24.

Castresana, J. (2000). Selection of conserved blocks from multiple alignments for their use in phylogenetic analysis. *Mol. Biol. Evol.* **17**, 540–552.

Chasiotis, H. and Kelly, S. P. (2008). Occludin immunolocalization and protein expression in goldfish. *J. Exp. Biol.* **211**, 1524–1534.

Chew, S. F., Jin, Y. and Ip, Y. K. (2001). The Loach *Misgurnus anguillicaudatus* reduces amino acid catabolism and accumulates alanine and glutamine during aerial exposure. *Physiol. Biochem. Zool.* **74**, 226–237.

Chew, S. F., Wong, M. Y., Tam, W. L. and Ip, Y. K. (2003). The snakehead *Channa asiatica* accumulates alanine during aerial exposure, but is incapable of sustaining locomotory activities on land through partial amino acid catabolism. *J. Exp. Biol.* **206**, 693–704.

Choe, K. P., Edwards, S., Morrison-Shetlar, A. I., Toop, T. and Claiborne, J. B. (1999). Immunolocalization of Na^+/K^+-ATPase in mitochondrion-rich cells of the

atlantic hagfish (*Myxine glutinosa*) gill. *Comp. Biochem. Physiol. A* **124**, 161–168.

Choe, K. P., Morrison-Shetlar, A. I., Wall, B. P. and Claiborne, J. B. (2002).
Immunological detection of Na^+/H^+ exchangers in the gills of a hagfish, *Myxine glutinosa*, an elasmobranch, *Raja erinacea*, and a teleost, *Fundulus heteroclitus*. *Comp. Biochem. Physiol. A* **131**, 375–385.

Choe, K. P., O'Brien, S., Evans, D. H., Toop, T. and Edwards, S. L. (2004).
Immunolocalization of Na^+/K^+-ATPase, carbonic anhydrase II, and vacuolar H^+-ATPase in the gills of freshwater adult lampreys, *Geotria australis*. *J. Exp. Zool. A* **301A**, 654–665.

Claiborne, J. B., Edwards, S. L. and Morrison-Shetlar, A. I. (2002). Acid-base regulation in fishes: cellular and molecular mechanisms. *J. Exp. Zool.* **293**, 302–319.

Clark, A. J. and Summers, A. P. (2007). Morphology and kinematics of feeding in hagfish: possible functional advantages of jaws. *J. Exp. Biol.* **210**, 3897–3909.

Clifford, A. M., Goss, G. G. and Wilkie, M. P. (2015a). Adaptations of a deep sea scavenger: High ammonia tolerance and active NH_4^+ excretion by the Pacific hagfish (*Eptatretus stoutii*). *Comp. Biochem. Physiol. A* **182C**, 64–74.

Clifford, A. M., Goss, G. G., Roa, J. N. and Tresguerres, M. (2015b). A and ionic regulation in hagfish. In *Hagfish Biology* (eds. Edwards, S. L. and Goss, G. G., pp. 277–298. Boca Raton, Fl: CRC Press.

Clifford, A. M., Guffey, S. C. and Goss, G. G. (2014). Extrabranchial mechanisms of

systemic pH recovery in hagfish (*Eptatretus stoutii*). *Comp. Biochem. Physiol. A* **168**, 82–89.

Close, D. A., Yun, S.-S., McCormick, S. D., Wildbill, A. J. and Li, W. (2010). 11-deoxycortisol is a corticosteroid hormone in the lamprey. *Proc. Natl. Acad. Sci. U.S.A.* **107**, 13942–13947.

Collins, M. A., Yau, C., Nolan, C. P., Bagley, P. M. and Priede, I. G. (1999). Behavioural observations on the scavenging fauna of the Patagonian slope. *J. Mar. Biol. Assoc. UK* **79**, 963–970.

Cooper, A. J. and Plum, F. (1987). Biochemistry and physiology of brain ammonia. *Physiol. Rev.* **67**, 440–519.

Cox, G. K., Sandblom, E., Richards, J. G. and Farrell, A. P. (2011). Anoxic survival of the Pacific hagfish (*Eptatretus stoutii*). *J. Comp. Physiol. B* **181**, 361–371.

Crocker, C. E. and Cech, J. J., Jr (1998). Effects of hypercapnia on blood-gas and acid-base status in the white sturgeon, *Acipenser transmontanus*. *J. Comp. Physiol. B* **168**, 50–60.

Crocker, C. L. (1967). Rapid determination of urea nitrogen in serum or plasma without deproteinization. *Am. J. Med. Technol.* **33**, 361–365.

Currie, S. and Edwards, S. L. (2010). The curious case of the chemical composition of hagfish tissues-50 years on. *Comp. Biochem. Physiol. A* **157**, 111–115.

Davenport, H. W. (1974). *The ABC of Acid-Base Chemistry: The Elements of*

Physiological Blood-Gas Chemistry for Medical Students and Physicians. 6 ed. Chicago, IL: University of Chicago Press.

Davison, W., Baldwin, J., Davie, P. S., Forster, M. E. and Satchell, G. H. (1990). Exhausting exercise in the hagfish, *Eptatretus cirrhatus*: The anaerobic potential and the appearance of lactic acid in the blood. *Comp. Biochem. Physiol. A* **95**, 585–589.

Demaurex, N. and Grinstein, S. (1994). Na^+/H^+ antiport: modulation by ATP and role in cell volume regulation. *J. Exp. Biol.* **196**, 389–404.

Dobson, G. P. and Hochachka, P. W. (1987). Role of glycolysis in adenylate depletion and repletion during work and recovery in teleost white muscle. *J. Exp. Biol.* **129**, 125–140.

Doyle, W. L. and Gorecki, D. (1961). The so-called chloride cell of the fish gill. *Physiol. Zool.* **34**, 81–85.

Drazen, J. C., Yeh, J., Friedman, J. and Condon, N. (2011). Metabolism and enzyme activities of hagfish from shallow and deep water of the Pacific Ocean. *Comp. Biochem. Physiol. A* **159**, 182–187.

Dymowska, A. K., Hwang, P.-P. and Goss, G. G. (2012). Structure and function of ionocytes in the freshwater fish gill. *Respir. Physiol. Neurobiol.* **184**, 282–292.

Edgar, R. C. (2004). MUSCLE: multiple sequence alignment with high accuracy and high throughput. *Nucl. Acids Res.* **32**, 1792–1797.

Edsall, J. T. (1968). Carbon dioxide, carbonic acid and bicarbonate ion: Physical

properties and kinetics of interconversion. In *CO₂: Chemical, Biochemical, and Physiological Aspects*, pp. 15–27. NASA SP#188.

Edwards, S. L. and Marshall, W. S. (2013). Principles and patterns of osmoregulation and euryhalinity in fish. In *Fish Physiology: Euryhaline Fishes* (eds. McCormick, S. D., Farrell, A. P., and Brauner, C. J., pp. 1–45. San Diego: Fish physiology.

Edwards, S. L., Arnold, J., Blair, S. D., Pray, M., Bradley, R., Erikson, O. and Walsh, P. J. (2015). Ammonia excretion in the Atlantic hagfish (*Myxine glutinosa*) and responses of an Rhc glycoprotein. *Am. J. Physiol. Regul. Integr. Comp. Physiol.* **308**, R769–78.

Edwards, S. L., Claiborne, J. B., Morrison-Shetlar, A. I. and Toop, T. (2001). Expression of Na^+/H^+ exchanger mRNA in the gills of the Atlantic hagfish (*Myxine glutinosa*) in response to metabolic acidosis. *Comp. Biochem. Physiol. A* **130**, 81–91.

Elger, M. and Hentschel, H. (1983). Morphological evidence for ionocytes in the gill epithelium of the hagfish Myxine glutinosa. *Bull. Mt. Desert Island Biol. Lab.* **23**, 4–8.

Endeward, V., Cartron, J. P., Ripoche, P. and Gros, G. (2006). Red cell membrane CO_2 permeability in normal human blood and in blood deficient in various blood groups, and effect of DIDS. *Transfusion Clinique et Biologique* **13**, 123–127.

Esbaugh, A. J., Gilmour, K. M. and Perry, S. F. (2009). Membrane-associated carbonic anhydrase in the respiratory system of the Pacific hagfish (Eptatretus stouti). *Respir. Physiol. Neurobiol.* **166**, 107–116.

Evans, D. H. (1984). Gill Na$^+$/H$^+$ and Cl$^-$/HCO$_3^-$ exchange systems evolved before the vertebrates entered fresh water. *J. Exp. Biol.* **113**, 465–469.

Evans, D. H. (1982). Mechanisms of acid extrusion by two marine fishes: The teleost, *Opsanus beta*, and the elasmobranch, *Squalus acanthias*. *J. Exp. Biol.* **97**, 289–299.

Evans, D. H., Piermarini, P. M. and Choe, K. P. (2005). The multifunctional fish gill: Dominant site of gas exchange, osmoregulation, acid-base regulation, and excretion of nitrogenous waste. *Physiol. Rev.* **85**, 97–177.

Feder, M. E. and Burggren, W. W. (1985). Cutaneous gas exchange in vertebrates: design, patterns, control and implications. *Biol. Rev.* **60**, 1–45.

Felipo, V. and Butterworth, R. F. (2002). Neurobiology of ammonia. *Prog. Neurobiol.* **67**, 259–279.

Fernholm, B. (1998). Hagfish Systematics. In *The Biology of Hagfishes*, pp. 33–44. Dordrecht: Springer Netherlands.

Forster, M. E. (1989). Performance of the heart of the hagfish, *Eptatretus cirrhatus*. *Fish Physiol. Biochem.* **6**, 327–331.

Forster, M. E. (1990). Confirmation of the low metabolic rate of hagfish. *Comparative Biochemistry and Physiology Part A: Physiology* **96**, 113–116.

Forster, M. E., Axelsson, M., Farrell, A. P. and Nilsson, S. (2011). Cardiac function and circulation in hagfishes. *Canadian Journal of Zoology* **69**, 1985–1992.

Forster, M. E., Davison, W., Axelsson, M. and Farrell, A. P. (1992). Cardiovascular

responses to hypoxia in the hagfish, *Eptatretus cirrhatus*. *Resp. Physiol.* **88**, 373–386.

Forster, M. E., Russell, M. J., Hambleton, D. C. and Olson, K. R. (2001). Blood and Extracellular Fluid Volume in Whole Body and Tissues of the Pacific Hagfish, *Eptatretus stoutii*. *Physiol. Biochem. Zool.* **74**, 750–756.

Foskett, J. and Scheffey, C. (1982). The chloride cell: definitive identification as the salt-secretory cell in teleosts. *Science* **215**, 164–166.

Frick, N. T. and Wright, P. A. (2002). Nitrogen metabolism and excretion in the mangrove killifish *Rivulus marmoratus* II. Significant ammonia volatilization in a teleost during air-exposure. *J. Exp. Biol.* **205**, 91–100.

Galtier, N., Gouy, M. and Gautier, C. (1996). SEAVIEW and PHYLO_WIN: two graphic tools for sequence alignment and molecular phylogeny. *Comput. Appl. Biosci.* **12**, 543–548.

Glover, C. and Bucking, C. (2015). Feeding, digestion and nutrient absorption in hagfish. In *Hagfish Biology* (eds. Edwards, S. L. and Goss, G. G., pp. 299–320. Boca Raton: CRC press.

Glover, C. N., Blewett, T. A. and Wood, C. M. (2015). Novel route of toxicant exposure in an ancient extant vertebrate: nickel uptake by hagfish skin and the modifying effects of slime. *Environ. Sci. Technol.* **49**, 1896–1902.

Glover, C. N., Bucking, C. and Wood, C. M. (2013). The skin of fish as a transport

epithelium: a review. *J. Comp. Physiol. B* **183**, 877–891.

Glover, C., Bucking, C. and Wood, C. (2011). Adaptations to *in situ* feeding: novel nutrient acquisition pathways in an ancient vertebrate. *Proc. R. Soc. B* **278**, 3096–3101.

Goss, G. G. and Wood, C. M. (1990a). Na$^+$ and Cl$^-$ uptake kinetics, diffusive effluxes and acidic equivalent fluxes across the gills of Rainbow Trout: I. Responses to environmental hyperoxia. *J. Exp. Biol.* **152**, 521–547.

Goss, G. G. and Wood, C. M. (1990b). Na$^+$ and Cl$^-$ uptake kinetics, diffusive effluxes and acidic equivalent fluxes across the gills of Rainbow Trout: II. Responses to bicarbonate infusion. *J. Exp. Biol.* **152**, 549–571.

Goss, G. G. and Wood, C. M. (1991). Two-substrate kinetic analysis: a novel approach linking ion and acid-base transport at the gills of freshwater trout, *Oncorhynchus mykiss*. *J. Comp. Physiol. B* **161**, 635–646.

Goss, G., Gilmour, K., Hawkings, G., Brumbach, J. H., Huynh, M. and Galvez, F. (2011). Mechanism of sodium uptake in PNA negative MR cells from rainbow trout, *Oncorhynchus mykiss* as revealed by silver and copper inhibition. *Comp. Biochem. Physiol. A* **159**, 234–241.

Gouy, M., Guindon, S. and Gascuel, O. (2010). SeaView version 4: A multiplatform graphical user interface for sequence alignment and phylogenetic tree building. *Mol. Biol. Evol.* **27**, 221–224.

Griffith, R. W. (1991). Guppies, toadfish, lungfish, coelacanths and frogs: a scenario for the evolution of urea retention in fishes. *Environ. Biol. Fish.* **32**, 199–218.

Grosell, M. (2006). Intestinal anion exchange in marine fish osmoregulation. *J. Exp. Biol.* **209**, 2813–2827.

Grosell, M. and Genz, J. (2006). Ouabain-sensitive bicarbonate secretion and acid absorption by the marine teleost fish intestine play a role in osmoregulation. *Am. J. Physiol. Regul. Integr. Comp. Physiol.* **291**, R1145–56.

Guffey, S. C. and Goss, G. G. (2014). Time course of the acute response of the North Pacific spiny dogfish shark (*Squalus suckleyi*) to low salinity. *Comp. Biochem. Physiol. A* **171**, 9–15.

Guffey, S. C., Fliegel, L. and Goss, G. G. (2015). Cloning and characterization of Na$^+$/H$^+$ Exchanger isoforms NHE2 and NHE3 from the gill of Pacific dogfish *Squalus suckleyi*. *Comp. Biochem. Physiol. B* **188**, 46–53.

Gustafson, G. (1935). On the biology of *Myxine glutinosa*. *Arkiv for Zoologi* **28**, 1–8.

Hans, M. and Tabencka, Z. (1938). Über die Blutgefässe der Haut *Myxine glutinosa* L. *Bull. Acad. Pol. Sci.* **Ser. BII Zool**, 69–77.

Hardisty, M. W. (1979). *Biology of Cyclostomes*. London: Chapman and Hall.

Heimberg, A. M., Cowper-Sal-lari, R., Sémon, M., Donoghue, P. C. J. and Peterson, K. J. (2010). microRNAs reveal the interrelationships of hagfish, lampreys, and gnathostomes and the nature of the ancestral vertebrate. *Proc. Natl. Acad. Sci. U.S.A.*

107, 19379–19383.

Heisler, N. (1986a). Buffering and transmembrane ion transfer processes. In *Acid-Base Regulation in Animals* (ed. Heisler, N., pp. 3–47. Amsterdam: Elsevier Science Publishers bv.

Heisler, N. (1986b). Acid-Base regulation in fishes. In *Acid-Base Regulation in Animals* (ed. Heisler, N., pp. 309–356. Amsterdam.

Heisler, N. and Weitz, A. M. (1976). Extracellular and intracellular pH with changes of temperature in the dogfish *Scyliorhinus stellaris*. *Respir. Physiol. Neurobiol.* **26**, 249–263.

Henry, R. P. and Heming, T. A. (1998). Carbonic anhydrase and respiratory gas exchange. In *Fish Physiology: Fish Respiration* (eds. Perry, S. F. and Tufts, B., pp. 75–111. San Diego, CA: Fish physiology.

Henry, R. P., Lucu, Č., Onken, H. and Weihrauch, D. (2012). Multiple functions of the crustacean gill: osmotic/ionic regulation, acid-base balance, ammonia excretion, and bioaccumulation of toxic metals. *Front Physiol* **3**, 431.

Hirose, K., Tamaoki, B., Fernholm, B. and Kobayashi, H. (1975). In vitro bioconversions of steroids in the mature ovary of the hagfish, *Eptatretus burgeri*. *Comp. Biochem. Physiol. B* **51**, 403–408.

Holland, N. D. and Chen, J. (2001). Origin and early evolution of the vertebrates: New insights from advances in molecular biology, anatomy, and palaeontology. *Bioessays*

23, 142–151.

Huang, C.-H. and Peng, J. (2005). Evolutionary conservation and diversification of Rh family genes and proteins. *Proc. Natl. Acad. Sci. U.S.A.* **102**, 15512–15517.

Hung, C. Y. C., Tsui, K. N. T., Wilson, J. M., Nawata, C. M., Wood, C. M. and Wright, P. A. (2007). Rhesus glycoprotein gene expression in the mangrove killifish *Kryptolebias marmoratus* exposed to elevated environmental ammonia levels and air. *J. Exp. Biol.* **210**, 2419–2429.

Hwang, P.-P. and Lee, T.-H. (2007). New insights into fish ion regulation and mitochondrion-rich cells. *Comp. Biochem. Physiol. A* **148**, 479–497.

Hwang, P.-P., Lee, T.-H. and Lin, L.-Y. (2011). Ion regulation in fish gills: recent progress in the cellular and molecular mechanisms. *Am. J. Physiol. Regul. Integr. Comp. Physiol.* **301**, R28–47.

Idler, D. R. and Burton, M. P. (1976). The pronephroi as the site of presumptive interrenal cells in the hagfish *Myxine glutinosa* L. *Comp. Biochem. Physiol. A* **53**, 73–77.

Ip, Y. K., Chew, S. F. and Randall, D. J. (2001a). Ammonia toxicity, tolerance, and excretion. In *Fish Physiology: Nitrogen Excretion* (eds. Wright, P. A. and Anderson, P., pp. 109–148. New York: Academic Press.

Ip, Y. K., Randall, D. J., Kok, T. K. T., Barzaghi, C., Wright, P. A., Ballantyne, J. S., Wilson, J. M. and Chew, S. F. (2004). The giant mudskipper *Periophthalmodon*

schlosseri facilitates active NH_4^+ excretion by increasing acid excretion and decreasing NH_3 permeability in the skin. *J. Exp. Biol.* **207**, 787–801.

Ip, Y. K., Tay, A. S. L., Lee, K. H. and Chew, S. F. (2010). Strategies for surviving high concentrations of environmental ammonia in the swamp eel *Monopterus albus*. *Physiol. Biochem. Zool.* **77**, 390–405.

Ip, Y., Chew, S., Leong, I., Jin, Y., Lim, C. and Wu, R. (2001b). The sleeper Bostrichthys sinensis (Family Eleotridae) stores glutamine and reduces ammonia production during aerial exposure. *J. Comp. Physiol. B* **171**, 357–367.

Janssens, P. A. and Cohen, P. P. (1968). Biosynthesis of urea in the estivating African lungfish and in *Xenopus laevis* under conditions of water-shortage. *Comp. Biochem. Physiol. A* **24**, 887–898.

Janvier, P. (2007). Living primitive fishes and fishes from deep time. In *Fish Physiology: Primitive Fishes*, pp. 1–51. San DIego: Elsevier.

Janvier, P. (2010). microRNAs revive old views about jawless vertebrate divergence and evolution. *Proc. Natl. Acad. Sci. U.S.A.* **107**, 19137–19138.

Jensen, D. (1966). The hagfish. *Sci. Am.* **214**, 82–90.

Jow, L. Y., Chew, S. F. and Lim, C. B. (1999). The marble goby *Oxyeleotris marmoratus* activates hepatic glutamine synthetase and detoxifies ammonia to glutamine during air exposure. *J. Exp. Biol.* **202**, 237–245.

Karnaky, K. J. (1986). Structure and Function of the Chloride Cell of *Fundulus*

heteroclitus and Other Teleosts. *Integr. Comp. Biol.* **26**, 209–224.

Karnaky, K. J. (1998). Osmotic and ionic regulation. In *The Physiology of Fishes*, pp. 157–176. Boca Raton, FL: CRC Press.

Katoh, F., Tresguerres, M., Lee, K. M., Kaneko, T., Aida, K. and Goss, G. G. (2006). Cloning of rainbow trout SLC26A1: involvement in renal sulfate secretion. *Am. J. Physiol. Regul. Integr. Comp. Physiol.* **290**, R1468–78.

Katsu, Y., Kubokawa, K., Urushitani, H. and Iguchi, T. (2013). Estrogen-dependent transactivation of amphioxus steroid hormone receptor *via* both estrogen and androgen response elements. *Endocrinology* **151**, 639–648.

Keay, J. and Thornton, J. W. (2009). Hormone-activated estrogen receptors in annelid invertebrates: implications for evolution and endocrine disruption. *Endocrinology* **150**, 1731–1738.

Keay, J., Bridgham, J. T. and Thornton, J. W. (2006). The *Octopus vulgaris* estrogen receptor is a constitutive transcriptional activator: Evolutionary and functional implications. *Endocrinology* **147**, 3861–3869.

Kime, D. E. and Hews, E. A. (1980). Steroid biosynthesis by the ovary of the hagfish *Myxine glutinosa. Gen. Comp. Endocrinol.* **42**, 71–75.

Kime, D. E., Hews, E. A. and Rafter, J. (1980). Steroid biosynthesis by testes of the hagfish *Myxine glutinosa. Gen. Comp. Endocrinol.* **41**, 8–13.

Kirsch, R. and Nonnotte, G. (1977). Cutaneous respiration in three freshwater teleosts.

Respir. Physiol. Neurobiol. **29**, 339–354.

Laemmli, U. K. (1970). Cleavage of structural proteins during the assembly of the head of bacteriophage T4. *Nature* **227**, 680–685.

Lametschwandtner, A., Weiger, T., Lametschwandtner, U., Georgieva-Hanson, V., Patzner, R. A. and Adam, H. (1989). The vascularization of the skin of the Atlantic hagfish, *Myxine glutinosa* L. as revealed by scanning electron microscopy of the vascular corrosion casts. *Scanning Microsc.* **3**, 305–314.

Laurent, P., Wilkie, M. P., Chevalier, C. and Wood, C. M. (2000). The effect of highly alkaline water (pH 9.5) on the morphology and morphometry of chloride cells and pavement cells in the gills of the freshwater rainbow trout: relationship to ionic transport and ammonia excretion. *Can. J. Zool* **78**, 307–319.

Le, S. Q. and Gascuel, O. (2008). An improved general amino acid replacement matrix. *Mol. Biol. Evol.* **25**, 1307–1320.

Lerman, A. and Stumm, W. (1989). CO_2 storage and alkalinity trends in lakes. *Water Res.* **23**, 139–146.

Lesser, M. P., Martini, F. H. and Heiser, J. B. (1996). Ecology of the hagfish, *Myxine glutinosa* L. in the Gulf of Maine I. Metabolic rates and energetics. *J. Exp. Mar. Biol. Ecol.* **208**, 215–225.

Levi, G., Morisi, G., Colettp, A. and Catanzaro, R. (1974). Free amino acids in fish brain: Normal levels and changes upon exposure to high ammonia concentrations *in*

vivo, and upon incubation of brain slices. *Comp. Biochem. Physiol. A* **49**, 623–636.

Levine, S., Franki, N. and Hays, R. M. (1973a). A saturable, vasopressin-sensitive carrier for urea and acetamide in the toad bladder epithelial cell. *J. Clin. Invest.* **52**, 2083–2086.

Levine, S., Franki, N. and Hays, R. M. (1973b). Effect of Phloretin on water and solute movement in the toad bladder. *J. Clin. Invest.* **52**, 1435–1442.

Lin, L.-Y., Horng, J.-L., Kunkel, J. G. and Hwang, P.-P. (2006). Proton pump-rich cell secretes acid in skin of zebrafish larvae. *Am. J. Physiol. Cell Physiol.* **290**, C371–8.

Mallatt, J. and Paulsen, C. (1986). Gill ultrastructure of the Pacific hagfish *Eptatretus stouti*. *Am. J. Anat.* **177**, 243–269.

Mallatt, J., Conley, D. M. and Ridgway, R. L. (1987). Why do hagfish have gill "chloride cells" when they need not regulate plasma NaCl concentration? **65**, 1956–1965.

Malte, H. and Lomholt, J. P. (1998). Ventilation and gas exchange. In *The Biology of Hagfishes* (eds. Jørgensen, J. M., Lomholt, J. P., Weber, R. E., and Malte, H., pp. 223–234. Dordrecht: Springer Netherlands.

Manwell, C. (1963). The blood proteins of cyclostomes. A study in phylogenetic and ontogenetic biochemistry. In *The Biology of Myxine* (eds. Brodal, A. and Fänge, R., pp. 372–455. Oslo: Universitetsforlaget.

Marini, A. M. and Urrestarazu, A. (1997). The Rh (Rhesus) blood group polypeptides are related to NH_4^+ transporters. *Trends in Biochem. Sci.* **22**, 460–461.

Martini, F. H. (1998). The ecology of hagfishes. In *The Biology of Hagfishes*, pp. 57–77. Dordrecht: Springer Netherlands.

McCarthy, J. E. and Conte, F. P. (1966). Determination of volume of vascular and extravascular fluids in pacific hagfish *Eptatretus stoutii* (Lockington).p. 605. American Zoologist.

McDonald, D. G., Cavdek, V., Calvert, L. and Milligan, C. L. (1991). Acid-base regulation in the Atlantic hagfish *Myxine glutinosa. J. Exp. Biol.* **161**, 201–215.

McInerney, J. E. (1974). Renal sodium reabsorption in the hagfish, *Eptatretus stouti. Comp. Biochem. Physiol. A* **49**, 273–280.

McInerney, J. E. and Evans, D. O. (1970). Habitat Characteristics of the Pacific Hagfish, *Polistotrema stouti. J. Fish. Res. Bd. Can.* **27**, 966–968.

Mecke, D. (1985). L-glutamine, colorimetric method with glutamine synthetase. *Methods of enzymatic analysis* **8**, 364–369.

Mehrbach, C. (1973). Measurement of the apparent dissociation constants of carbonic acid in seawater at atmospheric pressure.

Miller, M. A., Pfeiffer, W. and Schwartz, T. (2010). Creating the CIPRES Science Gateway for inference of large phylogenetic trees. *Proceedings of the Gateway Computing Environments Workshop (GCE). 14 November 2010. New Orleans, LA.*

1–8.

Millero, F. J., Lee, K. and Roche, M. (1998). Distribution of alkalinity in the surface waters of the major oceans. *Mar. Chem.* **60**, 111–130.

Mommsen, T. P. and Walsh, P. J. (1989). Evolution of urea synthesis in vertebrates: the piscine connection. *Science* **243**, 72–75.

Mommsen, T. P. and Walsh, P. J. (1992). Biochemical and environmental perspectives on nitrogen metabolism in fishes. *Experientia* **48**, 583–593.

Morris, R. (1965). Studies on salt and water balance in *Myxine glutinosa* (L.). *J. Exp. Biol.* **42**, 359–371.

Munger, R. S., Reid, S. D. and Wood, C. M. (1991). Extracellular fluid volume measurements in tissues of the rainbow trout (*Oncorhynchus mykiss*) in vivo and their effects on intracellular pH and ion calculations. *Fish Physiol. Biochem.* **9**, 313–323.

Munz, F. W. and McFarland, W. N. (1964). Regulatory function of a primitive vertebrate kidney. *Comp. Biochem. Physiol. A* **13**, 381–400.

Munz, F. W. and Morris, R. W. (1965). Metabolic rate of the hagfish, *Eptatretus stoutii* (Lockington) 1878. *Comp. Biochem. Physiol. A* **16**, 1–6.

Musa-Aziz, R., Chen, L.-M., Pelletier, M. F. and Boron, W. F. (2009). Relative CO_2/NH_3 selectivities of AQP1, AQP4, AQP5, AmtB, and RhAG. *Proc. Natl. Acad. Sci. USA* **106**, 5406–5411.

Nakada, T., Westhoff, C. M., Kato, A. and Hirose, S. (2007). Ammonia secretion from fish gill depends on a set of Rh glycoproteins. *FASEB J.* **21**, 1067–1074.

Nawata, C. M., Hung, C. C. Y., Tsui, T. K. N., Wilson, J. M., Wright, P. A. and Wood, C. M. (2007). Ammonia excretion in rainbow trout (*Oncorhynchus mykiss*): evidence for Rh glycoprotein and H^+-ATPase involvement. *Physiol. Genomics* **31**, 463–474.

Near, T. J. (2009). Conflict and resolution between phylogenies inferred from molecular and phenotypic data sets for hagfish, lampreys, and gnathostomes. *J. Exp. Zool. B* **312B**, 749–761.

Nelson, D. L., Lehninger, A. L. and Cox, M. M. (2008). *Lehninger Principles of Biochemistry*. 5 ed. New York: W.H. Freeman.

Nishiyama, M., Chiba, H., Uchida, K., Shimotani, T. and Nozaki, M. (2013). Relationships between plasma concentrations of sex steroid hormones and gonadal development in the brown hagfish, *Paramyxine atami*. *Zool. Sci.* **30**, 967–974.

Nonnotte, G. and Kirsch, R. (1978). Cutaneous respiration in seven sea-water teleosts. *Respir. Physiol. Neurobiol.* **35**, 111–118.

Nozaki, M. and Sower, S. A. (2015). Hypothalamic-pituitary-gonadal endocrine system in the hagfish. In *Hagfish Biology* (eds. Edwards, S. L. and Goss, G. G., pp. 227–256. Boca Raton: CRC press.

Nozaki, M., Shimotani, T. and Uchida, K. (2007). Gonadotropin-like and

adrenocorticotropin-like cells in the pituitary gland of hagfish, *Paramyxine atami*; immunohistochemistry in combination with lectin histochemistry. *Cell. Tissue. Res.* **328**, 563–572.

Orlowski, J. (1997). Na^+/H^+ exchangers of mammalian cells. *J. Biol. Chem.* **272**, 22373–22376.

Paris, M., Pettersson, K., Schubert, M., Bertrand, S., Pongratz, I., Escriva, H. and Laudet, V. (2008). An amphioxus orthologue of the estrogen receptor that does not bind estradiol: Insights into estrogen receptor evolution. *BMC Evol. Biol.* **8**, 1.

Parks, S. K., Tresguerres, M. and Goss, G. G. (2007a). Interactions between Na+ channels and Na^+-HCO_3^- cotransporters in the freshwater fish gill MR cell: a model for transepithelial Na+ uptake. *Am. J. Physiol. Cell Physiol.* **292**, C935–44.

Parks, S. K., Tresguerres, M. and Goss, G. G. (2007b). Blood and gill responses to HCl infusions in the Pacific hagfish (*Eptatretus stoutii*). *Can. J. Zool* **85**, 855–862.

Parks, S. K., Tresguerres, M. and Goss, G. G. (2009). Cellular mechanisms of Cl-transport in trout gill mitochondrion-rich cells. *Am. J. Physiol. Regul. Integr. Comp. Physiol.* **296**, R1161–9.

Perry, S. F. (1997). The chloride cell: Structure and function in the gills of freshwater fishes. *Annu. Rev. Physiol.* **59**, 325–347.

Perry, S. F. and Gilmour, K. M. (2006). Acid-base balance and CO_2 excretion in fish: unanswered questions and emerging models. *Respir. Physiol. Neurobiol.* **154**, 199–

215.

Perry, S. F., Braun, M. H., Noland, M., Dawdy, J. and Walsh, P. J. (2010). Do
zebrafish Rh proteins act as dual ammonia-CO_2 channels? *J. Exp. Zool. A* **313**, 618–
621.

Perry, S. F., Gilmour, K. M., Bernier, N. J. and Wood, C. M. (1999). Does gill
boundary layer carbonic anhydrase contribute to carbon dioxide excretion: a
comparison between dogfish (*Squalus acanthias*) and rainbow trout (*Oncorhynchus
mykiss*). *J. Exp. Biol.* **202**, 749–756.

Perry, S. F., Vulesevic, B., Braun, M. and Gilmour, K. M. (2009). Ventilation in
Pacific hagfish (*Eptatretus stoutii*) during exposure to acute hypoxia or hypercapnia.
Respir. Physiol. Neurobiol. **167**, 227–234.

Peters, T., Forster, R. E. and Gros, G. (2000). Hagfish (*Myxine glutinosa*) red cell
membrane exhibits no bicarbonate permeability as detected by ^{18}O exchange. *J. Exp.
Biol.* **203**, 1551–1560.

Philpott, C. W. (1980). Tubular system membranes of teleost chloride cells: osmotic
response and transport sites. *Am. J. Physiol.* **238**, R171–84.

Piermarini, P. M. and Evans, D. H. (2001). Immunochemical analysis of the vacuolar
proton-ATPase B-subunit in the gills of a euryhaline stingray (*Dasyatis sabina*):
effects of salinity and relation to Na^+/K^+-ATPase. *J. Exp. Biol.* **204**, 3251–3259.

Piermarini, P. M., Verlander, J. W., Royaux, I. E. and Evans, D. H. (2002). Pendrin

immunoreactivity in the gill epithelium of a euryhaline elasmobranch. *Am. J. Physiol. Regul. Integr. Comp. Physiol.* **283**, R983–92.

Potter, I. C., Macey, D. J., Roberts, A. R. and Withers, P. C. (1996). Oxygen consumption by ammocoetes of the lamprey *Geotria australis* in air. *J. Comp. Physiol. B* **166**, 331–336.

Potter, I. C., Welsch, U., Wright, G. M., Honma, Y. and Chiba, A. (1995). Light and electron microscope studies of the dermal capillaries in three species of hagfishes and three species of lampreys. *J. Zool.* **235**, 677–688.

Pörtner, H. O., Boutilier, R. G., Tang, Y. and Toews, D. P. (1990). Determination of intracellular pH and PCO_2 after metabolic inhibition by fluoride and nitrilotriacetic acid. *Respir. Physiol. Neurobiol.* **81**, 255–273.

Putman, R. J. (1978). Flow of energy and organic matter from a carcase during decomposition: Decomposition of small mammal carrion in temperate systems 2. *Oikos* **31**, 58–68.

Rahman, N., Buck, J. and Levin, L. R. (2013). pH sensing *via* bicarbonate-regulated "soluble" adenylyl cyclase (sAC). *Front Physiol* **4**, 343.

Randall, D. J. and Wright, P. A. (1989). The interaction between carbon dioxide and ammonia excretion and water pH in fish. **67**, 2936–2942.

Randall, D. J., Wilson, J. M., Peng, K. W., Kok, T. W., Kuah, S. S., Chew, S. F., Lam, T. J. and Ip, Y. K. (1999). The mudskipper, *Periophthalmodon schlosseri*,

actively transports NH_4^+ against a concentration gradient. *Am. J. Physiol.* **277**, R1562–7.

Rauther, M. (1937). Kiemen der anamnier-kiemendarm-derivate der Cyclostomen und fische. die driisenartigen derivate des kiemendarmes und kiemengange bei den Cyclostomen und fischen. In *Handbuch der vergleichenden Anatomie der Wirbeltiere*, pp. 211–278. Berlin: Urban & Schwarzenberg.

Read, L. J. (1975). Absence of ureogenic pathways in liver of the hagfish Bdellostoma cirrhatum. *Comparative Biochemistry and Physiology Part B: Comparative Biochemistry* **51**, 139–141.

Reid, S. D., Hawkings, G. S., Galvez, F. and Goss, G. G. (2003). Localization and characterization of phenamil-sensitive Na+ influx in isolated rainbow trout gill epithelial cells. *J. Exp. Biol.* **206**, 551–559.

Riegel, J. A. (1978). Factors affecting glomerular function in the pacific hagfish *Eptatretus stouti* (Lockington). *J. Exp. Biol.* **73**, 261–277.

Robertson, J. D. (1976). Chemical composition of the body fluids and muscle of the hagfish *Myxine glutinosa* and the rabbit-fish *Chimaera monstrosa*. *J. Zool.* **178**, 261–277.

Robertson, J. D. (1954). The chemical composition of the blood of some aquatic chordates, including members of the tunicata, cyclostomata and osteichthyes. *J. Exp. Biol.* **31**, 424–442.

Roos, A. and Boron, W. F. (1981). Intracellular pH. *Physiol. Rev.* **61**, 296–434.

Rossier, B. C., Baker, M. E. and Studer, R. A. (2015). Epithelial sodium transport and its control by aldosterone: The story of our internal environment revisited. *Physiol. Rev.* **95**, 297–340.

Ruben, J. A. and Bennett, A. F. (1980). Antiquity of the vertebrate pattern of activity metabolism and its possible relation to vertebrate origins. *Nature* **286**, 886–888.

Saha, N. and Ratha, B. K. (2007). Functional ureogenesis and adaptation to ammonia metabolism in Indian freshwater air-breathing catfishes. *Fish Physiol. Biochem.* **33**, 283–295.

Sanderson, L. A., Wright, P. A., Robinson, J. W., Ballantyne, J. S. and Bernier, N. J. (2010). Inhibition of glutamine synthetase during ammonia exposure in rainbow trout indicates a high reserve capacity to prevent brain ammonia toxicity. *J. Exp. Biol.* **213**, 2343–2353.

Sardella, B. A., Baker, D. W. and Brauner, C. J. (2009). The effects of variable water salinity and ionic composition on the plasma status of the Pacific Hagfish (*Eptatretus stoutii*). *J. Comp. Physiol. B* **179**, 721–728.

Sayer, M. D. J. and Davenport, J. (1987). The relative importance of the gills to ammonia and urea excretion in five seawater and one freshwater teleost species. *J. Fish Biol.* **31**, 561–570.

Schultz, A. G., Guffey, S. C., Clifford, A. M. and Goss, G. G. (2014). Phosphate

absorption across multiple epithelia in the Pacific hagfish (*Eptatretus stoutii*). *Am. J. Physiol. Regul. Integr. Comp. Physiol.* **307**, R643–652.

Shelton, R. G. J. (1978). On the Feeding of the Hagfish *Myxine Glutinosa* in the North Sea. *J. Mar. Biol. Assoc. UK* **58**, 81–86.

Sidell, B. D. and Beland, K. F. (1980). Lactate dehydrogenases of Atlantic hagfish: physiological and evolutionary implications of a primitive heart isozyme. *Science* **207**, 769–770.

Sidell, B. D., Stowe, D. B. and Hansen, C. A. (1984). Carbohydrate is the preferred metabolic fuel of the hagfish (*Myxinie glutinosa*) heart. *Physiol. Zool.* **57**, 266–273.

Sinha, A. K., Liew, H. J., Nawata, C. M., Blust, R., Wood, C. M. and De Boeck, G. (2013). Modulation of Rh glycoproteins, ammonia excretion and Na$^+$ fluxes in three freshwater teleosts when exposed chronically to high environmental ammonia. *J. Exp. Biol.* **216**, 2917–2930.

Sinha, A. K., Matey, V., Giblen, T., Blust, R. and De Boeck, G. (2014). Gill remodeling in three freshwater teleosts in response to high environmental ammonia. *Aquat. Toxicol.* **155**, 166–180.

Smart, G. (1976). The effect of ammonia exposure on gill structure of the rainbow trout (*Salmo gairdneri*). *J. Fish Biol.*

Smith, C. R. (1985). Food for the deep sea: utilization, dispersal, and flux of nekton falls at the Santa catalina basin floor. *Deep Sea Res. A* **32**, 417–442.

Smith, C. R. and Baco, A. R. (2003). Ecology of whale falls at the deep-sea floor. *Oceanogr. Mar. Biol.* **41**, 311–354.

Smith, H. W. (1930). Metabolism of the lung-fish *Protopterus æthiopicus*. *J. Biol. Chem.* **88**, 97–130.

Smith, H. W. (1932). Water regulation and its evolution in the fishes. *Q. Rev. Biol.* 7, 1–26.

Smith, K. L., Jr and Hessler, R. R. (1974). Respiration of Benthopelagic Fishes: In situ Measurements at 1230 Meters. *Science* **184**, 72–73.

Sower, S. A., Moriyama, S., Kasahara, M., Takahashi, A., Nozaki, M., Uchida, K., Dahlstrom, J. M. and Kawauchi, H. (2006). Identification of sea lamprey GTHβ-like cDNA and its evolutionary implications. *Gen. Comp. Endocrinol.* **148**, 22–32.

Srivastava, J., Barber, D. L. and Jacobson, M. P. (2007). Intracellular pH sensors: design principles and functional significance. *Physiology (Bethesda)* **22**, 30–39.

Stamatakis, A. (2014). RAxML version 8: a tool for phylogenetic analysis and post-analysis of large phylogenies. *Bioinformatics* **30**, 1312–1313.

Steffensen, J. F., Johansen, K., Sindberg, C. D., Sørensen, J. H. and Møller, J. L. (1984). Ventilation and oxygen consumption in the hagfish, *Myxine glutinosa* L. *J. Exp. Mar. Biol. Ecol.* **84**, 173–178.

Strahan, R. (1962). Survival of the hag, *Paramyxine atami* Dean, in diluted sea water. *Copeia* **1962**, 471.

Strahan, R. (1963). The Behaviour of Myxinoids. *Acta Zoologica* **44**, 73–102.

Talavera, G. and Castresana, J. (2007). Improvement of phylogenies after removing divergent and ambiguously aligned blocks from protein sequence alignments. *Syst. Biol.* **56**, 564–577.

Takahashi, A., Amemiya, Y., Sarashi, M., Sower, S. A. and Kawauchi, H. (1995). Melanotropin and corticotropin are encoded on two distinct genes in the lamprey, the earliest evolved extant vertebrate. *Biochem. Biophys. Res. Commun.* **213**, 490–498.

Tay, A. S. L., Chew, S. F. and Ip, Y. K. (2003). The swamp eel *Monopterus albus* reduces endogenous ammonia production and detoxifies ammonia to glutamine during 144 h of aerial exposure. *J. Exp. Biol.* **206**, 2473–2486.

Taylor, J. R. (2009). Intestinal HCO_3- secretion in fish: A widespread mechanism with newly recognized physiological functions.

Taylor, J. R. and Grosell, M. (2006). Evolutionary aspects of intestinal bicarbonate secretion in fish. *Comp. Biochem. Physiol. A* **143**, 523–529.

Thomson, R. C., Plachetzki, D. C., Mahler, D. L. and Moore, B. R. (2014). A critical appraisal of the use of microRNA data in phylogenetics. *Proc. Natl. Acad. Sci. USA* **111**, E3659–68.

Tresguerres, M., Barott, K. L., Barron, M. E. and Roa, J. N. (2014). Established and potential physiological roles of bicarbonate-sensing soluble adenylyl cyclase (sAC) in aquatic animals. *J. Exp. Biol.* **217**, 663–672.

Tresguerres, M., Katoh, F., Fenton, H., Jasinska, E. and Goss, G. G. (2005). Regulation of branchial V-H$^+$-ATPase, Na$^+$/K$^+$-ATPase and NHE2 in response to acid and base infusions in the Pacific spiny dogfish (*Squalus acanthias*). *J. Exp. Biol.* **208**, 345–354.

Tresguerres, M., Parks, S. K. and Goss, G. G. (2006a). V-H$^+$-ATPase, Na$^+$/K$^+$-ATPase and NHE2 immunoreactivity in the gill epithelium of the Pacific hagfish (*Epatretus stoutii*). *Comp. Biochem. Physiol. A* **145**, 312–321.

Tresguerres, M., Parks, S. K. and Goss, G. G. (2007a). Recovery from blood alkalosis in the Pacific hagfish (*Eptatretus stoutii*): Involvement of gill V–H$^+$–ATPase and Na$^+$/K$^+$–ATPase. *Comp. Biochem. Physiol. A* **148**, 133–141.

Tresguerres, M., Parks, S. K., Katoh, F. and Goss, G. G. (2006b). Microtubule-dependent relocation of branchial V-H+-ATPase to the basolateral membrane in the Pacific spiny dogfish (*Squalus acanthias*): a role in base secretion. *J. Exp. Biol.* **209**, 599–609.

Tresguerres, M., Parks, S. K., Sabatini, S. E., Goss, G. G. and Luquet, C. M. (2008). Regulation of ion transport by pH and [HCO$_3^-$] in isolated gills of the crab *Neohelice (Chasmagnathus) granulata*. *Am. J. Physiol. Regul. Integr. Comp. Physiol.* **294**, R1033–R1043.

Tresguerres, M., Parks, S. K., Salazar, E., Levin, L. R., Goss, G. G. and Buck, J. (2010). Bicarbonate-sensing soluble adenylyl cyclase is an essential sensor for a homeostasis. *Proc. Natl. Acad. Sci. USA* **107**, 442–447.

Tresguerres, M., Parks, S. K., Wood, C. M. and Goss, G. G. (2007b). V-H$^+$-ATPase translocation during blood alkalosis in dogfish gills: interaction with carbonic anhydrase and involvement in the postfeeding alkaline tide. *Am. J. Physiol. Regul. Integr. Comp. Physiol.* **292**, R2012–R2019.

Tsui, T. K. N., Hung, C. Y. C., Nawata, C. M., Wilson, J. M., Wright, P. A. and Wood, C. M. (2009). Ammonia transport in cultured gill epithelium of freshwater rainbow trout: the importance of Rhesus glycoproteins and the presence of an apical Na$^+$/NH$_4^+$ exchange complex. *J. Exp. Biol.* **212**, 878–892.

Tsui, T., Randall, D. J., Chew, S. F., Jin, Y., Wilson, J. M. and Ip, Y. K. (2002). Accumulation of ammonia in the body and NH$_3$ volatilization from alkaline regions of the body surface during ammonia loading and exposure to air in the weather loach *Misgurnes anguillicaudatus*. *J. Exp. Biol.* **651-659**.

Uchida, K., Moriyama, S., Chiba, H., Shimotani, T., Honda, K., Miki, M., Takahashi, A., Sower, S. A. and Nozaki, M. (2010). Evolutionary origin of a functional gonadotropin in the pituitary of the most primitive vertebrate, hagfish. *Proc. Natl. Acad. Sci. U.S.A.* **107**, 15832–15837.

Urbina, M. A. and Glover, C. N. (2015). Effect of salinity on osmoregulation, metabolism and nitrogen excretion in the amphidromous fish, inanga (*Galaxias maculatus*). *J. Exp. Mar. Biol. Ecol.* **473**, 7–15.

Urbina, M. A., Glover, C. N. and Forster, M. E. (2012). A novel oxyconforming response in the freshwater fish *Galaxias maculatus*. *Comp. Biochem. Physiol. A* **161**,

301–306.

Urbina, M. A., Meredith, A. S., Glover, C. N. and Forster, M. E. (2014). The importance of cutaneous gas exchange during aerial and aquatic respiration in galaxiids. *J. Fish Biol.* **84**, 759–773.

Veauvy, C. M., McDonald, M. D., Audekerke, J. V., Vanhoutte, G., Camp, N. V., Linden, A. V. D. and Walsh, P. J. (2005). Ammonia affects brain nitrogen metabolism but not hydration status in the Gulf toadfish (*Opsanus beta*). *Aquatic Toxicology* **74**, 32–46.

Verdouw, H., Van Echteld, C. and Dekkers, E. (1978). Ammonia determination based on indophenol formation with sodium salicylate. *Water Res.* **12**, 399–402.

Wakabayashi, S., Shigekawa, M. and Pouyssegur, J. (1997). Molecular physiology of vertebrate Na^+/H^+ exchangers. *Physiol. Rev.* **77**, 51–74.

Walsh, P. J. (1997). Evolution and regulation of urea synthesis and ureotely in (batrachoidid) fishes. *Annu. Rev. Physiol.* **59**, 299–323.

Walsh, P. J. and Smith, C. P. (2001). Urea transport. In *Fish Physiology: Nitrogen Excretion* (eds. Wright, P. A. and Anderson, P., pp. 297–307. New York: Academic Press.

Walsh, P. J., Danulat, E. and Mommsen, T. P. (1990). Variation in urea excretion in the gulf toadfish *Opsanus beta*. *Mar. Biol.* **106**, 323–328.

Walsh, P. J., Mayer, G. D., Medina, M., Bernstein, M. L., Barimo, J. F. and

Mommsen, T. P. (2003). A second glutamine synthetase gene with expression in the gills of the gulf toadfish (*Opsanus beta*). *J. Exp. Biol.* **206**, 1523–1533.

Walsh, P. J., Veauvy, C. M., McDonald, M. D., Pamenter, M. E., Buck, L. T. and Wilkie, M. P. (2007). Piscine insights into comparisons of anoxia tolerance, ammonia toxicity, stroke and hepatic encephalopathy. *Comp. Biochem. Physiol. A* **147**, 332–343.

Walsh, P., Wang, Y., Campbell, C., De G Boeck and Wood, C. (2001). Patterns of nitrogenous waste excretion and gill urea transporter mRNA expression in several species of marine fish. *Mar. Biol.* **139**, 839–844.

Wang, Y., Heigenhauser, G. J. and Wood, C. M. (1994). Integrated responses to exhaustive exercise and recovery in rainbow trout white muscle: acid-base, phosphogen, carbohydrate, lipid, ammonia, fluid volume and electrolyte metabolism. *J. Exp. Biol.* **195**, 227–258.

Wang, Y., Heigenhauser, G. J. and Wood, C. M. (1996). Ammonia movement and distribution after exercise across white muscle cell membranes in rainbow trout. *Am. J. Physiol.* **271**, R738–50.

Weihrauch, D., Wilkie, M. P. and Walsh, P. J. (2009). Ammonia and urea transporters in gills of fish and aquatic crustaceans. *J. Exp. Biol.* **212**, 1716–1730.

Weinrauch, A. M., Edwards, S. L. and Goss, G. G. (2015). Anatomy of the Pacific hagfish (*Eptatretus stoutii*). In *Hagfish Biology* (eds. Edwards, S. L. and Goss, G. G., pp. 1–40. Boca Raton: CRC Press.

Weisbart, M. and Idler, D. R. (1970). Re-examination of the presence of corticosteroids in two cyclostomes, the atlantic hagfish (*Myxine glutinosa* L.) and the sea lamprey (*Petromyzon marinus* L.). *J. Endocrinol.* **46**, 29–43.

Weisbart, M., Dickhoff, W. W., Gorbman, A. and Idler, D. R. (1980). The presence of steroids in the sera of the Pacific hagfish, *Eptatretus stouti*, and the sea lamprey, *Petromyzon marinus*. *Gen. Comp. Endocrinol.* **41**, 506–519.

Weiss, R. F. (1974). Carbon dioxide in water and seawater: the solubility of a non-ideal gas. *Mar. Chem.* 203–215.

Wells, P. and Pinder, A. (1996). The respiratory development of Atlantic salmon. I. Morphometry of gills, yolk sac and body surface. *J. Exp. Biol.* **199**, 2725–2736.

Wells, R. M., Forster, M. E., Davison, W., Taylor, H. H., Davie, P. S. and Satchell, G. H. (1986). Blood oxygen transport in the free-swimming hagfish, *Eptatretus cirrhatus*. *J. Exp. Biol.* **123**, 43–53.

Welsch, U. and Potter, I. C. (1998). Dermal capillaries. In *The Biology of Hagfishes*, pp. 273–283. Dordrecht: Springer Netherlands.

Whitten, S. T., García-Moreno E, B. and Hilser, V. J. (2005). Local conformational fluctuations can modulate the coupling between proton binding and global structural transitions in proteins. *Proc. Natl. Acad. Sci. U.S.A.* **102**, 4282–4287.

Wicks, B. J. and Randall, D. J. (2002). The effect of sub-lethal ammonia exposure on fed and unfed rainbow trout: the role of glutamine in regulation of ammonia. *Comp.*

347

Biochem. Physiol. A **132**, 275–285.

Wilkie, M. P. (2002). Ammonia excretion and urea handling by fish gills: present understanding and future research challenges. *J. Exp. Zool.* **293**, 284–301.

Wilkie, M. P. and Wood, C. M. (1991). Nitrogenous waste excretion, acid-base regulation, and ionoregulation in rainbow trout (*Oncorhynchus mykiss*) exposed to extremely alkaline water. *Physiol. Zool.* **64**, 1069–1086.

Wilkie, M. P. and Wood, C. M. (1995). Recovery from high pH exposure in the rainbow trout: White muscle ammonia storage, ammonia washout, and the restoration of blood chemistry. *Physiol. Zool.* **68**, 379–401.

Wilkie, M. P., Claude, J. F., Cockshutt, A., Holmes, J. A., Wang, Y. S., Youson, J. H. and Walsh, P. J. (2006). Shifting patterns of nitrogen excretion and amino acid catabolism capacity during the life cycle of the sea lamprey (*Petromyzon marinus*). *Physiol. Biochem. Zool.* **79**, 885–898.

Wilkie, M. P., Pamenter, M. E., Duquette, S., Dhiyebi, H., Sangha, N., Skelton, G., Smith, M. D. and Buck, L. T. (2011). The relationship between NMDA receptor function and the high ammonia tolerance of anoxia-tolerant goldfish. *J. Exp. Biol.* **214**, 4107–4120.

Wilkie, M. P., Stecyk, J. A. W., Couturier, C. S., Sidhu, S., Sandvik, G. K. and Nilsson, G. E. (2015). Reversible brain swelling in crucian carp (*Carassius carassius*) and goldfish (*Carassius auratus*) in response to high external ammonia and anoxia. *Comp. Biochem. Physiol. A* **184**, 65–75.

Wilkie, M. P., Turnbull, S., Bird, J., Wang, Y. S., Claude, J. F. and Youson, J. H. (2004). Lamprey parasitism of sharks and teleosts: high capacity urea excretion in an extant vertebrate relic. *Comp. Biochem. Physiol. A* **138**, 485–492.

Wilkie, M. P., Wang, Y., Walsh, P. J. and Youson, J. H. (1999). Nitrogenous waste excretion by the larvae of a phylogenetically ancient vertebrate: the sea lamprey (*Petromyzon marinus*). **77**, 707–715.

Wilkie, M. P., Wright, P. A., Iwama, G. K. and Wood, C. M. (1993). The physiological responses of the Lahontan cutthroat trout (*Oncorhynchus clarki henshawi*), a resident of highly alkaline Pyramid Lake (ph 9.4), to challenge at pH 10. *J. Exp. Biol.* **175**, 173–194.

Wilson, J. M., Randall, D. J., Donowitz, M., Vogl, A. W. and Ip, A. K. (2000). Immunolocalization of ion-transport proteins to branchial epithelium mitochondria-rich cells in the mudskipper (*Periophthalmodon schlosseri*). *J. Exp. Biol.* **203**, 2297–2310.

Wisner, R. L. and McMillan, C. B. (1995). Review of new world hagfish of genus Myxine (Agnatha, Myxinidae) with descriptions of nine new species. *Fish. Bull.* **93**, 530–550.

Wood, C. and Evans, D. H. (1993). Ammonia and urea metabolism and excretion in fish. In *Molecular genetics of avian proteins*, CRC Marine science series 379-426.

Wood, C. M. (1991). Acid-base and ion balance, metabolism, and their interactions, after exhaustive exercise in fish. *J. Exp. Biol.* **160**, 285–308.

Wood, C. M. (2001). Influence of feeding, exercise, and temperature on nitrogen metabolism and excretion. In *Fish Physiology: Nitrogen Excretion* (eds. Wright, P. A. and Anderson, P., pp. 201–238. San Diego: Elsevier.

Wood, C. M. and Nawata, C. M. (2011). A nose-to-nose comparison of the physiological and molecular responses of rainbow trout to high environmental ammonia in seawater versus freshwater. *J. Exp. Biol.* **214**, 3557–3569.

Wood, C. M., Kajimura, M., Mommsen, T. P. and Walsh, P. J. (2005a). Alkaline tide and nitrogen conservation after feeding in an elasmobranch (*Squalus acanthias*). *J. Exp. Biol.* **208**, 2693–2705.

Wood, C. M., Walsh, P. J., Chew, S. F. and Ip, Y. K. (2005b). Greatly elevated urea excretion after air exposure appears to be carrier mediated in the slender lungfish (*Protopterus dolloi*). *http://dx.doi.org/10.1086/432919*.

Wright, P. A. (1995). Nitrogen excretion: three end products, many physiological roles. *J. Exp. Biol.* **198**, 273–281.

Wright, P. A. and Wood, C. M. (1985). An analysis of branchial ammonia excretion in the freshwater rainbow trout: Effects of environmental pH change and sodium uptake blockade. *J. Exp. Biol.* **114**, 329–353.

Wright, P. A. and Wood, C. M. (1988). Muscle ammonia stores are not determined by pH gradients. *Fish Physiol. Biochem.* **5**, 159–162.

Wright, P. A. and Wood, C. M. (2009). A new paradigm for ammonia excretion in

aquatic animals: role of Rhesus (Rh) glycoproteins. *J. Exp. Biol.* **212**, 2303–2312.

Yancey, P. H. (2005). Organic osmolytes as compatible, metabolic and counteracting cytoprotectants in high osmolarity and other stresses. *J. Exp. Biol.* **208**, 2819–2830.

You, G., Smith, C. P., Kanai, Y., Lee, W. S., Stelzner, M. and Hediger, M. A. (1993). Cloning and characterization of the vasopressin-regulated urea transporter. *Nature* **365**, 844–847.

Zimmer, A. M. and Wood, C. M. (2015). Ammonia first? The transition from cutaneous to branchial ammonia excretion in developing rainbow trout is not altered by exposure to chronically high NaCl. *J. Exp. Biol.* **218**, 1467–1470.

Zimmer, A. M., Brauner, C. J. and Wood, C. M. (2014). Ammonia transport across the skin of adult rainbow trout (*Oncorhynchus mykiss*) exposed to high environmental ammonia (HEA). *J. Comp. Physiol. B* **184**, 77–90.

Zintzen, V., Roberts, C. D., Anderson, M. J., Stewart, A. L., Struthers, C. D. and Harvey, E. S. (2011). Hagfish predatory behaviour and slime defence mechanism. *Sci. Rep.* **1**, 131.